[redacted]

NASA TM X-1280

POSTFLIGHT EVALUATION OF ATLAS-CENTAUR AC-6

(Launched August 11, 1965)

By Staff of the Lewis Research Center

Lewis Research Center
Cleveland, Ohio

NATIONAL AERONAUTICS AND SPACE ADMINISTRATION

[redacted]

[redacted]

CONTENTS

I. SUMMARY

The sixth Atlas Centaur vehicle (AC-6) was successfully launched from the Eastern Test Range, Complex 36B, on August 11, 1965, at 0931:04.430 EST. A 2084-pound dynamic model of the Surveyor payload was placed in a simulated lunar transfer trajectory. Vehicle systems operated satisfactorily and all the flight objectives were accomplished.

Lift-off within 4 seconds of the window opening demonstrated the launch-on-time capability of the vehicle. Small deviations from the desired trajectory were accurately compensated for by the Centaur guidance system. Injection of the Surveyor model into a near-perfect lunar transfer trajectory would have resulted in an impact of the moon without a midcourse correction. To hit the precise target area on the lunar surface, the required correction would have been 4.25 meters per second, which is well within the spacecraft capability.

Normal thrust and impulse levels were obtained with both the Atlas and Centaur propulsion systems. However, a sizeable thrust overshoot on startup of the Centaur engines has not been resolved. A propellant-utilization system used for the first time on the Centaur, accurately controlled the fuel and oxidant consumption. The turnaround and retrothrust maneuver were performed without incident. Relatively high longitudinal modal excitations and lateral payload excitations were obtained at lift-off; these high perturbations are believed to be related to the launcher holddown arms.

Nominal temperatures were recorded for both the external vehicle skin and the payload compartment; however, abnormally low temperatures were measured in the forward equipment area, which may have resulted from leakage of cold helium purge gas. All vehicle electrical systems performed satisfactorily; the only difficulty with the RF systems was obtained with the C-band transponder. Most of the vehicle instrumentation yielded valid data.

The AC-6 vehicle was constructed with several new lightweight designs including the forward bulkhead, thrust barrel, interstage adapter and tank skin thickness reduction from 0.016 to 0.014 inch. No deficiencies were observed in any of these new structural elements.

II. INTRODUCTION

The AC-6 Atlas-Centaur vehicle, which was successfully launched from ETR Complex 36B on August 11, 1965 at 0931:04.430 EST, was the sixth in a series of development flights. (All symbols and abbreviations are defined in appendix A.) The AC-6 carried a 2084-pound dynamic model of the Surveyor payload that was successfully placed in a simulated lunar transfer trajectory. For a direct ascent and single-burn second stage, the space vehicle demonstrated a capability to launch on the proper azimuth for various times and days that the Earth and the moon were in the proper relation to each other. The launch windows for AC-6 were derived from the September-October launch opportunity dates to satisfy the requirements for the launch-on-time study as well as offering maximum launch opportunities and assuring a lunar miss. In order to have photographic coverage for use in potential failure analysis, the launch windows were biased by 6 hours to permit a daylight launch.

The AC-6 was the first vehicle flown wherein the Atlas sustainer stage operation was nominally terminated by a planned propellant depletion mode. A normal sustainer engine shutdown procedure consists of a "soft" shutdown phase and a "hard" shutdown phase.

From lift-off until booster engine cutoff, the Atlas is steered by a series of preprogramed pitch commands. At 8 seconds after booster engine cutoff, the Centaur guidance is admitted and is active throughout the remainder of the Atlas and Centaur portions of flight.

The following major changes to Centaur systems were incorporated on AC-6 to make it essentially an operational configuration:

(1) Nominal tank skin thickness changed from 0.016 to 0.014 inch

(2) Smaller LO_2 tank to eliminate slosh baffle and maintain vehicle stability

(3) Revised station 219 tank ring (modified T-shape)

(4) Station 408 ring modified to station 412 and revised (modified T-shape)

(5) Lightweight thrust barrel

(6) Lengthened insulation panels to accommodate longer LH_2 tank incurred by lowering the intermediate bulkhead

(7) Lightweight forward bulkhead

(8) Advanced propellant level indicating system

(9) Separate and independent Range Safety Command battery pack

(10) Lightweight dual range safety command receivers

(11) Electrically functional Surveyor destruct subsystem (with inert pyrotechnics)

(12) Redesigned lightweight interstage adapter

(13) Single 100 ampere-hour battery for both telemetry and missile power

Other Centaur changes that occurred between AC-5 and AC-6 were as follows:

(1) Revised location and alinement of attitude control engines

(2) Uprated hydraulic recirculation system

(3) Interstage-adapter shaped-charge area "finalized"

(4) New Atlas-Centaur separation guides

(5) Redesigned propellant ducts

(6) Minimum LO_2 ullage standpipe

(7) Redesigned power changeover switch

(8) No separate telemetry changeover switch

(9) Fusing of nonessential systems on main missile battery

The flight test control criteria for AC-6 as stated in Section 8.6 of the Unified Test Plan (ref. 1) were as follows:

Basic Structure:

(1) To demonstrate the structural integrity of the Atlas and Centaur vehicles during all powered phases of flight

(2) To demonstrate the structural and thermal integrity of the Centaur nose-fairing and insulation panels

Separation and Jettison:

(1) To demonstrate the satisfactory operation of the insulation-panel and nose-fairing-jettison systems

(2) To demonstrate the satisfactory operation of the Atlas-Centaur separation system

(3) To demonstrate the spacecraft separation system

Guidance:

(1) To verify the integrity of the guidance system

(2) To demonstrate the overall measuring accuracy of the guidance system

(3) To verify that the guidance system provides proper discrete and steering signals to the Atlas and Centaur flight-control systems during closed-loop flight

(4) To demonstrate that the guidance equations and associated trajectory parameters are satisfactory

(5) To obtain data on accuracy of Atlas-Centaur lunar orbit injection by postinjection DSIF tracking of the Surveyor dynamic model S-band transponder

Centaur Propulsion:

(1) To verify the ability of the Centaur propulsion system to start in the flight environment and then burn to guidance cutoff

(2) To obtain data on the performance of the Centaur main-engine system

(3) To obtain data on the performance of the H_2O_2 attitude-control system

Centaur Vehicle Systems:

(1) To verify that the flight-control system supplies the proper signal for attitude control and dynamic stability of the Centaur vehicle

(2) To obtain data on the capability of Centaur to perform the retromaneuver

(3) To obtain data on the performance of the following systems:

   (a) Hydraulic

   (b) Pneumatic

   (c) Electrical

   (d) Radiofrequency: telemetry, Azusa, and C-band beacon

   (e) Propellant utilization

   (f) Propellant level indicating

(4) To demonstrate the capability of the electromechanical timer for one-burn missions

Atlas Vehicle:

(1) To obtain data on the performance of all the Atlas systems (including the propellant-depletion system)

(2) To demonstrate the operation of the 165K-thrust MA-5 engine on the LV-3C vehicle

Launch Capability:

(1) To demonstrate the simulated lunar - launch-on-time (variable launch azimuth) capability of the Atlas-Centaur vehicle

Environment:

(1) To obtain data on the flight environment including pressures, temperatures, and vibration levels

(2) To obtain data on the spacecraft environment during the launch-to-spacecraft separation phase of flight

(3) To obtain data on the orbital environments, terminal behavior, and general postmission performance of vehicle systems until loss of all data links

The AC-6 sequence of flight events is presented in table II-I. Table II-II presents a weight summary for Atlas and Centaur. A schematic diagram of the flight is shown in figure II-1, and an illustration of the general arrangement of the Centaur stage is presented in figure II-2. Figure II-3 shows an illustration of the AC-6 dynamic model, SD-2.

TABLE II-I. - SEQUENCE OF FLIGHT EVENTS

Event	Time, sec		
	Programer	Nominal	Actual
Lock LH_2 vent valve		T - 7.00	T - 7.38
Programer start; 2-in. rise		T + 0	T + 0
Initiate roll program		T + 2	T + 2.3
Initiate pitch program		T + 15	T + 15.3
Open LH_2 vent valve command		T + 69	T + 69.6^{+0}_{-1}
Close LH_2 vent valve command, activate sustainer control, rate gyro gain to high	BECO + 0	T + 142.7	T + 141.6^{+0}_{-1}
Booster engine cutoff	BECO + 0	T + 142.7	T + 141.79
Jettison booster package	BECO + 3.1	T + 145.8	T + 144.87
Open LH_2 vent valve command	BECO + 7	T + 149.7	T + 149.6^{+0}_{-1}
Guidance admitted for steering control	BECO + 8.0	T + 150.7	
Jettison insulation panels	BECO + 30	T + 172.7	T + 171.62
Unlatch nose fairings	BECO + 54.5	T + 197.2	T + 195.57±0.5
Fire thruster bottles	BECO + 55	T + 197.7	T + 196.47
Start Centaur boost pumps	BECO + 62	T + 204.7	T + 203.57±0.5
Sustainer engine cutoff (due to LO_2 depletion) Vernier engine cutoff	SECO + 0	T + 234.8	T + 234.1^{+0}_{-1}
Close LO_2 and LH_2 vent valves, pressurize LO_2 and LH_2 tanks	SECO + 0	T + 234.8	T + 234.4^{+0}_{-1}
Start Centaur programer	SECO + 0	T + 234.8	T + 235.1^{+0}_{-1}
Start hydraulic recirculating pump	SECO + 0.5	T + 235.3	T + 235.6^{+0}_{-1}
SECO discrete backup command from guidance	SECO + 0	T + 234.8	T + 236.57
Separate first and second stages	SECO + 1.9	T + 236.7	T + 236.22
Prestart, steering reference to Centaur	SECO + 3.5	T + 238.3	T + 238.6^{+0}_{-1}
Start main engines, unnull main engine integrators, low rate gain, energize igniters	SECO + 8.5 (MES)	T + 243.3	T + 242.77
Main engine cutoff, H_2O_2 separate on, H_2O_2 roll integrators unnulled, high rate gain, low displacement gain	MECO + 0	T + 675.4	T + 679.07
MECO backup, PU null	SECO + 453.5 (t)	T + 688.3	T + 688.6^{+0}_{-1}
Safe Surveyor destruct	SECO + 454	T + 688.8	T + 689.6^{+0}_{-1}
Preseparation arming, extend landing gear, null main-engine integrators	t + 18	T + 706.3	T + 706.8^{+0}_{-1}

TABLE II-I. - Concluded. SEQUENCE OF FLIGHT EVENTS

Event	Time, sec		
	Programer	Nominal	Actual
Unlock omni antenna	t + 28.5	T + 716.8	$T + 717.1^{+0}_{-1}$
High power on, preseparation arming off	t + 49	T + 737.3	$T + 736.57^{+1}_{-0}$
Spacecraft electrical disconnect, switch guidance-spacecraft TLM channels	t + 54.5	T + 742.8	T + 742.57±0.5
Separate spacecraft	t + 60	T + 748.3	T + 747.57
Start 180° turn, admit guidance for attitude control	t + 65	T + 753.3	T + 752.97
End 180° turn, start retrothrust, prestart, start hydraulic recirculating pump	t + 185	T + 873.3	T + 872.57
Calibrate telemetry	t + 641	T + 1329.3	$T + 1329.7^{+0}_{-1}$
Open LO_2 and LH_2 vent valves	t + 1165	T + 1853.3	$T + 1853.3^{+0}_{-1}$
End retrothrust, power off	t + 1166	T + 1854.3	$T + 1854.1^{+0}_{-1}$

TABLE II-II. - WEIGHT SUMMARY

Centaur stage	Weight, lb
Basic hardware	
Body group	940
Propulsion group	1 192
Guidance group	310
Control group	117
Pressurization group	138
Electrical group	266
Separation equipment	80
Flight instrumentation	447
Miscellaneous equipment	153
Spacecraft	2 084
Total	5 727
Jettisonable hardware	
Nose fairing	2 006
Insulation panels	1 218
Total	3 224
Residuals	
LH_2 trapped	72
LO_2 trapped	68
Unburned [a] LH_2	91
Unburned [a] LO_2	203
Gaseous hydrogen	83
Gaseous oxygen	165
H_2O_2	52
Helium	5
Ice	12
Total	751
Expendables	
Main impulse H_2	4 966
Main impulse O_2	25 153
Gas boiloff on ground [b] H_2	27
Gas boiloff on ground [b] O_2	26
Inflight chill H_2	11
Inflight chill O_2	13
Boost-phase vent H_2	83
Boost-phase vent O_2	20
Sustainer-phase vent H_2	46
Sustainer-phase vent O_2	38
H_2O_2	49
Ice	50
Total	30 482
Total tanked weight	40 184
Minus ground vent	-53
Total Centaur weight at lift-off	40 131

Atlas stage	Weight, lb
Sustainer jettison weight	
Sustainer dry weight	5 667
Sustainer residuals	1 654
Unburned expendables	0
Interstage adapter	1 087
Unburned lubrication oil	17
Total	8 425
Booster jettison weight	
Booster dry weight	6 208
Booster residuals	1 117
Unburned lubrication oil	29
Total	7 354
Flight expendables	
Main impulse RP-1	75 829
Main impulse O_2	171 881
Helium panel purge	6
Oxidizer vent loss	15
Lubrication oil	173
Total	247 904
Ground [c] expendables	
Fuel	536
Oxidizer	1 698
Lubrication oil	3
Exterior ice	50
LN_2 in helium shrouds	140
Pre-ignition GO_2 loss	450
Total	2 877
Total tanked weight	266 560
Minus ground run	-2 877
Total Atlas weight at lift-off	263 683
Total Atlas-Centaur lift-off weight	303 814

[a] Includes flight performance reserve.
[b] Expended prior to Atlas ignition.
[c] Ground run time, 2.05 sec.

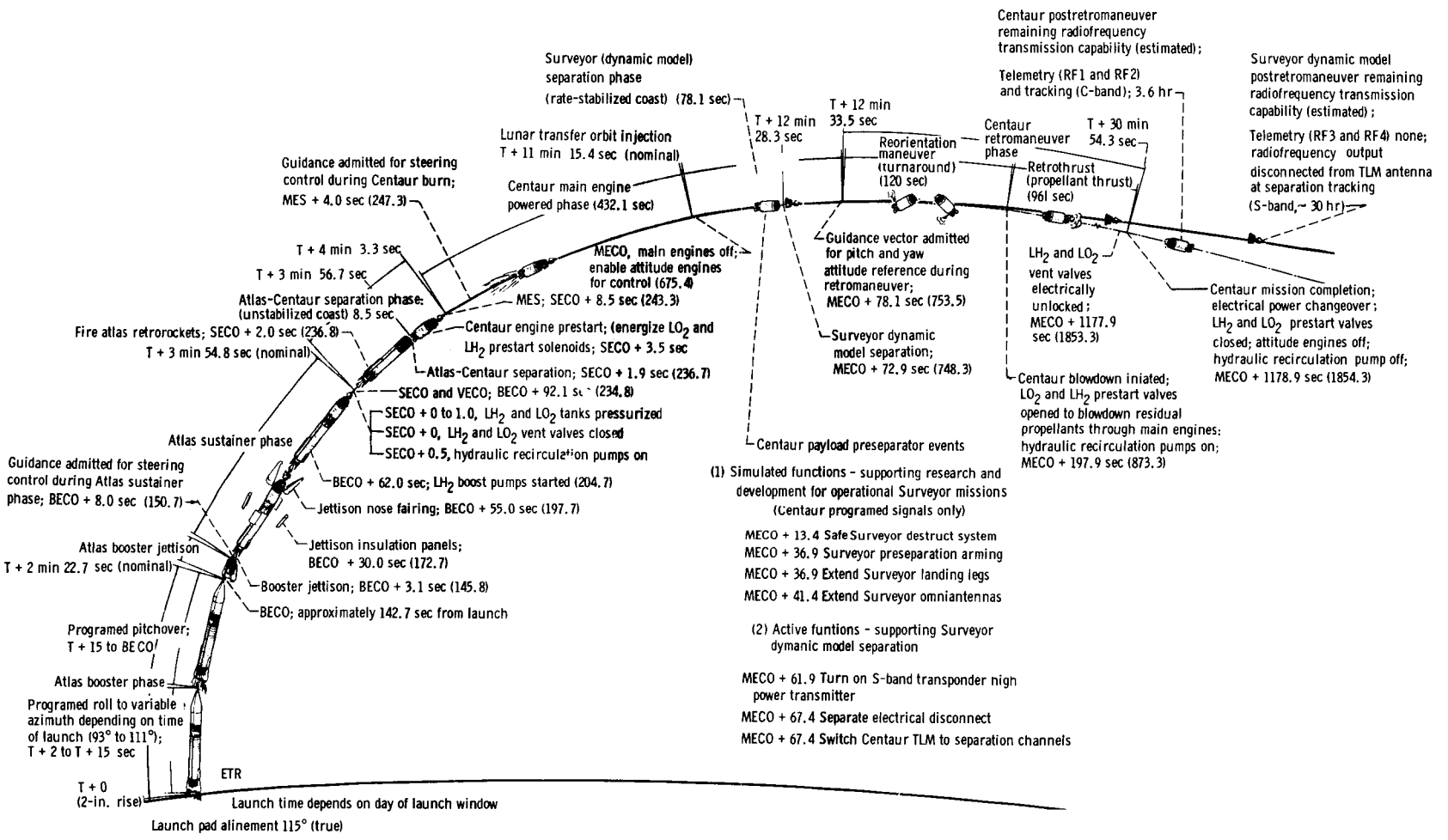

Figure II-1. - Atlas-Centaur-Surveyor dynamic model flight compendium. Times shown are preflight nominal. Actual times are given in table II-I.

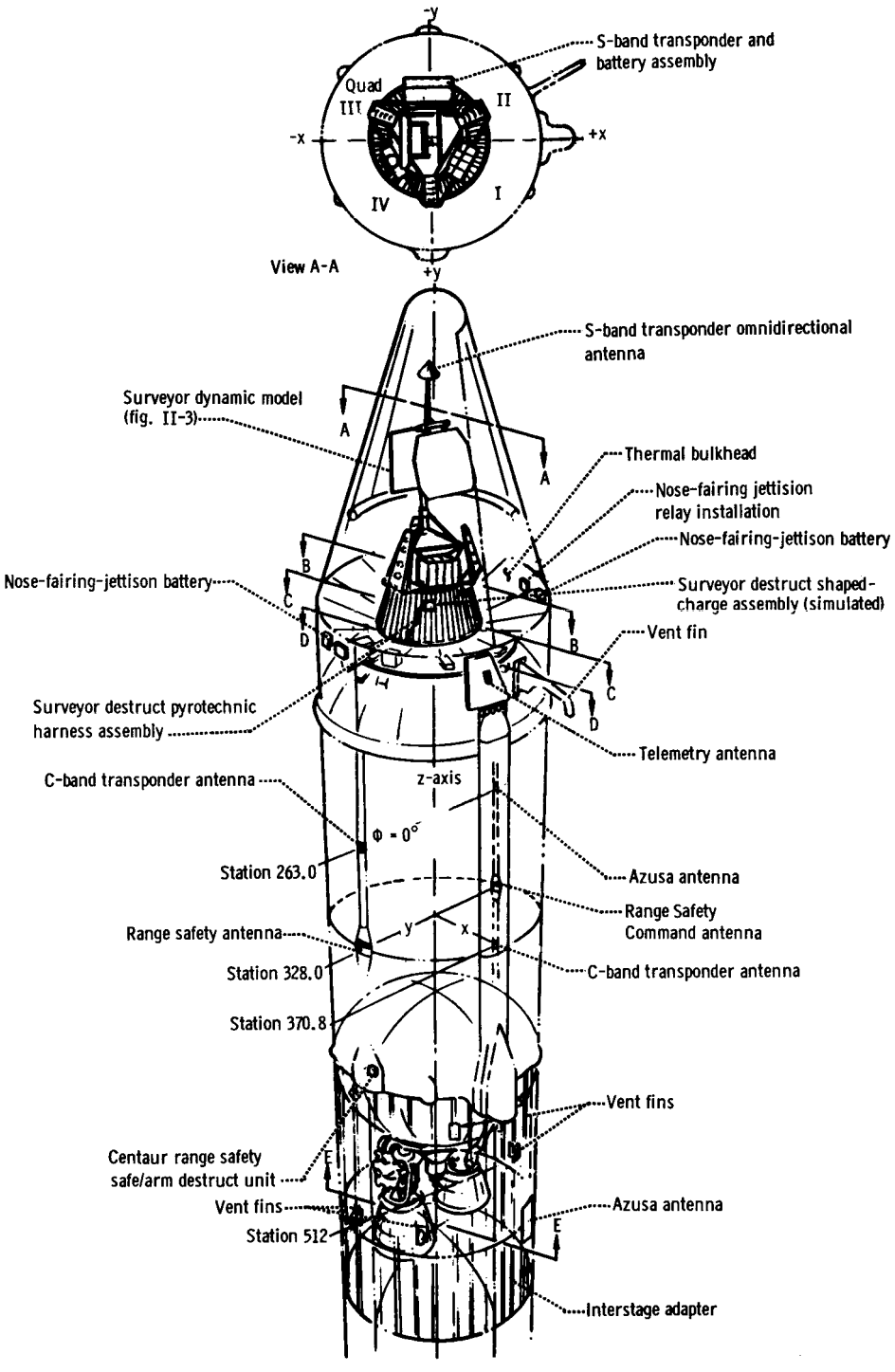

Figure II-2. - General arrangement of

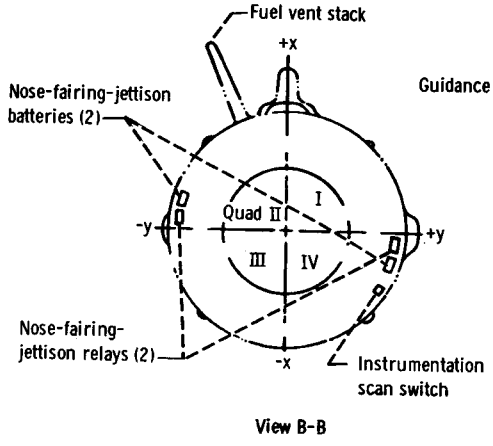

View B-B

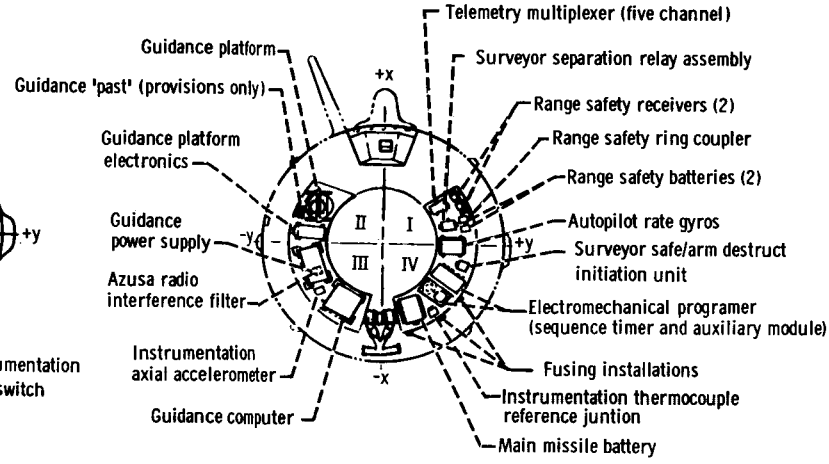

view C-C upper tier

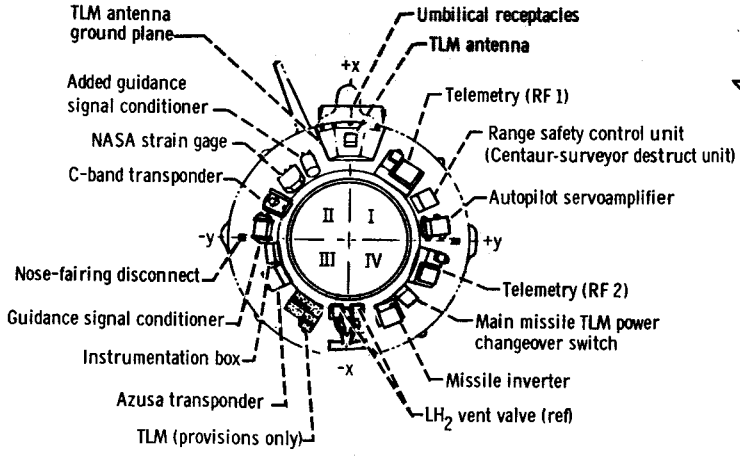

View D-D lower tier

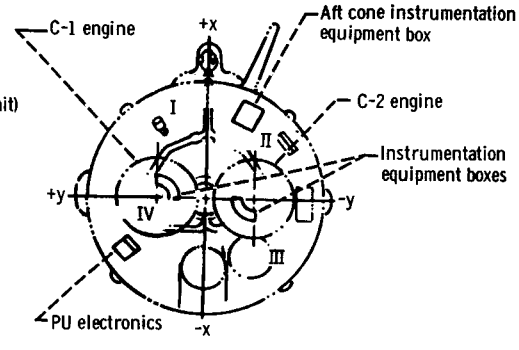

View E-E looking forward

Centaur 2D (AC-6) (ref. 1).

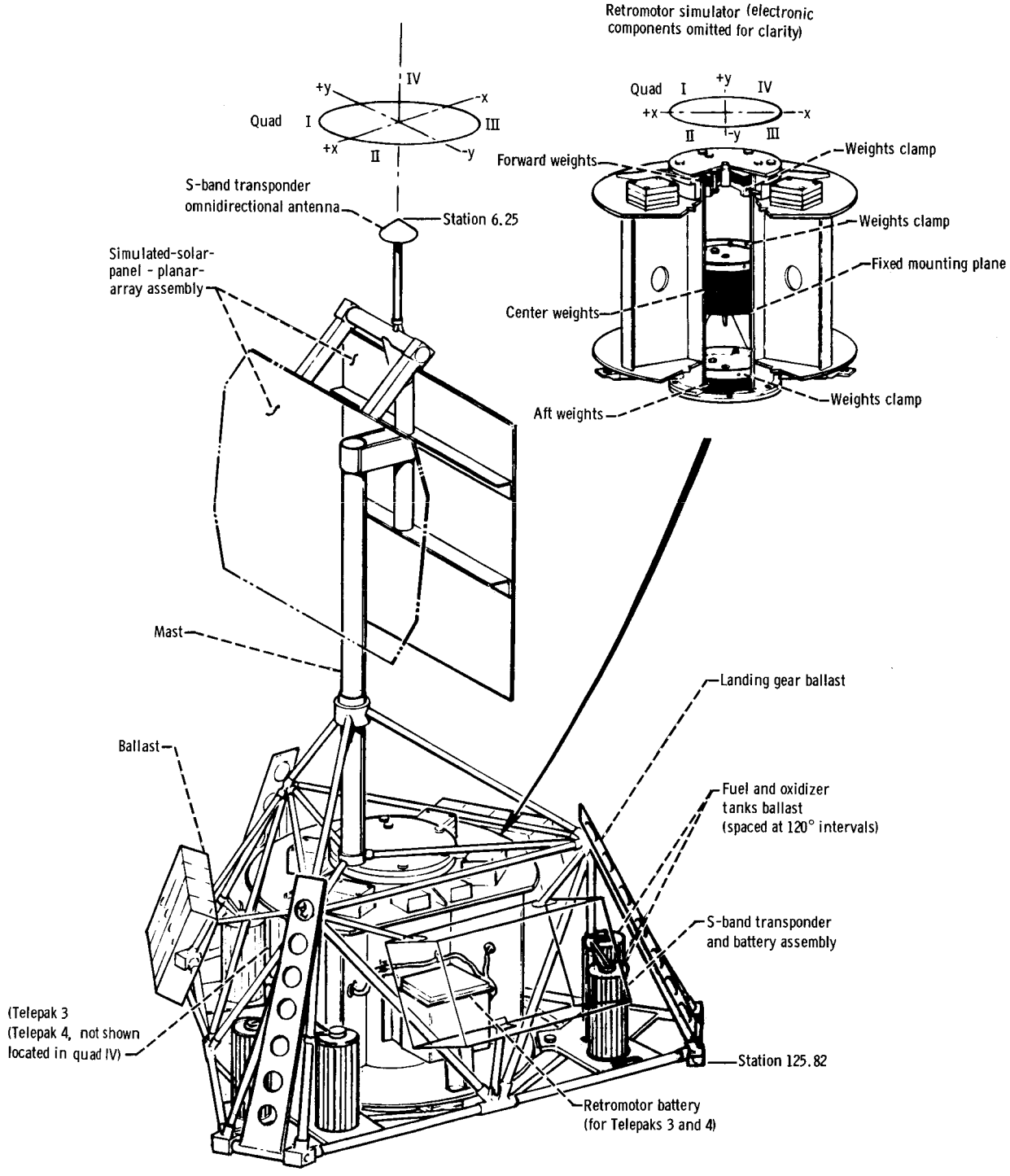

Figure II-3. - Surveyor dynamic model (SD-2) (ref. 1).

[redacted]

III. PRELAUNCH HISTORY

SUMMARY

Between the time the Atlas-Centaur launch vehicle arrives at ETR and launch day, it undergoes a series of preflight tests. These tests, which include (1) the Flight Control and Propellant Tanking Test, (2) the Flight Acceptance and Composite Test, and (3) the Composite Readiness Test, are to ensure that all airborne and ground-support systems are within specifications to support a successful launch. The tests were satisfactorily completed with only a few major anomalies.

ARRIVAL AND ERECTION

The Atlas-Centaur launch vehicle (AC-6) arrival at ETR began with the Atlas (151D) booster and the interstage adapter on May 14, 1965. The Centaur (2D) stage arrived May 25, 1965.

Vehicle erection on Complex 36B started on May 18 with the Atlas booster, followed by the interstage adapter on May 19, and the Centaur stage on May 27.

The Surveyor dynamic model arrived at ETR on May 14. The encapsulation of the model in preparation for preflight testing was accomplished on July 8 and it was mated to the launch vehicle on July 9. The encapsulated payload was demated on July 28 for final flight preparations and was remated to the launch vehicle on August 1 in preparation for launch.

PROPELLANT TANKING INTEGRATED TEST

The Propellant Tanking Integrated Test (Quad Tanking, ref. 2) is conducted to verify that the launch vehicle can be tanked with propellants and that all vehicle systems and the spacecraft can function properly under cryogenic and operational radiofrequency environments.

The Quad Tanking Test was conducted on July 13. The test began at 0520 EST and proceeded through to the scheduled 40-minute hold at T - 10 minutes at 0750 EST. Prior to T - 10 minutes, two major airborne equipment discrepancies were encountered. The first discrepancy occurred during the Guidance and Autopilot Test when the Atlas programer failed to act upon the guidance-generated BECO command. A rerun of this test was conducted successfully. After the Quad Tanking Test, the programer was removed from the vehicle and sent to GD/C, San Diego, for failure analysis. The second discrepancy occurred during LH_2 tanking when the C-1 pump inlet temperature would not meet the temperature requirements. The probable cause of this discrepancy was the hydrogen recirculation line. The

[redacted]

count was resumed at 0904 EST and, after several recycles between T - 5 minutes and T - 0, a simulated T - 0 occurred at 1000 EST. Other than the two major airborne equipment discrepancies, the results of the test were satisfactory.

PARTIAL TANKING TEST

A partial tanking test was conducted on July 29. The purpose of the test was to verify the fix of the hydrogen recirculation line by confirming the presence of LH_2 at the C-1 pump inlet. The tanking consisted of 28 percent Centaur LO_2, 58 percent Centaur LH_2, and no propellants loaded in the Atlas. Liquid temperatures were not indicated at the pump inlet during LH_2 loading, but were indicated $5\frac{1}{2}$ minutes after the start of LHe chilldown of the Centaur main engines. The test was completed with satisfactory results.

FLIGHT ACCEPTANCE COMPOSITE TEST

The Flight Acceptance Composite Test (FACT, ref. 3) is conducted to verify that the combined Atlas-Centaur-Surveyor dynamic model system is capable of operation with no detrimental interference when subjected to conditions simulating flight.

The FACT was conducted on July 28, beginning at 0905 EST. At T - 35 minutes a test to ensure that the Atlas inverter could be started and transferred to internal power was initiated. During the inverter start, trouble with a ground power supply was experienced and corrected. Subsequently, a second inverter start test was successfully performed. The test was resumed and proceeded normally with T - 0 occurring at 1226 EST. Other than the power supply problem, the test was completed with satisfactory results.

A second FACT was conducted on August 5. The purpose of the test was to check out the new Atlas programer that replaced the one that failed to start during the CRT test conducted on July 31. Prior to the start of the second test, the Atlas inverter was replaced because of the problems that were encountered during the first FACT. The test was satisfactorily accomplished.

COMPOSITE READINESS TEST

The Composite Readiness Test (CRT; ref. 4) is conducted to revalidate and verify the proper operation of the vehicle and GSE electrical systems.

The CRT was conducted on July 31. The test began at 1335 EST and proceeded until T - 5 minutes and 30 seconds at which time Atlas telemetry subsystem 1 was replaced because of a malfunction of two telemetry channels. The count was resumed and proceeded through to T - 0 at which time the count was recycled to T - 5 minutes because the second Atlas programer failed to start. The count was resumed and proceeded to the end of the test with a manual programer start and T - 0 occurred at 1559 EST. After the test, the programer was removed

and sent to GD/C, San Diego, for failure analysis.

A second CRT was conducted on August 6. The test was performed with satisfactory results.

LAUNCH

The first attempt to launch AC-6 was made on August 10 at ETR Complex 36B. The launch attempt was aborted at T - 1 minute because the Centaur destruct unit failed to arm. A recycle was started that enabled the second launch attempt to be conducted on August 11. The vehicle lifted off from ETR Complex 36B at 0931:04 EST. The vehicle systems performed nominally and injected the Surveyor dynamic model into a simulated lunar transfer orbit.

WEATHER

The atmospheric conditions on launch day were favorable, and permitted good photographic coverage. The cloud cover was from 20 percent between 20 000 to 40 000 feet to 80 percent between 250 000 to 300 000 feet. Surface winds ranged from 6 to 8 knots with visibility of 10 miles and a temperature of 84° F. Altitude variation of atmospheric pressure, temperature, and wind velocity component is presented in figures V-1 and 2.

LAUNCH ON TIME

The AC-6 launch and launch attempt demonstrated two important launch-on-time factors essential to the development of a capability to adjust to unknown factors that could cause the miss of a launch window. These factors were (1) the capability to preplan a countdown operation and execute the countdown to achieve a precise vehicle lift-off time and (2) the ability to turn around in 24 hours after an abort of a launch attempt.

The Atlas-Centaur AC-6 was launched on August 11, 1965, at 0931:04 EST, which was 4 seconds after the window-opening time. The ETR range countdown was scheduled for 280 minutes with preplanned holds of 60 and 40 minutes at T - 90 and T - 5 minutes, respectively. The countdown was successful thus demonstrating the ability to launch on time.

The launch attempt on August 10, 1965, was aborted after the countdown reached T - 1 minute and 35 seconds because the Centaur Range Safety Command system failed to arm. The vehicle was detanked, and preparations were made to attempt a launch on the following day. The second launch attempt was successful thus demonstrating the ability to turn a vehicle around and launch within a 24-hour period.

AC-6 PRELAUNCH HISTORY - 1965

Arrival of Atlas 156D	May 14
Arrival of interstage adapter	May 14
Arrival of payload	May 14
Erection of Atlas 156D	May 18
Erection of interstage adapter	May 19
Arrival of Centaur 6C	May 25
Erection of Centaur 6C	May 27
Arrival of insulation panels	June 1
Arrival of nose fairing	June 14
Erection of insulation panels	June 15
Encapsulation of payload	July 8
Mating of encapsulated payload	July 9
Quad tanking	July 13
Flight Acceptance Composite Test 1	July 28
Demating of payload	July 28
Partial tanking test	July 29
Mating of payload	August 1
Flight Acceptance Composite Test 2	August 5
Composite Readiness Test	August 6
Attempted launch	August 10
Launch	August 11

[redacted]

IV. MECHANICAL GROUND-SUPPORT EQUIPMENT AND FACILITIES

SUMMARY

All mechanical ground-support equipment and facility equipment functioned satisfactorily during the launch countdown. Minor problems, consisting of a failed hydrogen storage tank vent stack igniter and a possible leaking Centaur LO_2 flow-control valve were encountered.

PROPELLANT-LOADING SYSTEM

Performance of the propellant-loading system was satisfactory throughout the countdown with only two minor problems encountered. The hydrogen storage tank vent stack igniter failed at approximately T - 200 minutes. It was decided, with Range Safety concurrence, to continue the countdown without the burner. At approximately T - 60 minutes it was reported that the Centaur LO_2 loading flow-control valve leaked LO_2 into the Centaur tank. It was speculated that the valve may not have been in a fully closed position when the storage tank transfer pressure was raised to 145 psig.

LH_2 Systems

The liquid-hydrogen transfer system consists of a vacuum-jacketed LH_2 storage tank, a vaporizer for transfer pressure, a flow-control unit, and a vacuum-jacketed transfer line. The system delivers LH_2 at an approximate rate of 750 gpm. Gaseous helium is used for purging the transfer and storage-tank vent lines before and after tanking. The storage tank is pressurized to 12 psig for chilldown and 38 psig for transfer. On the AC-6 launch, however, the maximum transfer pressure achieved was 29.2 psig. This anomaly had also occurred on quad tanking but not on subsequent testing. This pressure, however, was adequate for LH_2 transfer.

LO_2 Systems

The LO_2 transfer system consists of a 38 000-gallon storage tank, a vaporizer for transfer pressure, a flow-control unit, and a topping system with an LN_2 subcooler. The system performed satisfactorily with the only anomaly being the Centaur flow-control-valve leakage mentioned previously.

LIQUID-HELIUM CHILLDOWN

Liquid-helium chilldown was initiated at T - 23 minutes. The LHe flow-

[redacted]

control and line-dump valves are both opened for chilldown. When the dump-valve temperature reaches -200° F, it is closed. C-1 and C-2 pump temperatures are controlled by the flow-control valve and a -310° F temperature is required for both pumps at 15 minutes prior to T - 0. There were no problems in the system, and approximately 180 gallons of LHe were used for pressurizing the storage Dewar, line chilldown, engine chilldown, and depressurizing the Dewar.

PRESSURIZATION SYSTEM

All pneumatic systems performed within required limits as follows:

Primary helium supply:

Minimum - 1500 psig from T - 90 minutes to engine start
Actual - 4500 psig

Emergency helium supply:

Minimum - 3500 psig from T - 90 minutes to engine start
Actual - 5000 psig

Routine GN_2 supply:

Minimum - 2300 psig from T - 90 minutes to engine start
Actual - 4500 psig

Environmental GN_2 supply:

Minimum - 900 psig from start of Centaur tanking to launch
Actual - 1900 psig

UMBILICAL BOOMS

This was the first Centaur launch to use horizontal swing booms. This system consists of one upper and one lower boom that are swung in opposite directions by separate hydraulic rotary actuators. Boom rotation is actuated by solenoid firing valves that are energized by the 2-inch motion signal. The lower boom rotation starts 0.25 second later than the upper boom as a result of a time-delay relay in the lower-boom firing circuitry.

Upper Boom

The upper boom has four electric umbilical plugs, the GH_2 vent line, and the Surveyor and Centaur air-conditioning ducts. The umbilical plugs are electrically ejected at approximately T - 4 seconds with a lanyard backup in the event of failure of the electric ejectors. This lanyard is retracted by a hydraulic cylinder. The upper boom rotation times are given in the following table:

Degrees from rest	Time, sec	Required time, sec
3	T + 0.53	Prior to T + 1.50
21	T + 1.50	Prior to T + 3.00
50	T + 3.89	Prior to T + 4.70

The lanyard cylinder retraction started at T - 2.75 seconds and completed its stroke in 0.80 second. The required timing is between 0.80 and 0.96 second.

Lower Boom

This boom supports the LO_2 and LH_2 transfer lines, the aft pneumatic panel lines, LH_2 and LO_2 fill and drain valve actuation and purge lines, the T - 0 electric umbilical, the insulation-panel purge-bottle charge line, and the interstage-adapter air-conditioning duct.

This boom has two lanyard cylinders, one for the T - 4 umbilicals and one for the T - 0 umbilicals. In most cases, these lanyards act as a backup for the primary disconnect mechanism (electric, pneumatic, or static lanyard). The T - 4 cylinder stroke started at T - 3.05 seconds and stopped at T - 1.78 seconds well within the 1.20- to 1.60-second requirement. The T - 0 cylinder stroke started at T + 0.20 second ending at T + 1.02 seconds or 0.82 second total. The required time is between 0.80 to 0.96 second. The lower boom rotation times are presented in the following table:

Degrees from rest	Time, sec	Required time, sec
13	T + 1.42	Prior to T + 1.7
35	T + 2.63	Prior to T + 3.2
55	T + 3.82	Prior to T + 4.4

ENVIRONMENT CONTROL SYSTEM

The environmental control system provided the required air-conditioning supply temperatures and flow rates to the vehicle, except for the flow to the interstage adapter. After the launch it was discovered that the orifice plate was installed backwards in the test tool used to set the flow rate to the interstage adapter. Tests run on October 8, 1965 showed that reversing the orifice plate causes a 25-percent error in calculated flow rate. Consequently, flow rate to the interstage adapter during the countdown exceeded the specified upper limit of 178 pounds per minute.

Air-conditioning-system performance during the launch countdown, from the start of LO_2 tanking until lift-off, was as follows:

Payload:

Requirements - 85°±5° F; 75±3.5 lb/min
Actual - 84° to 85° F; 74 lb/min
(temperature measurement at disconnect, landline measurement number CN1560T; ref. 5)

Centaur electronic compartment:

Requirements - 48°±5° F; 79±4 lb/min
Actual - 47° to 49° F; 82 to 73 lb/min
(temperature measurement in duct on umbilical tower, CN1191T).
From 08:00 EST until lift-off, pressure oscillations of as much as ±3 in. of water occurred in the ducts, at about 6-min intervals. Flow rates noted are based on mean pressure values.

Interstage adapter:

Requirements - 137.5°±7.5° F; 164±14 lb/min
Actual - Temperature at start of LO_2 tanking was 120° F and rose to 130° F in 25 min. During the remainder of the countdown, temperature rose slowly to a maximum of 134° F at lift-off (temperature measured in duct on umbilical tower, CN1274T). Temperature measured at the disconnect (CN1557T) was 5° to 6° F lower than CN1274T. Flow rate was 195 lb/min.

Atlas pod:

Requirements - 50° F maximum; 32 lb/min minimum
Actual - Temperature rose from 46.5° F at start of LO_2 tanking to 49.4° F at lift-off (temperature measured in duct at base of umbilical tower, AN1342T). Flow rate was between 40 and 41 lb/min.

Atlas thrust section:

Requirements - Over the range from 60 to 80 lb/min, minimum temperature ranges from 180° to 147° F.
Actual - Temperature rose from 165° F at start of LO_2 tanking to 170° F at T - 5 min. After switch-over to GN_2, temperature dropped to 169° F. Flow rate was 84 lb/min until T - 5 min and dropped to about 77 lb/min after switch-over to GN_2.

The air-conditioning GN_2 supply was supplemented by operation of the LN_2 vaporizer at Complex 36A, from 03:00 to 09:31 EST. This accounts for consumption of 2250 gallons of LN_2 from the Complex 36A Dewar.

The available and consumed quantities of the propellants and gases and their usage are given in table IV-I.

TABLE IV-I. - PROPELLANT AND GAS USAGE

Propellant or gas	Usage	Available	Consumed
GN_2	Routine use, scf	121 000	33 200
	Air conditioning, scf	1 555 000	490 000
	LN_2 tank pressurization, scf	52 200	23 100
	Launcher holddown, scf	13 800	Negligible
GHe	Insulation-panel and engine purge, scf	440 000	111 000
	Primary, scf	95 200	20 100
	Emergency, scf	49 000	15 100
LHe	gal	1 000	180
LO_2	gal	38 100	30 600
LH_2	gal	22 000	12 000
RP-1	gal	15 000	13 400
LN_2	Complex 36B, gal	25 750	3 250
	Complex 36A, gal	15 000	2 250

V. TRAJECTORY

SUMMARY

The Atlas-Centaur AC-6 vehicle, targeted for a September 28 launch opportunity, was launched on time August 11, 1965 at 0931:04.430 EST. The flight was so near nominal that the transfer orbit of the Surveyor model passed through the "paper moon" without the need of a midcourse correction. To place the payload in the desired target area on the lunar surface would have required a midcourse correction of only 4.25 meters per second. The booster launch vehicle exhibited the characteristic lofted trajectory profile, which has been observed in the previous flights (ref. 6). To account for this anomaly, a new drag model, which draws on flight observations as well as on wind-tunnel data, has been adopted. Most significant, aside from yielding a more satisfactory acceleration history, the new model reveals a substantial gain in payload capability for operational Surveyor flights. The Atlas sustainer engine operated with 1.6 percent higher specific impulse and 2.3 percent higher thrust levels than nominal. A further look at the engine model simulations may be suggested by this finding. Centaur engine specific impulse, though above acceptance test levels, was well within the three-sigma deviation of that predicted. The guidance system properly compensated for the "hot" booster and targeted to the proper injection conditions.

INTRODUCTION

Trajectory Definition

There are two main purposes for a postflight trajectory analysis effort. The first is to verify or improve the preflight trajectory simulation technique and thus to increase confidence in the FPR and payload capability calculations for operational flights. The second purpose is the determination of the best estimate of the actual vehicle performance. The analysis was performed first by comparing the preflight prediction with the observed trajectory and, second, by reconstructing the flight using the computer simulation.

The preflight or predicted trajectory was determined with the ground rules and weights of reference 7 and for the actual time of launch using a computer trajectory program. For trajectory evaluation, a guidance-based trajectory (GET) was accepted as the best estimate of the actual trajectory. Normally, the best estimate of trajectory (BET) consists of ground-based tracking data, which are received from AFETR in the form of position, velocity, and acceleration components. The reconstruction program, which was used as part of the trajectory analysis, required a smooth set of tracking data for matching. The GET data were found to be more consistent and smoother than the BET data. During the

first 20 seconds of flight, the ETR determined BET data were of poor quality because of the absence of optical tracking. Beyond T + 620 seconds, the noise level of the BET became excessive, because the range of the Glotrac, a high-precision tracking system, was exceeded at this time. After the loss of Glotrac, the three-sigma deviations of the tracking position and velocity components were one and two orders of magnitude, respectively, greater than prior to its loss. Even within the intermediate period between T + 20 and T + 620 seconds, the smoother GET provided a better opportunity to study trends and patterns in the component differences (residuals) of the actual and reconstructed trajectories.

The trajectory was reconstructed with the same computer program used to determine the preflight predicted trajectory. Performance and steering parameters were adjusted until the computed position and velocity components best matched the GET components in a weighted least-square sense. The adjusted values of the Atlas performance and steering parameters differed little for BET versus GET. However, the noise in the residuals was lower, and the selection of data points to be matched along the trajectory was less subjective with the smoother GET. The residuals, which resulted from the least-square match, were subjected to further investigation to determine changes in the model needed for a more satisfactory match and thus for a better simulation of the actual flight.

Rawinsonde Atmosphere Data

Atmospheric conditions and wind profiles at the time of launch are necessary for a proper postflight reconstruction. Launch conditions were determined at the site at 0940 EST, approximately 3 minutes after lift-off. Profiles of these measured temperatures and pressures as a function of altitude are compared with those assumed for the preflight trajectory (fig. V-1(a)). Only slight variations were evident between the measured and preflight values. Rawinsonde launch winds are presented in figure V-1(b). Zero magnitude winds, in lieu of light winds normal for September, were used in the preflight simulation of AC-6. The measured east-west components below 40 000 feet, where aerodynamic forces are most prevalent, agreed well with the preflight estimates; however, the north-south components in the same altitude region were approximately 20 feet per second out of the south. This wind, for an otherwise nominal flight, would have tended to bias the trajectory to the left of predicted. The presence of winds also affected the angle of attack throughout booster operation, as discussed in section IX, VEHICLE STRUCTURES AND SEPARATION SYSTEMS. Above an altitude of 40 000 feet, the winds have much less effect on the trajectory.

Comparisons of profiles of dynamic pressure q and Mach number M of the preflight simulation with the profiles derived from Rawinsonde data and the observed trajectory are presented in figure V-2. Both q and M from T + 60 to T + 120 seconds were higher for the actual than for the preflight predicted trajectory. It is noteworthy that this time corresponds to the interval of highest drag, and also that values of q and M higher than those predicted were seen on earlier Atlas-Centaur flights through this time interval.

Telemetry and Other Measured Data

The preflight trajectory, as previously mentioned, was determined for nominal or predicted conditions. Variations in any actual condition, which may cause a change in the trajectory, should be incorporated, when possible, in the postflight reconstruction. The measured atmosphere and winds are included. The best estimate of the actual propellant and hardware weights were used in the reconstruction and are compared in table V-I with those of the preflight. Actual histories of several parameters, which affect engine operation and which are variables of the propulsion models, were obtained from telemetry data. The operation of the Atlas engines was simulated by a computer-programed detailed propulsion model (DEPRO), which includes effects due to ambient pressure, propellant densities, and pump inlet pressures and to operation of the sustainer propellant-utilization (PU) system.

Ambient pressure was determined as a function of altitude from the launch atmosphere profile. The density of RP-1 was fixed at its launch time value of 50.38 pounds per cubic foot; that of LO_2 was calculated from telemetry temperature-pressure data. Propellant-tank ullage pressures, which are used in DEPRO to determine pump inlet pressures, and the history of sustainer PU valve position were other telemetered data used in the reconstruction.

The telemetered inlet temperatures and pressures and the PU valve position for the two Centaur engines were used in the Pratt & Whitney (P & W) Regression equations to determine variations of the thrust and specific impulse of the engines. Because the telemetry history of the LH_2 inlet temperature for the C-1 engine was not acceptable, it was replaced by the LH_2 temperature history of the C-2 engine in the reconstruction.

Time histories of vehicle thrust attitude in pitch and yaw, relative to the launch inertial reference coordinate system, were derived from the telemetered values of the time integrals of the three guidance system accelerometers. These attitude histories were used to steer the vehicle during the guided portion of the postflight reconstruction in lieu of the guidance equations. Experience with the reassembly of AC-4 showed that a guidance simulation distorted the iteration process of the reconstruction. The guidance equation corrected for performance dispersions that had been introduced by the adjusting procedure used to search for the best performance values. Use of guidance-derived attitudes avoided this distortion.

RESULTS

Trajectory parameters are presented in table V-II for the predicted, observed, and reconstructed trajectories. A detailed trajectory listing is presented in appendix C. The observed and reconstruction values are in good agreement with each other and are in fair agreement with the predicted values. Another indication that the actual flight was near that desired is that the injection orbit elements (table V-III) are in reasonable agreement. The actual values were determined from 48 hours of spacecraft tracking by JPL. Based on these observations, a midcourse correction of only 4.25 meters per second would have been required to impact in the desired lunar target area. This is well within the projected capabilities of the AC-7 spacecraft, the first Surveyor that will attempt a midcourse maneuver and soft lunar landing.

Values of vehicle performance were obtained from the trajectory reconstruction. In order to achieve a satisfactory fit of the observed trajectory, a modified aerodynamic drag model was used. A more detailed discussion of this model and its significance is presented later in this section. The reconstruction, as mentioned previously, was performed by adjusting vehicle performance and attitude parameters until the reconstructed trajectory best matched the observed velocity and position components in a weighted least-square sense (ref. 6). Prior to the reconstruction of the flight, several observations regarding the trajectory were apparent. As shown in figure V-3, the actual trajectory was to the right of and slightly lofted above the preflight profile. The bias to the right would appear to be a launch azimuth difference. The lofted trajectory had been the trend observed on previous Atlas-Centaur flights. Discrepancies in velocity (fig. V-4) and thrust acceleration (fig. V-5) indicated that there had also been greater-than-predicted acceleration during the booster phase. Both the lofted trajectory and the high thrust accelerations can result from better-than-predicted booster performance and/or a variation of the flight aerodynamic drag characteristics from those predicted. The study of a similar phenomenon on the AC-4 flight indicated that a discrepancy in the drag characteristics was the principal cause (ref. 6). This anomaly for AC-6 is discussed later in more detail. Velocity and thrust acceleration comparisons (figs. V-4 and 5) indicated performance other than the predicted performance during sustainer solo and Centaur phases. During sustainer solo operation, the differences, in part, can be attributed to the shift in BECO time for the predicted and actual flights.

For the reconstruction, five attitude factors were tuned during the Atlas phase of the reconstruction: (1) attenuation factor on the nominal booster pitch-rate profile, (2) initial pitch-over azimuth, (3) initial pitch attitude from T + 0 to T + 15 seconds, (4) and (5) attenuation factors on the sustainer pitch and yaw guidance-derived-attitude histories. In addition, the thrust and specific impulse levels, that is, reference values, of the booster and sustainer engines, and the effective time of BECO, were modified for the trajectory match. It should be noted that engine transient models, such as the booster engine decay model, were used in the reconstruction. Consequently, any deviation between the predicted booster engine shutdown model and the actual shutdown transient would be compensated for by a shift in the computed time of BECO. During Centaur phase, thrust and specific impulse of the engines were adjusted. Again, to compensate for any discrepancies in either the Centaur engine buildup model or the sustainer engine decay model, an effective time of MES was determined. Attenuation factors on the Centaur pitch- and yaw-attidude histories and constant drift rates in pitch and yaw completed the list of adjusted parameters for the Centaur reconstruction.

Atlas Parameters

The adjusted and the preflight propulsion parameters are presented in table V-IV. Preflight reference values and the reconstruction reference values of the propulsion model are compared. Additionally, specific inflight values, which are tabulated at T + 2 seconds for the Atlas and T + 300 seconds for the Centaur, are compared. These latter data show not only the difference in reference performance, but also the effect of deviations from predicted engine inlet conditions and PU valve histories.

Specific impulse and thrust of the engines were determined with the reference booster mixture ratio fixed at the preflight reference value. The adjusted reference specific impulse of the booster engines was slightly less (-1.3 percent) than the standard reference value, while engine thrust value maintained a near nominal value, up only 0.4 percent. Reference values of sustainer performance required larger adjustments. Increases in reference thrust and specific impulse of 2.3 and 1.6 percent, respectively, were needed. These adjustments were significantly greater than the three-sigma deviations of this engine and therefore were of concern. A similar increase in specific impulse was obtained over near-constant thrust regions of sustainer solo operation, when the slope-impulse technique (ref. 6) was applied to the reciprocal of guidance-based thrust accelerations. This check, in addition to the relatively small and random thrust acceleration residuals of the reconstruction during sustainer solo (fig. V-6) supports the higher sustainer performance.

An improvement in the match of observed position and velocity components was further attained by adjusting attitude parameters of the trajectory. A cross-range drift to the right by the actual trajectory from the predicted is indicated in figure V-3(c). In order to account for this cross-range drift, the initial roll to pitch-over azimuth was adjusted. The actual pitch-over azimuth was determined as 94.92°, which is 0.38° greater than that indicated for the launch time. Integration of the telemetered roll rate during the initial 15 seconds after 2-inch motion gave an azimuth of 94.9°, in good agreement with the computed adjusted value. An attenuation factor on booster pitch-rate history was increased 0.5 percent, possibly compensating for step errors in the autopilot or uncorrected drifting of the autopilot. The initial pitch attitude of both the booster and the sustainer steering profiles required minor adjustments to improve the trajectory match.

The final residuals of thrust acceleration, velocity, and position components during Atlas operation are presented in figures V-6(a), 7(a), and 8(a). Except during engine transient times, the velocity residuals were below 3 feet per second, and position residuals were below 60 feet.

Centaur Parameters

The match of position and velocity components during the Centaur phase was not as good as the Atlas match. Reconstruction residuals for this phase are presented in figures V-6(b), 7(b), and 8(b). Maximum velocity and position residuals were approximately 5 feet per second and 200 feet, respectively, except for the last 20 seconds of powered flight. During this portion of the flight, the pseudo-guidance simulation and possible limitation of the engine model may have contributed substantially to the relatively poor fit.

The thrust acceleration residuals (fig. V-6(b)) showed a pattern of error amplitudes that could be correlated with the larger amplitudes of the Centaur PU valve cycle shown in figure 5 of section VII. This correlation is particularly evident between T + 340 and T + 380 seconds, and after T + 660 seconds, at which time it was indicated that the PU valves were at the LO_2-rich limit. This correlation suggests that the PU valve may have, at times, exceeded the limits of

the engine performance model, which had been derived for small variations in inlet conditions and PU valve angle.

The reconstructed Centaur thrust level, derived with the P & W engine model for the measured engine conditions, was less than 1 percent below the acceptance test value (table V-IV). The adjusted reference specific impulse was determined as 435.9 seconds, well within the range of acceptable dispersion. An independent calculation of specific impulse was made with the slope-impulse technique, which requires a constant thrust (the mean of a sinusoidal thrust will satisfy the constant thrust requirement). For this method, a specific impulse of 435.5 seconds, consistent with the reconstruction value, was obtained.

An engine build-up model was derived for the reconstruction from the thrust acceleration history following the Centaur engine ignition signal. To compensate for errors in the engine transient models of sustainer shutdown and main engine startup, the time of the main engine start (MES) signal was adjusted in the reconstruction. The computed MES was 242.63 seconds, approximately 0.14 second earlier than the measured discrete event (table V-II).

As in the Atlas reconstruction, it was necessary to adjust the guidance-based attitude histories used to orient the vehicle in the reconstruction. To reduce the residuals of velocity and position during the Centaur phase, the attitude histories, in pitch and yaw, respectively, were adjusted with attenuation factors of 0.9978 and 0.9976 and with a drift rate of 0.00011 degree per second to the left in the yaw plane and 0.00080 degree per second up in pitch plane.

Aerodynamic (Drag) Models

Reconstruction of the AC-4 trajectory (ref. 6) and preliminary attempts of reconstruction of AC-6 indicated that the standard drag coefficient C_X model did not accurately represent flight axial forces. This preflight model (Model I of fig. V-9) is employed to compute drag simply as the product q, C_X, and the reference area, A.

When this model was incorporated in the AC-6 reconstruction, a large residual pattern resulted during the high-dynamic-pressure (q) period of the flight from T + 60 to T + 110 seconds (fig. V-10). A similar pattern was observed in the AC-4 reconstruction, and the drag model was believed to be at fault. On the basis of AC-4 results, as well as flight data of other Atlas flights, GD/C formulated a new drag model (Model II of fig. V-9). This model separates the drag into three major components, q-sensitive drag, base force, and holddown force. The q-sensitive drag, with fore body and aft body contributions, is dependent on Mach number, dynamic pressure, and vehicle cross-sectional area. The base force results from recirculation of mass from the engine exhaust jets to the base of the vehicle. The magnitude of this base force is generally determined from flight measurements rather than wind tunnel tests.

The holddown force improves the match of thrust acceleration obtained by optical tracking during the first 10 seconds after 2-inch motion (fig. V-11).

This force is believed to be caused by the restraining forces of the launcher and effects of ground proximity. This force was included as an exponential force decaying from a maximum at lift-off to zero at 10 seconds.

The drag models and their reconstruction acceleration residuals are presented in figures V-9 and 10. The GD/C drag model (Model II) is of the form

$$DRAG_{II} = -4500(1.0 - P_{amb}/P_{sl}) + qAC_{x_{II}} + 41.29(10.0 - t)^{2.3917}$$

where

P_{amb}/P_{sl} ratio of ambient pressure to sea level pressure

A reference area, 78.5 sq ft

C_x standard drag coefficient

t time from lift-off ($0 \leq t \leq 10$), sec

The first expression on the right of the equation gives the base force, with a vacuum value of 4500 pounds; the last term gives the holddown force with a maximum value of approximately 10 000 pounds.

The inclusion of Model II, which greatly improved the trajectory match, still left a residual pattern between T + 60 and T + 80 seconds (fig. V-10). Since the booster engine thrust was increased from 154 000 pounds for AC-4 to 165 000 pounds for AC-6, it could be anticipated that the vacuum base force would increase with the higher jet pressure associated with the uprated engines. Consequently, a third drag model, patterned after the GD/C Model II, was derived specifically for the AC-6 reconstruction. In addition to adjusting the base-force term and the drag coefficients, the initial holddown force was tailored to the optical tracking data (fig. V-11). The resulting drag model (Model III) is of the form

$$DRAG_{III} = -5000(1.0 - P_{amb}/P_{sl}) + qAC_{x_{III}} + 16.516(10 - t)^{2.3917}$$

where $0 \leq t \leq 10$. This model increased the vacuum base force from 4500 to 5000 pounds, readjusted the C_x function (fig. V-9), and reduced the holddown force to 40 percent of that of Model II. The effects on thrust acceleration residuals with this revised model are shown in figures V-10 and 11.

Model III did not significantly change the values of the reconstruction booster performance parameters from those determined by Model II. The thrust increased 0.03 percent, and specific impulse decreased by 0.04 percent for Model III. Sustainer performance showed no change in specific impulse and a 0.05-percent decrease in computed thrust level.

A net payload increase for an operational vehicle, AC-15, of 83 pounds for Model II and 85 pounds for Model III results when the new models replace the standard drag model, Model I. The results of the reconstruction presented in

the tables and figures were obtained with Model III. In summary, Model II, the new standard preflight drag model, yields a good acceleration match for AC-6. This can be further improved as indicated by the results based on Model III; however, the differences in residuals for the two models are small and may be within inherent flight-to-flight variation. Regardless of which model was used, there still existed large residuals in thrust acceleration and velocity during the 10 seconds prior to BECO. These residuals, evident in figures V-6 and 8, suggest the need for further study of the drag and/or propulsion models, if the same patterns of residuals repeat in future flights.

Atlas Propellant Residuals

An indication of the accuracy of the engine performance models is how well they predict the amount of each propellant remaining in the vehicle tanks. Previous reconstructions have indicated that the Atlas propulsion model could be improved by increasing the number of independent variables considered (ref. 8). However, this new model has not been incorporated into the simulations used in this analysis. The current Atlas propulsion model is referred to as the 6 variable DEPRO; the proposed new model (ref. 8) is referred to as the 12 variable DEPRO.

Estimates of the fuel and oxidizer residuals in the Atlas tanks were made on the basis of sensor uncovery times. It was indicated that approximately 294 pounds of RP-1 and 418 pounds of LO_2 remained. The postflight reconstruction, which included simulation of measured sustainer PU valve position that was on the LO_2-rich limit most of the flight, indicated that approximately 490 pounds of RP-1 and 123 pounds of LO_2 were left. Thus, the total residuals were about 100 pounds less than estimated and were accepted as adequate for the purposes of the reconstruction; however, the imbalance between fuel and oxidizer residuals was larger than desired. There is evidence that this may be a result of an inadequacy on the part of the 6 variable DEPRO model.

Using the data of reference 8, which indicated approximately a 0.5-percent decrease in booster mixture ratio when the 12 variable model was used rather than the 6 variable model, showed that the oxidant-fuel ratio of the residuals from the reconstruction could be changed from about 0.25 to 1.92. This value would be in better agreement with the estimated residual oxidant-fuel ratio of 1.42. Consequently, the use of the 12 variable model should yield a better estimate of the propellant residuals. An accurate means of predicting the residuals is needed in preflight simulations, so that the booster engines may be properly orificed and the sustainer PU valve suitably biased prior to flights.

TABLE V-I. - TRAJECTORY ANALYSIS WEIGHT SUMMARY

Weight, lb	Preflight[a] estimate	Postflight estimate	Trajectory reconstruction
Total at lift-off	302 073	303 536	[b]303 536
At BECO (before staging)	79 117	-------	80 529
Booster jettison[c]	7 355	7 354	[b]7 356
Insulation	1 226	1 225	[b]1 225
Nose fairing	1 995	2 005	[b]2 005
Total at separation	44 562	44 833	44 731
Sustainer residual propellant[d]	475	712	613
Sustainer jettison[c]	7 700	7 713	[b]7 710
Centaur and payload at lift-off	39 848	39 892	[b]39 892
Boost-phase Centaur loss:	3 461	3 484	[b]3 484
Oxidant	(126)	(58)	([b]58)
Fuel	(58)	(129)	([b]129)
Hardware and miscellaneous	(3 277)	(3 297)	([b]3 297)
Centaur at separation	36 387	36 408	[b]36 408
Total weight at MECO	6 372	6 474	6 580
Centaur residual propellant:[d]	188	294	400
Oxidant	(107)	(203)	(333)
Fuel (including PU residual)	(81)	(91)	(67)
Centaur jettison	4 084	4 096	[b]4 096
Payload	2 100	2 084	[b]2 084

[a]Based on data of appendix A of ref. 7.
[b]Based on the best postflight weight estimate.
[c]Includes residual lubrication oil and trapped propellant.
[d]Propellant above pump inlet.

TABLE V-II. - TRAJECTORY PARAMETER COMPARISON

Parameter	BECO	Insulation jettison	Nose-fairing jettison	SECO	Separation	MES
Time,[a] sec						
Planned[b]	142.061	172.061	197.061	235.268	237.268	243.768
Actual	141 79	171.62	196.47	234.10	236.22	242.77
Reconstruction	[c]141.879	171.72	196.49	234.39	236.22	[c]242.634
Altitude, n. mi.						
Planned	31.430	47.682	60.261	78.391	79.307	82.178
Actual[d]	31.841	48.324	61.092	79.289	80.277	83.223
Reconstruction	31.893	48.377	61.103	79.426	80.279	83.170
Range, n. mi.						
Planned	42.024	80.056	115.444	177.484	181.019	192.494
Actual	42.271	80.488	116.076	177.921	181.716	193.434
Reconstruction	42.383	80.624	116.106	178.441	181.720	193.200
Relative velocity,[e] ft/sec						
Planned	8073	8861	9680	11 334	11 327	11 280
Actual	8152	8972	9810	11 487	11 483	11 430
Reconstruction	8172	8976	9810	11 496	11 490	11 444
Inertial velocity, ft/sec						
Planned	9313	10 141	10 984	12 664	12 659	12 616
Actual	9390	10 251	11 113	12 817	12 815	12 767
Reconstruction	9410	10 254	11 113	12 827	12 822	12 780
Axial load factor, g's						
Planned	5.700	1.252	1.426	1.378	0.00024	0.00024
Actual	5.69	1.27	1.45	-----	-------	-------
Reconstruction	5.757	1.278	1.454	1.471	.00024	.00024

[a]Time from 2-in. motion (0931:04.430 EST). Planned and reconstruction times refer to the beginning of thrust decay or weight separation. Actual times are taken from table II-I.

[b]All planned values are taken from a simulated trajectory based on ref. 7 and using the actual time of launch.

[c]Effective time compatible with the engine build-up simulation used in reconstruction.

[d]All actual values were determined from corrected telemetry guidance data.

[e]Velocity referenced to a coordinate system fixed with rotating Earth.

TABLE V-III. - SPACECRAFT ORBIT PARAMETERS

Parameter	Predicted[a]	Actual[b]	Reconstruction
Time[c] of epoch, sec	678	679.2	679.32
Inclination, deg	28.59	28.56	28.55
True anomaly, deg	-5.89	-5.76	-5.75
Semimajor axis, n. mi.	229 843.56	224 365.98	224 364.23
Perigee altitude,[d] n. mi.	90.14	90.19	90.94
Apogee altitude,[d] n. mi.	452 708.95	441 753.77	441 749.52
Eccentricity	0.9846	0.9842	0.9842
Period, days	31.989	30.853	30.852
Energy, sq ft/sec^2	-5 039 728	-5 162 766	[e]-5 162 808
Injection conditions			
Latitude, deg	23.034	22.981	22.984
Longitude, deg	307.258	307.449	307.539
Radius, n. mi.	3 543.43	3 543.20	3 543.79
Flight path angle,[f] deg	-3.039	-2.968	-2.966
Azimuth,[g] deg	108.143	108.166	109.249
Relative velocity, ft/sec	34 647.21	34 645.67	34 640.18

[a]Data obtained from Lewis Research Center preflight nominal trajectory.
[b]Data obtained by Jet Propulsion Laboratory from spacecraft tracking.
[c]Time measured from 2-in. motion (from 0931:04.430 EST).
[d]Measured above a spherical 3444-nautical-mile-radius Earth.
[e]Reconstruction trajectory terminated at Jet Propulsion Laboratory determined energy.
[f]Angle between relative velocity vector and local horizontal.
[g]Angle of relative velocity vector measured clockwise from true north.

TABLE V-IV. - PROPULSION PARAMETERS FOR RECONSTRUCTION

Parameter	Reference values			Specific inflight values[a]		
	Standard[b]	Reconstruction	Ratio	Preflight	Postflight	Ratio
Booster						
Thrust (sea level), lb	330 000	331 155	1.0035	325 536	325 232	0.9991
Flow rate, lb/sec	1306.9	1328.3	1.0164	1291.9	1298.7	1.0053
Specific impulse (sea level), sec	252.5	249.3	.9874	252.0	250.3	.9936
Mixture ratio, O/F	2.28:1	2.28:1	1.0000	2.25:1	2.18:1	.9689
Sustainer and vernier						
Thrust[c] (sea level), lb	59 000	60 351	1.0229	58 342	60 332	1.0341
Flow rate, lb/sec	275.2	277.1	1.0069	273.4	275.6	1.0080
Specific impulse (sea level), sec	214.4	217.8	1.0159	213.4	218.9	1.0258
Mixture ratio, O/F	2.27:1	2.27:1	1.0000	2.40:1	2.48:1	1.0333
Centaur						
Thrust (vacuum), lb	29 939.00	29 684.5	0.9915	29 939.0	29 730.9	0.9930
Flow rate, lb/sec	68.904	68.045	.9883	68.904	68.255	.9906
Engine specific impulse (vacuum), sec	434.5	435.9	1.0033	434.5	435.6	1.0025
Vehicle specific impulse[d] (vacuum), sec	434.0	435.4	1.0032	434.0	435.0	1.0024
Mixture ratio (engine), O/F	5.045:1	5.045:1	1.0000	5.045:1	5.086:1	1.0081

[a]For Atlas booster and sustainer, values are for T + 2 sec, for Centaur, values are for T + 300 sec for the corresponding inlet conditions.

[b]The standard reference values used in the reconstruction are the class values for Atlas engines and acceptance test values for the Centaur engines.

[c]Includes total vernier thrust.

[d]Includes 8.72 lb of thrust and 0.103 lb/sec of flow charged to boost pumps.

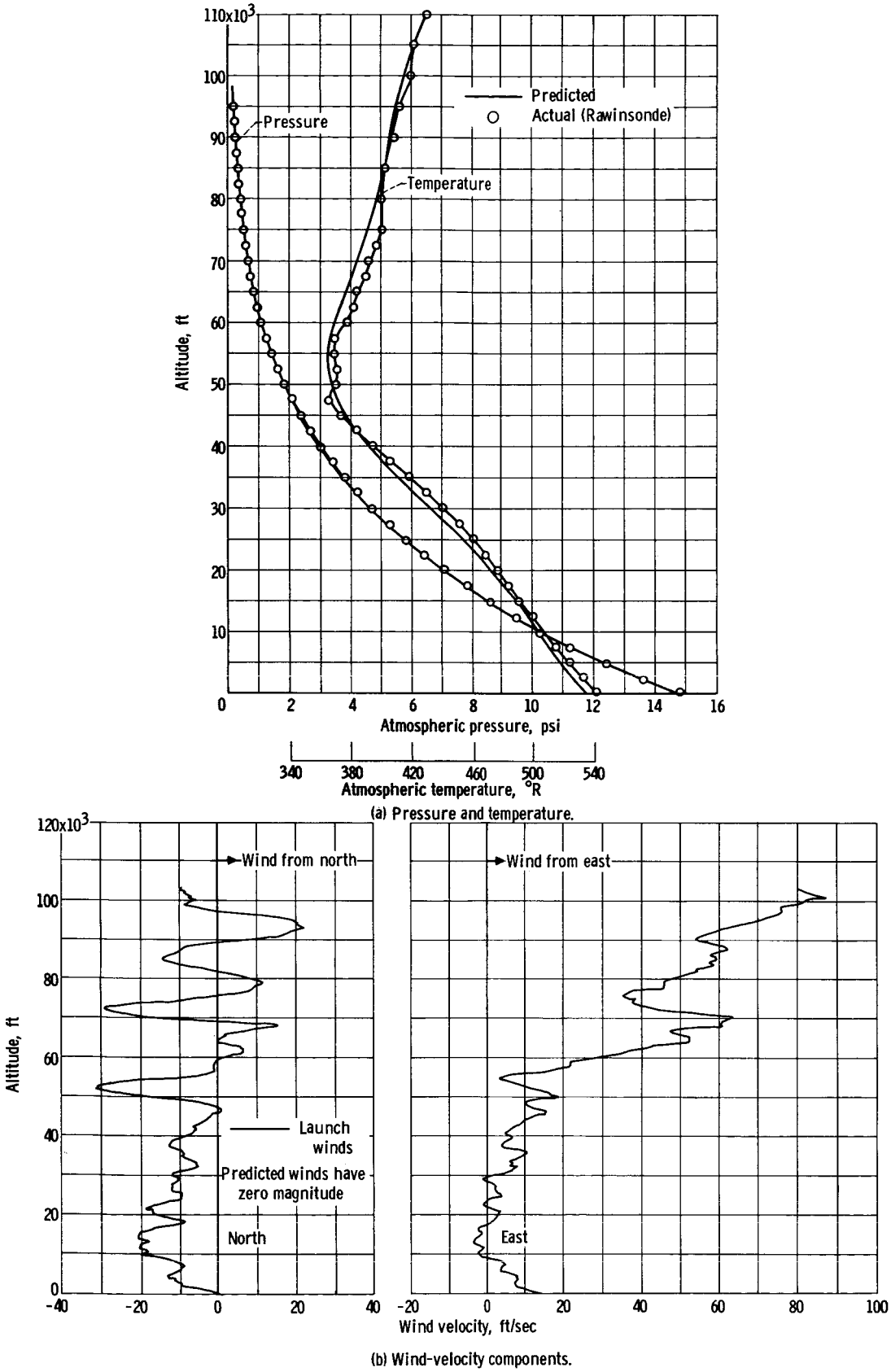

Figure V-1. - Atmospheric conditions at time of launch. Rawinsonde run 997 at 9:40 EST, August 11, 1965.

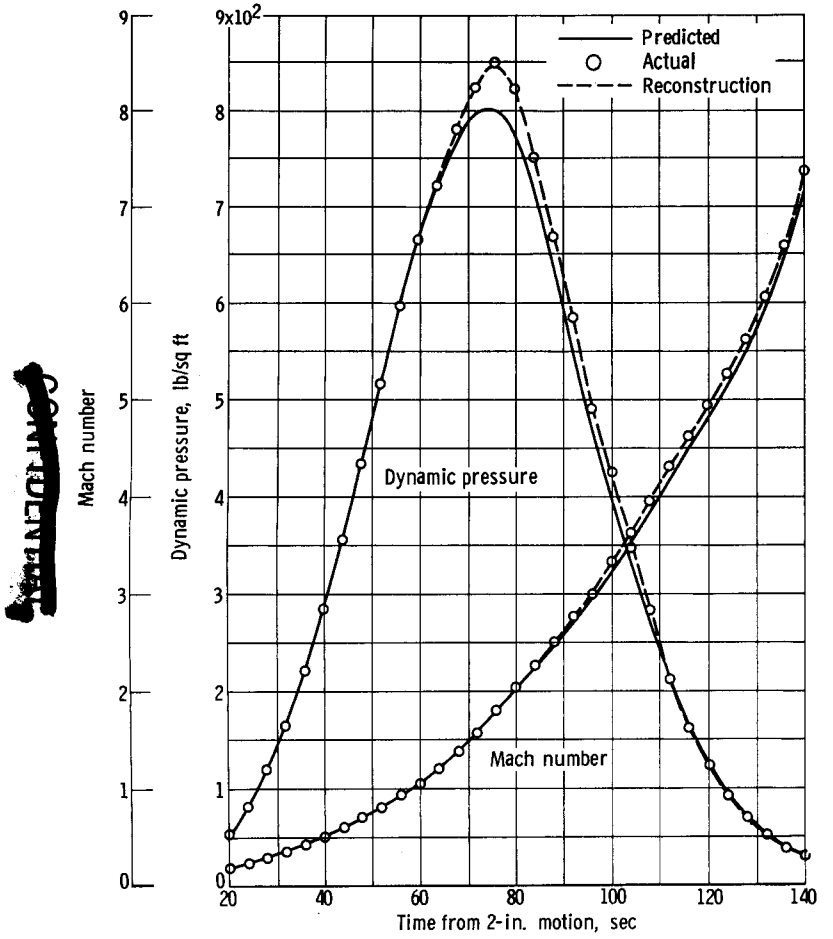

Figure V-2. - Comparison of aerodynamic parameters for AC-6.

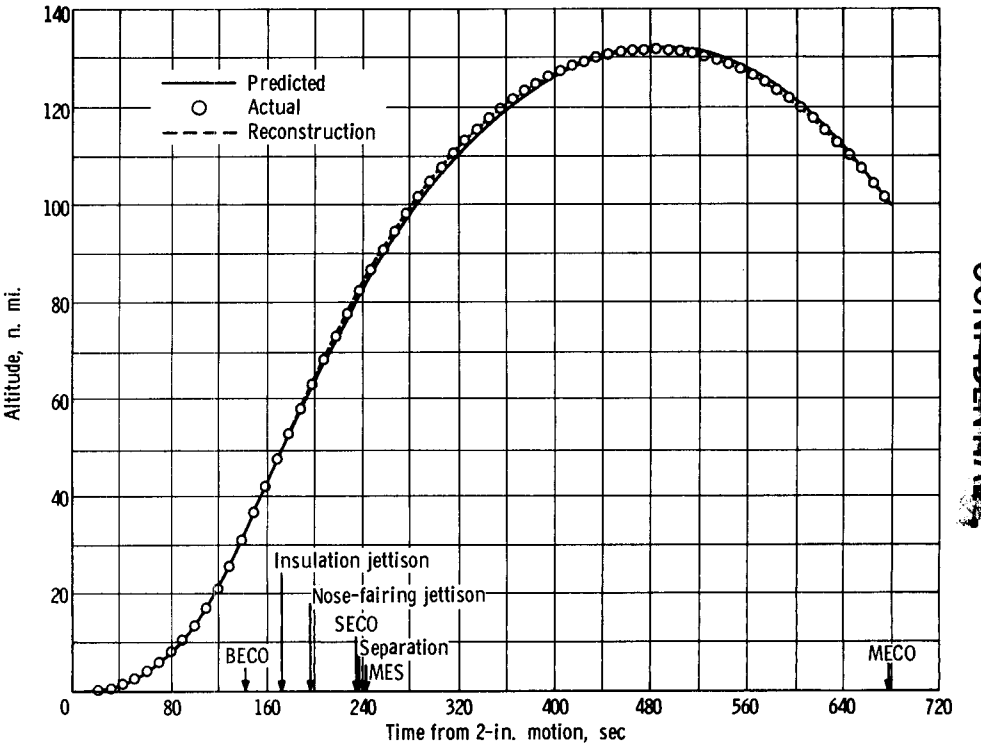

(a) Altitude-time relation.

Figure V-3. - Trajectory position comparison.

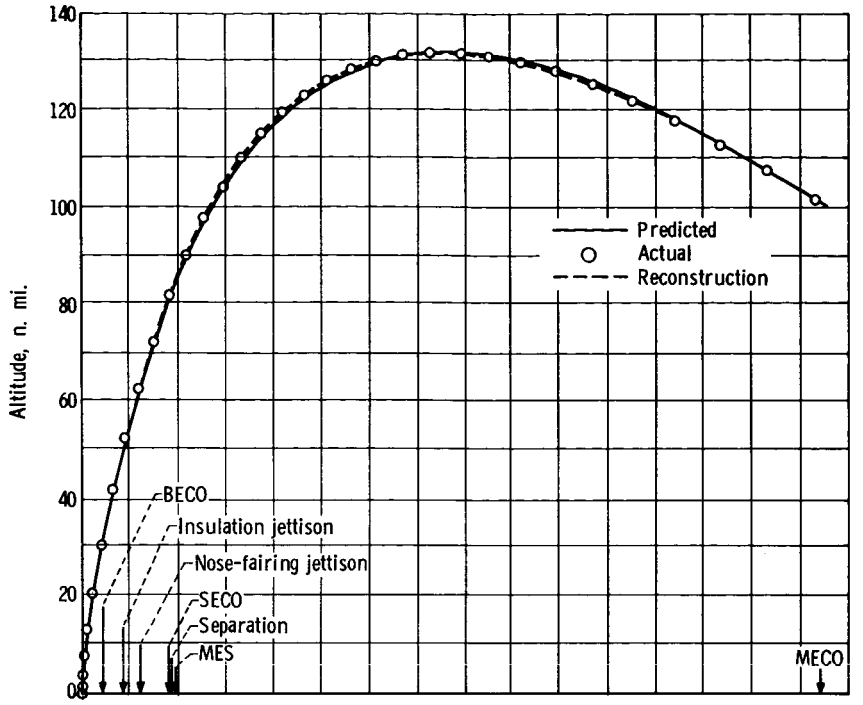

(b) Vertical plane.

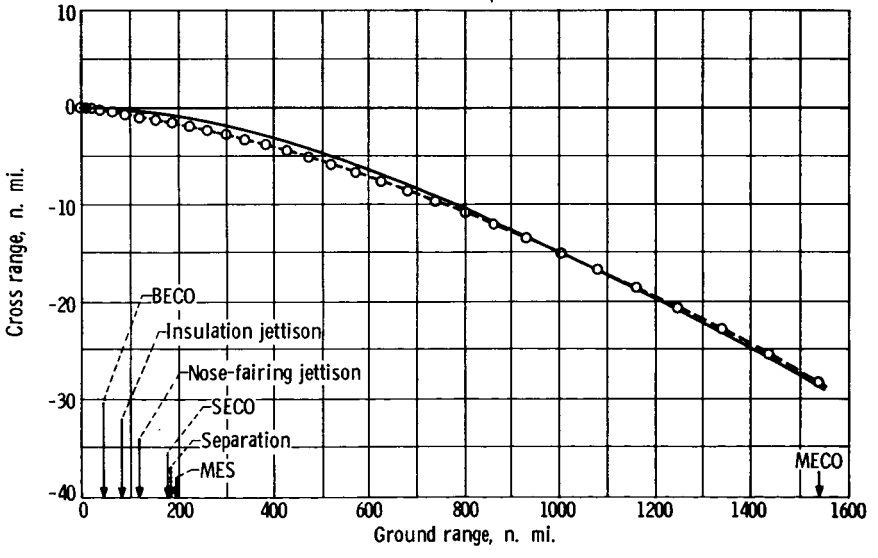

(c) Horizontal plane.

Figure V-3. - Concluded.

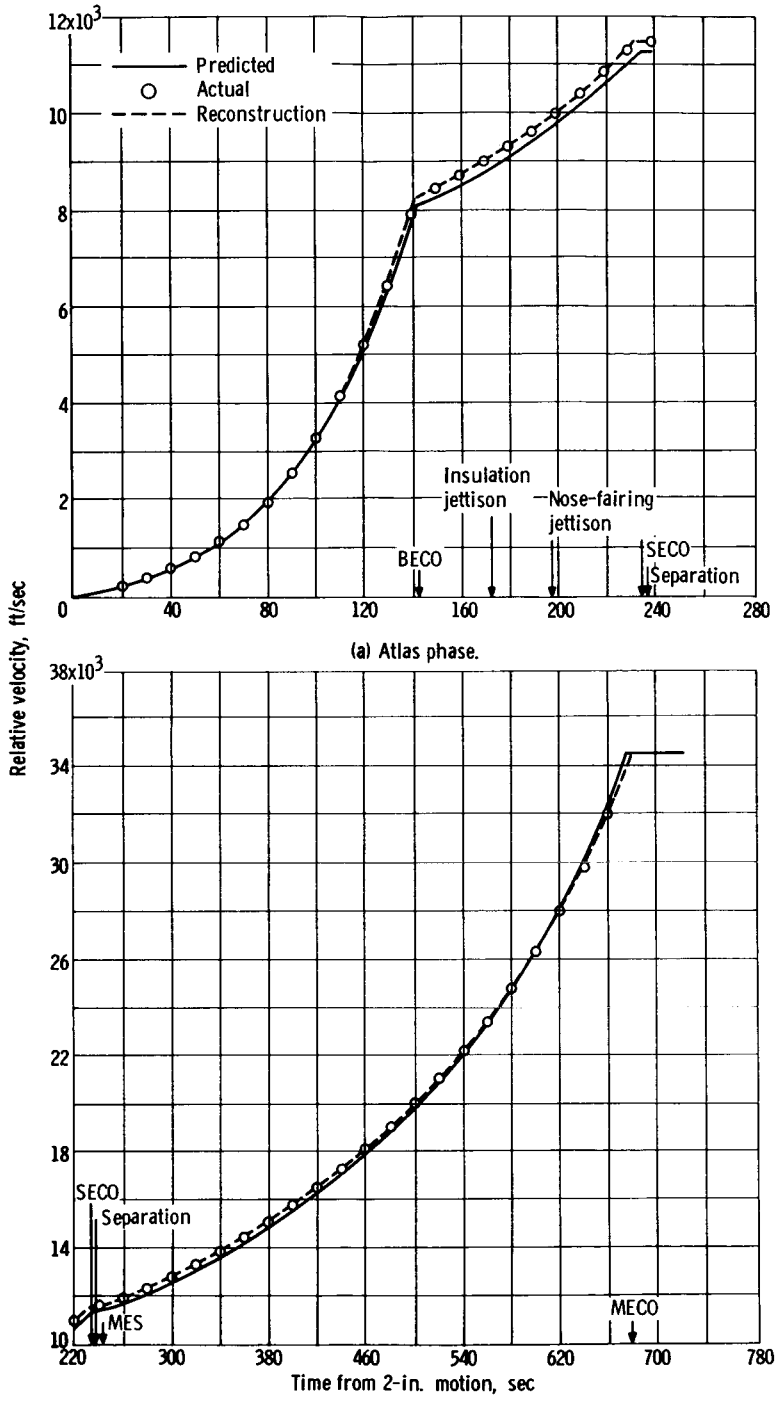

(a) Atlas phase.

(b) Centaur phase.

Figure V-4. - Trajectory comparison. Velocity relative to atmosphere including wind effects.

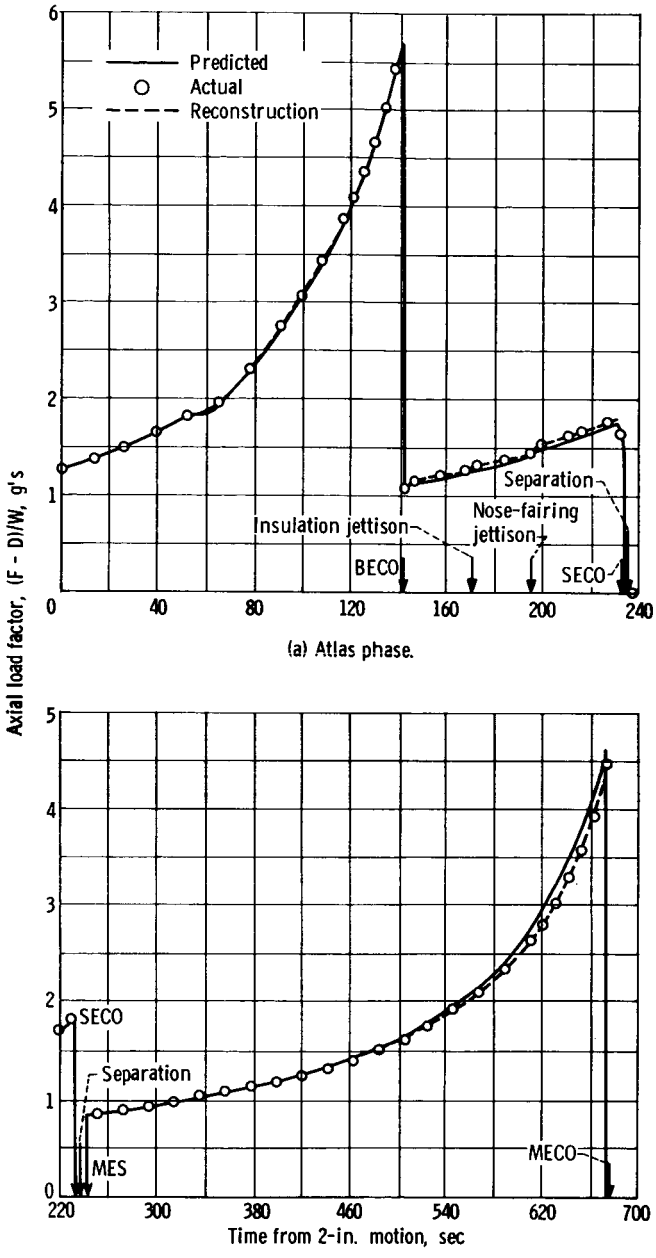

(a) Atlas phase.

(b) Centaur phase.

Figure V-5. - Trajectory comparison. Thrust acceleration (axial load factor).

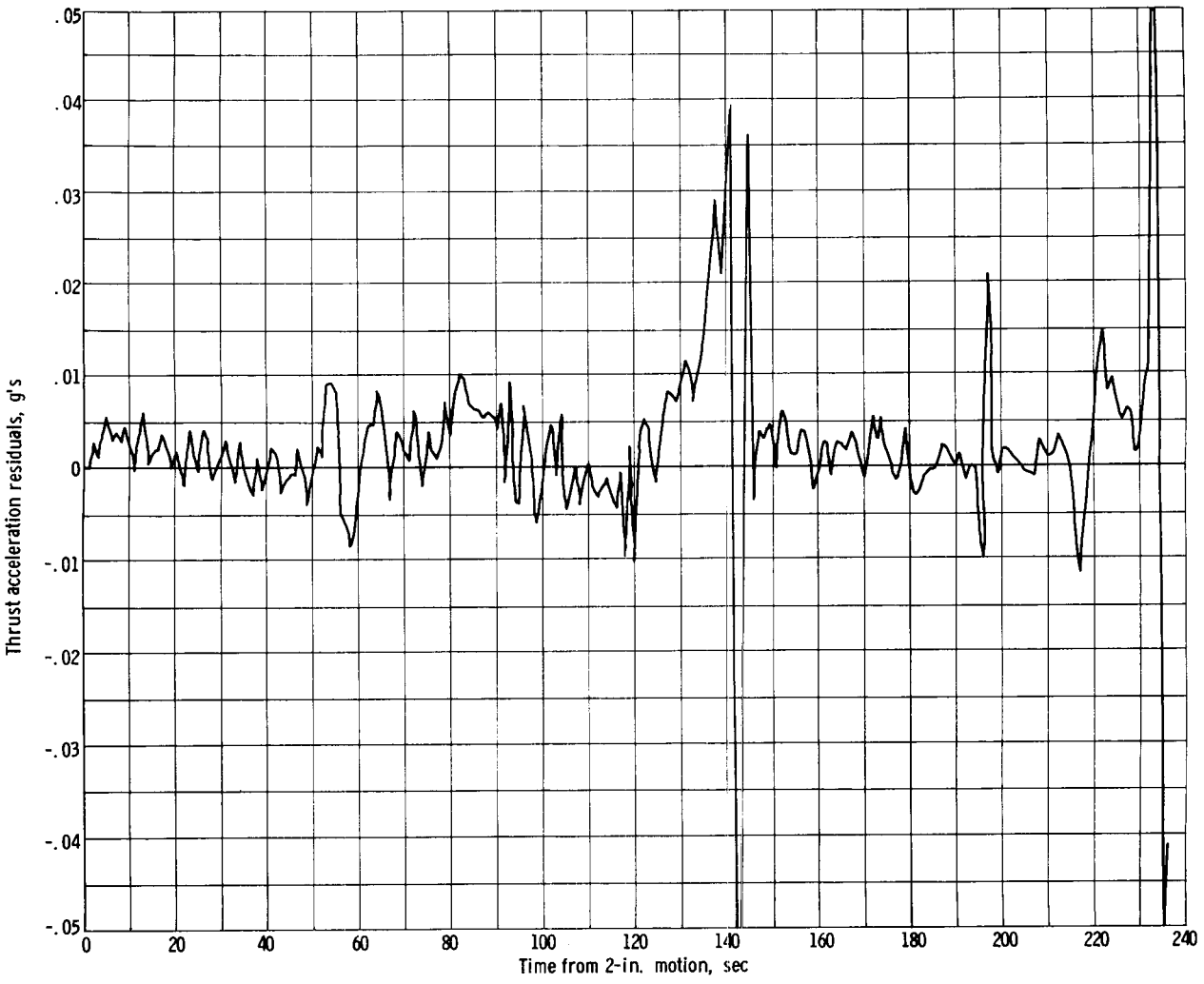

(a) Atlas phase.

Figure V-6. - Thrust acceleration residuals (reconstruction minus GET).

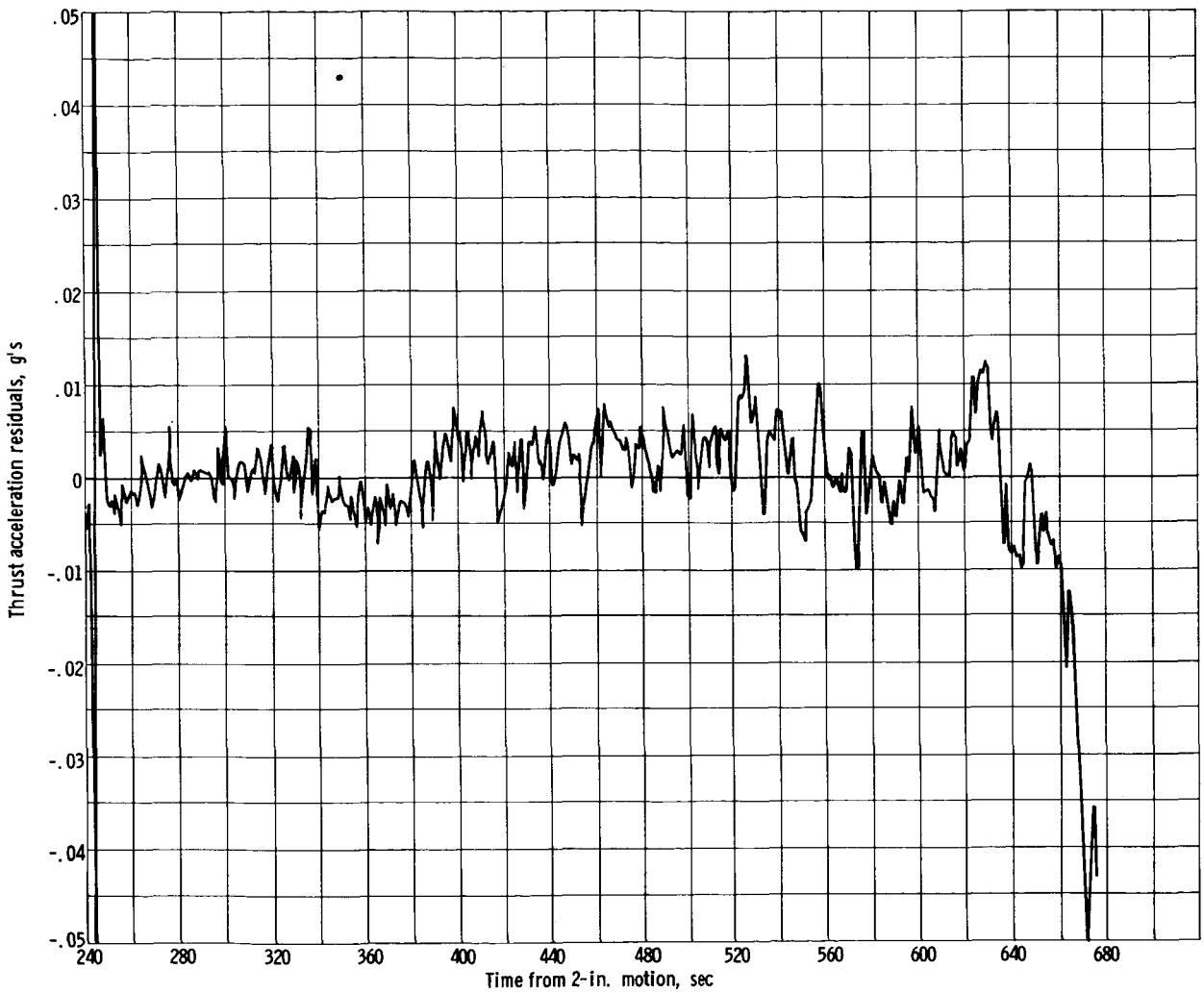

(b) Centaur phase.

Figure V-6. - Concluded.

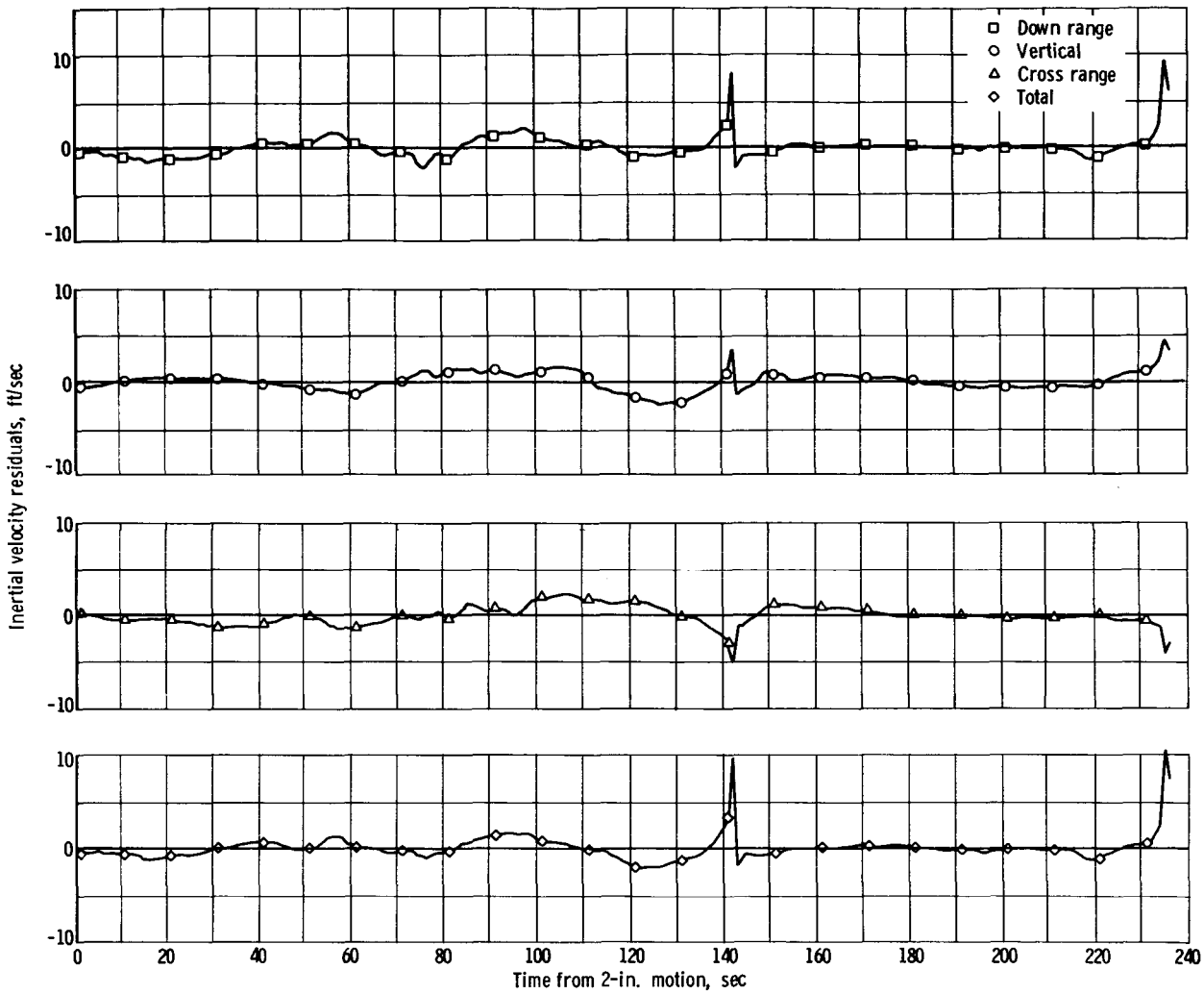

(a) Atlas phase.

Figure V-7. - Velocity component residuals (reconstruction minus GET).

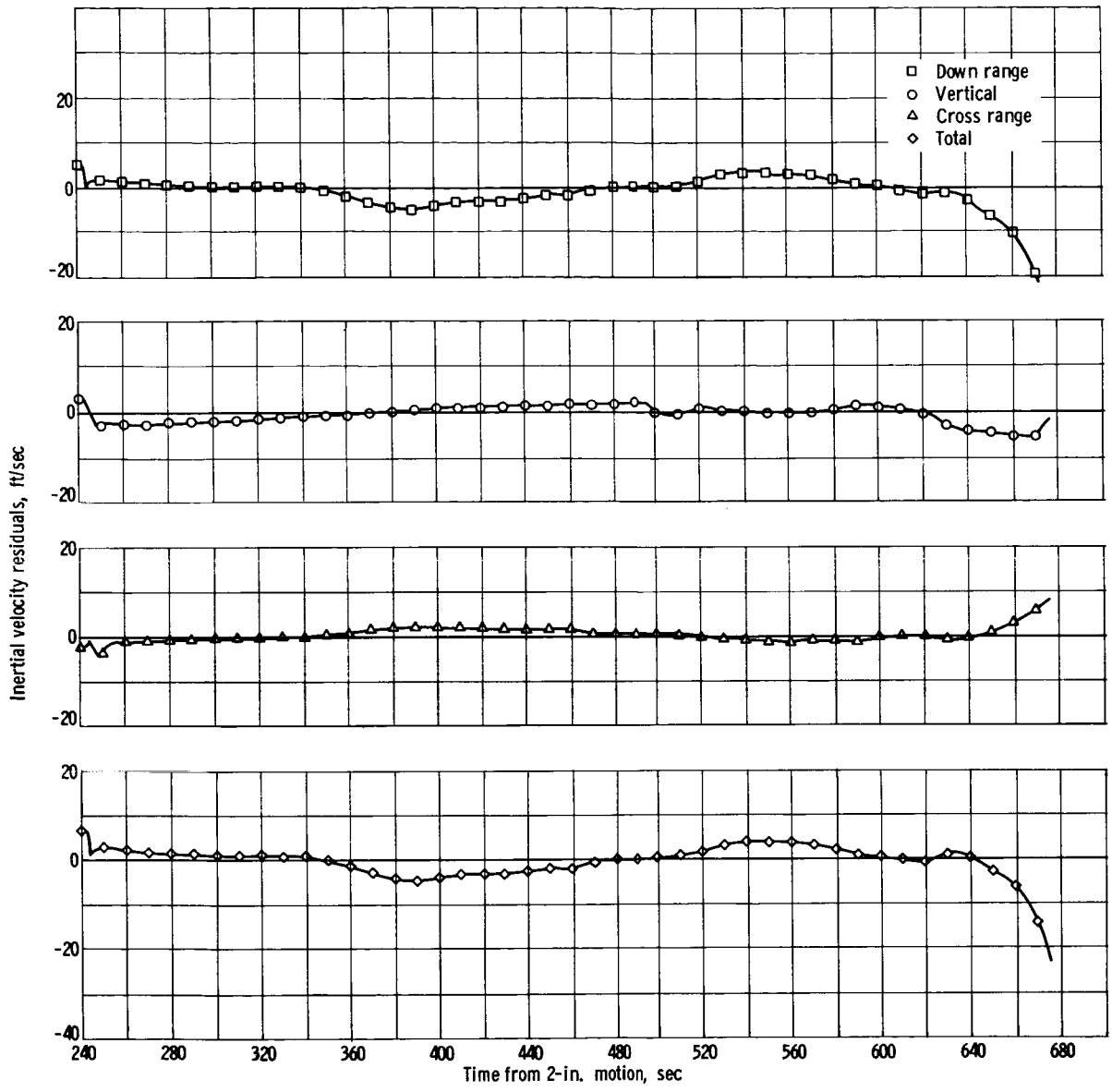

(b) Centaur phase.

Figure V-7. - Concluded.

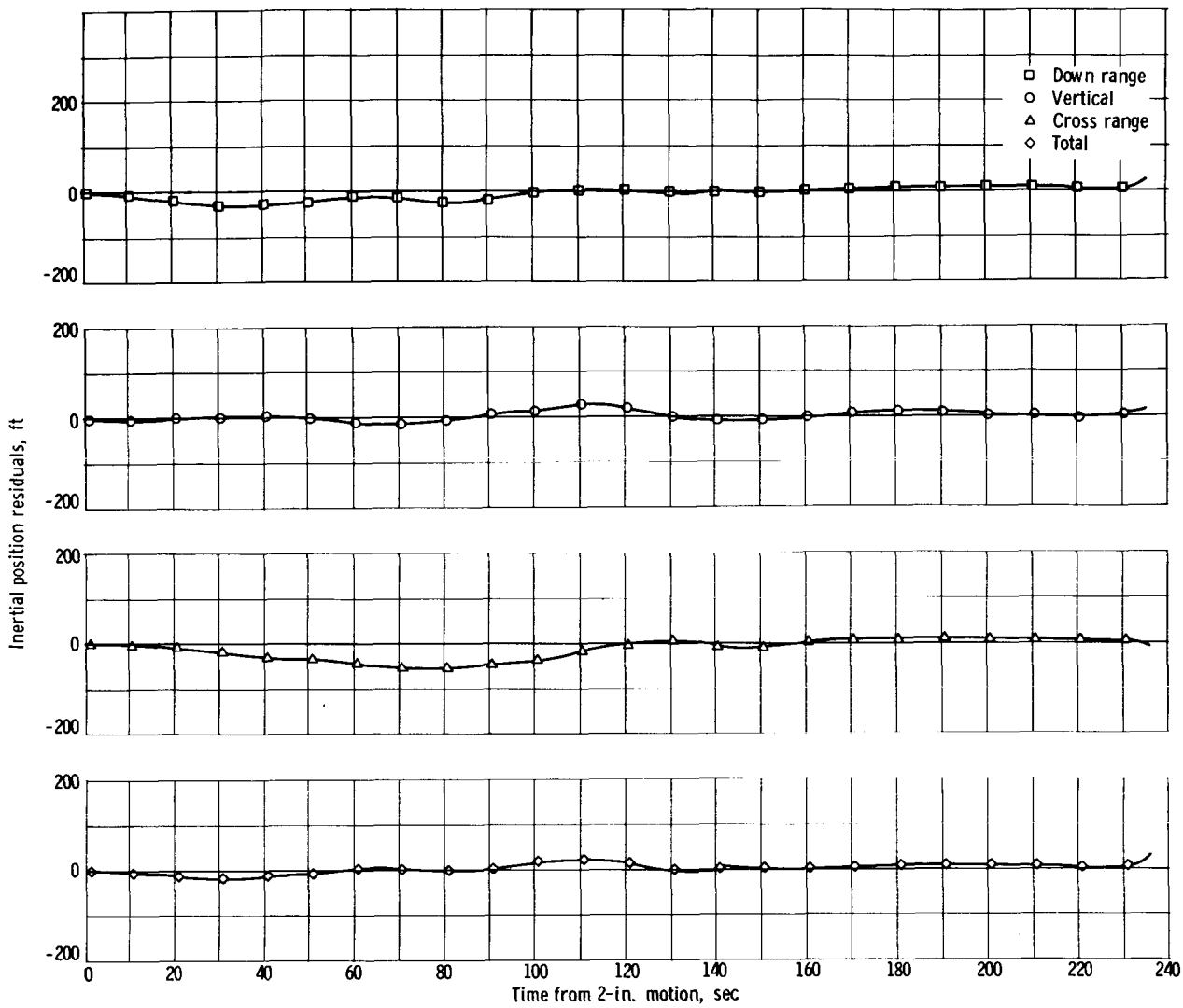

(a) Atlas phase.

Figure V-8. - Position component residuals (reconstruction minus GET).

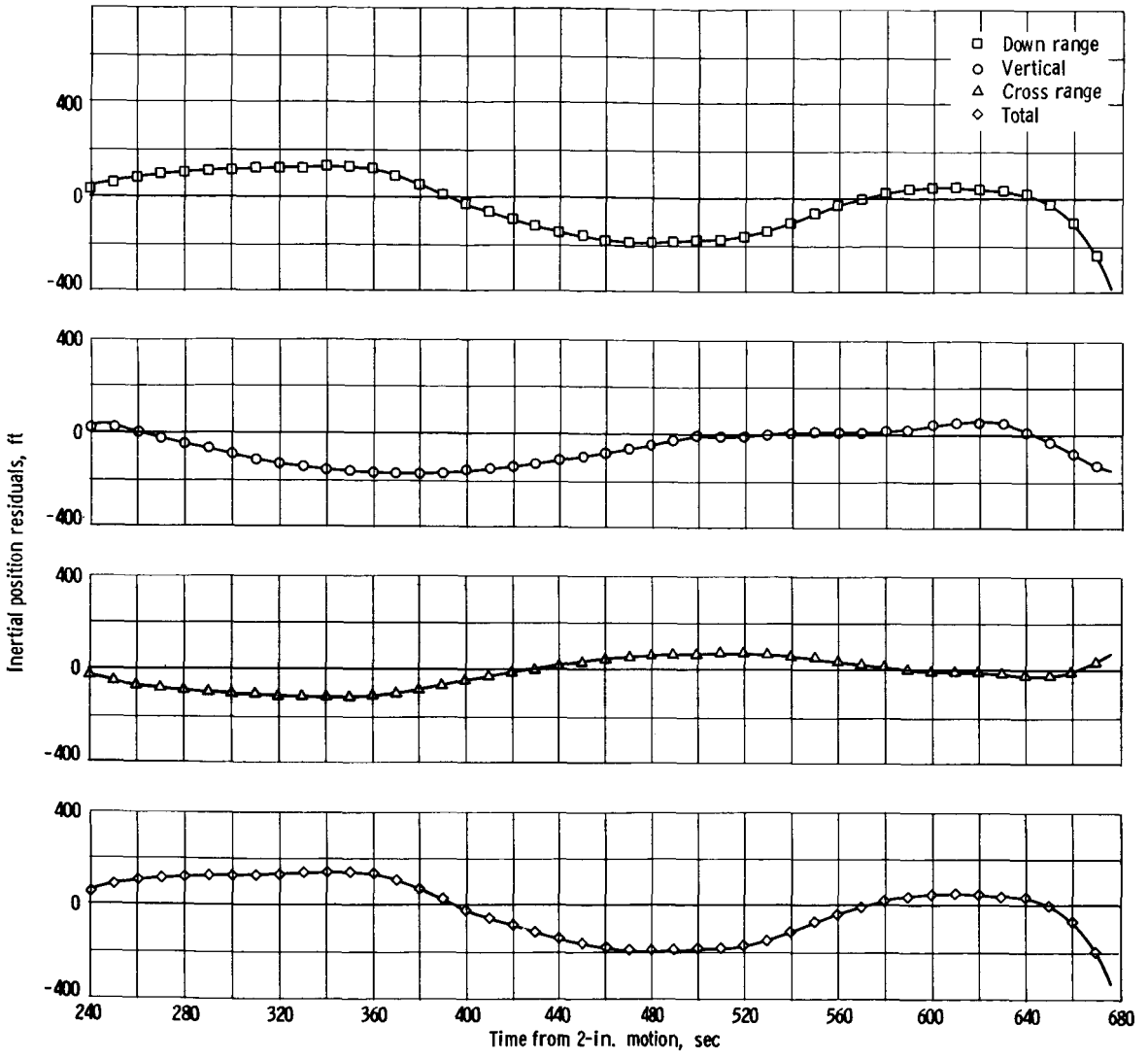

(b) Centaur phase.

Figure V-8. - Concluded.

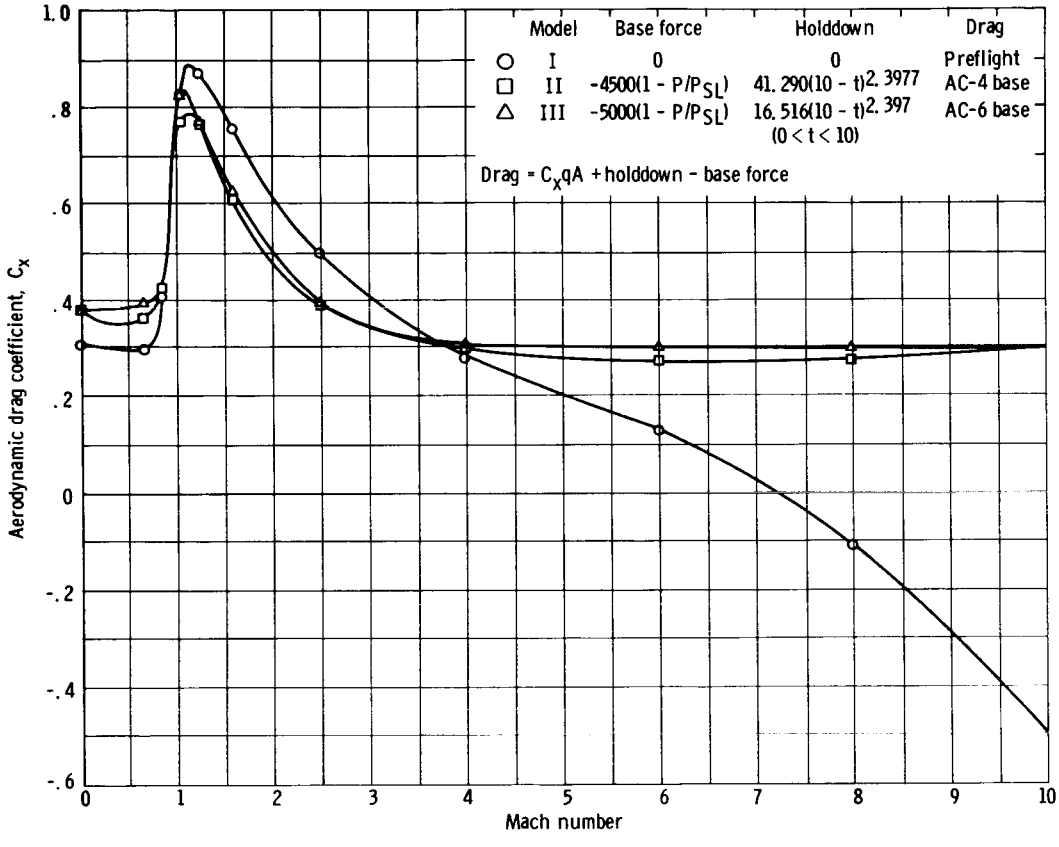

Figure V-9. - Comparison of aerodynamic drag coefficient models.

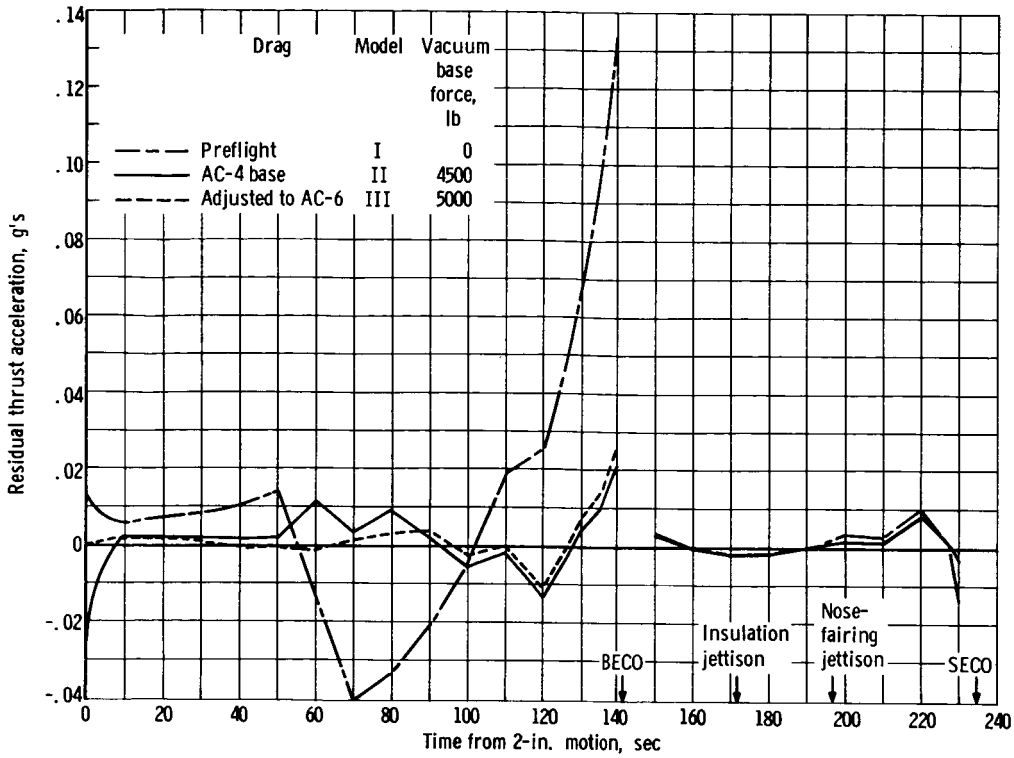

Figure V-10. - Comparison of residual thrust acceleration for three drag models.

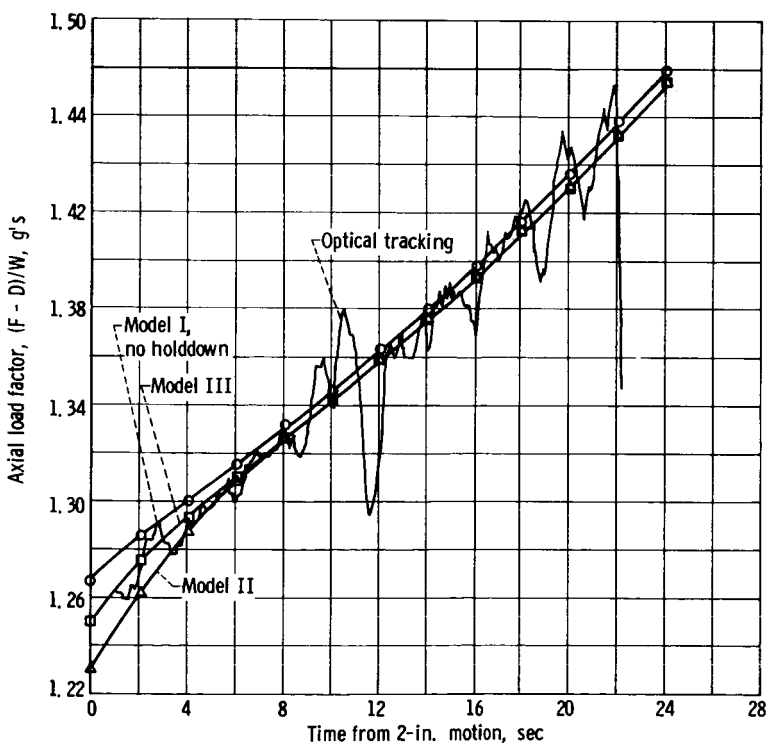

Figure V-11. - Effect of holddown force models on thrust acceleration.

VI. PROPULSION

SUMMARY

The Atlas and the Centaur propulsion systems both performed adequately for the AC-6 flight. For the first time, a successful vehicle retromaneuver was demonstrated.

ATLAS

The AC-6 was the first successful Centaur flight to utilize 165 000-pound-thrust booster engines. Some Atlas steady-state operating conditions are presented in table VI-I. All propulsion system parameters appeared normal through the booster phase of flight. Nominal performance adjusted for engine inlet conditions (ref. 6) in terms of thrust specific impulse, and mixture ratio is presented in table VI-II. The Atlas propulsion system appeared to operate nominally throughout the flight.

CENTAUR

Major changes in the AC-6 propulsion system included:

(1) Installation of RL10A-3-1 engines

(2) Strengthened propellant supply ducts to withstand RL10A-3-1 engine-shutdown pressure spikes

(3) Installation of a separate LHe chilldown manifold and overboard vent for each engine

(4) Increase in boost-pump lead or deadhead time

(5) Relocation of the venturi in the C-1 LO_2 duct bleed system

(6) Installation of duel-element temperature probes for both the LH_2 and LO_2 turbopump inlets

Additional system changes resulting from the failure of the C-1 LH_2 turbopump inlet temperature probe to indicate liquid during quad tanking (see section III, PRELAUNCH HISTORY) include the following:

(1) Relocation of the venturis in the LH_2 duct recirculation systems to the junction with the main LH_2 supply duct

(2) Insulation added on both the dual-element probes and the LH_2 recirculation system branch lines

(3) Installation of foam insulation rings on the LH_2 supply ducts extended to cover the engine inlet flange

(4) Reversal of the flow direction in the LH_2 duct purge system

One primary discrepancy occurred during the operation of the Centaur propulsion system: a thrust chamber pressure overshoot, in excess of that normally experienced, occurred on both engines during the start transient. Although the effect of this overshoot on the AC-6 flight was negligible, had conditions been more severe, the engines might have failed to accelerate.

MAIN ENGINES

During a typical engine start transient, the turbopump speed and engine chamber pressure rise to their peak at approximately the same time. When flow commences from the engine turbopumps to the combustion chamber, a corresponding drop in pump inlet pressure occurs. Following the peak transient flow, when flow rate begins to stabilize, pump inlet pressure increases toward a steady-state operating level. This recovery of pump inlet pressure normally takes place just prior to the peaking of engine chamber pressure and turbopump speed.

Turbopump speed and engine chamber pressure during the start transient for both the flight and the engine acceptance tests are presented in figures VI-1 and 2. Although chamber pressure and turbopump speed peaked at approximately the same time during flight, turbopump speed began its rise early relative to chamber pressure. The chamber pressure lag could have resulted from a temporary starvation of flow to the LO_2 turbopumps.

Turbopump inlet pressures and temperatures during the start transient for flight and for the engine acceptance tests are presented in figures VI-3 and 4. Both the LO_2 and the fuel pump inlet pressures on AC-6 dropped to values considerably below those of the acceptance tests and also below those experienced on previous flights. The recovery of LO_2 pump inlet pressure during the AC-6 start transient did not take place until approximately 0.2 second following the time of peak chamber pressure. This presents additional evidence of flow starvation to the LO_2 turbopumps.

Plots of fuel and LO_2 pump NPSP during the flight start transient are presented in figures VI-5 and 6, respectively. The NPSP for both LO_2 and fuel dipped to near the saturation line, whereas on previous flights, the minimum values were well above the steady-state operating limit.

The foregoing sequence of events suggests that both LO_2 turbopumps momentarily cavitated. The combination of chamber pressure and turbopump speed overshoot, the fact that the turbopump speed led the chamber pressure during the start transient, and the lag in LO_2 pump inlet pressure recovery indicate that the LO_2 turbopumps were momentarily unloaded. The speed overshoot could have been caused by a combination of unloading the LO_2 turbopumps and the high pres-

sure ratio across the turbine that resulted from the lag in chamber pressure rise. A quick recovery of LO_2 flow following the momentary cavitation would then account for the chamber pressure overshoot. The dip in fuel pump NPSP is considered a result of high transient flow rates and probably did not contribute to the overshoot.

The most likely causes of the LO_2 turbopump cavitation are as follows:

(1) Gas bubble formation in the sump at the LO_2 boost-pump inlet causing the LO_2 boost pump and the engine LO_2 turbopump to cavitate during the flow transient following MES

(2) Improperly filled propellant lines resulting from a combination of excessive air-conditioning heat input and minimum chilldown

(3) Warm turbopump housing temperatures resulting from excessive heat input from air conditioning and insufficient cooldown

The adequacy of the propellant tank burp at SECO to suppress boiling and to provide boost-pump NPSH is evaluated by subtracting the saturation pressure corresponding to the boost-pump inlet temperature from the ullage pressure after burp. Although AC-6 did not have instrumentation to measure LO_2 boost-pump inlet temperature, a correlation was made by using data from past flights. The subtraction of the saturation pressure, corresponding to this temperature, from the ullage pressure resulted in a -1.0-psi effective burp pressure margin, whereas all previous flights had positive margins of at least 1.0 psi. This negative burp pressure margin could have created a quantity of gas at the boost-pump inlet. During the flow transient following MES, this gas could then have been drawn through the propellant feed system causing the boost pump and the engine LO_2 pumps to cavitate. To ensure against the recurrence of this problem, the burp pressure is to be increased for all future vehicles.

Although the LO_2 turbopump inlet temperature probes indicated liquid at main engine start, gas could have been trapped in the low-pressure ducts upstream of the probes or could have existed at the probes at saturated liquid temperatures. Ground tests are currently being conducted to determine the effects of propellant ducts partly filled with gas at main engine start.

Figures VI-7 and 8 demonstrate higher turbopump housing temperatures at engine start compared with those of previous flights. Failure of the fuel pump housing temperature to stabilize at 120° R during the booster phase, as experienced on previous flights, is considered to have resulted from the difference in ground air conditioning. The contention is that, on previous flights, the combination of LHe chilldown and GN_2 air conditioning was sufficient to create a layer of nitrogen frost on the turbopump housing. During the booster phase, the housing temperature could only warm to the melting temperature of the nitrogen frost; however, conditions on AC-6 were probably such that no nitrogen frost layer formed. The warm LO_2 pump housing temperature is also considered to be a result of excessive air conditioning. The effects of warm housing temperatures will be further investigated by additional ground testing.

The use of RL10A-3-1 as opposed to RL10A-3 engines is considered to have had a negligible effect on the problem of overshoot. Extensive ground testing

on both engines has revealed little difference during the start transient.

The start total impulse calculated to 95 percent of rated thrust was 2860 and 3095 pound-seconds for the C-1 and C-2 engines, respectively. The differential total impulse between engines was well within specifications.

Engine steady-state operation appeared normal. Table VI-III compares some flight steady-state values with their nominal or predicted values. The C-1 fuel pump inlet temperature, which had created problems during quad tanking (see section III, PRELAUNCH HISTORY), failed to record throughout the entire flight. Engine thrust, specific impulse, and mixture ratio during steady state are presented in table VI-IV. The high mixture ratios at MES + 100 seconds are a result of activation of the propellant utilization system at MES + 90 seconds (see section VII, PROPELLANT SYSTEMS).

Main engine cutoff appeared normal. The cutoff total impulse was calculated to be 2250 and 2400 pound-seconds for the C-1 and C-2 engines, respectively. Although the differential impulse of 150 pound-seconds between engines was satisfactory, the engine specification value of total cutoff impulse, 1180±150 pound-seconds per engine, was exceeded. Even though excessive total cutoff impulse also occurred on all previous flights, it is not considered a major problem. The engine manufacturer bases its specification values on simple electrical circuitry used at the factory. The more complex vehicle electrical system creates a longer delay in engine valve closure at MECO. Preflight guidance corrections compensate for the "excessive" cutoff impulse obtained during flight.

Engine inlet temperatures and pressures for the engine retrothrust operation are noted in figures VI-9 to 12. All indications are that the retrothrust operation was highly successful. For further details on this subject see sections VII, PROPELLANT SYSTEMS; XII, FLIGHT CONTROL; and the attitude control portion of this section.

Boost Pumps

Boost-pump start command was initiated at approximately 39.1 seconds prior to main engine start compared with a predicted time of 39.2 seconds. First indications of turbine inlet pressures occurred 1.5 and 1.6 seconds after BPS command for the oxidizer and fuel units, respectively. These times are considerably below the preflight estimate of 6.7 seconds required to expel the gases trapped in the peroxide bladder and lines. As shown in figure VI-13, turbine inlet pressures reached steady-state values of 140 and 88 psia for the fuel and oxidizer units, respectively, which compare favorably with preflight acceptance test values of 139.5 and 89.9 psia. Inlet pressure oscillations similar to those experienced on previous ground and flight tests were evident. Maximum amplitudes were experienced at the fuel turbine for the last 65 seconds of boost-pump operation.

Both the oxidizer and the fuel turbines accelerated normally to steady-state speeds of 38 400 and 51 150 rpm, respectively (fig. VI-14) just prior to prestart command. No indications of overspeed tendencies were noted during the

separation sequence. The separation phase was of some concern because the overspeed control system had been found faulty and was intentionally disconnected prior to flight.

A momentary increase in oxidizer boost-pump turbine speed, approximately 500 rpm, occurred at MES + 1.2 seconds. At this particular time in the start sequence, the turbine speed should be decreasing steadily as a result of the increased boost-pump oxidizer flow as the engine accelerates. This slight increase in speed may be attributed to either (1) momentary reduction in liquid-oxygen flow to the engines caused by engine pump cavitation, or (2) ingestion of gas through the boost pump at MES resulting in momentary cavitation of the boost pump.

Both boost pumps operated normally during the Centaur burn portion of the flight with steady-state turbine speeds of 33 600 and 46 850 rpm for the oxidizer and fuel units, respectively. Based on the preflight acceptance test data and inflight peroxide bottle pressure of 307 psia, the corresponding turbine speeds expected during flight were 32 000 and 46 380 rpm. Variations in propellant flow rates during the period of propellant utilization system control resulted in essentially no change in turbine speeds, with the exception of the last 50 seconds of engine operation. During this period, a 600-rpm decrease in fuel-boost-pump turbine speed was evident. This slight reduction in turbine speed may have been caused either by the propellant utilization valve (which was in the fuel-rich position for the majority of this time period), or by the previously noted large oscillations in the fuel turbine inlet pressure during the last 65 seconds of operation. The cause cannot be determined, but the magnitude of the speed reduction is well within acceptable limits.

Post-MECO boost-pump turbine speed decay is shown in figure VI-15. Fuel unit speed decay is questionable because the data are of poor quality. The oxidizer unit trace is typical of previous flight data with the exception that the coastdown time is from 65 to 100 seconds longer than any previous flight. This extended coastdown time may have been a result of low propellant level of this flight resulting in quicker gas pullthrough in the weightless environment.

Boost-pump turbine bearing temperatures are shown in figure VI-16. The oxidizer unit temperature was 243° F at MECO and continued to increase to a maximum value of 300° F as a result of heat "soak-back." Corresponding values for the fuel unit were 320° and 372° F. The maximum values obtained were well below the 400° F upper limit permitted during acceptance testing. Landline instrumentation indicated turbine housing skin temperatures of 82° and 93° F for the oxidizer and fuel units, respectively, just prior to lift-off.

Instrumentation to monitor headrise across the boost pumps was not available on this flight; the performance of the pumps in this respect may be obtained from the engine inlet conditions. These data are presented in the section covering main engine performance.

Attitude Control and Hydrogen Peroxide Systems

AC-6 was the first vehicle to have the attitude control engines mounted in-

board of the interstage adapter. As a result of this relocation, the A or 1.5 pound-thrust engines were rotated 25° outboard to reduce exhaust gas impingement on adjacent equipment (see fig. VI-17).

The H_2O_2 bottle pneumatic pressure is shown in figure VI-18. A relatively long time was required to pressurize the bottle but this was expected with the small quantity of H_2O_2 tanked. The gradual drop in bottle pressure after lift-off was also normal since the pressure regulator is referenced to ambient pressure.

Data indicated proper conditioning of the H_2O_2 system prior to launch. Figure VI-19 shows the P-2 fuel supply temperature. The trace appears normal with a slight rise as the system was being pressurized and a drop after lift-off due to discontinuation of the ground air conditioning at that time. The supply lines were filled with gas until the H_2O_2 engines were first fired at MECO. Thus the lines had a small total mass and reacted rapidly to ambient temperature changes. At MECO, the attitude control engines were enabled and fired to correct for main engine shutdown disturbances. The flow of warm H_2O_2 from the bottle was responsible for the sharp increase in temperature at this time. After the end of the retromaneuver, when the tube heaters were turned off, the supply lines increased in temperature, followed by a decrease and then another increase. These changes are attributed to solar heating with the vehicle rolling so that the supply lines were alternately in and out of the sun's rays.

Data that indicate the attitude control engine firing times are shown in figure VI-20. The P-1, A-2, and A-4 engines were fired for a short period just after MECO to correct for small pitch and roll errors caused by main engine thrust cutoff. The small requirement for attitude control at this time indicates a very smooth main engine shutdown. At MECO + 73.7 seconds, P-2 and A-1 engines fired for about 15 seconds with intermittent firing of A-2. This was the result of a programed function to turn the vehicle 180°. The engines were cut off when the turning rate reached a limit of 1.6 degrees per second. At MECO + 146.7 seconds, P-1, A-3, and A-4 engines came on to stop the turning. The start of retrothrust began at MECO + 193.5 seconds. Shortly thereafter, a yaw-roll error was indicated by the firing of A-2, A-3, and A-4 engines. This error continued for the duration of the retromaneuver, with constantly decreasing magnitude. Since the disturbance did not exist prior to the start of blowdown, and since the magnitude of the disturbance decreased with time, it is apparent that it was caused by misalinement of the retrothrust vector with the vehicle center of gravity and possibly a small amount of unbalanced impingement forces. With the exception of the preceding disturbances, the entire retromaneuver was performed relatively smoothly. Prior to the flight, there was some speculation that liquid hydrogen might freeze and partially block the cooldown valve discharge tubes through which the hydrogen is exhausted. However, the small requirement for the attitude control engines and the times at which they were fired indicate that there was no appreciable blockage of the discharge tubes.

The H_2O_2 bottle was tanked with 109 pounds. Approximately 9 pounds were expended in ground tests, resulting in a lift-off weight of 100 pounds. Based on a nominal H_2O_2 flow rate of 6.18 pounds per minute for the boost pumps, the total boost-pump requirement was calculated to be 49 pounds. The total weight

of H_2O_2 expended by the attitude control system was less than 5 pounds, based on the indicated firing times of the attitude control engines and nominal flow rates of 0.0194 and 0.0097 pound per second for the 3- and 1.5-pound-thrust engines, respectively. Therefore, there were approximately 46 pounds of H_2O_2 remaining in the tank at the completion of the mission.

HYDRAULIC SYSTEMS

Atlas

The booster hydraulic system performance was nominal throughout the boost phase (fig. VI-21). Steady-state airborne hydraulic pressure levels were obtained approximately 7 seconds following engine start. The 7-second time period included accumulator charging and the gimbal flow requirements just after lift-off (fig. VI-22). Steady-state pressures of 3103 psia at the pump discharge and 3211 psia at the B-1 accumulator were maintained until BECO and then dropped to zero as expected.

The sustainer hydraulic power changeover occurred in approximately 8 seconds. This time period included accumulator charging, engine control valve, and gimbal flow requirements just after lift-off (figs. VI-22 and 23). Steady-state pressure levels of 3036 psia at the pump discharge and 3163 psia in the vernier engine portion of the circuit were maintained until BECO. Normal pressures in support of gimbal flow requirements commanded by the autopilot and the admission of guidance were observed during BECO and after booster-package jettison.

An unexpected drop of approximately 500 psi at lift-off + 137 seconds with no flow demand of any significance has been attributed to a pressure transducer malfunction. The dropout was not reflected in any form on the sustainer-vernier pressure trace, which is derived from the same hydraulic circuit downstream of the pump.

Centaur

Evaluation of the data received from the AC-6 flight shows that both the C-1 and C-2 hydraulic systems operated properly. Engine positions as a function of time are shown in figure VI-24. The new rematched recirculation system effectively started nulling both engines as MES - 7.6 seconds. Nulling rates of 1.6 degrees per second maximum and a minimum of 0.5 degree per second were higher than those achieved on previous flights. A change in nulling rates occurred at MES - 6.4 seconds as a result of slight vehicle rate changes imparted by a minor Atlas-Centaur separation disturbance. Feedback positions at MES - 0.2 second indicate that the vehicle was pitching upward, yawing right, and rolling counterclockwise. Vehicle rates imparted by engine start differential impulse were effectively eliminated in the allotted time between MES and MES + 4 seconds. Guidance corrections, required after rate suppression, were accomplished in an 8-second interval between MES + 4 and MES + 12 seconds. The whole start transient in terms of engine gimbal was milder than any that occurred on previous flights. The only other hydraulic demand of any significance was made at MES + 253.8 seconds in response to a guidance input.

The uprated recirculation system pressures just prior to MES reached values of 127 psia for C-1 and 126 psia for C-2, as shown in figure VI-25. Main system pressures reached and maintained steady-state values of 1112 psia for C-1 and 1116 psia for C-2. The expected drop in pressure at MES + 4 seconds with guidance readmission was not noticeable.

Engine position changes needed to compensate for the transient differential impulse during shutdown are shown in figure VI-24(b). The maximum engine positions reached were 1.6 degrees for C-1 pitch, 1.3 degrees for C-2 pitch, -2.6 degrees for C-1 yaw, and 0.7 degree for C-2 yaw. Movement to these positions during shutdown indicates that compensation was made for vehicle downward pitch, right yaw, and counterclockwise roll.

The recirculation system pumps were restarted by the programer and continued to function properly until the end of the retromaneuver. Engine positions during retromaneuver were basically those that existed just prior to MECO (fig. VI-24(b)). Attitude errors in the pitch plane were sufficient to cause a sinusoidal type response of the engines. A corresponding peak to peak displacement of approximately 0.4 degree occurred on both engines for three cycles lasting 300 seconds.

Hydraulic system manifold temperatures at lift-off were 66° F for C-1 and 72° F for C-2, as shown in figure VI-26. The expected temperature drop through boost phase occurred and was comparable to that observed on AC-4. At MES + 0, C-1 reached a low of 58° F and C-2 settled to 61° F. Temperature rise rates during main pump operation were nominal. Temperatures at MECO were 178° F on C-1 and 193° F on C-2. Rates of temperature drop after MECO + 300 seconds were linear at 1.7° F per minute. The temperatures at lift-off + 1500 seconds were 122° F for C-1 manifold and 125° F for C-2 manifold.

TABLE VI-I. - ATLAS STEADY-STATE OPERATING CONDITIONS

Parameter	Time from lift-off, sec	Nominal value	Flight value
Booster			
B-1 pump speed, rpm	100	[a]6340	6610
B-2 pump speed, rpm	100	[a]6279	6494
B-1 LO_2 pump inlet pressure, psia	95.6	[b]58.7	65.7
B-2 LO_2 pump inlet pressure, psia	95.6	[b]58.7	67.2
B-1 fuel pump inlet pressure, psia	95.6	[b]56.2	53.0
B-2 fuel pump inlet pressure, psia	95.6	[b]56.2	54.9
B-1 thrust chamber pressure, psia	100	[a]577.5	578
B-2 thrust chamber pressure, psia	100	[a]577.5	581
Gas-generator chamber pressure, psia	100	[a]531	541
Sustainer			
Pump speed, rpm	200	[a]10 114	9984
Fuel pump inlet pressure, psia	195	[b]46.9	51.1
LO_2 pump inlet pressure, psia	195	[b]41.5	42.1
LO_2 pump inlet temperature, °F	195	[b]-284.2	-281.5
Fuel pump discharge pressure, psia	200	---------	894
Gas-generator discharge pressure, psia	200	[a]762	791
LO_2 injector manifold pressure, psia	200	---------	823
Thrust chamber pressure, psia	200	[a]704.2	696
Vernier			
V-1 thrust chamber pressure, psia	200	[a]359	373
V-2 thrust chamber pressure, psia	200	[a]360	371

[a]Acceptance test data.
[b]DEPRO predicted value.

TABLE VI-II. - ATLAS PERFORMANCE (DEPRO PROGRAM)[a]

	Flight value	Predicted value
Thrust at lift-off, lb		
Boosters	326 765	326 622
Sustainer	56 807	56 919
Verniers, axial	1 491	1 518
Total	385 063	385 059
Thrust at BECO, lb		
Boosters	375 411	376 363
Sustainer	80 512	79 515
Verniers, axial	1 705	1 744
Total	457 628	457 622
Thrust at SECO, lb		
Sustainer	79 760	79 250
Verniers, axial	1 704	1 744
Total	80 464	80 994
Specific impulse at lift-off, sec		
Boosters	251.8	252.9
Sustainer and verniers	213.0	213.9
Total	245.1	246.0
Specific impulse at BECO, sec		
Boosters	288.0	287.7
Sustainer and verniers	306.8	304.2
Total	291.0	290.5
Specific impulse at SECO, sec		
Total	306.8	303.4
LO_2 to fuel mixture ratio		
Lift-off	2.30	2.28
BECO	2.39	2.34
SECO	2.54	2.55

[a]See ref. 6 for explanation of this technique.

TABLE VI-III. - CENTAUR ENGINE STEADY-STATE OPERATING CONDITIONS

Parameter	Nominal	MES + 90 sec	
		C-1	C-2
LH_2 pump total inlet pressure, psia	35.0	34.4	33.4
LH_2 pump inlet temperature, ^{o}R	38.8	------	38.9
LO_2 pump total inlet pressure, psia	59.8	59.6	59.9
LO_2 pump inlet temperature, ^{o}R	176.6	173.5	174.0
LO_2 pump speed, rpm	11 350	11 125	11 462
LH_2 turbine inlet temperature, ^{o}R	331	326.9	337.1
LH_2 venturi upstream pressure, psia	649	672.8	681.5
Chamber pressure, psia	300	293.5	291.1

TABLE VI-IV. - CENTAUR PERFORMANCE (AC-6 FLIGHT)

Parameter	Acceptance run	Time from MES, sec									
		50	90	100	150	200	250	300	350	400	435
Chamber pressure, psia	293.6	293.5	293.5	297.5	292.7	292.7	292.3	292.7	292.7	291.7	293.4
C-1 engine (SN 1895)											
Thrust, lb:	14 934										
PWA regression method[a]		14 930	14 928	15 131	14 965	14 934	15 014	14 869	14 884	14 901	15 111
PWA C* method[a]		14 580	14 575	14 977	14 473	14 494	14 515	14 512	14 465	14 438	14 670
Specific impulse, sec:	434.0										
PWA regression method		433.7	433.8	430.6	433.2	433.6	432.5	434.7	434.5	434.2	431.1
PWA C* method		436.4	436.5	432.8	437.3	437.0	436.5	436.8	437.4	437.1	434.6
Mixture ratio:	5.0										
PWA regression method		5.030	5.024	5.409	5.097	5.040	5.183	4.896	4.925	4.958	5.350
PWA C* method		4.873	4.862	5.449	4.689	4.751	4.859	4.800	4.663	4.732	5.166
C-2 engine (SN 1896)											
Chamber pressure, psia	293.9	291.1	291.1	295.1	290.3	288.7	289.5	289.5	289.5	289.5	291.4
Thrust, lb:	15 005										
PWA regression method		15 021	15 022	15 309	15 068	15 051	14 943	14 963	14 933	14 889	15 175
PWA C* method		14 401	14 401	14 804	14 308	14 212	14 310	14 323	14 259	14 279	14 519
Specific impulse, sec:	435.0										
PWA regression method		434.1	434.1	429.3	433.3	433.6	435.3	435.0	435.5	436.1	431.8
PWA C* method		438.1	438.1	435.0	438.8	439.1	438.3	438.1	439.0	438.7	436.8
Mixture ratio:	5.09										
PWA regression method		5.151	5.150	5.693	5.242	5.212	4.986	5.025	4.961	4.869	5.417
PWA C* method		4.722	4.722	5.264	4.565	4.511	4.687	4.724	4.534	4.595	4.980

[a]See appendix C of ref. 6 for explanation of these techniques.

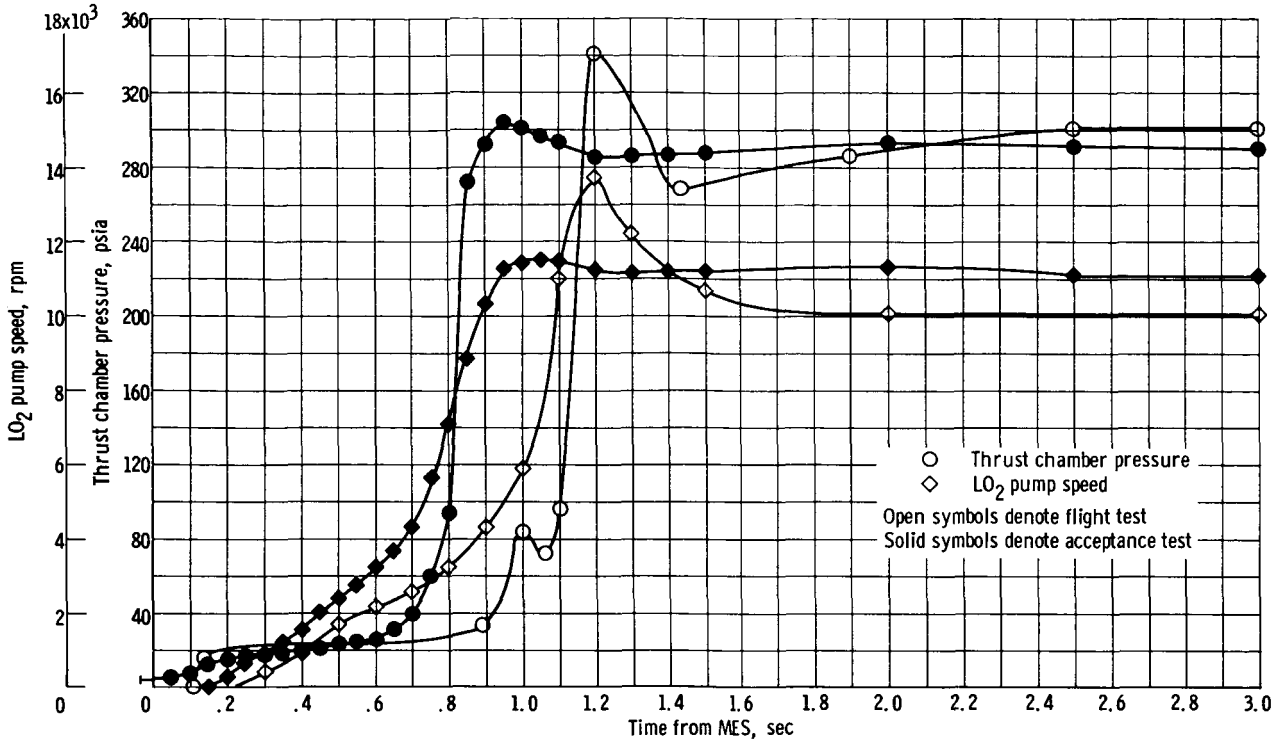

Figure VI-1. - C-1 engine (serial no. 641895) flight and final acceptance test run start transient characteristics.

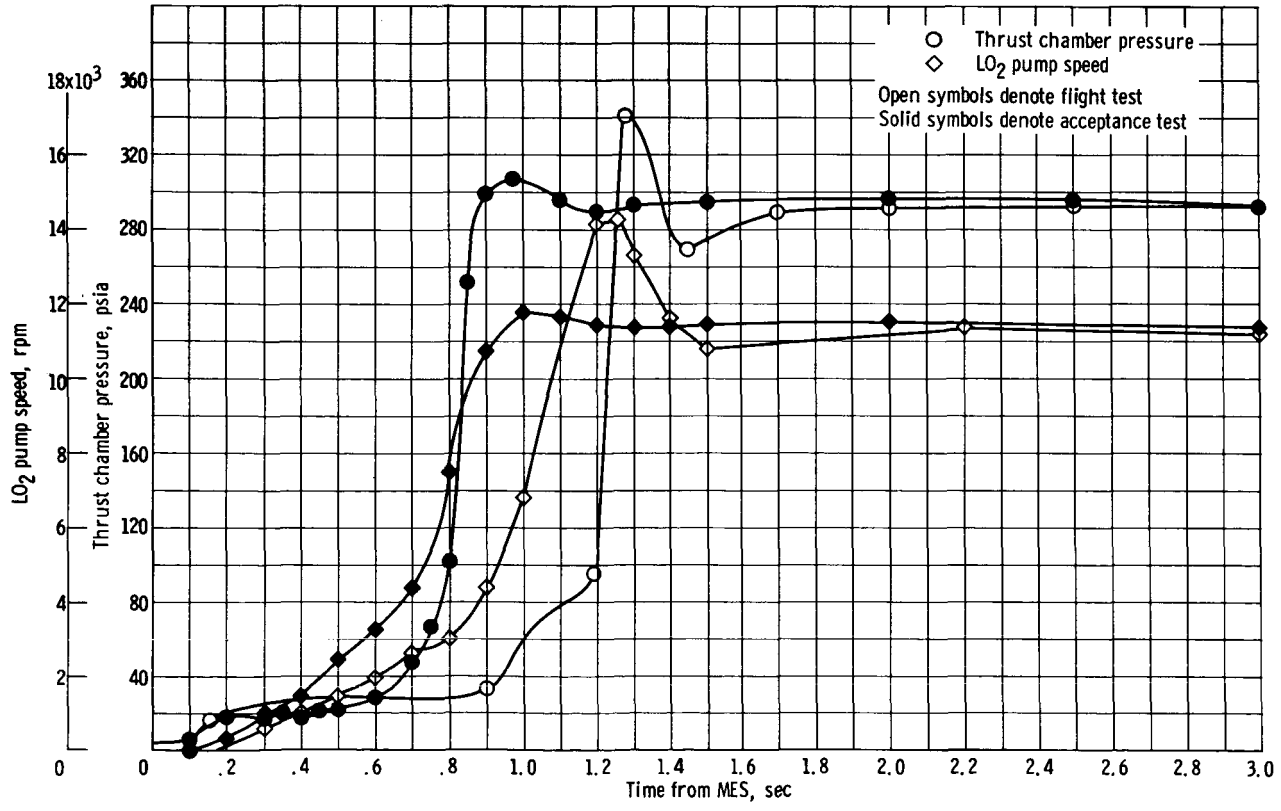

Figure VI-2. - C-2 engine (serial no. 641896) flight and final acceptance test run start transient characteristics.

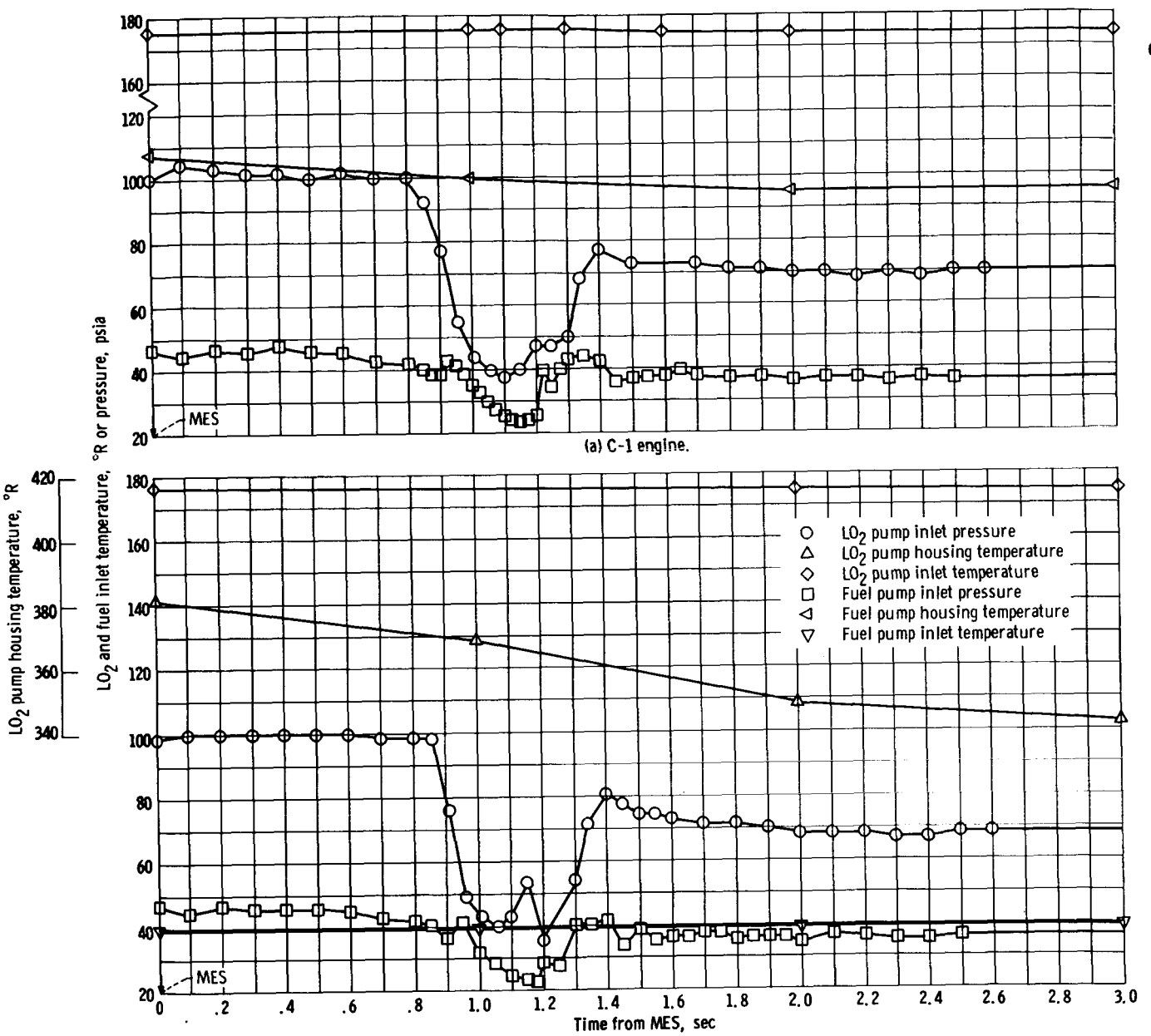

(a) C-1 engine.

(b) C-2 engine.

Figure VI-3. - AC-6 flight start transient fuel and LO_2 pump conditions.

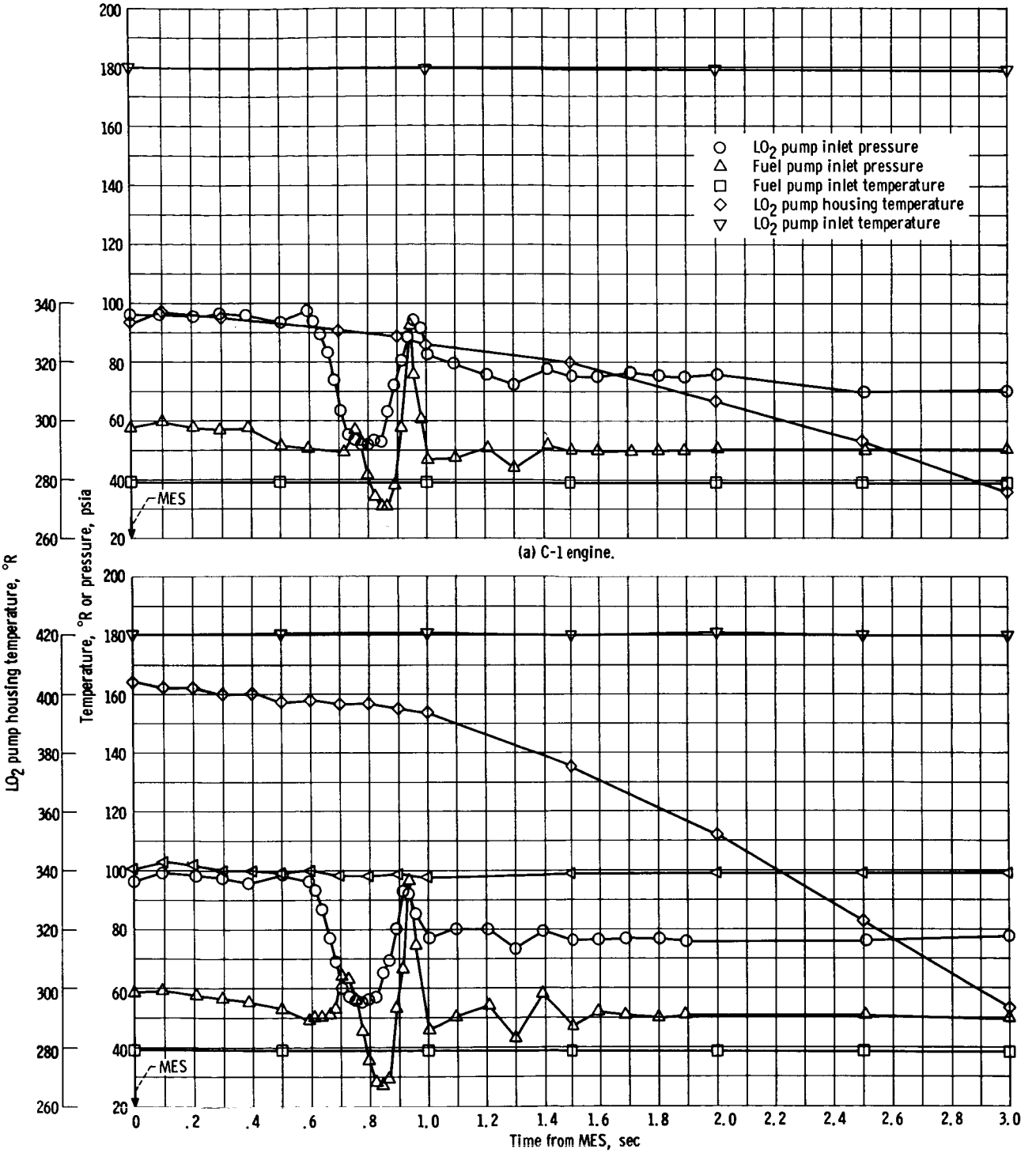

(a) C-1 engine.

(b) C-2 engine.

Figure VI-4. - AC-6 final acceptance test start transient fuel and LO_2 pump conditions.

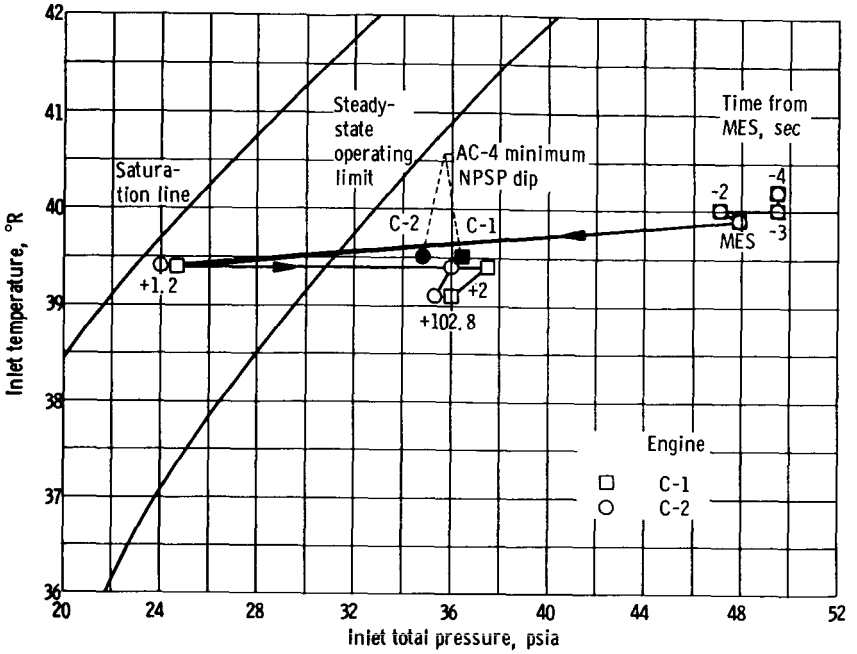

Figure VI-5. - Fuel pump inlet conditions near engine start. (C-2 engine temperatures used for C-1 engine; C-1 engine data not valid.)

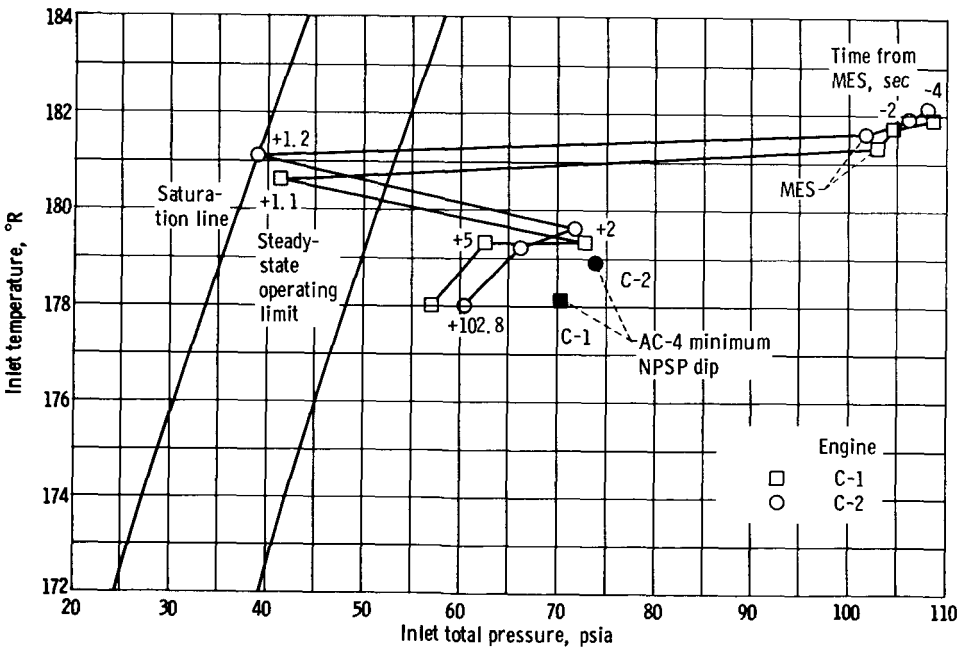

Figure VI-6. - LO_2 pump inlet conditions near engine start.

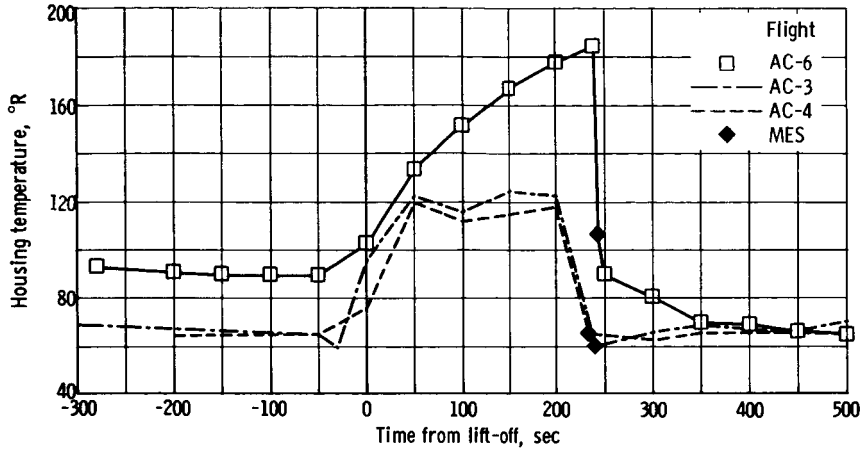

Figure VI-7. - C-1 engine fuel pump housing temperature.

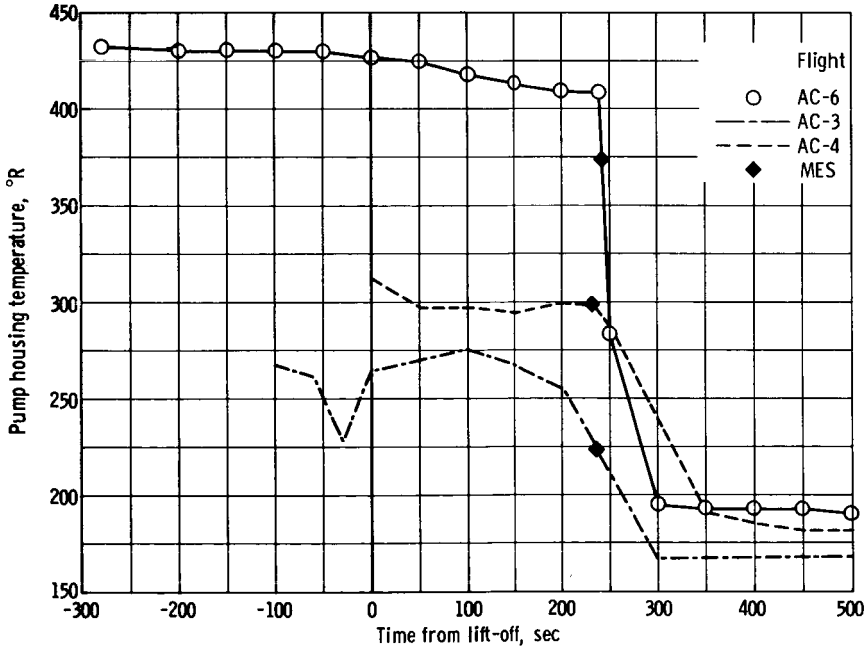

Figure VI-8. - C-2 engine LO_2 pump housing temperature.

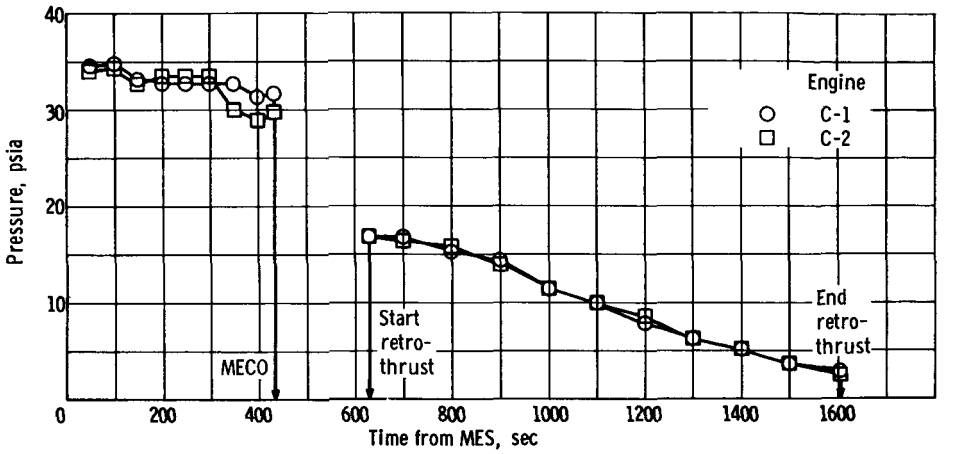

Figure VI-9. - Fuel pump inlet pressures through end of retrothrust.

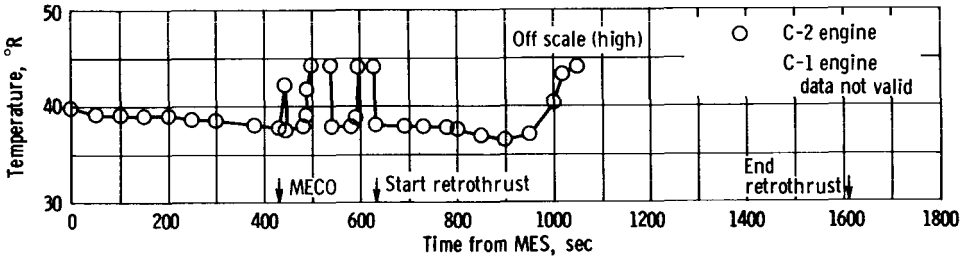

Figure VI-10. - Fuel pump inlet temperature through end of retrothrust.

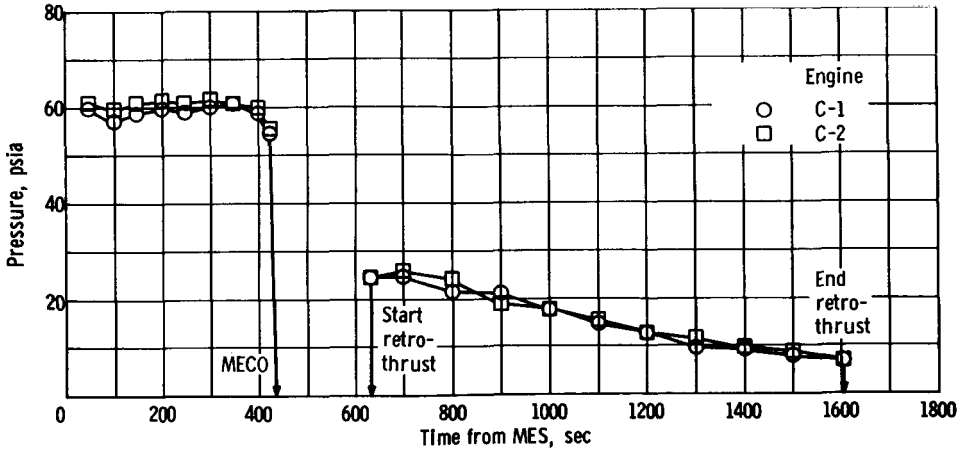

Figure VI-11. - LO_2 pump inlet pressures through end of retrothrust.

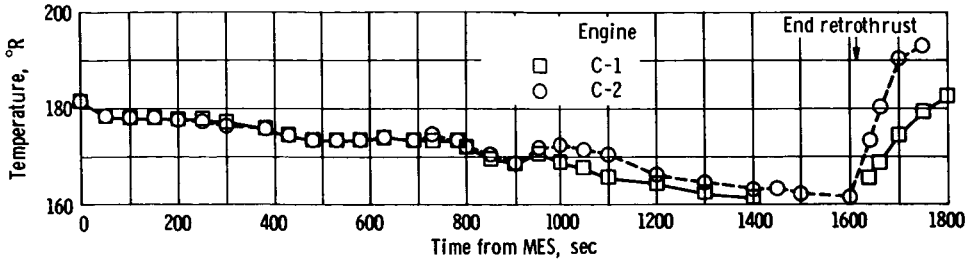

Figure VI-12. - LO_2 pump inlet temperature through end of retrothrust.

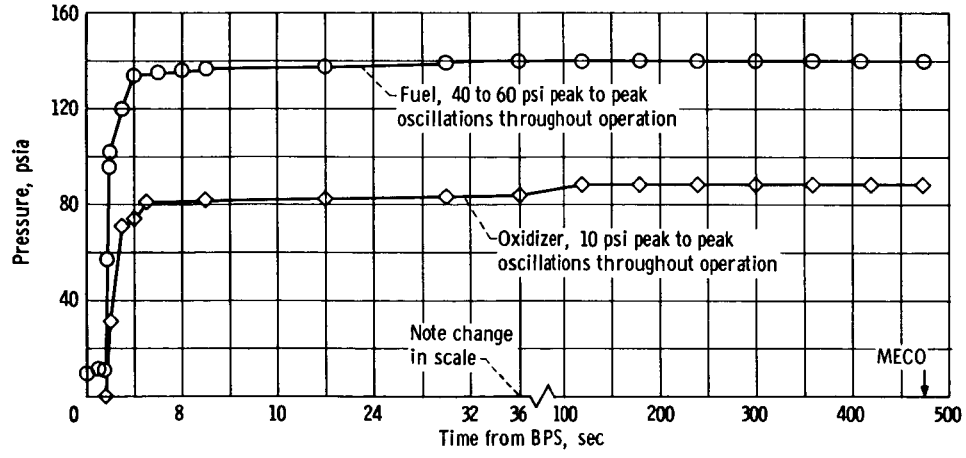

Figure VI-13. - Boost pump turbine inlet pressure.

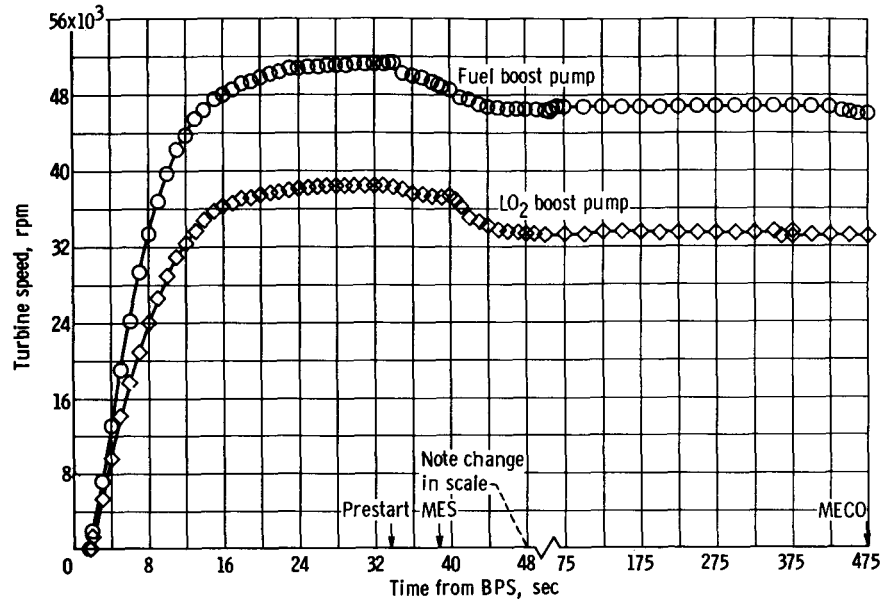

Figure VI-14. - Boost pump turbine speed.

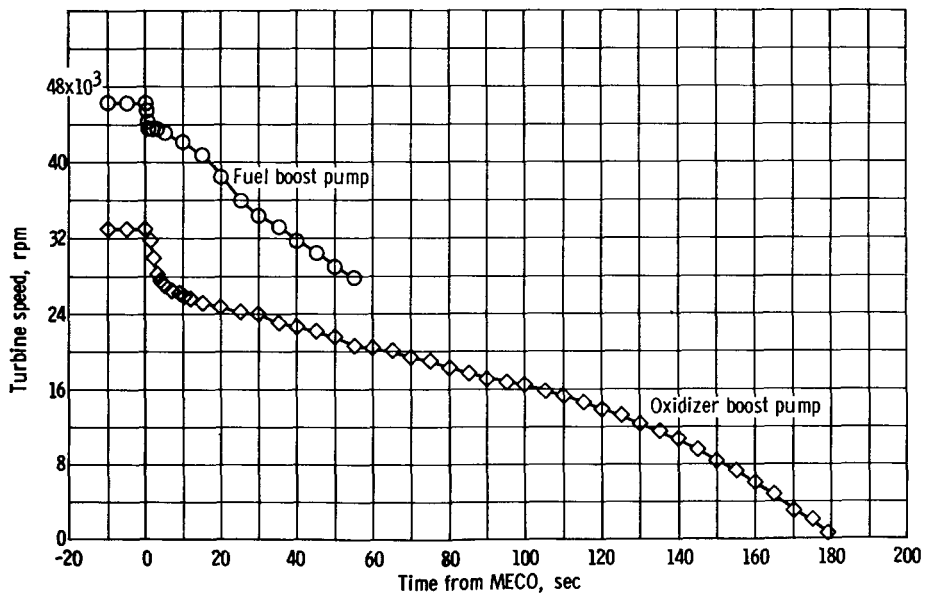

Figure VI-15. - Boost pump turbine speed coastdown (post-MECO). (Fuel boost pump data questionable from 0 to 55 sec, and completely invalid after 55 sec.)

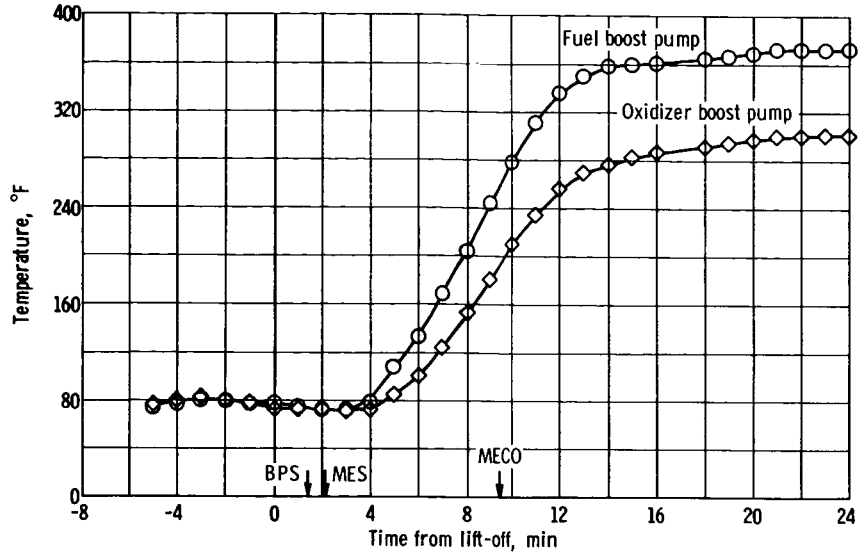

Figure VI-16. - Boost pump turbine bearing temperature.

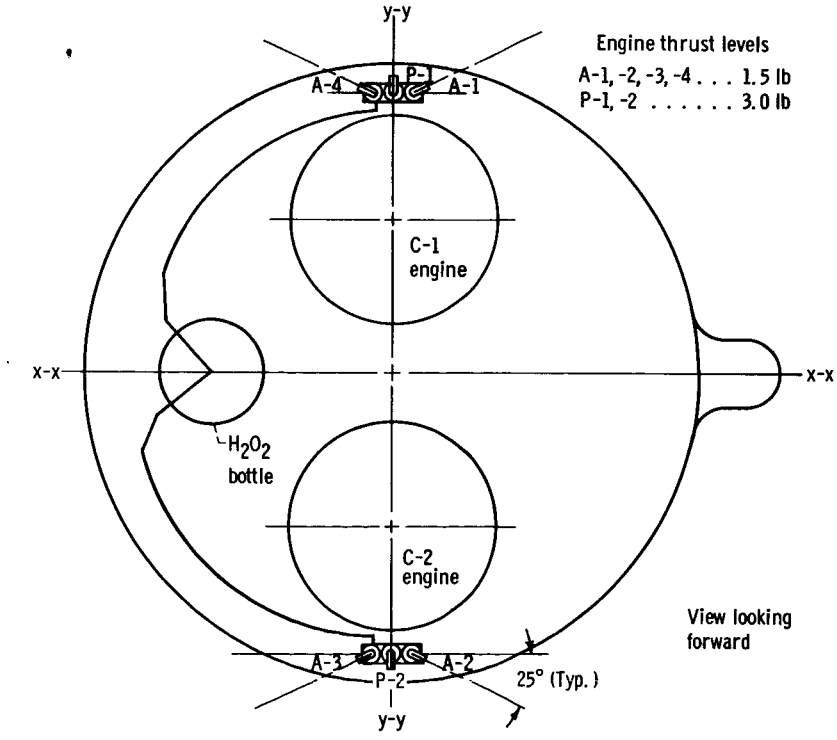

Figure VI-17. - Attitude control engines system schematic drawing.

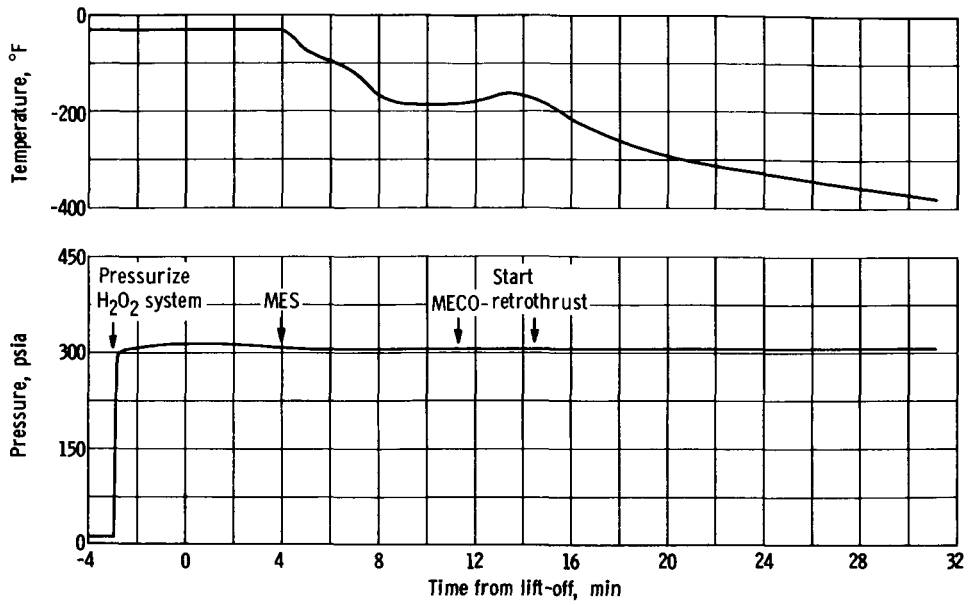

Figure VI-18. - Engine compartment temperature and H_2O_2 bottle pressure.

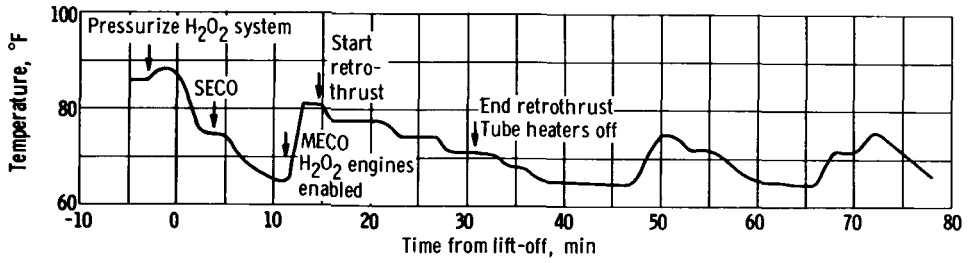

Figure VI-19. - P-2 engine H_2O_2 supply temperature.

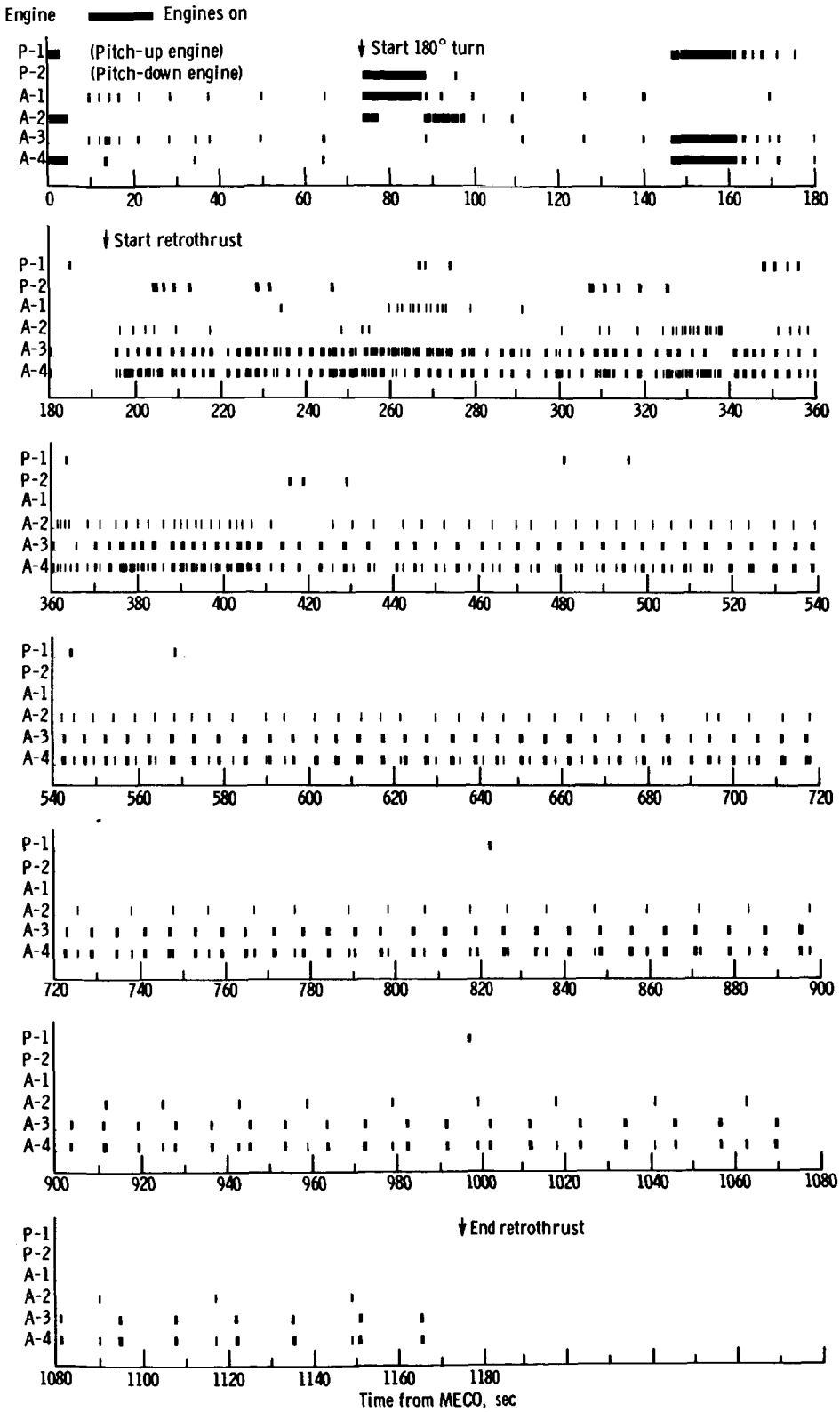

Figure VI-20. - Hydrogen peroxide engine commands history.

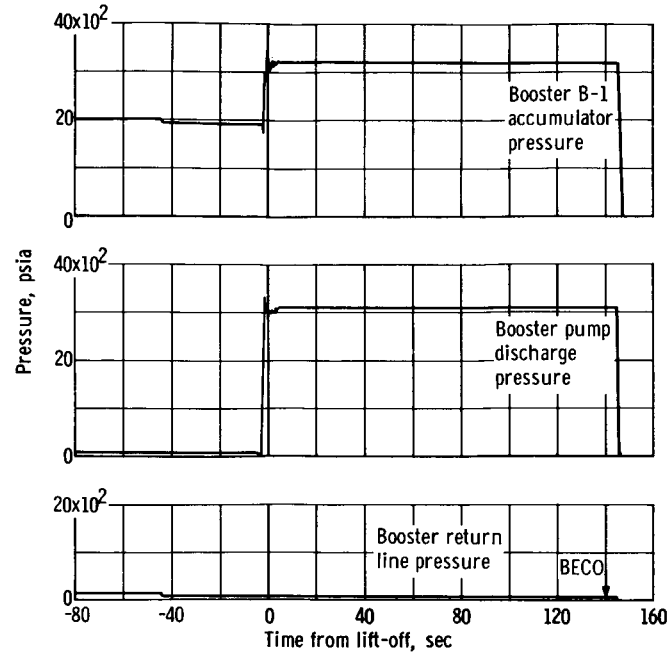

Figure VI-21. - Booster hydraulic pressures.

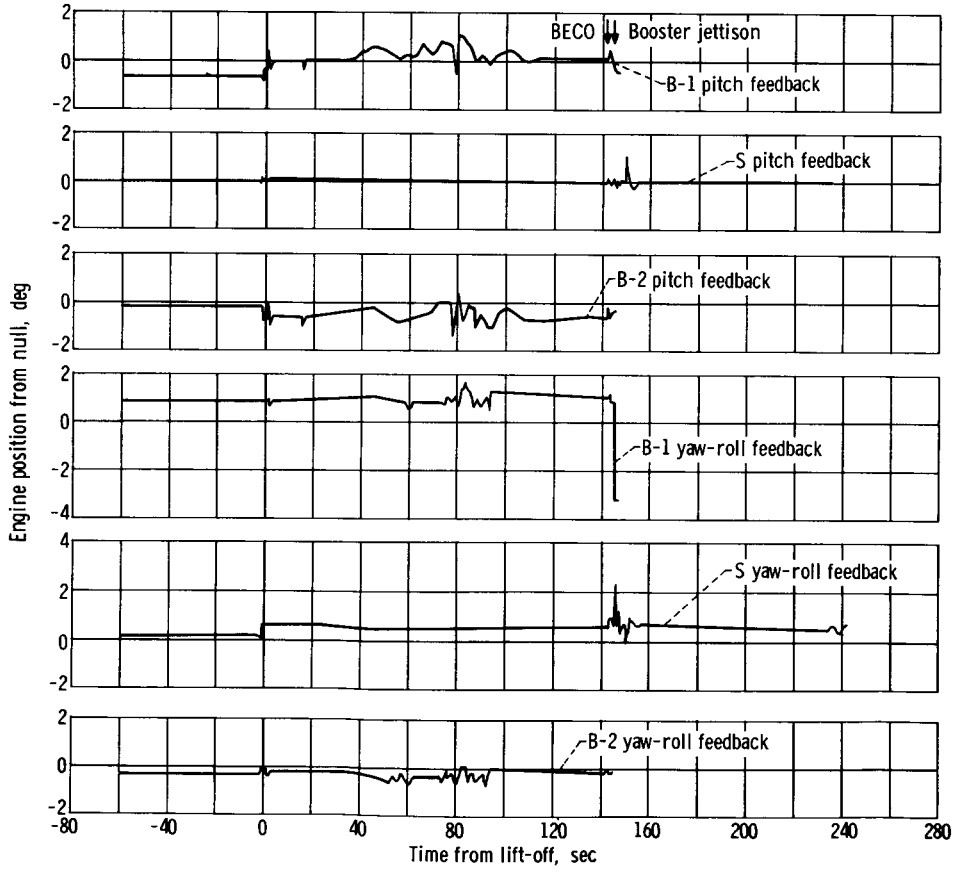

Figure VI-22. - B-1, S, B-2 engine positions.

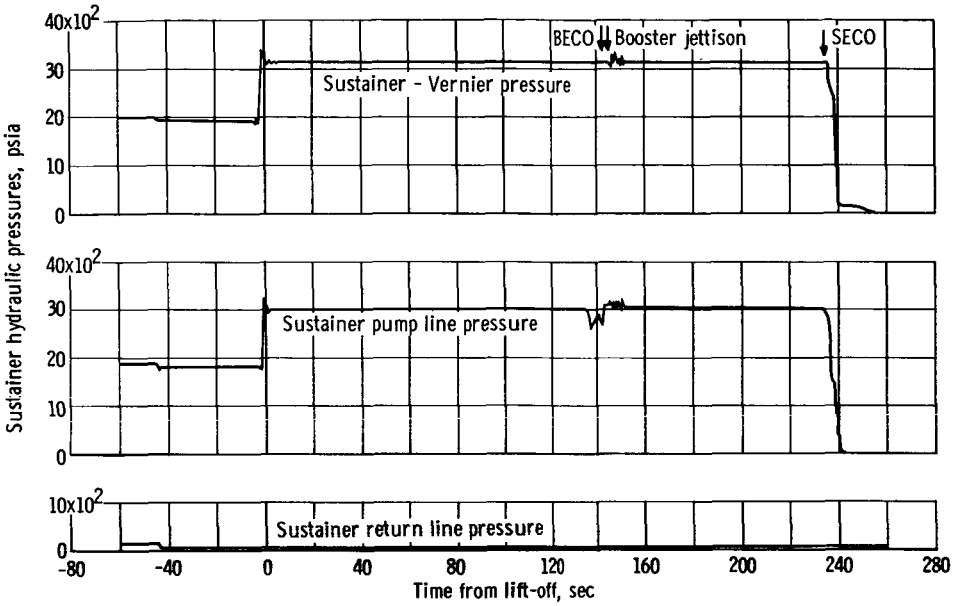

Figure VI-23. - Sustainer hydraulic pressures.

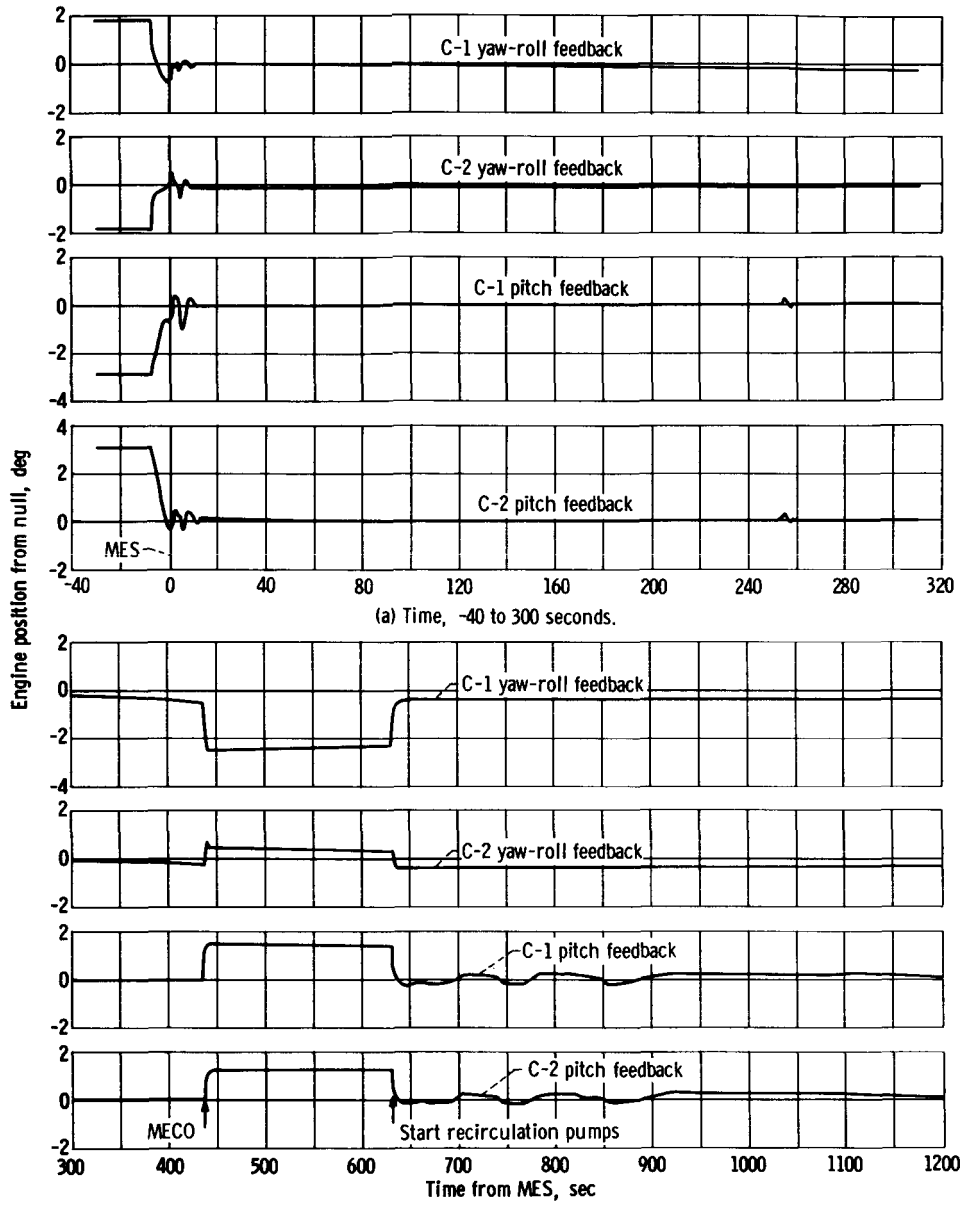

(a) Time, -40 to 300 seconds.

(b) Time, 300 to 1200 seconds.

Figure VI-24. - C-1 and C-2 engine positions.

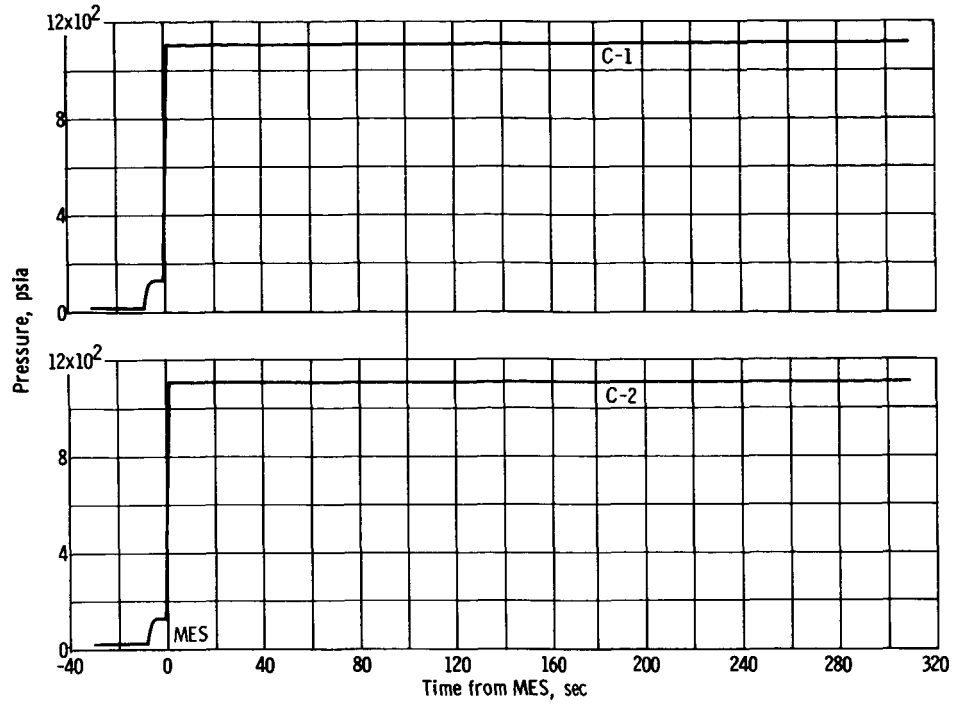

Figure VI-25. - C-1 and C-2 main hydraulic power package pressures.

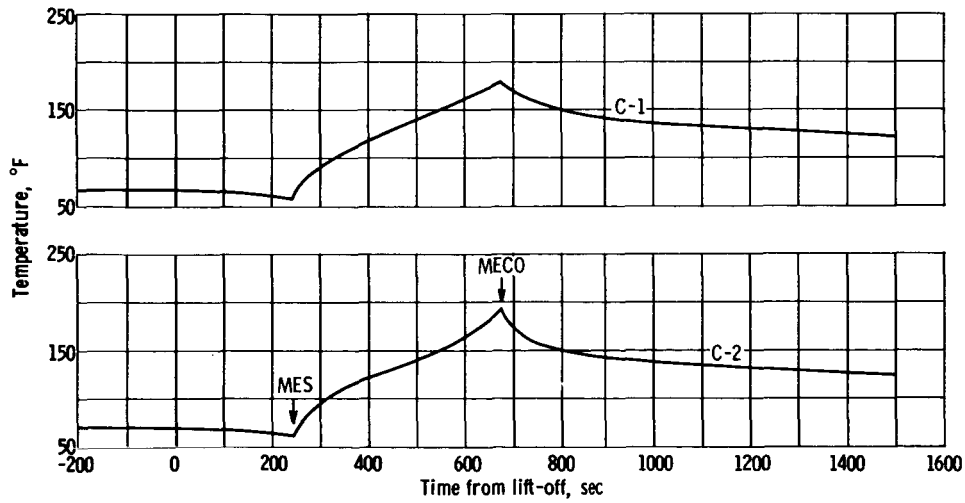

Figure VI-26. - Hydraulic manifold C-1 and C-2 temperatures.

[redacted]

VII. PROPELLANT SYSTEMS

SUMMARY

The Centaur propellant systems performed satisfactorily in support of the AC-6 flight. Additions to AC-6 were (1) a dual-element hot-wire liquid level sensor system for controlling precise topping levels during tanking and (2) a propellant utilization (PU) system to optimize propellant consumption. Topping rates were easily controlled to maintain minimum ullage levels. The PU system accurately controlled depletion of propellant quantities to within 5 pounds of LH_2 at the time the liquid levels receded below the bottom of the PU probes in the tank.

Tank pressurization and venting were successful throughout the flight, and the vent valves controlled within specified pressure limits. The pressure rise rate (3.73 psi/min) in the LH_2 tank was lower than expected during initial primary vent-valve lockup, T - 7 to T + 67 seconds. This was believed to be a result of cold helium purge gas leaking through the forward bulkhead seal and possibly some GH_2 leakage through the vent valve. The AC-6 was tanked to a minimum ullage, and the boiling on unlocking the low-pressure relief valve appears to have resulted in about 50 pounds of LH_2 entrainment.

Blowdown of the residual propellants through the engines to provide retromaneuver thrust was accomplished without incident. Pressure decay rates in the LH_2 and LO_2 tanks were in good agreement with predicted values based on conditions with 50 percent of the propellants settled.

The Atlas sustainer stage operation was successfully terminated in a planned propellant depletion mode by the fuel-depletion system. This was the first time this system was utilized to initiate sustainer engine cutoff.

CENTAUR PROPELLANT LOADING

The AC-6 Centaur tank was the first to utilize a new propellant level indicating system (PLIS) for loading propellants to proper flight levels. The system consisted of three dual-element hot-wire liquid level sensors in the hydrogen tank and four dual-element hot-wire level sensors in the LO_2 tank, as shown in figure VII-1. In conjunction with the PLIS, a refined topping system was installed to enable propellant "topping flow" rates as low as 3 gpm for fine level control.

To assure proper liquid levels at lift-off (T - 0), propellants were "topped" until T - 90 seconds. The requirement at this time was that the topping-low sensor be wet in the hydrogen tank and the topping-high sensor be

[redacted]

wet in the LO_2 tank. This requirement was adequately met, as shown in figure VII-2, with the LO_2 topping-high sensor indicating dry at T - 73.5 seconds and the LH_2 topping-low sensor going dry at T - 26 seconds. Propellant weights at lift-off are summarized in table VII-I.

CENTAUR PROPELLANT UTILIZATION SYSTEM

System Description

The AC-6 flight was the first test of the Centaur propellant-utilization (PU) system that demonstrated the capability of the system to operate in a closed-loop configuration. The system, as shown in figure VII-3, is used during tanking to indicate propellant masses and during flight to optimize propellant consumption. In flight, the mass of propellant remaining in each tank is sensed by a capacitance-type probe (transducer assembly) and compared in a bridge-type circuit. If the mass ratio of propellants (oxidizer to fuel ratio) in the tanks at any time varies from a predetermined value (usually 5), an error signal is sent to the proportional servopositioner that controls the LO_2 engine flow valves. If the mass ratio is greater than 5, the LO_2 flow to the engines is increased to return the mass ratio within the tanks to 5. If the mass ratio is less than 5, the LO_2 flow to the engines is decreased. Since the sensing probes do not extend the full length of both tanks, PU control is not effected until approximately 90 seconds after main engine start. For this 90 seconds of engine burn, the LO_2 flow-control valves are nulled (locked at a nominal flow mixture ratio of 5).

System Performance

All prelaunch checks of the system were within required limits and specifications. The PU LH_2 and LO_2 quantity readouts during tanking are shown in figure VII-4. Again, it should be noted that the PU probes do not extend the full length of the tanks and, therefore, do not indicate the final amount of tanked propellants. Table VII-II summarizes prelaunch checks of the PU system.

Inflight performance of the PU system was satisfactory. The liquid levels reached the top of the LO_2 probe at MES + 89.5 seconds and the LH_2 probe at MES + 95.1 seconds. The PU valves, as shown in figure VII-5, nulled by the programer until MES + 90 seconds, were unnulled properly and immediately moved to the LO_2-rich position and remained there until MES + 193.5 seconds. During this time (MES + 90 to MES + 193.5 sec), 228±25 pounds of excess LO_2 were consumed; 160 pounds of error bias, plus 68 pounds of tanking error and engine mixture ratio error accumulated during the first 90 seconds of engine burn. The PU valves oscillated about null from MES + 193.5 to MES + 423.6 seconds (Δ time = 281.1 sec). During this time, the system corrected for a -514±100 pound steady-state LO_2 error; that is, the valves decreased the LO_2 flow so that the engines burned at a fuel-rich mixture ratio. All these calculations have been made with the assumption that nominal engine inlet conditions existed throughout engine burn. At MES + 423.6 seconds, the LO_2 level passed the bottom of the LO_2 probe, and 2.2 seconds later, the LH_2 level receded below the bottom of the LH_2

probe. At this time, the flow control valves went to the LO_2-rich stops and remained there until MECO. Figure VII-6 shows the propellant quantities as indicated by the PU probes as a function of time during engine burn.

System Accuracy

At LO_2 probe uncovery (level passing the bottom of the probe) 25.8 pounds of LH_2 were indicated by the LH_2 probe (hydrogen remaining in tank above bottom of probe). This represents the 2.2-second uncovery time difference between the LO_2 and LH_2 probes. The error bias, which was 160 pounds of LO_2, was effectively reduced to 123 pounds as a result of a larger amount of gaseous hydrogen than expected remaining in the tank. Therefore, at LO_2 probe uncovery, 24.6 pounds of LH_2 (123 lb LO_2 at a ratio of 5 equals 24.6 lb LH_2) indicated by the probe. The PU system error then would be 25.8 - 24.6 = 1.2 pounds of LH_2. A conservative number for PU error would be less than 5 pounds of LH_2 indicated by the LH_2 probe above the probe bottom at the time the LO_2 level passed the bottom of the LO_2 probe.

PROPELLANT RESIDUALS AT MECO

Liquid Residuals

The LO_2 and LH_2 residuals were calculated by using the time that the propellant levels passed the bottom of the PU probes as a reference point. The total LO_2 residual was 271.1 pounds with 202.8 pounds of this being burnable LO_2. The total LH_2 residual was 163.2 pounds with 91.3 pounds of this being burnable LH_2. For calculations of these residuals see appendix B.

Gaseous Residuals

The gaseous residuals of 83 pounds of GH_2 and 165 pounds of GO_2 were calculated by using ullage temperature and pressure data at MECO obtained from figures VII-7 and 8, respectively. The hydrogen residual calculations were made by utilizing the temperature profile in the tank at MECO and reflect temperature stratification in the tank. The oxygen residual was based on the three ullage temperature measurements in the tank.

CENTAUR PROPELLANT TANK PRESSURIZATION

Powered-Flight Phase

The LO_2 and LH_2 tank pressures were controlled throughout the AC-6 flight, as shown in figure VII-7. It should be noted that the LH_2 pressure rise rate during initial number 1 vent-valve lockup, T - 7 to T + 69 seconds, was low (3.73 psi/min). As a result, the number 2 vent valve did not relieve until T + 67 seconds, only 2 seconds before the number 1 vent valve was unlocked and tank pressure was relieved to allow pressures to remain within structural limits.

The cause of the low pressure rise rate is believed to be twofold. A leak in the forward station 208 seal allowed very cold helium purge gas, from between the LH_2 tank and the insulation panels, to escape into the forward equipment area and cool the forward bulkhead. Evidence of such a leak was indicated by the low temperatures of electronic equipment in the forward bulkhead area prior to lift-off. (See section VIII for equipment temperatures.) In addition, the primary hydrogen vent valve may not have been fully seated. Photographic coverage gives evidence of continued hydrogen venting from the vent fin during the early seconds of flight.

Tank ullage temperatures are shown in figure VII-8. The LO_2 tank ullage temperature remained essentially at saturation, indicating thermal equilibrium in the tank throughout the flight. The LH_2 tank ullage temperature reflected changes in pressure as expected. The temperature measurement, which was located on the forward bulkhead, again indicated an abrupt temperature drop to LH_2 temperatures at MECO, which provided evidence of LH_2 spray from the boost-pump volute bleed hitting the forward bulkhead. In addition to the ullage temperatures shown in figure VII-8, several additional temperature measurements were made in the tank, as shown in figure VII-9 for the period of engine burn. These measurements were utilized to obtain a temperature profile in the tanks at MECO to enable accurate calculations of gaseous residuals and give some indication of temperature stratification.

Step pressurization of the propellant tanks (burp) to provide the proper NPSH for boost-pump start was normal. The pressure data are summarized in the following table:

Tank	Initial pressure, psia	Final pressure, psia	ΔP, psid
LO_2	29.5	33.3	3.8
LH_2	19.2	21.6	2.4 (1-sec spike)
		20.4	1.2

Pneumatic system operation was also normal and in good agreement with ground testing. Helium bottle pressure was 2820 psia at lift-off and had decreased to 2580 psia by T + 550 seconds. The engine controls pressure regulator and the H_2O_2 controls pressure regulator were 448 to 460 psig and 307 to 314 psig, respectively. The latter was slightly higher until the boost pumps were started as a result of normal regulator lockup. Helium consumption for the burp prior to boost pump start was 0.292 pound.

Propellant Tank Venting

Venting of the LH_2 and LO_2 tanks, as required to maintain a scheduled tank pressure profile, was accomplished successfully on the AC-6 flight. The hydrogen vent flow rate, which was the only one monitored, was invalid because of a

loss of pressure instrumentation at the venturi flowmeter. However, based on known liquid levels at T - 0 and start of PU control, the total propellant ventage prior to Centaur staging has been estimated as follows:

	Propellants, lb	
	LO_2	LH_2
Total propellants tanked	25 521	5 278
Ground boiloff: LH_2 = 0.45 lb/sec (T - 26 to T - 7 sec) LO_2 = 0.326 lb/sec (T - 73.5 to T - 0 sec)	26	9
Total propellants at T - 0	25 495	5 269
Propellants consumption, engine chilldown to PU probe uncovery: LO_2 T + 234.4 to T + 332.5 sec LH_2 T + 234.4 to T + 338.5 sec Remaining propellants and ventage at PU start Actual propellants at PU start	5 197 20 298 20 240	1 122 4 147 4 018
Total propellants vented	58	129

The GO_2 vented was low as expected, but the indicated hydrogen ventage was high. Previous flights indicated that the total hydrogen vented during this time was about 70 to 80 pounds. This increased ventage on AC-6 (129 lb - 80 lb = 49 lb) may be attributed to liquid entrainment during periods of tank blowdown after vent-valve lockup periods. A sudden drop in pressure upon unlocking the lower relief valve produces boiling, and with a very low ullage (about 13 cu ft on AC-6), liquid droplets could easily be entrained in the vent discharge.

Retromaneuver Blowdown

Current separation requirements between the spacecraft and Centaur are 336 kilometers in 5 hours. To effect this separation distance, Centaur is turned 180° to the injection velocity at T + 752.8 seconds, and a retrothrust is applied at T + 872.8 seconds, terminating at T + 1853.8 seconds. The thrust force is provided by venting residual hydrogen through the chilldown valves and residual oxygen through the engine nozzles. Analysis of flight data indicated that the spacecraft-Centaur separation distance after 5 hours was 1300 to 1600 kilometers, which is considerably in excess of the minimum separation requirement.

Tank pressure histories during the retromaneuver, as shown in figure VII-10 were normal, and agreed well with analytical predictions for the 50 percent liquid settled case. Pressure in the LH_2 tank increased from MECO to start of retroblowdown at an average rate of about 0.77 psi per minute, then showed a

gradual decline. Pressure in the LO_2 tank continued to increase at an average rate of about 0.33 psi per minute until 87 seconds after the start of retroblowdown before the downtrend was observed. From the shape of the tank pressure profiles, it appeared that venting of mixed phase or trapped liquid occurred during this period.

Tank pressures in both tanks continued to decay from T + 960 seconds to the end of the retromaneuver at T + 1853.8 seconds. The average rate of pressure decay was 0.96 psi per minute in the LH_2 tank, and 1.18 psi per minute in the LO_2 tank. Tests (ref. 9) had shown that, under suitable conditions, solid hydrogen would form and tend to adhere to the vent duct when LH_2 was exhausted to an ambient pressure below its triple point. The tank pressure history and attitude control duty cycles in this period, however, showed no apparent evidence of any adverse effects due to solid hydrogen formation in the chilldown vent ducts. At T + 1853.8 seconds, the blowdown valves closed, and both tanks experienced a gradual rise in pressure.

BOOSTER FUEL DEPLETION SYSTEM

The flight of AC-6 was the first Centaur mission in which the sustainer stage flew to propellant depletion and utilized propellant depletion systems (LO_2 and fuel) to initiate SECO. The fuel depletion system had flown for the first time on AC-4 in an open-loop configuration. Pressure switches, used to detect LO_2 depletion, had served only as a backup for triggering engine shutdown on all previous flights. An additional backup signal to the propellant depletion scheme was provided by Centaur guidance, capable of SECO initiation at 0.7 g.

The most probable mode of shutdown, based on propellant tanking, is the depletion of LO_2 before fuel. This was the case experienced in the flight of AC-6. In order to detect LO_2 depletion, two series-connected sustainer-engine-fuel manifold-pressure switches are activated by a decay in fuel-manifold pressure that results from a drop in LO_2 pump NPSH. When both pressure switches close, a signal is transmitted to the autopilot to initiate SECO (fig. VII-11).

In the event that fuel depletes first, detection is made by two magnetostrictive sensors, mounted on a common probe and located in the fuel tank, with the sensing point at station 1194.27 (fig. VII-12). Two series-connected sensor controller units located in the B-1 pod receive the "dry" feedback signals from the sensors and, in turn, relay a 28-volt signal to the autopilot. Both sensors must indicate "dry" before a shutdown signal can be transmitted.

In addition to the functional system just described, there is a duplicate and independent evaluation system with similar sensors located in the fuel tank, with the sensing fuel level at station 1168.50. These sensors are positioned sufficiently high in the tank to be uncovered on all flights (evaluation system will be flown through AC-8 only). Outputs from this system are transmitted to the telemetry system alone and are not utilized for any command functions (fig. VII-13).

The fuel-depletion system operated without anomalies on AC-6 as indicated

by telemetry measurements of each of the four sensor controller relays. The data were quite similar to those obtained from the AC-4 flight. The evaluation sensors indicated approximately four uncover-cover cycles during a 2.2-second period commencing at T + 208.5 seconds (fig. VII-14). Slosh oscillations of this nature were expected because of the location of the probe near the tank wall with exposure to undampened fuel movement. At T + 210.7 seconds, the evaluation sensors remained dry until after retrorocket firing. At T + 237.2 and T + 241.8 seconds, sensor A indicated wetting for 1/2-second periods as a result of fuel sloshing.

The functional sensors remained covered with fuel until 2.5 seconds following SECO (T + 236.6 sec). At this time the sensors were uncovered due to the forward movement of the fuel after retrorocket firing. Sensor A gave three momentary wet signals at T + 240.6 and T + 246.1 seconds (2 cycles) before remaining dry, indicating continued fuel movement. Had not the engines sensed LO_2 depletion, there would have been 2.5 seconds additional burn time remaining until the fuel-depletion system would have triggered shutdown.

TABLE VII-I. - AC-6 PROPELLANT LOADING

	Propellant	
	LH_2	LO_2
Sensor required to be wet at T - 90 sec	Topping low	Topping high
Sensor station number	174.99	373.16
Volume[a] at sensor, cu ft	1256.69	370.94
Ullage volume at sensor, cu ft	11.22	6.58
LH_2 topping-low sensor dry at sec	T - 26	--------
LO_2 topping-high sensor dry at sec	-------	T - 73.5
Ullage pressure, psia	21.8	30.5
Density[b], lb/cu ft	4.2	68.8
Weight in tank at time sensor goes dry, lb	5278	25 521
LH_2 boiloff to vent-valve lock at T - 7 sec, lb	9	--------
LO_2 boiloff to T - 0 sec, lb	-------	26
Ullage volume at lift-off, cu ft	13.5	6.9
Weight at lift-off, lb	5269	25 495

[a]Volumes include 1.85 cu ft LO_2 and 2.53 cu ft LH_2 for lines from boost pumps to turbopump inlet valves.

[b]Densities are taken from curves for vapor pressure against density from ref. 10.

TABLE VII-II. - PROPELLANT UTILIZATION SYSTEM

PREFLIGHT CHECKS

Time, min	PU valve slew rates, deg/sec		
	C - 1	C - 2	Limits
T - 44	9.20	9.35	6 to 12
T - 9	9.50	9.20	6 to 12

PU valve crossover points (time of check, T - 59 min)

The following equation must be satisfied:

$5\ LH_2 - LO_2 = 160 \pm 300$ lb

For check:

$LH_2 = 2\ 880$
$LO_2 = 14\ 045$

therefore

$5\ LH_2 - O_2 = 355$ lb

Full quantity check (time = T - 52 min)

Propellant	Quantity, lb	Requirement, lb
LH_2	3 860	3 880±200
LO_2	19 425	19 400±1000

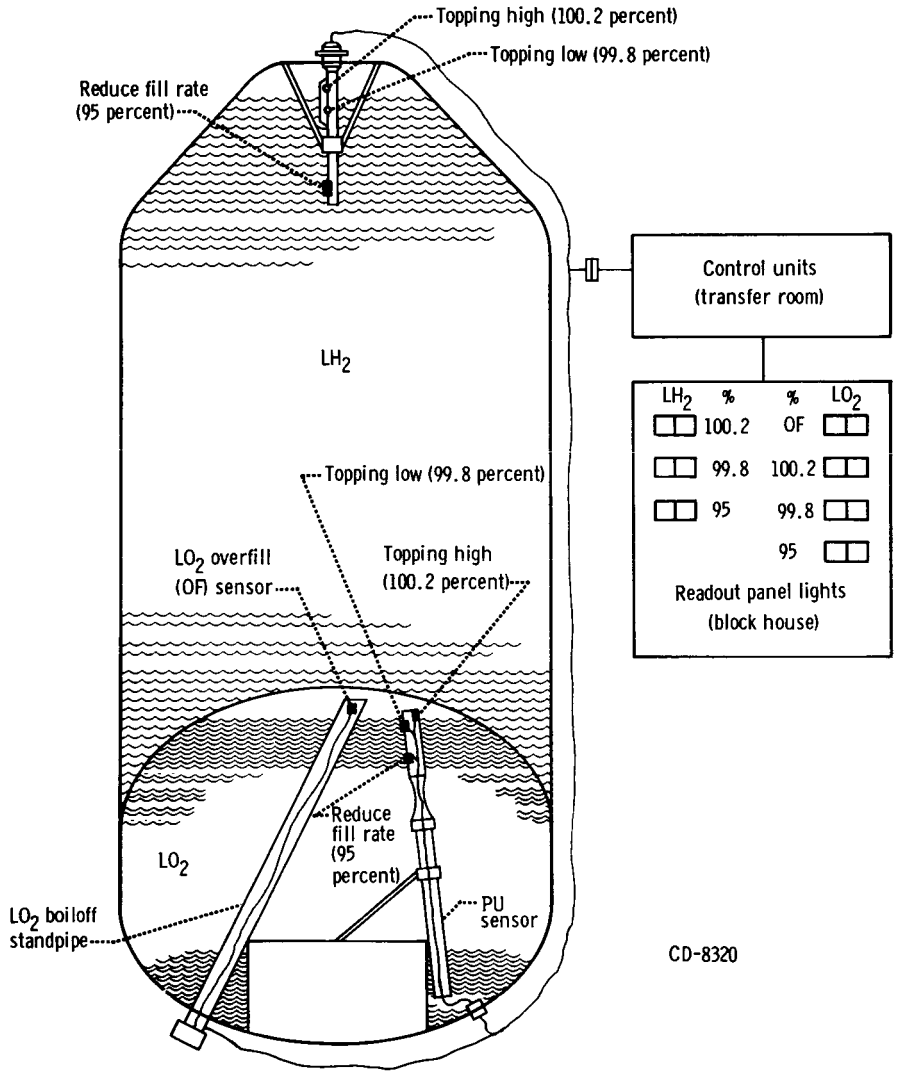

Figure VII-1. Centaur propellant level indicating system.

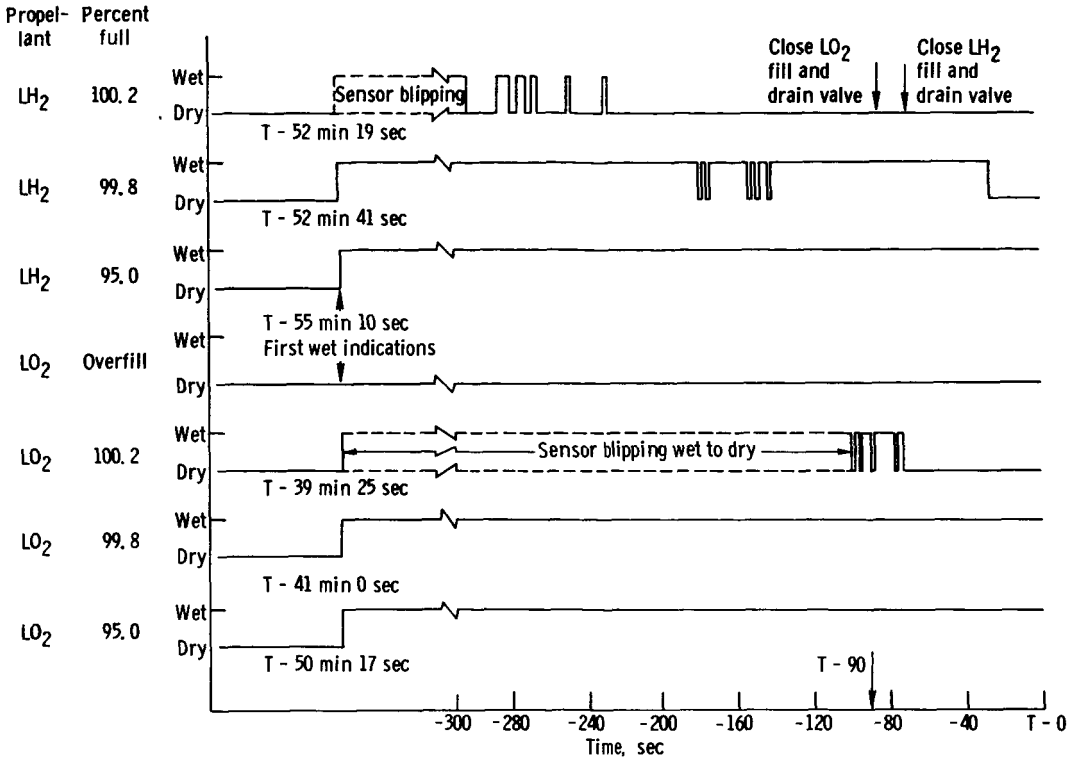

Figure VII-2. - Centaur propellant level indicating system operation.

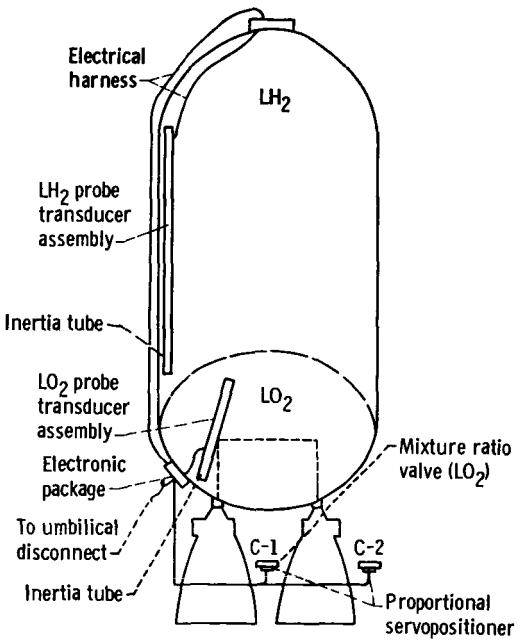

Figure VII-3. - Centaur propellant utilization system schematic.

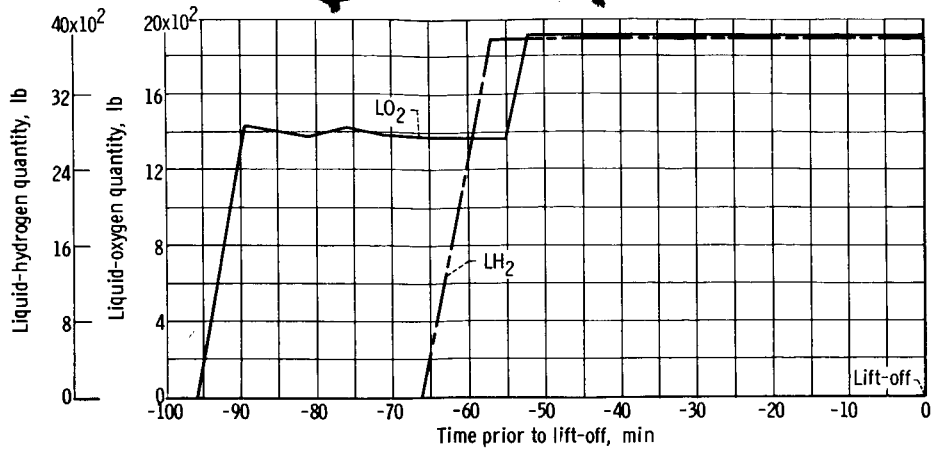

Figure VII- 4. - Propellant utilization liquid-oxygen and liquid-hydrogen quantities.

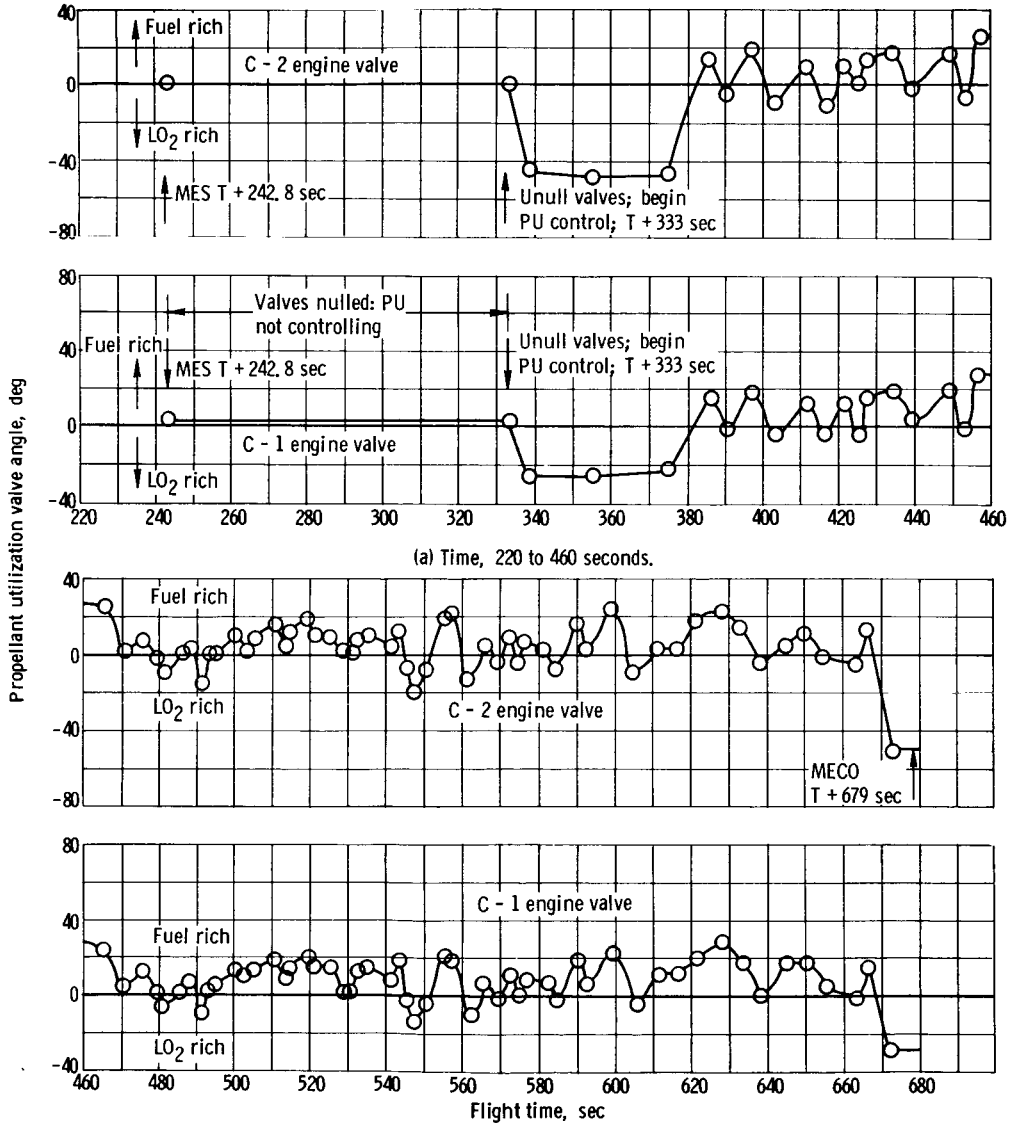

(a) Time, 220 to 460 seconds.

(b) Time, 460 to 680 seconds.

Figure VII-5. - Propellant utilization valve angle as function of time.

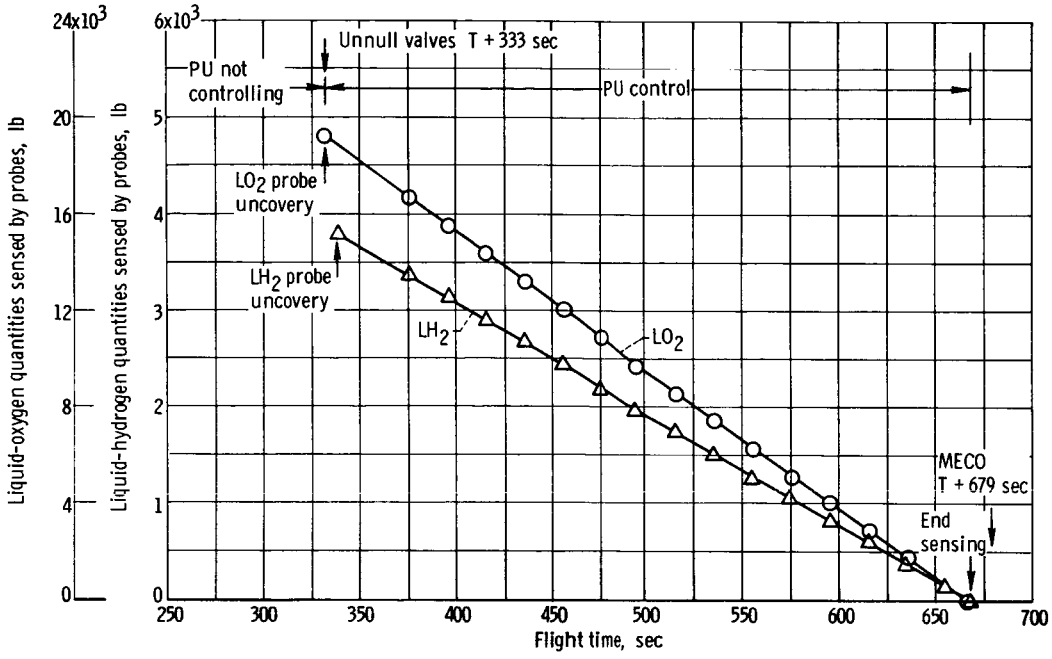

Figure VII-6. - Propellant quantities from propellant-utilization probes.

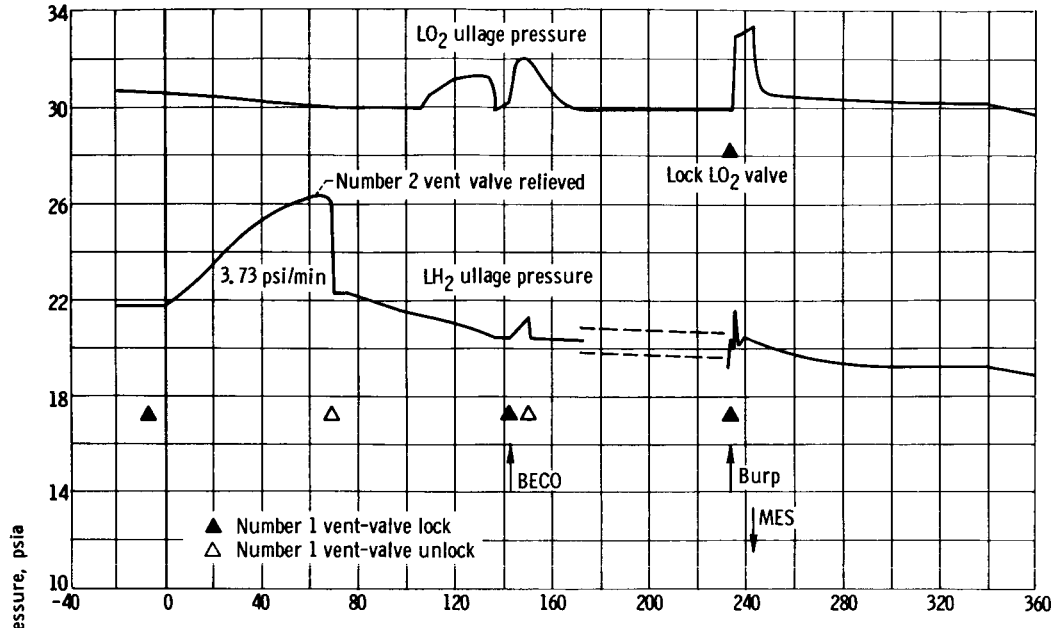

(a) Time, -40 to 360 seconds. Pressure varied during period from insulation-panel jettison (T + 172.7 sec) to SECO (T + 234.8 sec) at approximately 1 cps. The dashed lines indicate the maximum excursions: most were less.

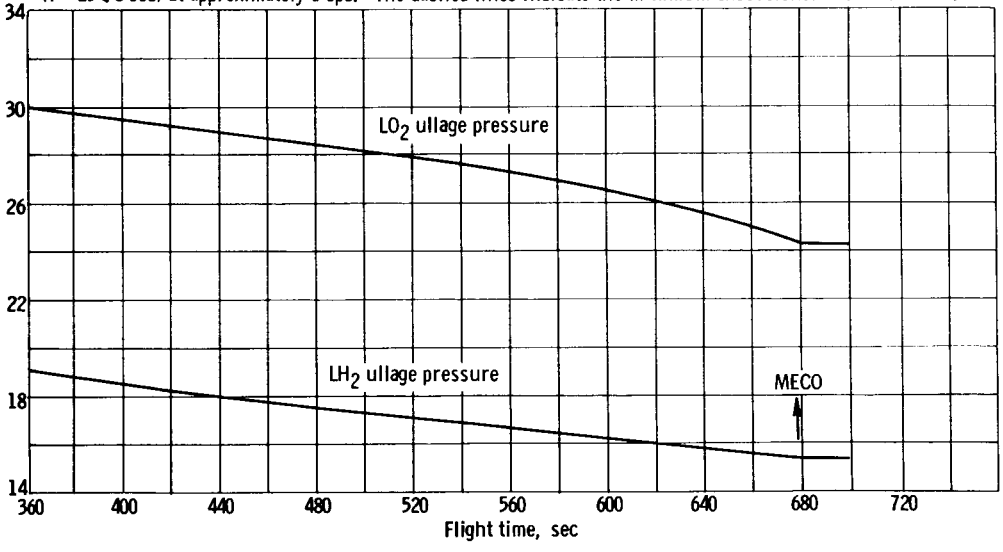

(b) Time, 360 to 720 seconds.

Figure VII-7. - Propellant tank pressures.

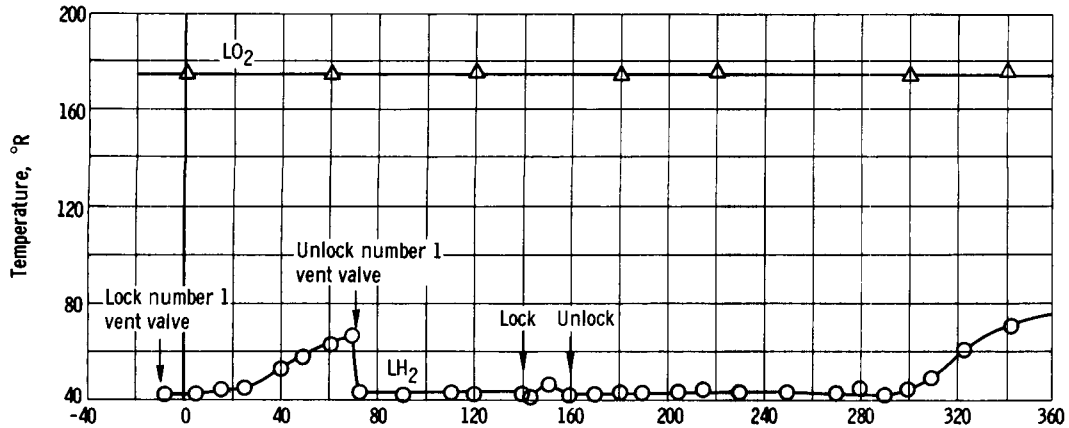

(a) Time, -40 to 360 seconds. Liquid-hydrogen temperature measurement at station 162, CF100T; liquid-oxygen temperature measurement at station 370, CF6T.

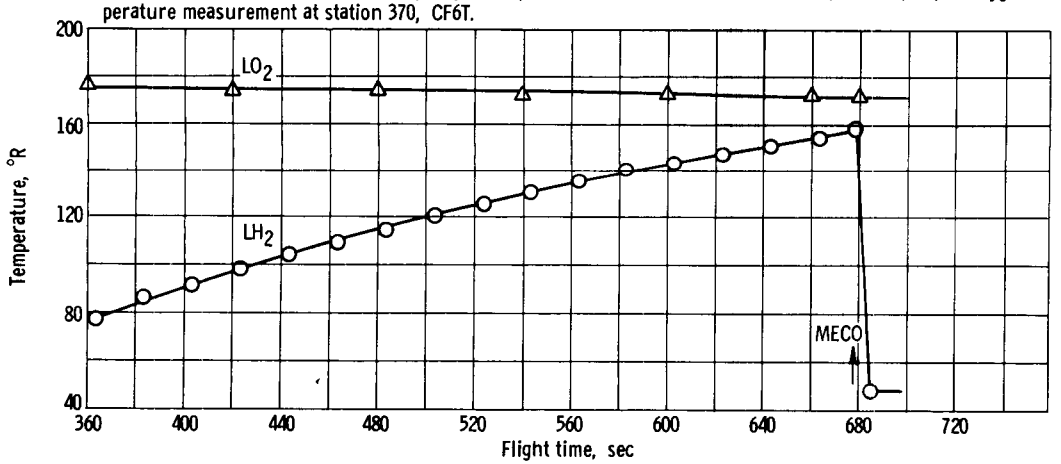

(b) Time, 360 to 720 seconds. Sudden temperature drop at MECO is spray from liquid-hydrogen boost-pump volute bleed hitting forward bulkhead.

Figure VII-8. - Propellant tank ullage temperatures.

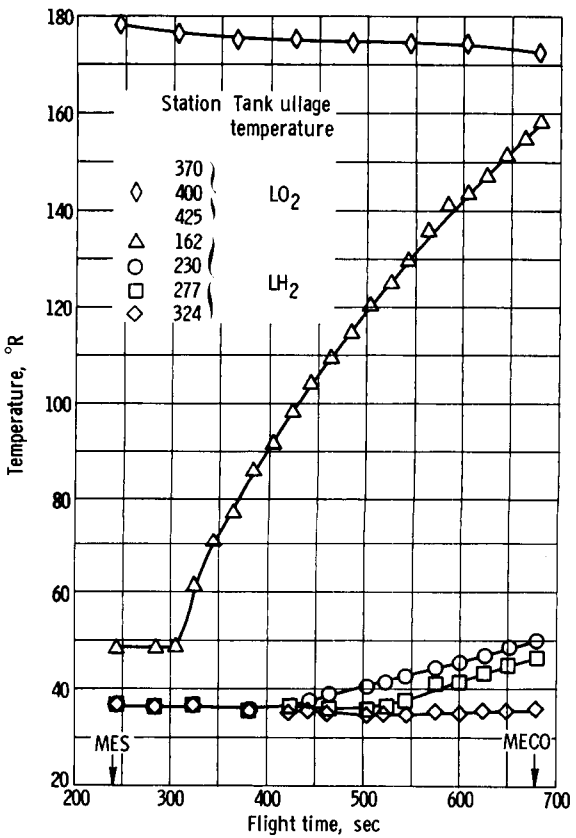

Figure VII-9. - Propellant tank ullage temperature during engine burn.

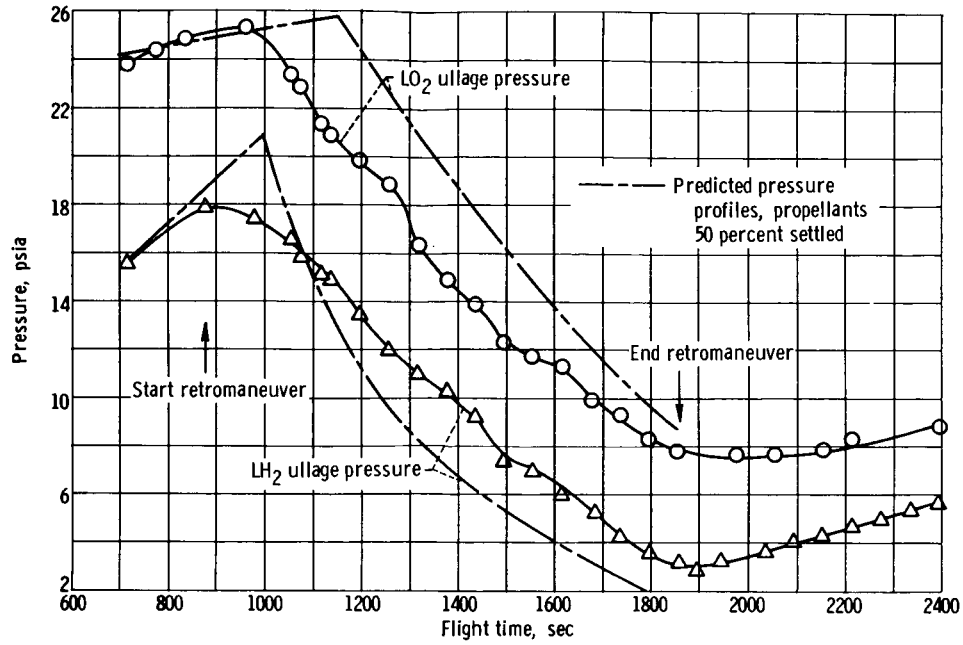

Figure VII-10. - Propellant tank pressures during retromaneuver.

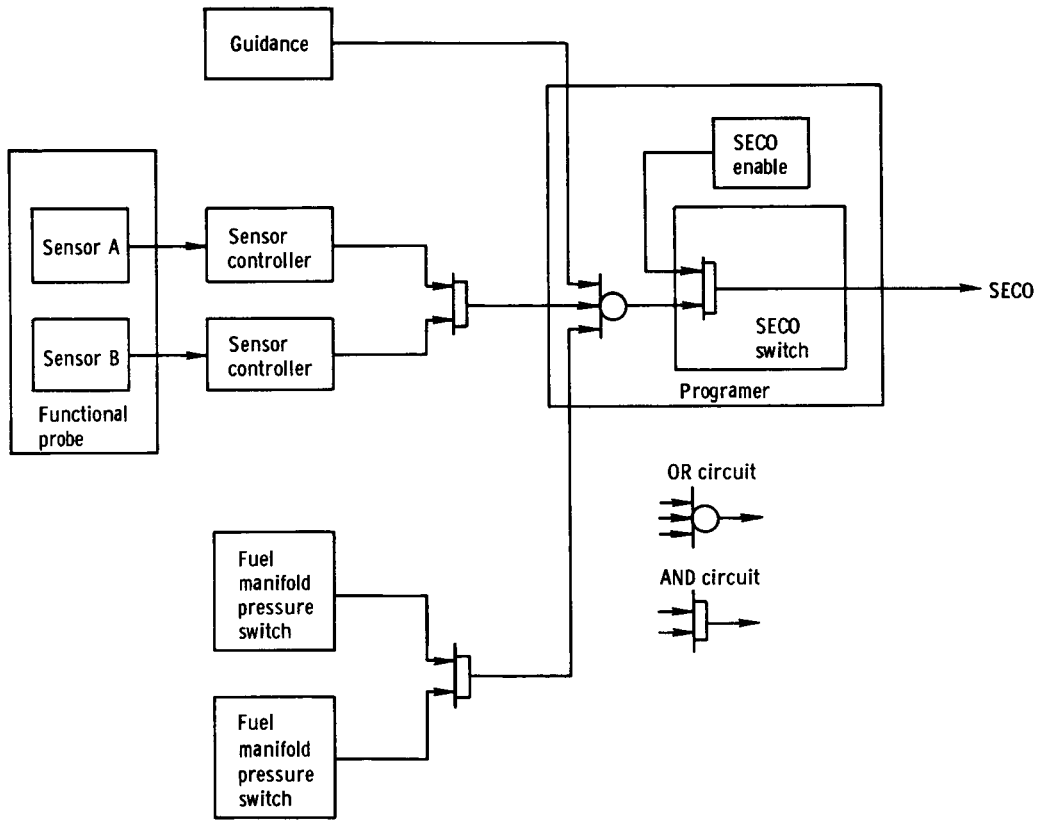

Figure VII-11. - Booster fuel depletion system circuit.

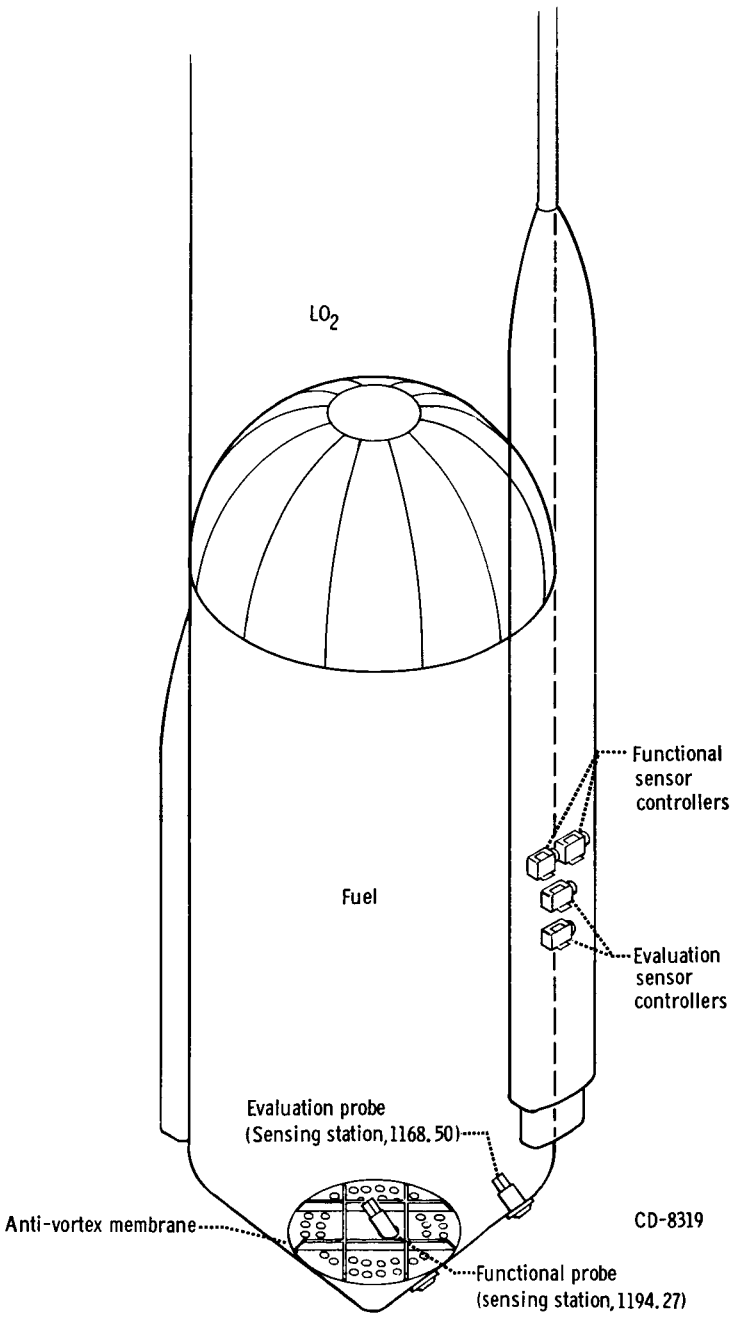

Figure VII-12. - Location of booster fuel depletion system sensors.

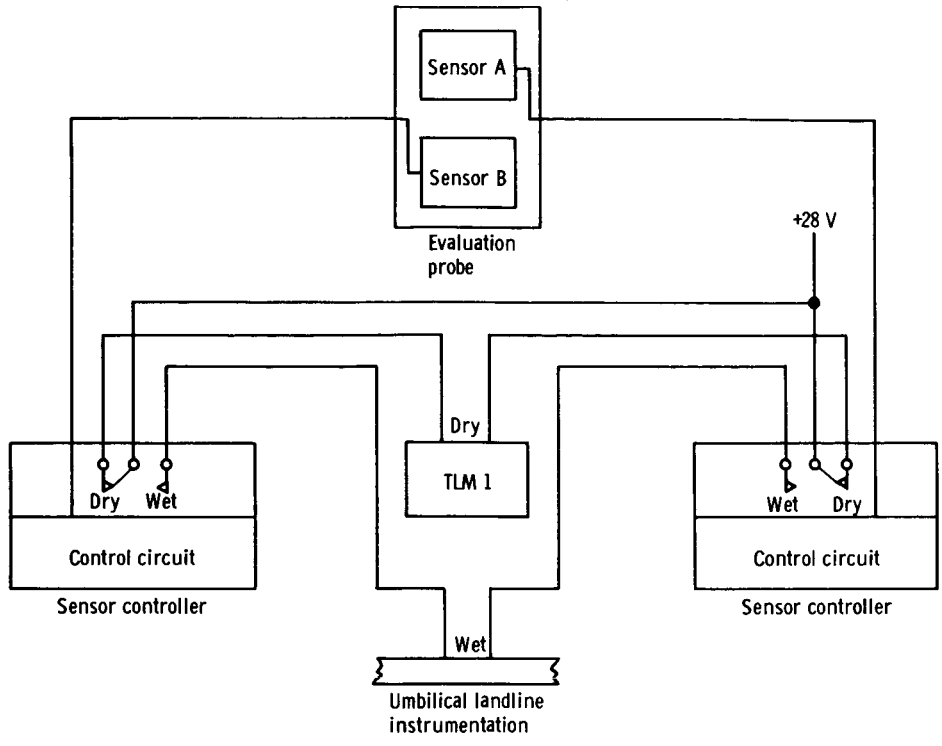

Figure VII-13. - Booster fuel depletion evaluation sensor system circuit.

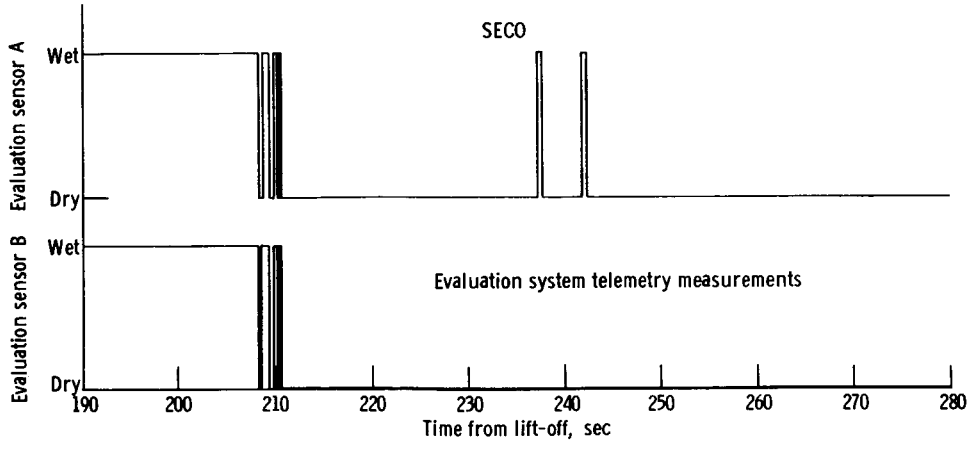

Figure VII-14. - Booster fuel depletion system evaluation sensors operation.

[redacted]

VIII. ENVIRONMENTAL TEMPERATURES

SUMMARY

The AC-6 environmental temperature profiles during flight were generally satisfactory, indicating adequate thermal control. Limited use of Thermolag provided additional protection for the nose-fairing and insulation panels, and the maximum skin temperatures due to aerodynamic heating were in good agreement with predicted values. Maximum measured flight temperatures were 1450° F at the nose-cap stagnation point and 826° F on the leading edge of the hydrogen vent stack. The high indicated nose-cap temperatures, however, were erroneous due to a poor thermocouple installation.

Internal temperatures in the payload compartment and the Centaur thrust section were nominal. In the Centaur forward equipment area some unusually low temperatures were experienced, particularly at the number 1 telemetry package, which had a skin temperature of -16° F or lower at lift-off. These low temperatures indicated the possibility of a cold helium gas leak through the station 208 seal.

EXTERNAL THERMAL ENVIRONMENT NOSE-FAIRING AND INSULATION PANELS

Measured external temperatures on the nose-fairing and insulation panels are shown in figures VIII-1 to 4. Table VIII-I also compares maximum measured temperatures with the predicted temperatures. The maximum measured temperature on the phenolic nose cap was 1450° F compared with a preflight prediction of 850° F. However, the nose-cap measurements were not valid because of a poor thermocouple installation. The thermocouples in the nose cap had been potted with a low-temperature epoxy that pyrolized at about 400° F. Consequently, the epoxy charred, insulated the thermocouple from the nose cap, and the small isolated mass sensed the higher response to aerodynamic heating as evidenced by the higher temperatures. The thermocouple did not accurately reflect the nose-cap temperature. This theory has been substantiated by postflight tests.

The maximum temperature experienced as a result of aerodynamic heating on the leading edge of the hydrogen vent stack was 826° F at a point 18 inches outboard from the nose fairing. This thermocouple installation was integral with the vent stack and was not compromised as in the case of the nose cap. The maximum temperature was less than the predicted 1025° F.

Heating effects on the conical surface of the nosecone were much less and did not exceed 265° F. These temperatures were well below the critical bond (glue) line temperature of 500° F. The effect of the Thermolag used to protect select areas can be noted by comparing figures VIII-2(a) and (b). Temperatures measured under the Thermolag at station 72 were approximately 80° F less than

[redacted]

those without Thermolag. Measured temperatures on the insulation panels along the positive x-axis without Thermolag indicated a peak value of approximately 300° F.

INTERNAL TEMPERATURE CONTROL

Payload Compartment

The payload compartment environmental control and temperature instrumentation are shown in figure VIII-5. The temperature histories of the payload compartment are shown in figure VIII-6. All the temperatures at lift-off gave assurance that a satisfactory thermal environment was maintained throughout the countdown. The Surveyor ambient temperature (CY7T), which was 85° F at lift-off, indicated that the environment in the vicinity of the retromotor was sufficient to meet the requirement of 85°±5° F at lift-off. The temperatures of the spacecraft separation latches, which have a lower temperature limit of 35° F, varied from 73° to 85° F at lift-off.

An attempt was made on this flight to determine the feasibility of monitoring and controlling the conditioning gas temperature at the ground side of the duct disconnect while maintaining the temperature of the gas within the lower airborne duct at 85°±5° F. Figure VIII-7 shows a comparison of these temperatures and indicates that a temperature setting of 83° F on the ground controlling sensor would have met the 85°±5° F requirement. These data will be verified by repeating this procedure on future vehicles.

Interstage Adapter

Extensive temperature instrumentation was installed on the AC-6 interstage adapter to measure the thermal environment. This instrumentation is shown in figure VIII-8. Table VIII-II is a summary of maximum measured temperatures on the AC-6 interstage adapter. Figure VIII-9 is a typical temperature history of the interstage skin.

INTERNAL THERMAL ENVIRONMENT CENTAUR ELECTRONICS COMPARTMENT

Temperatures in the forward equipment area are shown in figures VIII-10 and 11. It can be noted from the thermal mapping of figure VIII-11 that some of the components experienced abnormally low temperatures at lift-off. In particular, the temperature measurement on telemetry package number 1 went off scale at -16° F. These telemetry units have been tested over the range of 20° to 110° F, but the maximum or minimum allowable operating temperatures are not known. A summary of the critical measurements is given in the following table:

[redacted]

Centaur electronics compartment temperature survey		
Equipment	Lift-off temperature, °F	Allowable range, °F
Telemetry package number 1	Below -16	----------
Guidance platform	59	30 to 130
Autopilot servoamplifier	33	10 to 130
C-band transponder	39	-35 to 160
Inverter	68	200(max)

Difficulties with the cold temperatures in the forward compartment were experienced during the quad tanking test and the first launch attempt. Inspection revealed a leak in the forward station 208 seal that allowed cold helium purge gas from between the insulation panels and the tank to leak into the area and cool the components. An attempt was made to repair the seal, but it appears that the failure recurred.

Centaur Thrust Section

Data from the Centaur thrust section indicated adequate thermal control. The H_2O_2 manifold temperature of 80° F at lift-off was below the 120° F maximum allowable. The propellant-utilization electronics package skin temperature of 70° F was well within the 20° to 120° F range allowed.

TABLE VIII-I. - NOSE-FAIRING AND INSULATION-PANEL MAXIMUM TEMPERATURES

Measurement	Station	Axis	Measured		Predicted		Thermo-lag	Remarks
			Temperature, °F	Time, sec	Temperature, °F	Time, sec		
Nose-cap stagnation point	---	--	1450	146	850	149	No	Questionable thermocouple installation; data invalid
30° from stagnation point	---	--	1352	139	751	146	No	
Nose-fairing conical surface	19	+y	262	121	375	140	No	
	72	+y	230	121	375	140	No	
	125	+y	220	130	375	140	No	
	72	+x	152	130	180	110	Yes	
	72	-x	188	160	180	110	Yes	
Nose-fairing barrel section	185	+y	155	125	200	130	No	
Wiring tunnel	314	+x	184	125	165	120	No	
Boost-pump fairing	362	+x	270	135	260	125	No	
	400	+x	295	130	260	125	No	
Leading edge of H_2 vent stack	---	--	826	150	1025	150	No	
Umbilical island	---	--	100	197	120	197	No	

[redacted]

TABLE VIII-II. - INTERSTAGE ADAPTER MAXIMUM TEMPERATURES

Measurement	Station	Quadrant	Measured		Predicted	
			Temperature, °F	Time, sec	Temperature, °F	Time, sec
AA224T	444	I	116	127	180	120
AA225T	465	I	140	120	176	126
AA226T	484	I	154	130	175	127
AA227T	499	I	152	130	170	133
AA244T	418	III	164	117	114	135
AA669T	430	I	180	127	183	120
AA670T	450	I	220	120	180	120
AA671T	450	II	135	130	180	120
AA672T	461	II	130	137	180	120
AA673T	490	II	110	120	169	133
AA674T	510	II	105	120	215	170
AA675T	419	II	230	126	290	142
AA676T	422	IV	150	120	188	160
AA677T	503	IV	120	160	230	170
AA814T	507	III	250	130	290	142
AA821T	535	-y-axis	262	130	290	142

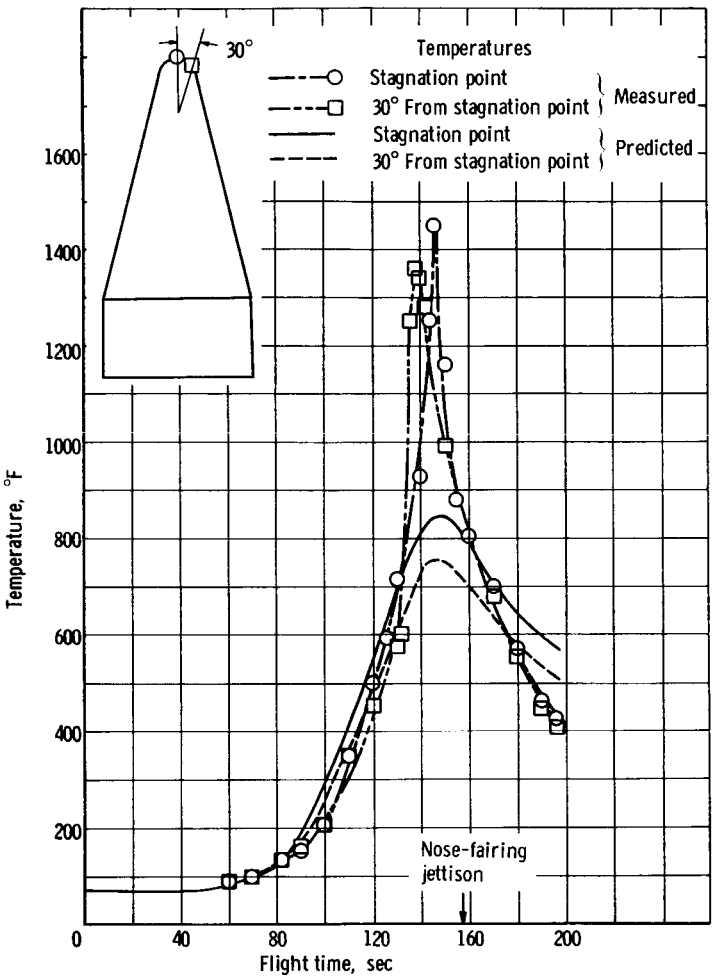

Figure VIII-1. - Nose-cap temperatures.

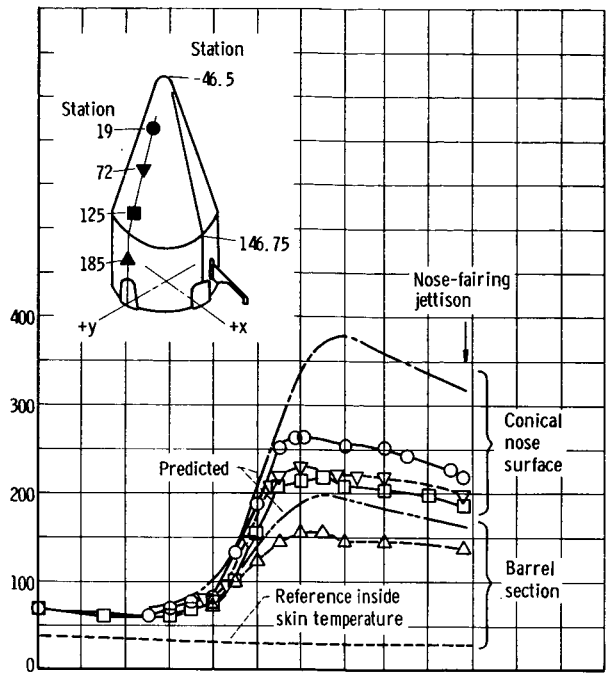

(a) y-Axis. Temperature measurements shown are in center of 4-inch-diameter area not covered with Thermolag. Other areas of nose fairing covered by Thermolag T-230.

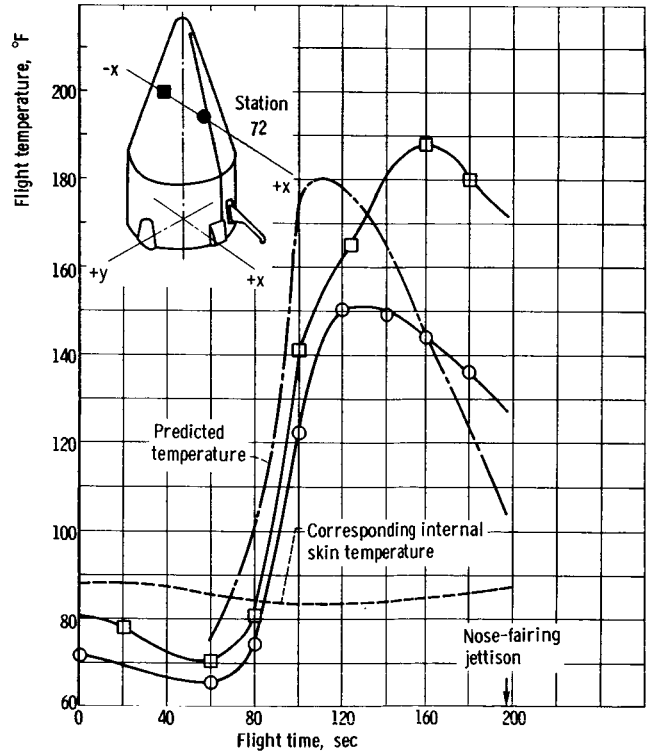

(b) x-Axis. Thermocouples covered with layer of Thermolag 0.046 to 0.056-inch thick.

Figure VIII-2. - Nose-fairing skin temperatures.

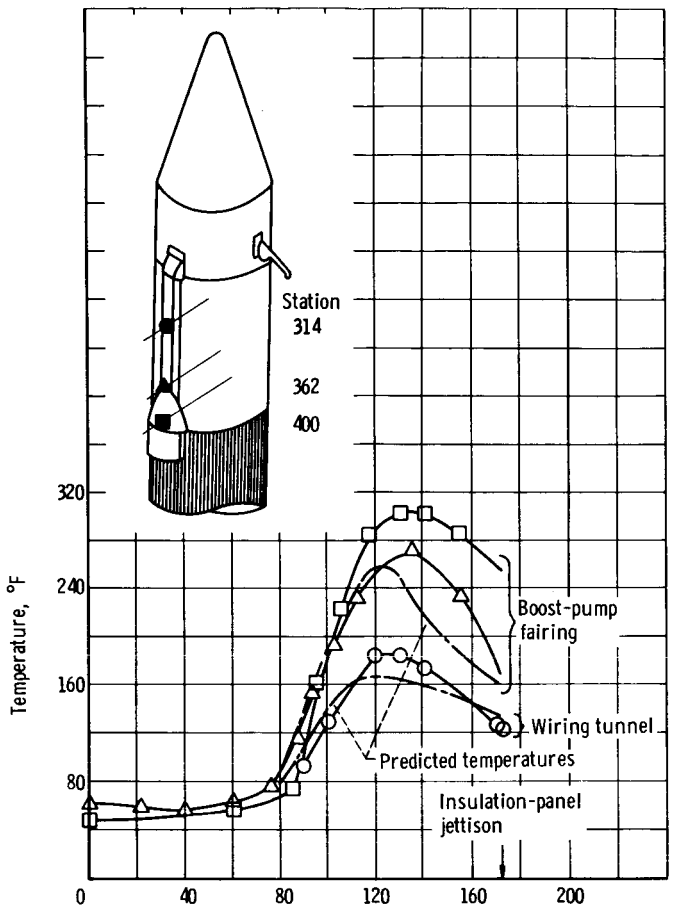

(a) Insulation panel protuberance temperatures.

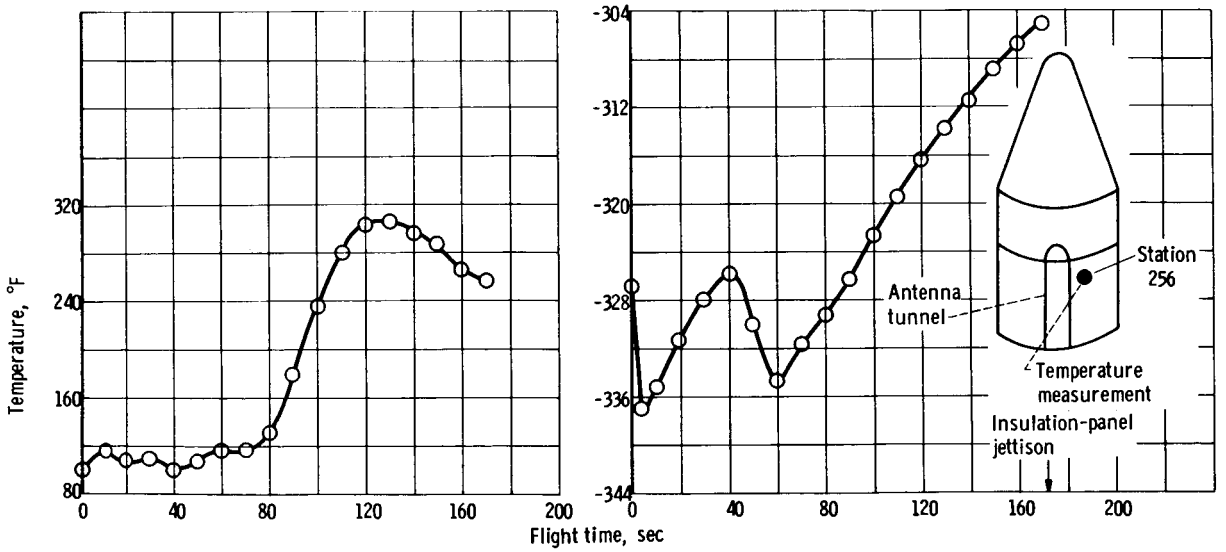

(b) Outside temperature.

(c) Inside temperature.

Figure VIII-3. - Insulation panel temperatures.

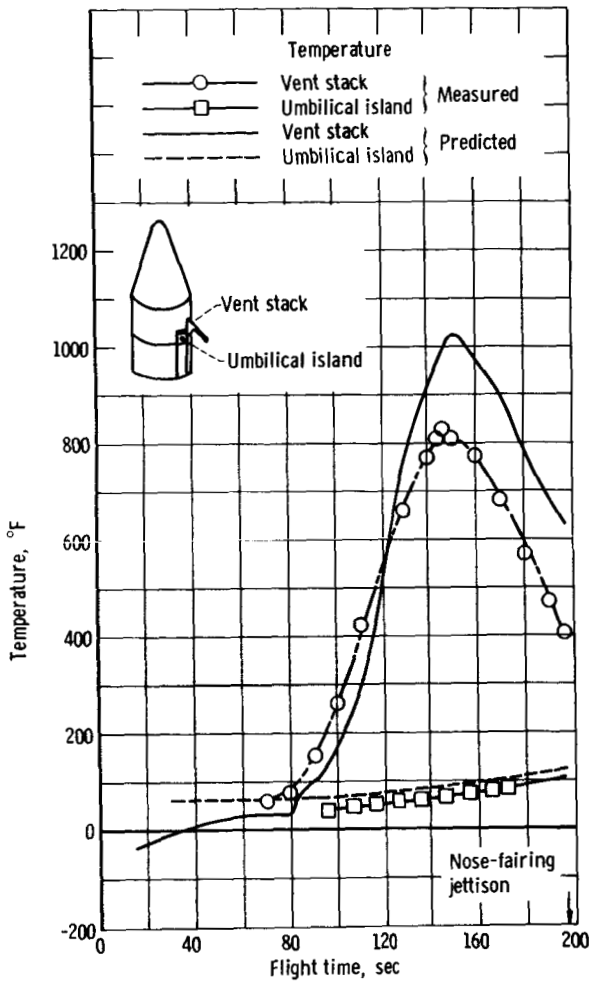

Figure VIII-4. - Protuberance temperatures.

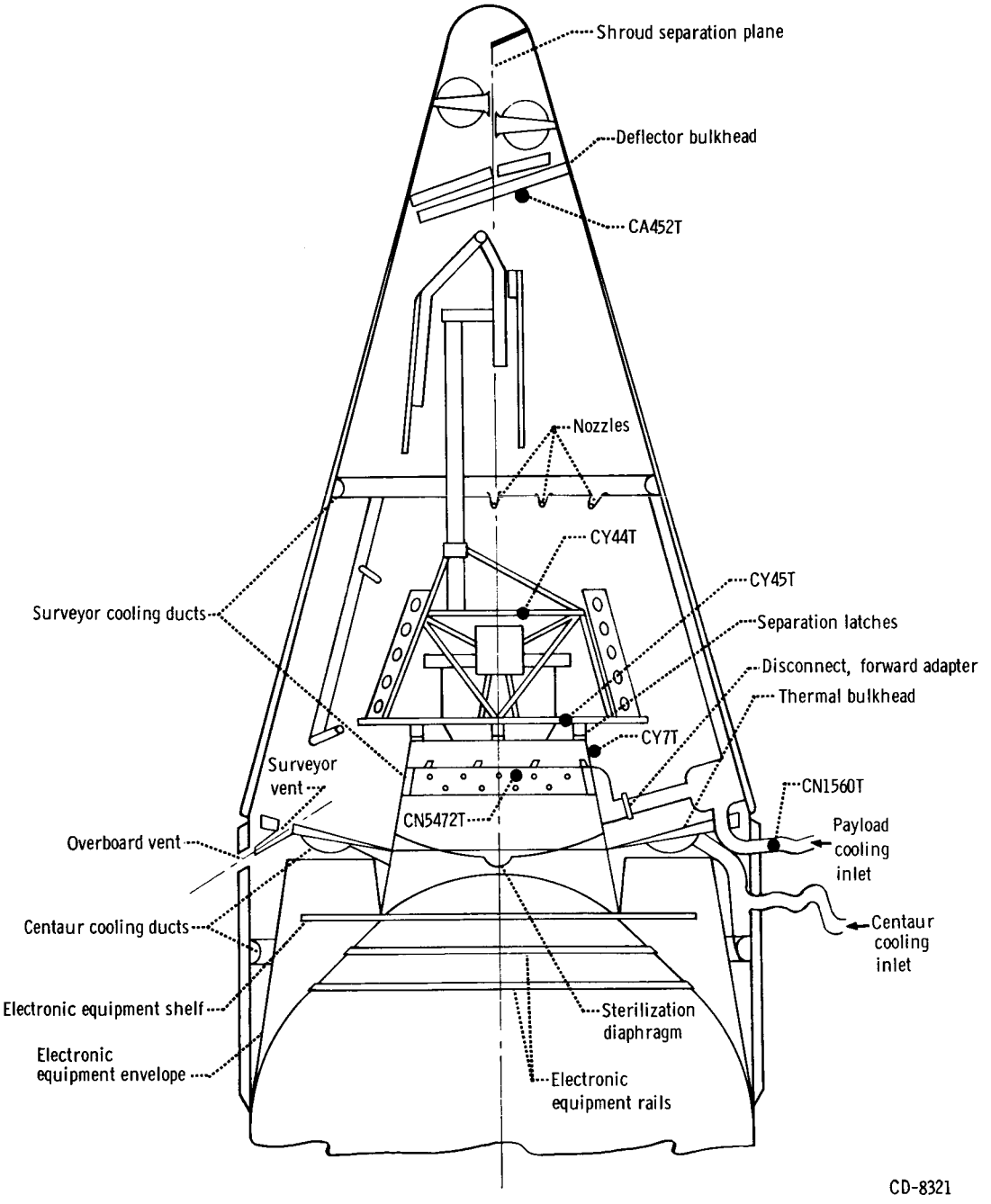

Figure VIII-5. - Surveyor compartment environmental control and temperature instrumentation.

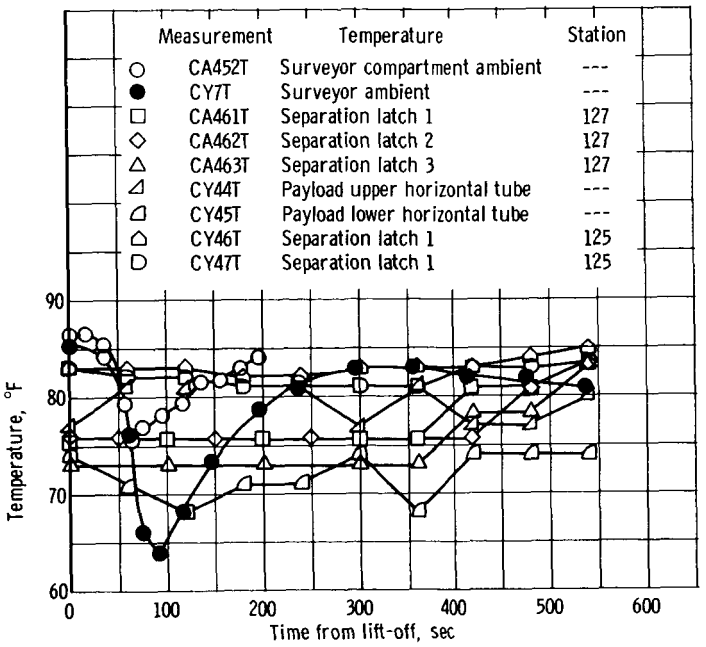

Figure VIII-6. - Payload compartment temperature history. (See fig. VIII-5 for temperature measurement locations.)

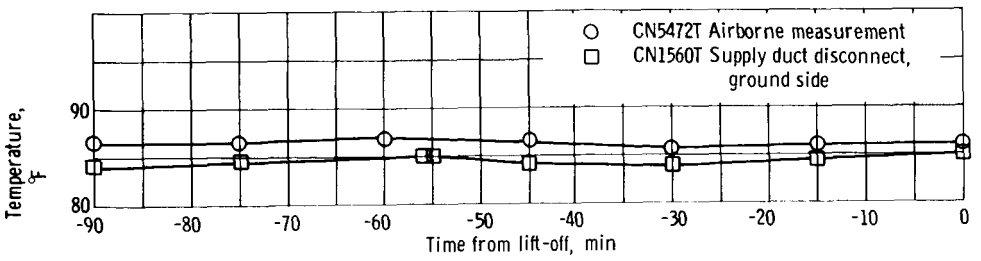

Figure VIII-7. - Payload compartment thermal conditioning gas supply temperature history.

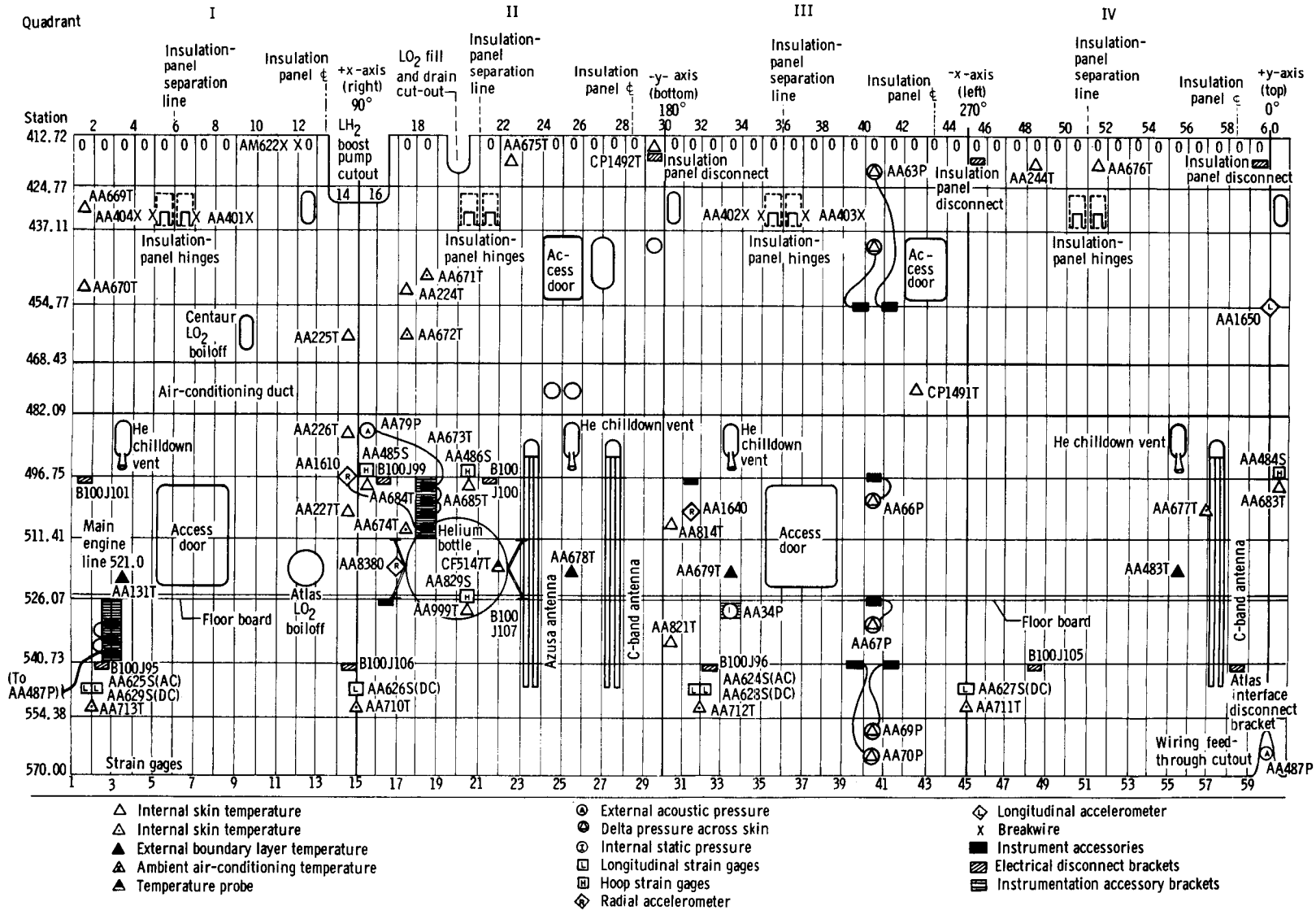

Figure VIII-8. - AC-6 interstage adapter instrumentation.

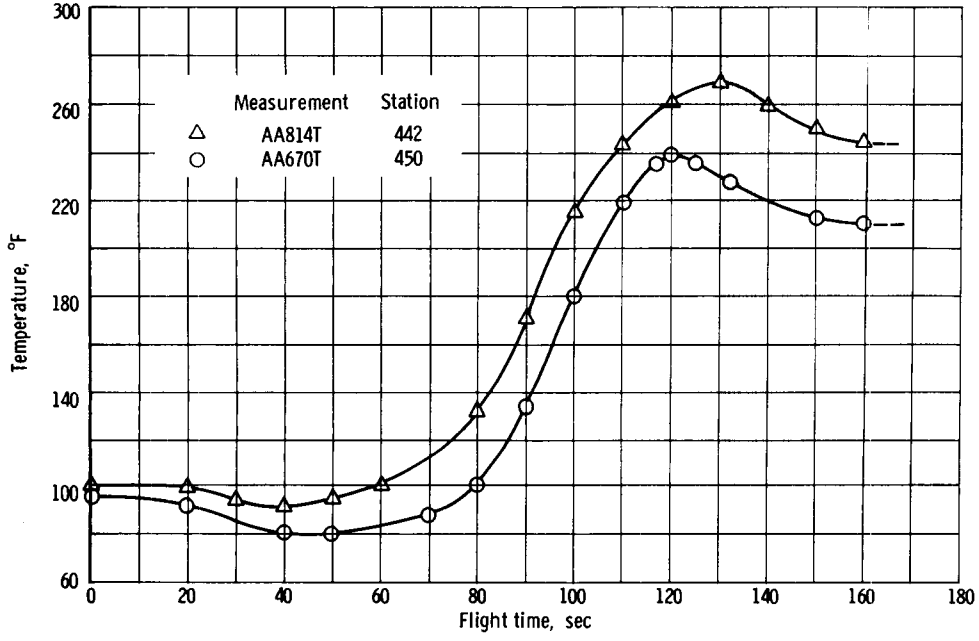

Figure VIII-9. - Typical interstage adapter skin temperature history.

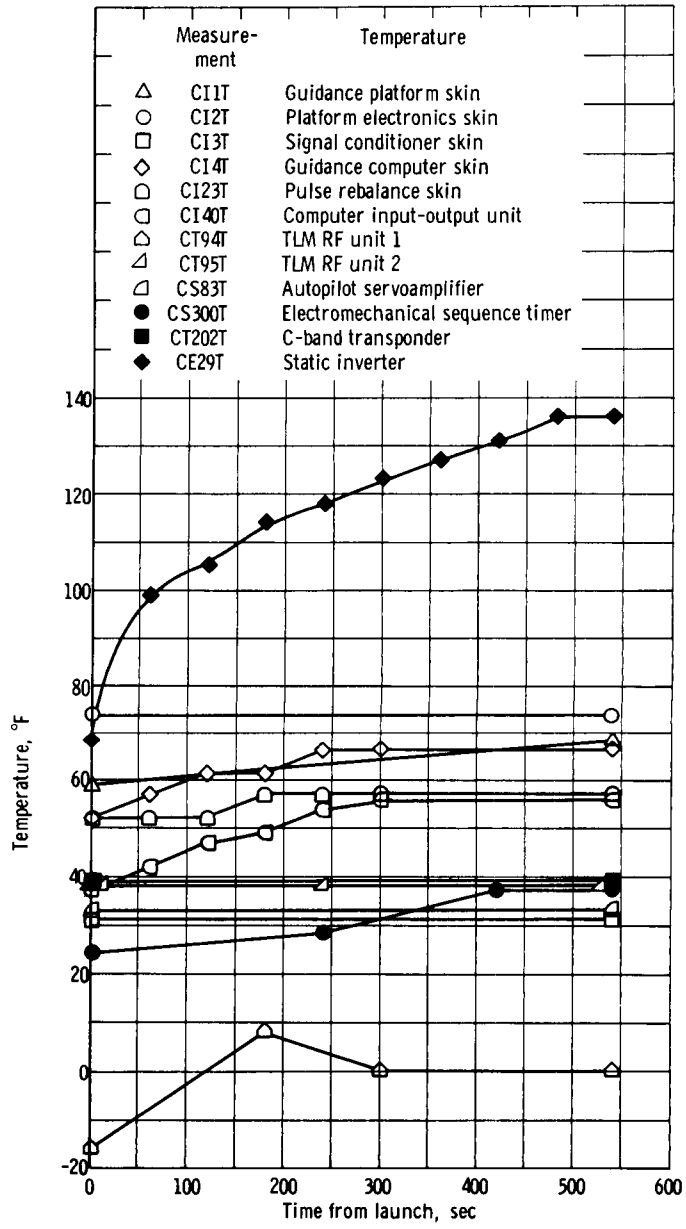

Figure VIII-10. - Electronics compartment temperature history.

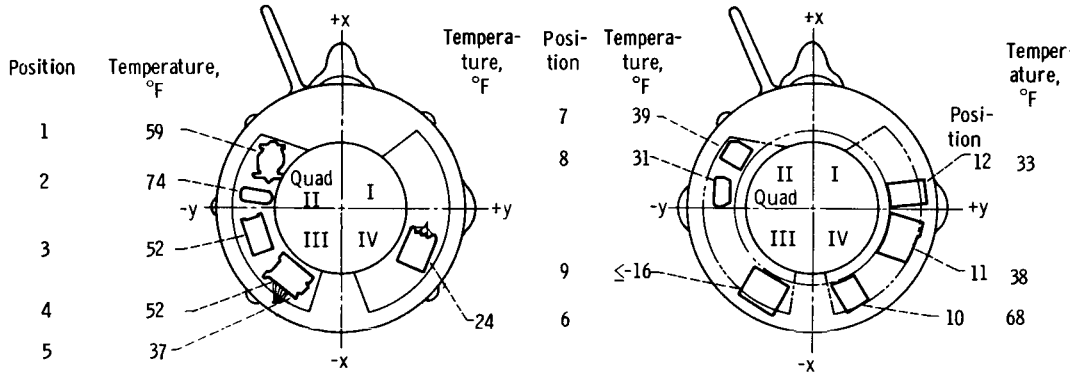

Upper tier (station 172)

Lower tier (station 183)

1 Guidance platform
2 Electronics guidance platform
3 Guidance pulse rebalance
4 Guidance computer
5 Computer input-output unit
6 Electromechanical sequence timer
7 C-band transponder
8 Guidance signal conditioner
9 Telemetry package 1
10 Inverter
11 Telemetry package 2
12 Autopilot servoamplifier

Figure VIII-11. - Thermal mapping of Centaur electronics compartment at lift-off.

[redacted]

IX. VEHICLE STRUCTURES AND SEPARATION SYSTEMS

SUMMARY

The structural integrity was demonstrated, and all mission objectives of structural significance were achieved on the AC-6 flight. The peak longitudinal load factor experienced during the flight was 5.7 g's at BECO. Aerodynamic drag loads peaked during transonic flight as expected. Bending loads induced by wind shears and gusts on this flight were small. The peak bending moment occurred at T + 82 seconds at station 812 and attained a value of 1.79×10^6 inch-pounds.

Intimate contact was maintained between the Centaur LH_2 tank and the insulation panels until panel separation. A minimum positive differential pressure of 10.7 psi across the Atlas intermediate bulkhead was experienced during launch. Interstage adapter panel excitation could not be evaluated due to the loss of the accelerometer on the panel skin.

The separation systems functioned properly within the established preflight limits, and all the separations were accomplished successfully. A tumbling rate of 1.82 degrees per second was encountered on the spacecraft subsequent to its separation from the Centaur stage. This compares with an allowable value of 3.00 degrees per second.

FLIGHT LOADS

Longitudinal Loads

There are two sources of longitudinal loads on flight vehicles: one is the inertial load resulting from axial acceleration, and the other is a result of aerodynamic drag forces. Vehicle axial acceleration is known both from onboard accelerometers and from a knowledge of total engine thrust. The inertial loads can then be calculated from known mass distribution. For this flight, the total axial load and drag load history through atmospheric flight was calculated from strain gage data (station 547) and compared with analytical values based on wind-tunnel drag coefficient data. This comparison is shown in figure IX-1. It can be seen that the measured and calculated values agree quite well except at approximately T + 60 seconds (Mach 1) and after T + 104 seconds. This was attributed to the fact that the strain gage data were of poor quality and difficult to interpret accurately.

Vehicle Bending Moments

Though the Atlas-Centaur vehicle is launch restricted from inflight winds,

[redacted]

these winds during the month of August are usually very mild. The launch availability during this month was estimated to be 100 percent. This was the case on the AC-6 launch opportunity, as was shown both by preflight Rawinsonde runs and by measured (strain gage and angle of attack) bending moment data. All bending loads were well within the vehicle limit capability.

A comparison of predicted and actual bending loads encountered on this flight is shown in figure IX-2. The predicted range was based on T - 2 hours (0611 EST) Rawinsonde run and $\pm 30(1 - \cos)/2$ feet-per-second gust criteria loads. The measured bending moments are based on the flight angle-of-attack data. The bending moments were calculated in each case at station 812, which is the station of peak loading. The maximum bending moment occurred at T + 82 seconds, attaining a value of 1.79×10^6 inch-pounds. This is within the limit allowable of 5.6×10^6 inch-pounds at this station.

There were four strain gages mounted on the interstage adapter at station 547. One each of these gages was located on the principal axes. As previously mentioned, the data obtained from these gages were of poor quality. Further, because of the low bending moment amplitudes encountered on this flight, the relative magnitude of the errors resulting from the poor quality data could be sizeable. A comparison between the bending moment history calculated from strain gage responses, angle-of-attack data, and two Rawinsonde runs is shown in figure IX-3. The Rawinsonde balloons were launched at 0611 EST and 0940 EST, the latter approximately 10 minutes after vehicle lift-off. It is seen that the bending loads obtained from these various sources are in substantial agreement, leading to increased confidence in preflight analytical procedures.

The measured angle-of-attack histories in the pitch and yaw planes are shown in figures IX-4 and 5. In each case they are compared with calculated angles of attack based on the two previously mentioned Rawinsonde runs. It is seen that, in general, the trends are in agreement. The apparent divergence between measured and calculated values in the pitch plane could be a result of the relatively low angles of attack encountered on this flight. It is felt that, in a more severe wind environment, the agreement would be better. Comparison of the two Rawinsonde runs (figs. IX-4 and 5) gives an indication of the variability of winds aloft. As has been evidenced on past flights, the time dependence of these winds is relatively minor, particularly in the time domain of interest in establishing launch vehicle loads environment.

Gust Bending Moments

All previous Atlas-Centaur vehicles have been launched into mild wind environments, and the AC-6 flight was no exception. The gust loads encountered (with the exception of AC-2) have also been very small. These loads are monitored by the high-frequency strain measurements at station 547 on the interstage. A review of these high-frequency strain responses showed a maximum strain increment of 20 microinches per inch at T + 78 seconds, which is equivalent to a gust bending moment of 0.145×10^6 inch-pounds. This bending moment increment represents a gust of approximately 4 feet per second. It is apparent that the gusts encountered on this flight were well below the design criteria of 30 feet per second.

PAYLOAD ADAPTER LOADS

There are three strain gages mounted on the payload adapter longerons directly aft of the separation latch points. Data from these gages indicate only compression loads in the adapter from launch to T + 700 seconds, at which time the vehicle went out of range of receiving stations at Antigua. The history of the adapter loads through T + 700 seconds, as calculated from the strain gages, is shown in figure IX-6. The loads increase steadily from launch to BECO attaining a peak value of 4000 pounds per latch point. There are subsequent lesser compression load discontinuities at SECO and MECO. From known values of payload weight, a peak longitudinal load factor of 5.78 g's can be calculated at BECO. At this time, measured axial acceleration showed a value of approximately 5.7 g's, which is within the accuracy of the strain gage data.

Payload adapter strain gage data from the AC-6 flight at the time of launch have been expanded and indicate the following results:

(1) At T + 0.78 second, a bending moment of 80 000 inch-pounds occurred in the payload adapter at station 143. This is equivalent to a 1.2-g lateral load factor shown in figure IX-7.

(2) Oscillation of the payload from T + 0.6 to about T + 1.1 seconds had a frequency of about 10 cps.

(3) The relatively high bending (twice that encountered on AC-4 during launch) may have been a result of a dynamic load from the launcher kick struts that give a third kick at 0.5 to 0.6 second after lift-off.

(4) The design load factors for this time of flight are 1.95 g's lateral and 1.8 g's longitudinal. The flight load factors are within these limits.

Insulation Panel Hoop Tension Loads

The Fiberglas honeycomb LH_2 tank insulation panels are bolted to each other along four longitudinal seams and to the Centaur tank at station 412. At T + 171.9 seconds, the flexible linear-shaped-charge severence system was activated, and the panels were severed free from the vehicle. To preclude the possibility of panel flutter during the flight, the panels were installed on the tank with a pretension (hoop) load. This pretension load ensures intimate contact between the panels and the tank throughout the flight and further provides a built-in spring to assist in panel separation and jettison.

From a consideration of nominal preduction tolerances, temperatures, and tank internal pressure, it was estimated analytically that a panel hoop load of approximately 82 pounds per inch would be attained at launch. Landline strain gage data recorded during the quad tanking test revealed that the panel hoop load varied between 71 and 82 pounds per inch over the panel length at T + 0 second, indicating that approximately nominal pretension conditions were attained in the panels on this flight. Continuous strain gage data through the tanking test showed a constant hoop load. A return of all gage readings to the

ambient hoop load levels during detanking indicated that the structural integrity of the panels was maintained throughout the tanking process.

During flight, the hoop load in the panels varied because of changes in tank internal pressure and panel temperature. Based on this analysis, the maximum value attained during the flight was 115 pounds per inch at T + 70 seconds. This compares with an allowable hoop load in excess of 206 pounds per inch. It may, therefore, be concluded that the insulation panels were structurally intact throughout the flight. A history of the predicted range and the actual panel hoop loads is shown in figure IX-8.

Interstage Adapter Differential Pressure Environment

The AC-6 interstage adapter was the first of the operational lightweight adapters to be test flown. The operational adapter is approximately 400 pounds lighter than those flown on AC-4 and AC-5. This weight reduction was accomplished by a reduction in area of both stringers and frames, while the basic skin gage remained unchanged at 0.032 inch. The skin panel size of the AC-6 adapter is approximately 4.5 by 13.5 inches compared with 8.5 by 14.5 inches used on the previous adapters.

Differential pressure gages located in a vertical line at the negative y-axis of the adapter skin recorded a maximum crushing pressure of 2.1 pounds per square inch, which was well within the structural allowable of 3.5 pounds per square inch. The interstage adapter was subjected to a crushing pressure environment throughout most of the atmospheric flight as expected. Pressure data are shown in figure IX-9.

Centaur Propellant Tank Pressures

Recorded pressures in the Centaur LO_2 and LH_2 tanks were normal throughout suborbital flight as was the differential pressure across the intermediate bulkhead. Detailed plots of the variation of pressure as a function of time are shown in figure VII-7. The pressure curves fall well within the structural allowables of 25 psig for the LH_2 tank and 42 psig for the LO_2 tank throughout the flight.

Atlas Intermediate Bulkhead Differential Pressure

The Atlas LO_2 tank ullage pressure programing system, incorporated to maintain sufficient bulkhead differential pressure during launch transient with 165K booster engines, was effective. It was designed to reduce Atlas LO_2 tank pressure approximately 5 psi for the first 20 seconds of flight. A satisfactory differential pressure across the intermediate bulkhead of 10.7 to 13.6 psi was maintained for this period of time. At T + 20 seconds, the return to full flight pressure in the LO_2 tank was initiated by the programer and completed approximately 3 seconds later.

A minimum value of 7.8 psi differential pressure across the bulkhead was

experienced at T + 92 seconds. The maximum value of 25.8 psi occurred immediately following BECO at T + 144 seconds. Though the upper and lower differential pressure limits have not been clearly established, a minimum value of 2.0 psi was considered desirable. The range of differential pressures encountered on the AC-6 flight was compatible with previous flight experience. Differential pressure, LO_2, and fuel tank ullage pressure histories for this flight are shown in figure IX-10.

SEPARATION SYSTEMS

To optimize the payload, several structural elements were jettisoned during powered flight. In chronological order these were as follows:

(1) Booster-package jettison

(2) Centaur insulation-panel jettison

(3) Nose-fairing jettison

(4) Atlas-Centaur separation

(5) Centaur-Surveyor separation

The booster-package jettison was fully developed during the Atlas research and development program, and no problems have been encountered with this system on any of the Atlas-Centaur flights. On the AC-6 flight, booster-package jettison was successfully accomplished at T + 144.9 seconds. The insulation-panel jettison and nose-fairing and Atlas-Centaur separations have been demonstrated on previous flights. Centaur-Surveyor separation was the only one to be demonstrated for the first time on the AC-6 flight. The performance of each of these systems (except booster-package separation) on this flight is given in the discussion that follows.

Insulation-Panel Separation

Four breakwires were located on the insulation-panel jettison hinges to record panel separation. These breakwires provided an "on-off" type of measurement. A review of these measurements reveals that all the panels were jettisoned simultaneously at T + 171.9 seconds. This conclusion can be verified by noting the cessation of all insulation-panel-instrumentation data at this time. A second verification of panel separation can be deduced from the tank hoop strain increase, which also occurred at this time. This increase indicates that the hoop stress relief provided by the panels had been removed showing intimate contact between the panels and the Centaur tank.

This successful separation serves to demonstrate the capability of the shaped-charge system to withstand repeated cryogenic cycling, particularly in the area of station 219 where temperatures of -320° F are encountered. The AC-6 linear-shaped-charge-separation hardware experienced one partial Centaur tanking and one full cryogenic abort without degradation of its pyrotechnic components.

On previous vehicles, aborts had been followed by a complete replacement of the pyrotechnic system hardware. Confidence in the abort capability of the system was based on the following preflight test program:

(1) A series of cryogenic unlatch tests simulating flight aborts and rain

(2) A system qualification test program consisting of 38 successive, succesful flight-type hardware "breadboard" tests, subjecting all test hardware to the extreme limits of vibration, humidity, cryogenic and elevated temperatures, vacuum conditions, and flight aborts

The recovery and thorough inspection of the AC-6 wiring tunnel panel gave further indication that the insulation panels successfully separated and jettisoned from the vehicle. This panel, recovered by a U.S. Navy destroyer at 21°21' north lattitude and 71°17' west longitude (near Grand Turk Island in the Caribbean), was thoroughly inspected by cognizant GD/C and NASA engineers and found to be in reasonable condition considering the impact loads it obviously sustained during reentry and on contact with the water. The panel was intact with the exception of one missing hinge, one aft corner of the panel, and the "bolt-on" boost-pump fairing. The inside surface of the panel showed some local delamination of the skin. Charring of the detonator fairing and shaped-charge retainer indicates that the panel was in an aft end first attitude during reentry. Charring of the fracture surfaces indicates that the aft corner broke off prior to or during reentry.

Nose-Fairing Separation

Separation of the nose fairing was signaled by the linear-motion indicator connecting the fairing halves to the spacecraft mast at T + 196.49 seconds. The approximately 7-inch travel of these potentiometers was accomplished in 0.04 second. No excessive vibrations were observed on the accelerometers at this time.

The thrustor bottle compartment pressure dropped from 14.7 psia at launch to flight vacuum prior to nose-fairing jettison. At nose-fairing jettison there was a pressure peak of about 3 psi due to thrustor bottle pressure. This peak is slightly less than pressures developed during the Lewis Research Center Space Power Chamber tests of the nose fairing. Though this measurement may be somewhat inaccurate because of the 6-cycle-per-second maximum response of the transducer, it does indicate the pressure was within acceptable limits.

Atlas-Centaur Separation

The stage-separation process was initiated by the linear-shaped-charge firing at T + 236.20 seconds which severed the interstage adapter at station 413. The retrorockets fired at approximately T + 236.3 seconds to decelerate the Atlas. Acceleration data indicated that all eight rockets ignited.

Information obtained from rate gyros indicated that the Centaur did not rotate about its center of gravity appreciably during the separation process

[redacted]

(less than 0.05 deg). The rate and displacement gyros indicated that the Atlas rotated about its yaw axis approximately 0.27 degree at the time it cleared the Centaur. The predicted yaw rotation would result in a lateral motion of 2.3 inches at station 413 after 9 feet of axial motion relative to the Centaur. The observed motion due to rotation was 2.7 inches.

The gyros also indicated that the Atlas rotated somewhat about its pitch axis, but to a greater degree than is normally experienced. The departure noted from the norm appears to lie in a residual turning rate seen in the Atlas prior to separation. The Atlas was displaced in a negative direction prior to SECO and was initiating a corrective pitch when SECO occurred. The resulting positive pitch motion was not nulled out as the neutral position was passed after the engine was shut down, but continued into the separation interval. Therefore, the interstage adapter and the Centaur were moving together at the time of shaped-charge firing, and there was a vertical motion of the Centaur that moved it with the Atlas rotation, tending to prevent interference. By considering the change in the Atlas angular rate during staging, it appears that the clearance between the vehicles was reduced by 0.3 inch (out of a nominal 15 in.) toward the positive y-direction, which still leaves approximately 14.7 inches clearance. The predicted vertical motion at station 413 after 9 feet of longitudinal travel is -2.7 inches.

Spacecraft Separation System

Separation latches. - The separation latches at the Centaur Surveyor interface were designed to hold the spacecraft rigidly to the payload adapter and to provide the impulse during spacecraft separation. A cross-sectional view of the latch assembly and strain gage location is shown in figure IX-11. Not shown are the springs that provide the separation impulse. The separation latches are preloaded in tension to eliminate relative motion between the spacecraft and spacecraft adapter. As seen in figure IX-12, all three latches maintained the preload until spacecraft separation. The initial preload in all the latches was set at 2400 pounds before launch. Two of the gages drifted away from their nominal value prior to lift-off. This is thought to be zero shift in the strain gage since there is no known mechanism by which this preload could be relieved during the countdown.

Variations in preload during the flight were all less than 300 pounds from their prelaunch value. This level of variation does not affect the functional performance of the latch mechanism. At spacecraft separation, data from the gages showed the expected sudden release of the preload, indicating that the latch pin-pullers functioned successfully. Data from three deflection gages, one on each of the latch springs, also confirms a successful separation. Analysis of the spacecraft tip-off rate induced by the latch springs is discussed in the following section.

Spacecraft separation. - Analysis of the variation of signal strength from the S-band transponder revealed a tumbling rate of 1.8 degrees per second of the Surveyor spacecraft after separation from Centaur. A check of the Surveyor polar signal strength patterns for the omnidirectional antenna reveals that the frequency rate of tumbling is the same as the frequency of signal strength.

[redacted]

Linear potentiometers are located at each of the three points where the spacecraft is locked to the payload adapter to measure the position of each of the attachment points with relation to the spacecraft. Figure IX-13 shows the location of these potentiometers and a time record of their output. These data show that initiation of separation at all three points is within 5 milliseconds, but that the potentiometers located on the positive y-axis (CY2D) reached full scale 90 milliseconds after the other two potentiometers. These potentiometers indicated that a positive pitch rate existed at separation, and this fact agrees with the tumbling rate based on S-band signal variation.

Each of the three latches holding the Surveyor to the Centaur payload adapter has two sets of springs tending to separate Centaur and the spacecraft. The stronger set of these springs provides force for separation, while the weaker set of springs is used to make the potentiometer follow the motion of the spacecraft as well as to impart a small force to the separation. Calculations by analog computer show that, if all the force derived from the spring of potentiometer CY2D were removed from the system, the tumbling rate of Surveyor would only be 0.85 degree per second. This calculated rate includes the initial tumbling rate before separation of the combined Centaur-Surveyor, which was determined from the pitch and yaw rate gyros as

$$\text{Yaw rate} = -0.244 \text{ deg/sec}$$

$$\text{Pitch rate} = 0.12 \text{ deg/sec}$$

From this calculation, indications are that a higher unbalanced force was necessary to obtain the 1.8-degree-per-second tumbling rate that existed and that there was a high probability of a partial "hang-up" of one of the main separation springs. Also noted was that one extensiometer travel was only about 90 percent as much as the other two.

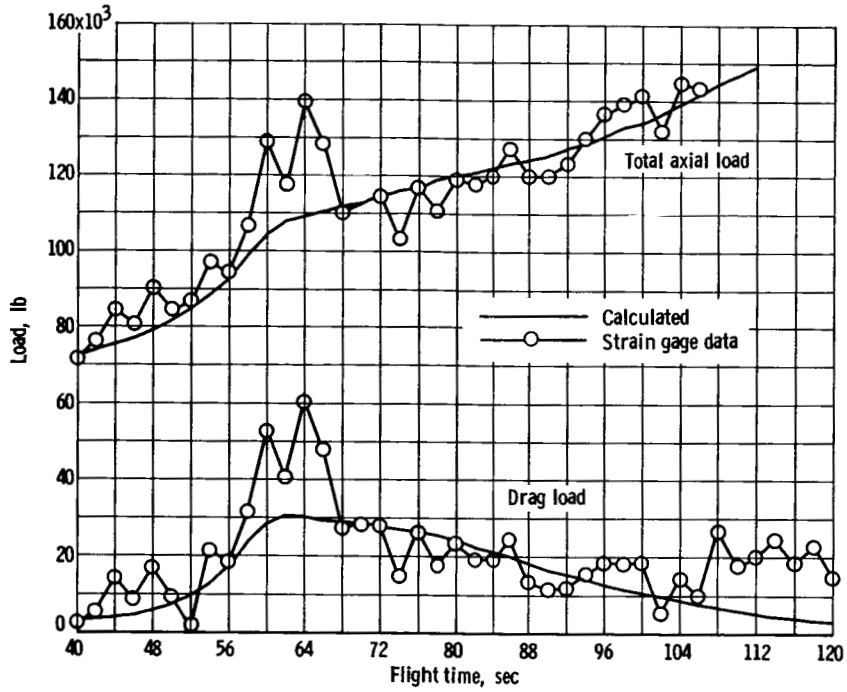

Figure IX-1. - Comparison of history of calculated and measured drag and total axial load on AC-6 flight.

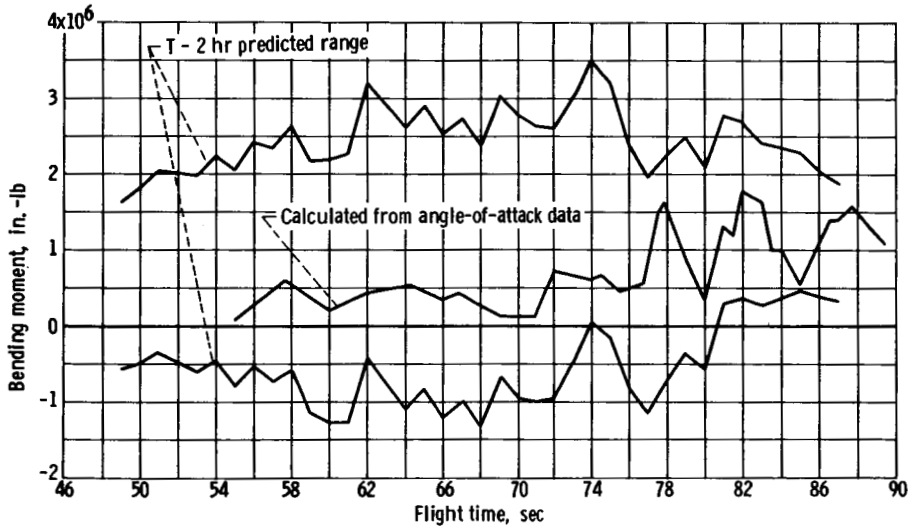

Figure IX-2. - AC-6 flight bending moment history at station 812 based on measured angle-of-attack data and range of bending moments predicted on basis of T - 2 hours (0611 EST) Rawinsonde run.

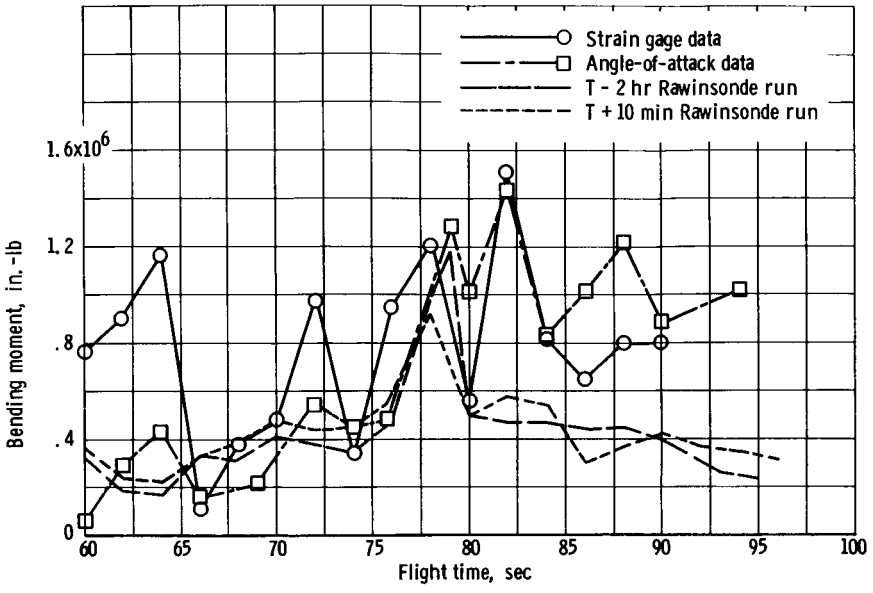

Figure IX-3. - AC-6 flight bending moment history at station 547.

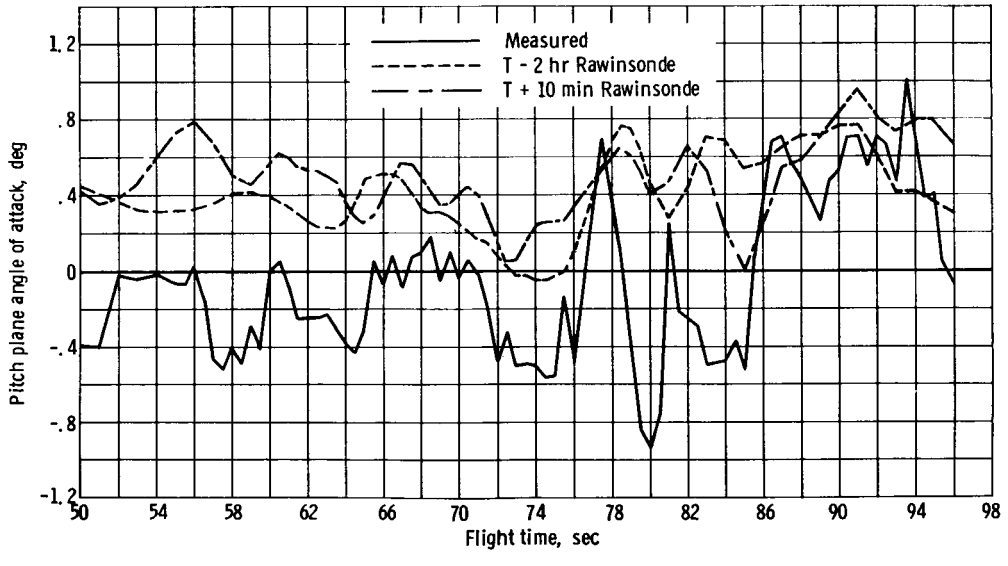

Figure IX-4. - Comparison of measured pitch plane angle of attack and computed values based on Rawinsonde soundings just before and after vehicle launch.

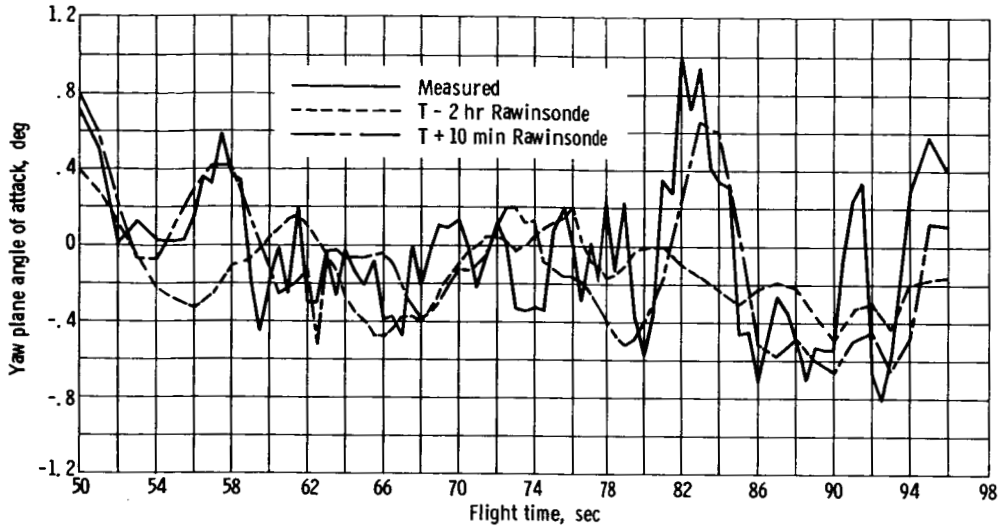

Figure IX-5. - Comparison of measured yaw plane angle of attack and computed values based on Rawinsonde soundings just before and after vehicle launch.

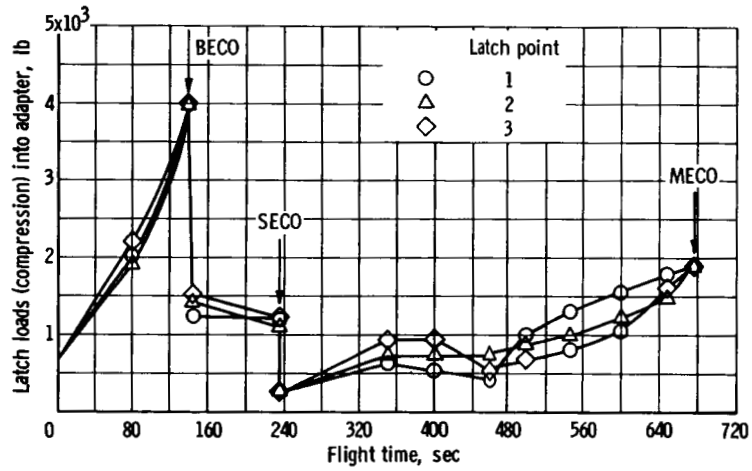

Figure IX-6. - Loads in payload adapter at separation latch points.

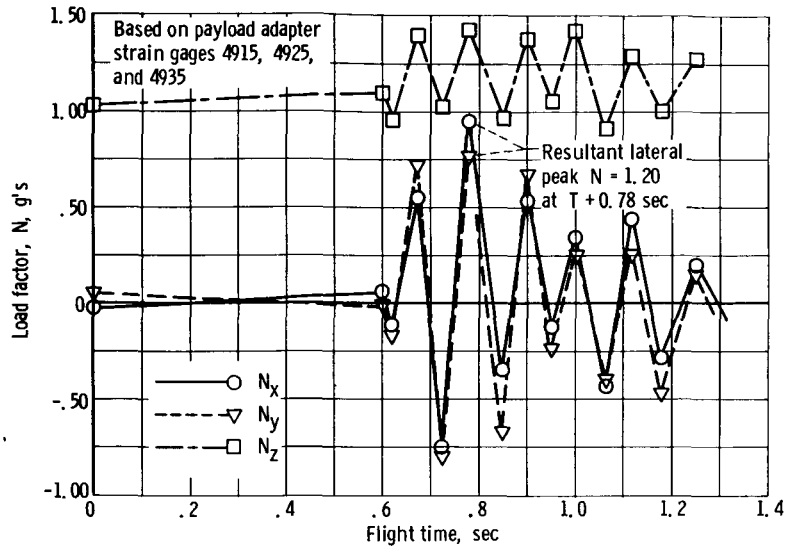

Figure IX-7. - Payload lateral and longitudinal load factors at launch. Design load factors at launch are 1.8 g's longitudinal and 1.95 g's lateral.

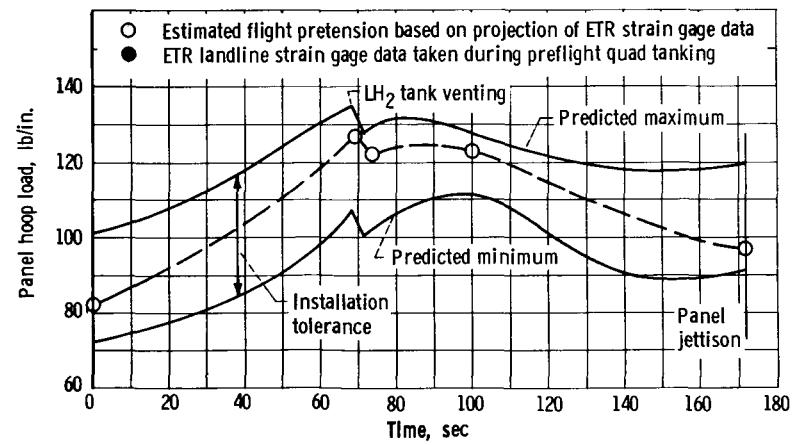

Figure IX-8. - AC-6 insulation panel hoop load as function of time. The spring rates are: K_{panel} = 0.166 inch of radial motion/psi and K_{tank} = 0.008 inch of radial motion/psi.

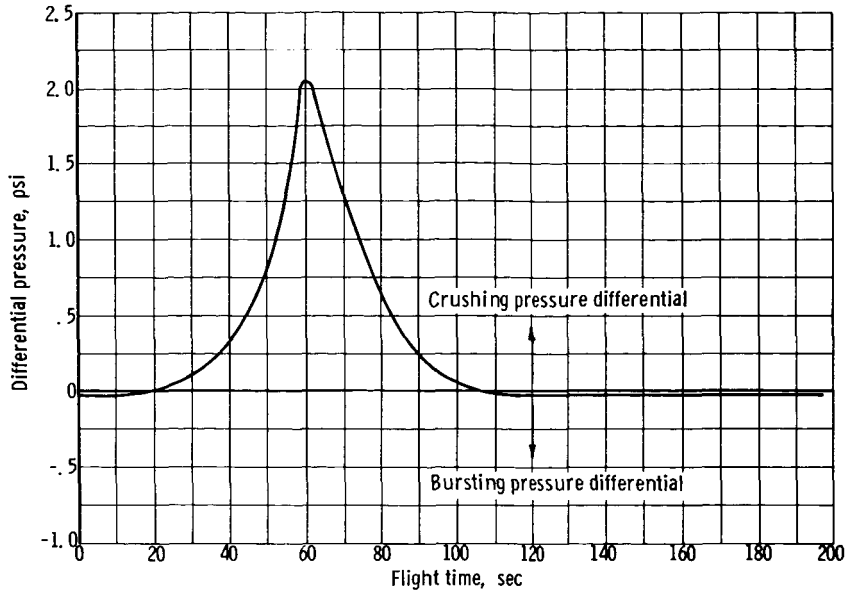

Figure IX-9. - Interstage adapter (AC-6) pressure differential history at station 557 in quadrant III (AA69P).

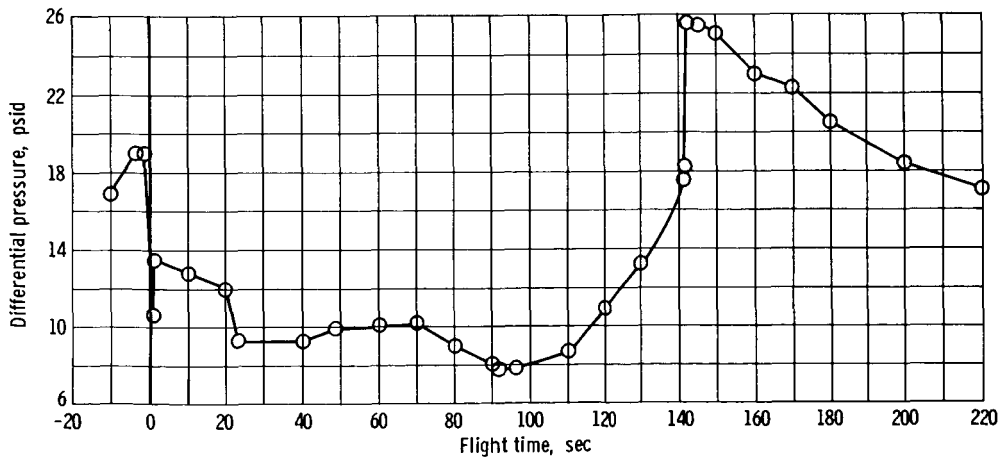

(a) Intermediate bulkhead differential pressure.

Figure IX-10. - Atlas pressure histories for AC-6.

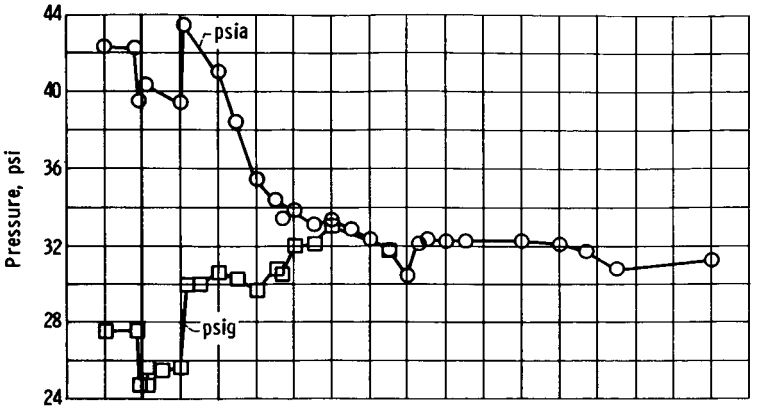

(b) LO_2 tank ullage pressure.

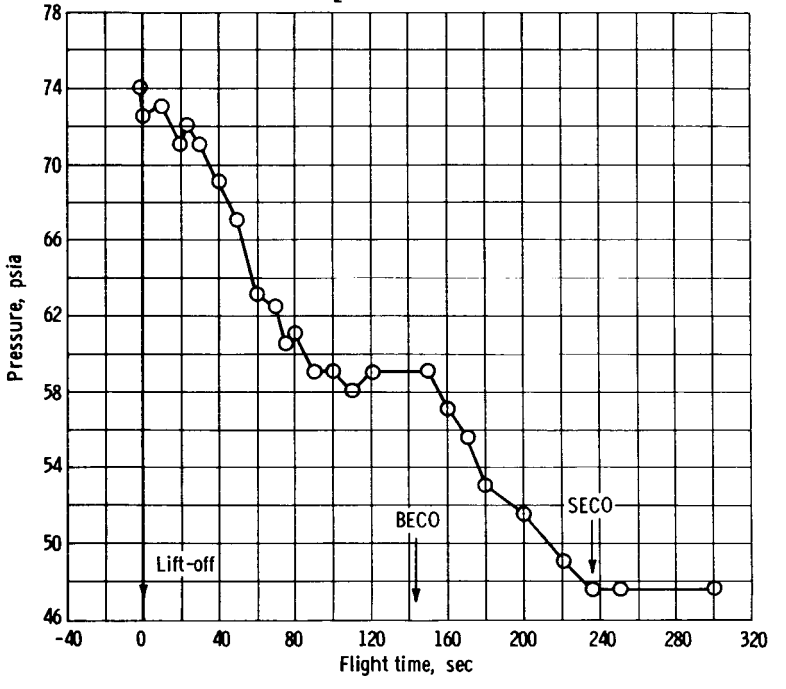

(c) Fuel tank ullage pressure.

Figure IX-10. - Concluded.

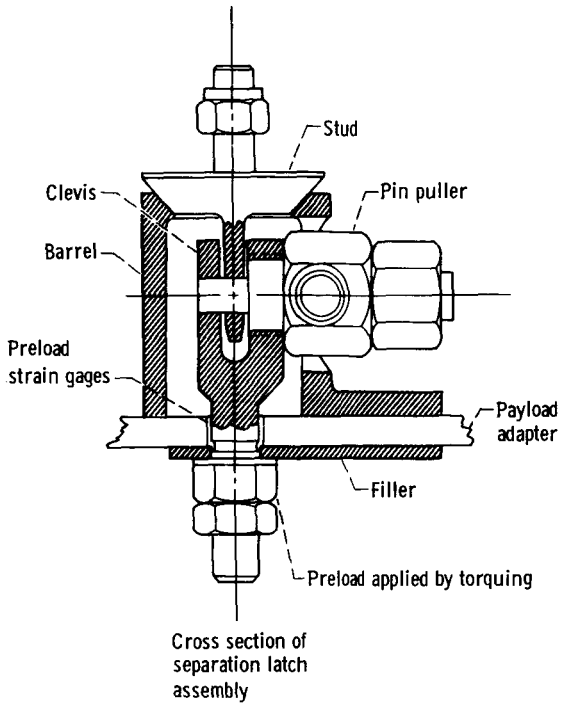

Figure IX-11. - Cross-sectional view of Centaur surveyor separation latch assembly.

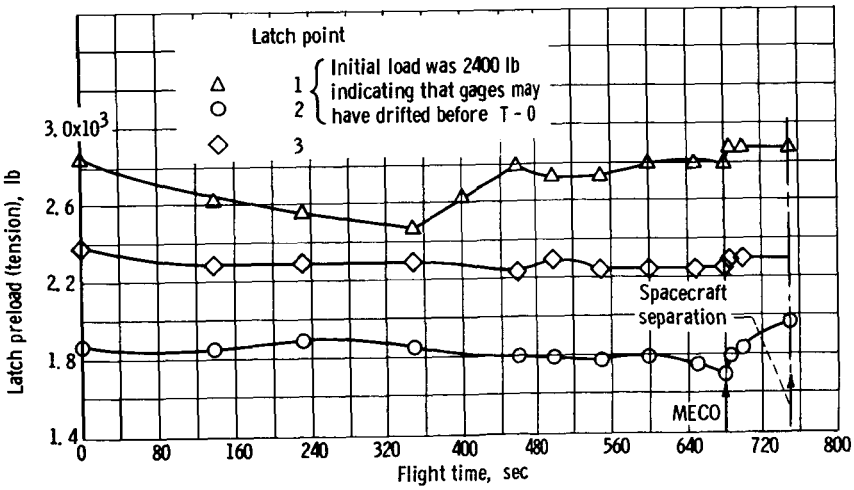

Figure IX-12. - Centaur-Surveyor separation latch preload.

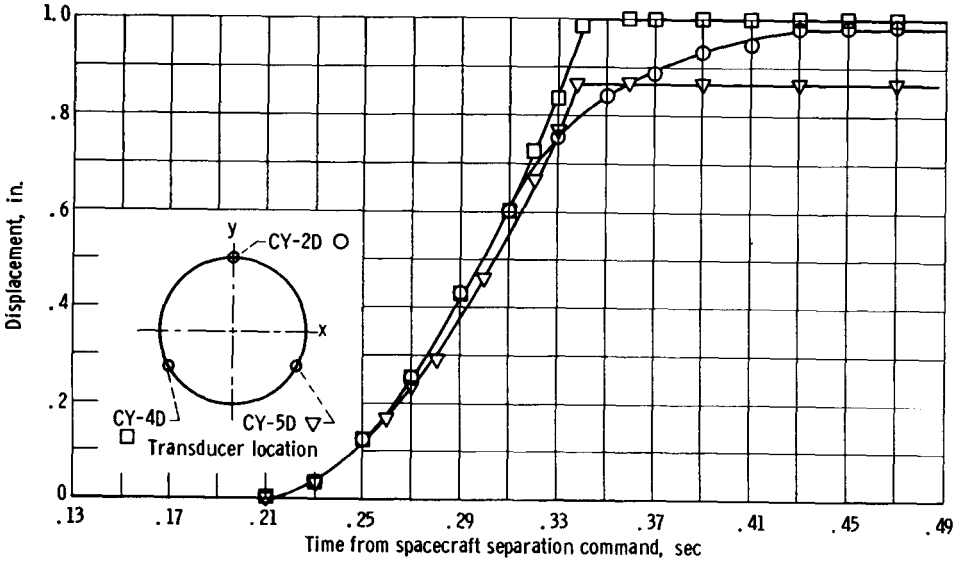

Figure IX-13. - Surveyor displacement from Centaur at separation. Spacecraft separation command issued at T + 747.57 seconds.

[redacted]

X. VEHICLE DYNAMICS

SUMMARY

Longitudinal modal excitations and lateral payload excitation were high at lift-off for the AC-6 flight. The vehicle-flight-vibration environment as well as the lateral modal excitation were similar to previous flights. At SECO, an engine shutdown pressure oscillation caused a 90-cps longitudinal vibration unobserved on previous flights.

MODAL DYNAMICS

Longitudinal excitations were observed approximately at the same times as in previous flights, as is shown in figure X-1. Lift-off perturbations resulting from launcher release and from Atlas LO_2 pressurization, as shown on z-axis accelerometers, were 0.47 g single amplitude around a 1.25-g centerline with a frequency of 7 cps. This amplitude was approximately three times greater than that observed on the AC-2, AC-3, and AC-4 flights, but about the same as that on the AC-5 launch. The peak disturbance occurred at about 0.2 second after 2-inch rise. At this time, struts bearing on the base of the Atlas vehicle were raised by the vehicle motion which caused the launcher holddown arms to rotate. Another longitudinal acceleration peak observed at 0.6 second after 2-inch rise had a single amplitude of 0.4 g (around a 1.25-g centerline) with a frequency of 7.0 cps. At the same time, large disturbances were indicated by the roll-rate gyro, displacement gyro, Surveyor separation-plane y-axis accelerometer, and Surveyor mast tip y-axis accelerometer. The roll signals indicated that, up to 0.6 second, the vehicle had rolled 0.16° whereupon it snapped back to 0° in less than 0.01 second. The Surveyor separation-plane accelerometer signals indicated a single amplitude of 0.80 g about a 0-g centerline, and the Surveyor mast tip accelerometer indicated a single amplitude of 4.0 g's about a 0-g centerline. Specifications for the Surveyor allows a 1.25-g single-amplitude vibration at the Surveyor-Centaur separation plane.

Surveyor displacement potentiometers measuring relative motion between the mast tip and the nose fairing showed a single-amplitude displacement of 0.48 inch at this time. These disturbances (at 0.6 sec) occurred at approximately 22 inches of vehicle rise and coincided with a load peak measured on the launcher kick strut at the same rise during tests conducted before this flight.

"Pogo" type oscillations occurred slightly earlier in the AC-6 than in the AC-4 flight and had a maximum single amplitude of 0.16 g about a centerline varying from 2.0 to 5.4 g's, as shown in figure X-1. The frequency for "pogo" was 12 cps. An engine cutoff transient was observed at BECO on z-axis accelerometers with a single amplitude of 0.7 g around a 1.28-g centerline and a frequency of 70 cps. This amplitude was approximately half that noted on pre-

ceding flights. Unlike previous flights, the AC-6 flight also had longitudinal oscillations caused by an engine cutoff transient at SECO detected on z-axis accelerometers (one located at station 1057 and the other at station 450 on the interstage adapter) that indicated a single amplitude of 5.3 g's about a 1.6-g centerline with a frequency of 90 cps. At the same time, a y-axis accelerometer and a tangential accelerometer on Surveyor were excited at the same 90-cps frequency. The y-axis accelerometer (on spacecraft mast tip) had a single amplitude of 0.30 g around a 0-g centerline, and the tangential accelerometer had a single amplitude of 0.35 g about a 0-g centerline. Again these disturbances did not exceed specifications for the Surveyor vehicle.

Lateral bending mode deflections are shown in figure X-2 as calculated from Centaur pitch- and roll-rate gyros (located at station 173). The design allowable modal deflections at station 173 are also shown in figure X-2. The allowable deflections are only critical from 44 to 80 seconds after 2-inch rise. During this period, only deflections in the yaw plane were observed since the low-range pitch-rate gyro was off scale. The observed yaw-plane first-modal deflection during the critical time period was less than 10 percent of the design deflection, and the yaw-plane second-modal deflection during the critical time period was less than 5 percent of the design deflections. The pitch-plane modal deflections observed before and after the critical time period for both first and second modes were approximately the same as the yaw-plane modal deflections at the same times. Since the deflections in both planes were nearly equal for both the actual case and for the design criteria, it can be assumed that the pitch-plane modal deflections do not exceed the design criteria during the critical time period.

Figure X-3 shows the comparison of first-mode maximum bending deflections during AC-2, AC-3, AC-4, and AC-6 flights. From this comparison it can be seen that the lateral first-mode deflections for this flight were about the same as in other flights. The first- and second-mode frequencies plotted against time are shown in figure X-4 and are very close to the theoretical values calculated before the flight.

VIBRATIONS

The vibration profile of AC-6 was similar to previous flights. At launch and transonic/max Q, the vibration environment was predominantly Gaussian with sinusoids superimposed. After the transonic region, the only vibrations evident were caused by flight events such as booster engine cutoff, Atlas-Centaur separation, etc.

All the accelerometers indicated a perturbation at booster jettison that is believed to be noise, since it was also visible on some temperature measurements. At 197.5 seconds after launch, the accelerometer indicating outboard acceleration located on compartment A of the spacecraft (CY58φ) oscillated between data channel band edge in a mode that is typical of instrumentation failure. The transducer located on the LH_2 duct (CA601φ) gave a questionable vibration indication starting at approximately 243 seconds after 2-inch rise.

The maximum vibrations are given in table X-I. Radial vibration in the

[redacted]

interstage adapter was fairly low; AA161φ ($Q_1 + Q_2$ station 497) gives the highest level, which was 40.0 g's (double amplitude) and occurred during launch. The maximum vibration indicated by the spacecraft accelerometers was 32.0 g's (double amplitude) retromotor attachment 1 z-axis (CY52φ), which occurred at 235.8 seconds after launch. The foot of the spacecraft experienced maximum vibration at launch that was equal to 2.0 g's (double amplitude) with a frequency of 8.7 cps and was measured on CY50φ located at station 125 and sensitive to the y-direction. The maximum vibration that the mast of the spacecraft experienced was 8.4 g's (P-P) indicated by an accelerometer located at the top of mast that read in the y-direction (CY55φ).

In order to gain an insight into how the actual flight vibration compares with the qualification levels that were used in designing vehicle and spacecraft components, a power spectrum analysis was performed on all usable accelerometer measurements. The power spectral density plots (fig. X-5) included in this report are for the flight times at which maximum vibration occurred. The densities were obtained by using very short analysis times (0.5 sec or less) to eliminate variations with flight time. The spectrum analyzer used was a General Applied Science Laboratories Model SA12 real-time low-frequency heterodyne analyzer.

Examination of the power spectral density (fig. X-5(b)) for the maximum radial vibration in the interstage adapter (quoted previously as 40 g's double amplitude) shows that there are sinusoids at 200, 300, and 400 cps, and the data channel starts to attenuate at 220 cps. If the 400-cps component is assumed to be noise (inverter crosstalk) the maximum energy level is 0.88 g^2/cps at a frequency of 300 cps.

As seen from figures X-5(f) to (o), the vibration profile of the spacecraft was predominantly sinusoidal, with the maximum levels being below the separation plane qualification level. The foot area accelerometer (CY50φ) indicated 0.036 g^2/cps, at a frequency of 25 cps, retroattachment area accelerometer (CY549) indicated 0.1 g^2/cps at a frequency of 25 cps, and the top-of-the-mast accelerometer (CY55φ) indicated 1.15 g^2/cps at a frequency of 50 cps.

AC-6 instrumentation included two microphones, one located on compartment A (CY61Y) and the other at the top of mast (CY60Y). The maximum dynamic sound pressure measured in each microphone area was 0.0695 psi (single amplitude) and 0.0727 psi (single amplitude), respectively, these values being close to the qualification level (ref. 11) of 145 decibels (rms) (fig. X-6 gives the amplitude as function of spectrum for launch).

At shaped-charge firings, Centaur insulation-panel jettison, the Atlas-Centaur separation there were shock loads induced in the spacecraft. This shock vibration was not indicated by all spacecraft accelerometers because of their low-frequency response (the frequency of this shock was of the order of 600 to 700 cps). Accelerometer (CY54φ) (best frequency response) indicated a 12.0-g (single amplitude) maximum amplitude shock lasting for approximately 0.05 second. The other high-frequency response accelerometers in the area (CY53φ and CY52φ), indicated 12.5 g's (single amplitude) and 16.0 g's (single amplitude), respectively, after correcting for roll-off. The nature of this shock is such that it could conceivably cause damage to the spacecraft packages if it is

not quickly damped out. Spacecraft amplification factors are currently being investigated to evaluate this situation better. Figures X-7 to 9 show both the raw data and amplitude spectrum (resulting from Fourier analysis) of this shock. The amplitude indicated by the amplitude spectrum is less than the raw data value. This is to be expected since the raw data is triangular in appearance.

TABLE X-I. - MAXIMUM VIBRATIONS OBSERVED DURING COMPLETE AC-6 FLIGHT

Location	Measurement number	Time after 2-inch motion, sec	Maximum g's, double amplitude	Frequency band of data channel, cps	Comments
Interstage adapter z-axis Q_1 and Q_2, station 455	AA165φ	142	4.2 g's	0 to 45	BECO
Panel radial Q_2 and Q_3, station 503	AA164φ	Only deflection was at Atlas booster jettison (noise)			
Interstage adapter radial Q_1 and Q_2, station 497	AA161φ	1	40.0 g's	0 to 220	Launch
Interstage adapter radial helium bottle, station 519	AA838φ	236.2	10.0 g's	0 to 1200	Atlas-Centaur separation shock-type transient
LH_2 duct near y-section, station 453 Q_2	CA601φ	171.7	13.03 g's	0 to 160	Transducer failed at 242.9 sec
Spacecraft vibrations: Compartment A, strain normal	CY59S	-----	1200 μin./in.	0 to 660	Launch
Foot accelerometer, 0° at station 125 x-axis sensitivity	CY49φ	0.6	1.2 g's	0 to 160	90 cps
Foot accelerometer, 0° at station 125 y-axis sensitivity	CY50φ	0.45	2.0 g's	0 to 220	8.7 cps
Foot accelerometer, 270° at station 125, sensitive in tangential direction	CY51φ	0.65	1.6 g's	0 to 330	8.7 cps
Retroattachment 1, z-axis sensitivity	CY52φ	171.7 235.8	11.2 g's 32.0 g's	0 to 600	Shock-type transient
Retroattachment 2, z-axis sensitivity	CY53φ	235.8	25.0 g's	0 to 790	Atlas-Centaur separation shock-type transient
Retroattachment 3, z-axis sensitivity	CY54φ	235.8	24.0 g's	0 to 1000	Atlas-Centaur separation shock-type transient
Top of mast, y-axis sensitivity	CY55φ	0.68	8.4 g's	0 to 80	10 cps
Top of mast, x-axis sensitivity	CY56φ	0.5	3.0 g's	0 to 60	10 cps
Compartment A, accelerometer outboard sensitivity	CY57φ	0.68	3.0 g's	0 to 450	10 cps
Compartment A, accelerometer z-axis sensitivity	CY58φ	171.7	1.6 g's	0 to 110	
Compartment A, outboard sensitivity	CY61Y	Launch	147.6 decibels	0 to 2100	0.0695 psi single amplitude
Top of mast	CY60Y	Launch	148.0 decibels	0 to 1200	0.0727 psi single amplitude

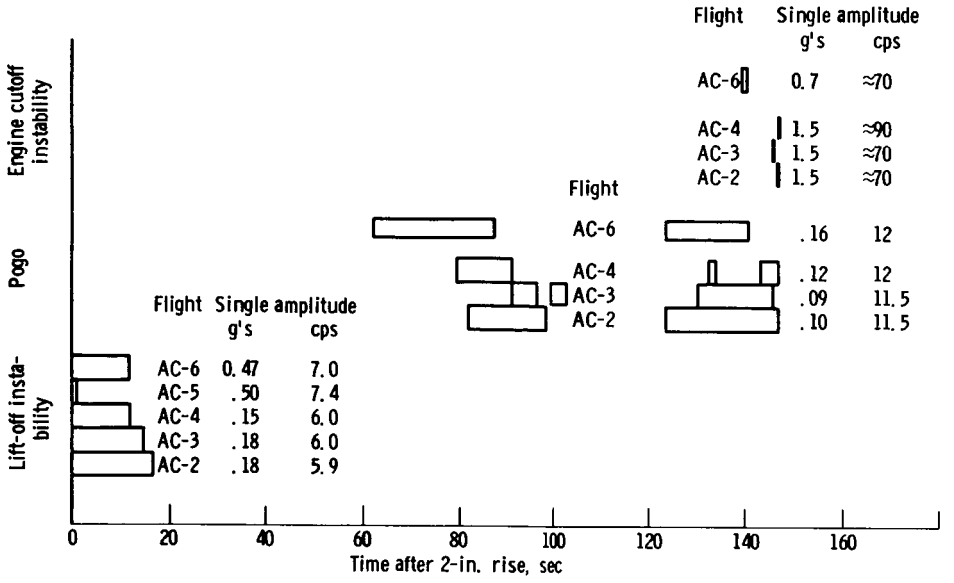

Figure X-1. - Longitudinal oscillation occurrences, frequencies, and maximum amplitudes for Atlas-Centaur flights.

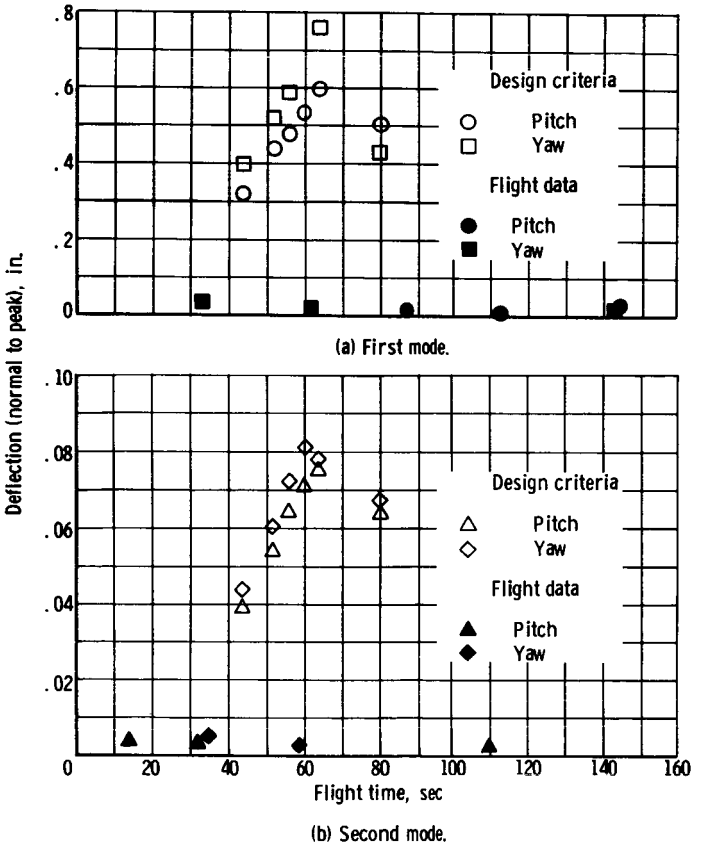

(a) First mode.

(b) Second mode.

Figure X-2. - Flight data and design criteria for wind-gust modal amplitudes (pitch and yaw planes at station 173).

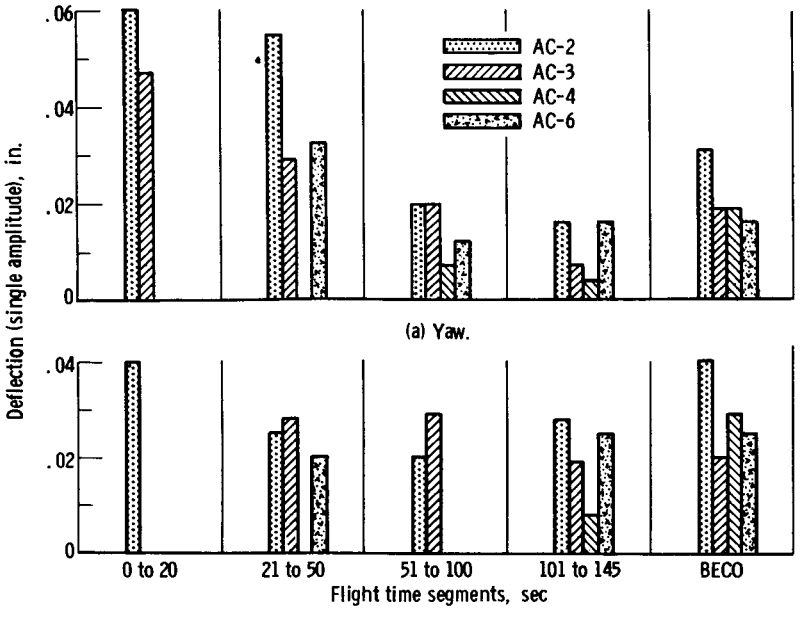

Figure X-3. - Maximum first modal amplitudes at station 173 for AC-2, AC-3, AC-4, and AC-6 flights.

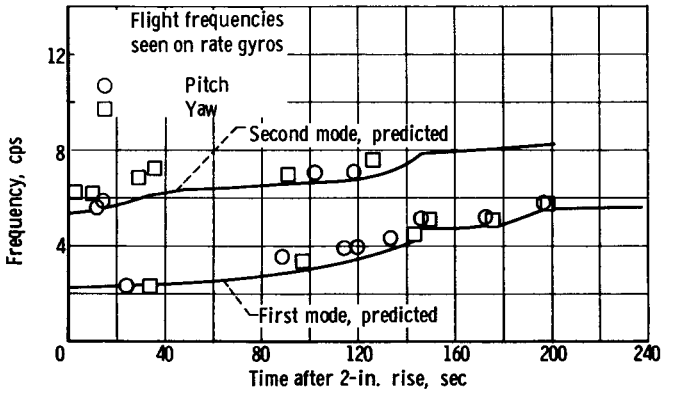

Figure X-4. - Comparison of flight bending frequencies with theoretical bending frequencies.

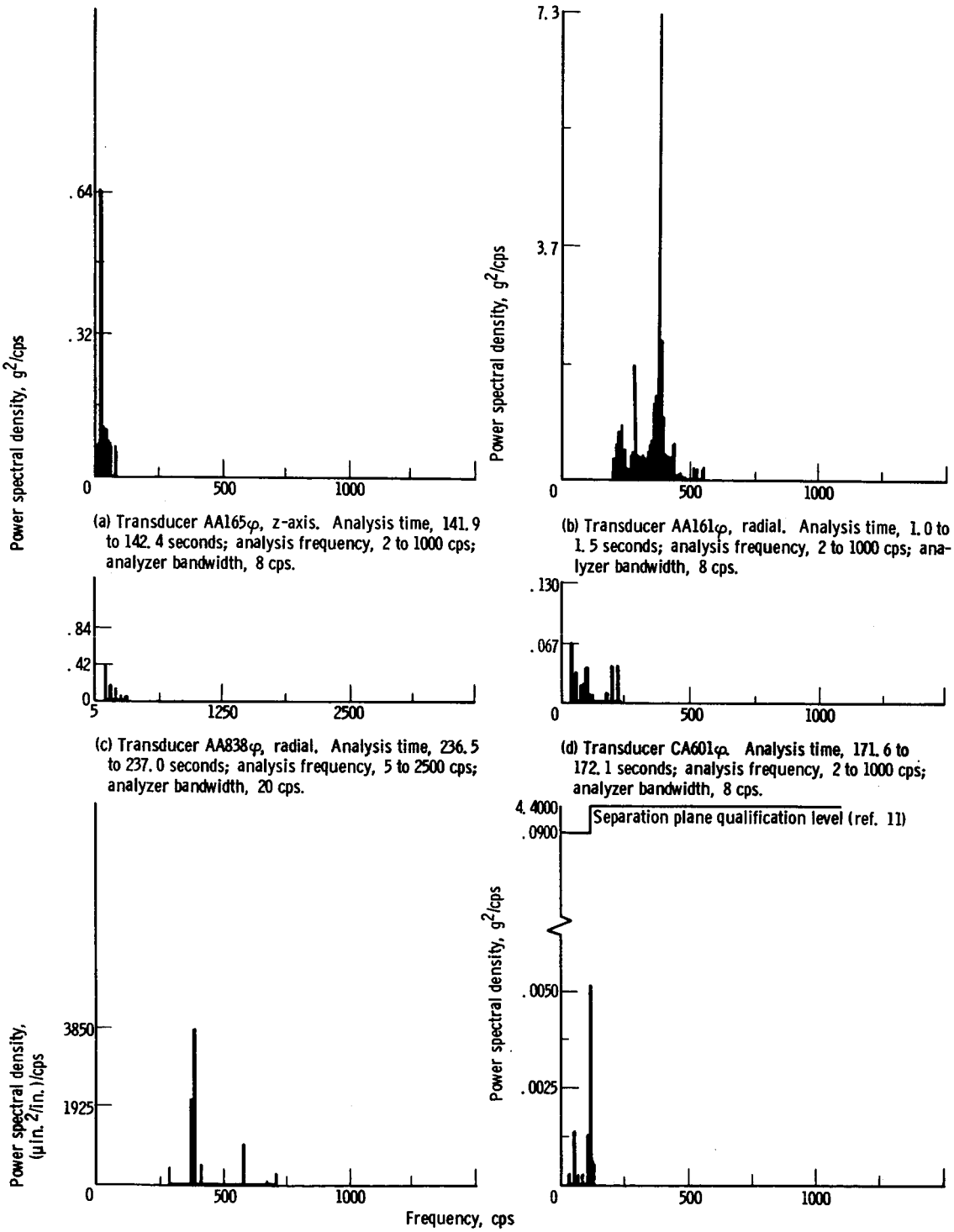

(a) Transducer AA165φ, z-axis. Analysis time, 141.9 to 142.4 seconds; analysis frequency, 2 to 1000 cps; analyzer bandwidth, 8 cps.

(b) Transducer AA161φ, radial. Analysis time, 1.0 to 1.5 seconds; analysis frequency, 2 to 1000 cps; analyzer bandwidth, 8 cps.

(c) Transducer AA838φ, radial. Analysis time, 236.5 to 237.0 seconds; analysis frequency, 5 to 2500 cps; analyzer bandwidth, 20 cps.

(d) Transducer CA601φ. Analysis time, 171.6 to 172.1 seconds; analysis frequency, 2 to 1000 cps; analyzer bandwidth, 8 cps.

(e) Transducer, CY59S. Analysis time, 0 to 0.5 second; analysis frequency, 2 to 1000 cps; analyzer bandwidth, 8 cps.

(f) Transducer CY49φ, x-axis. Analysis time, 0.5 to 1.0 second; analysis frequency, 2 to 1000 cps; analyzer bandwidth, 8 cps.

Figure X-5. - Vibration power spectrum.

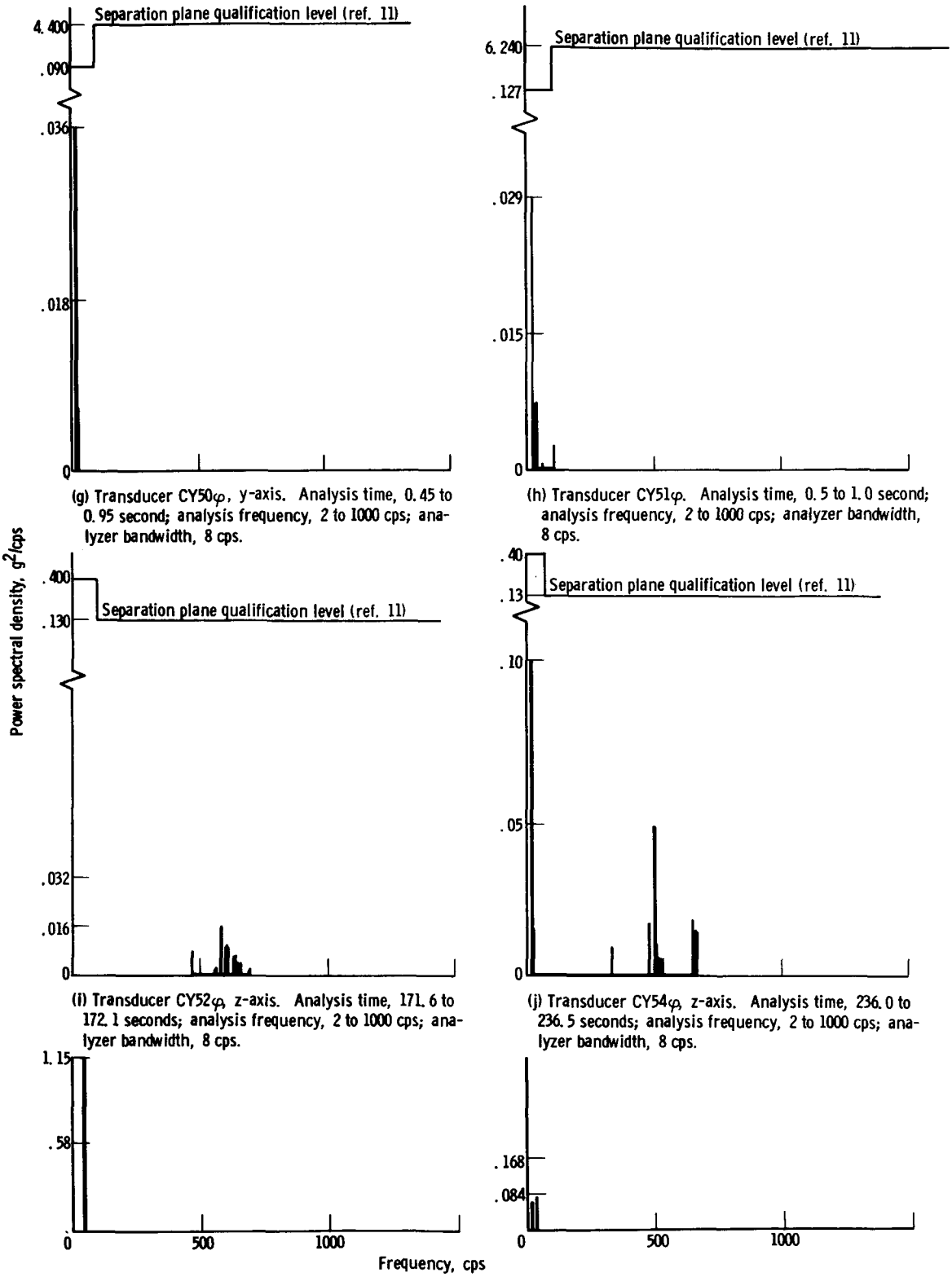

(g) Transducer CY50φ, y-axis. Analysis time, 0.45 to 0.95 second; analysis frequency, 2 to 1000 cps; analyzer bandwidth, 8 cps.

(h) Transducer CY51φ. Analysis time, 0.5 to 1.0 second; analysis frequency, 2 to 1000 cps; analyzer bandwidth, 8 cps.

(i) Transducer CY52φ, z-axis. Analysis time, 171.6 to 172.1 seconds; analysis frequency, 2 to 1000 cps; analyzer bandwidth, 8 cps.

(j) Transducer CY54φ, z-axis. Analysis time, 236.0 to 236.5 seconds; analysis frequency, 2 to 1000 cps; analyzer bandwidth, 8 cps.

(k) Transducer CY55φ, y-axis. Analysis time, 0.55 to 1.05 seconds; analysis frequency, 2 to 1000 cps; analyzer bandwidth, 8 cps.

(l) Transducer CY56φ, x-axis. Analysis time, 0.5 to 1.0 second; analysis frequency, 2 to 1000 cps; analyzer bandwidth, 8 cps.

Figure X-5. - Continued.

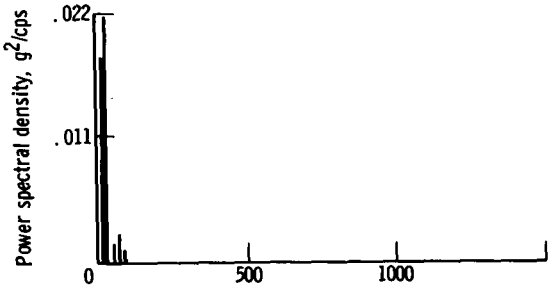

(m) Transducer CY57φ, normal axis. Analysis time, 0.5 to 1.0 second; analysis frequency, 2 to 1000 cps; analyzer bandwidth, 8 cps.

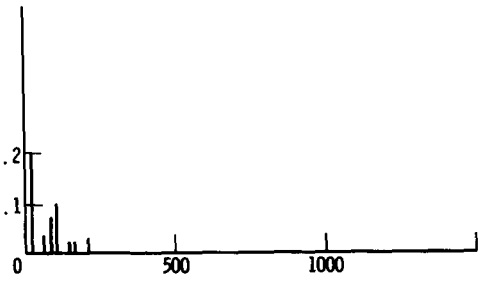

(n) Transducer CY58φ, z-axis. Analysis time, 171.5 to 172 seconds; analysis frequency, 2 to 1000 cps; analyzer bandwidth, 8 cps.

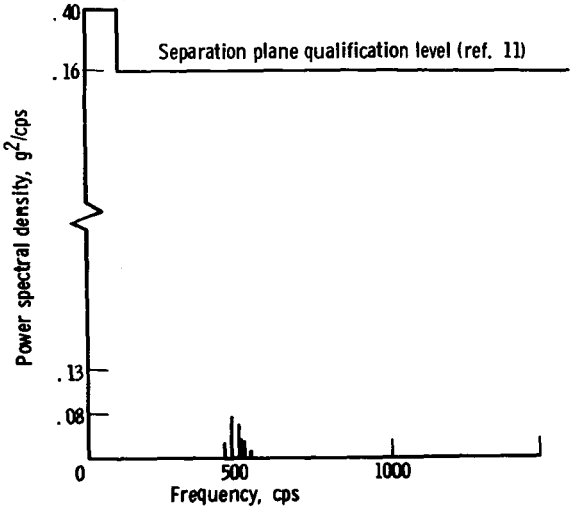

(o) Transducer CY53φ, z-axis. Analysis time, 235.6 to 236.1 seconds; analysis frequency, 2 to 1000 cps; analyzer bandwidth, 8 cps.

Figure X-5. - Concluded.

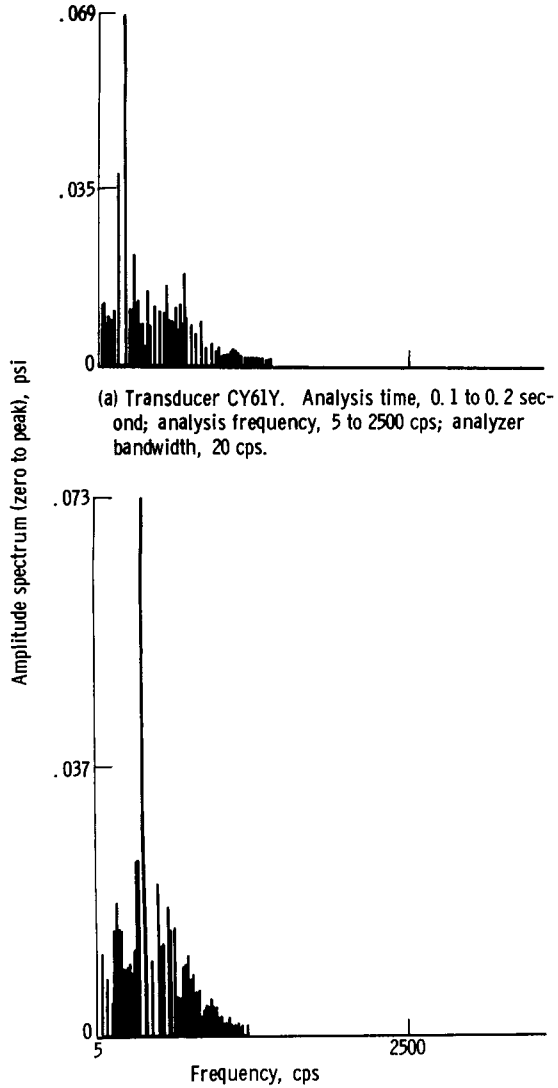

(a) Transducer CY61Y. Analysis time, 0.1 to 0.2 second; analysis frequency, 5 to 2500 cps; analyzer bandwidth, 20 cps.

(b) Transducer CY60Y. Analysis time, 1.0 to 1.2 seconds; analysis frequency, 5 to 2500 cps; analyzer bandwidth, 20 cps.

Figure X-6. - Sound pressure level.

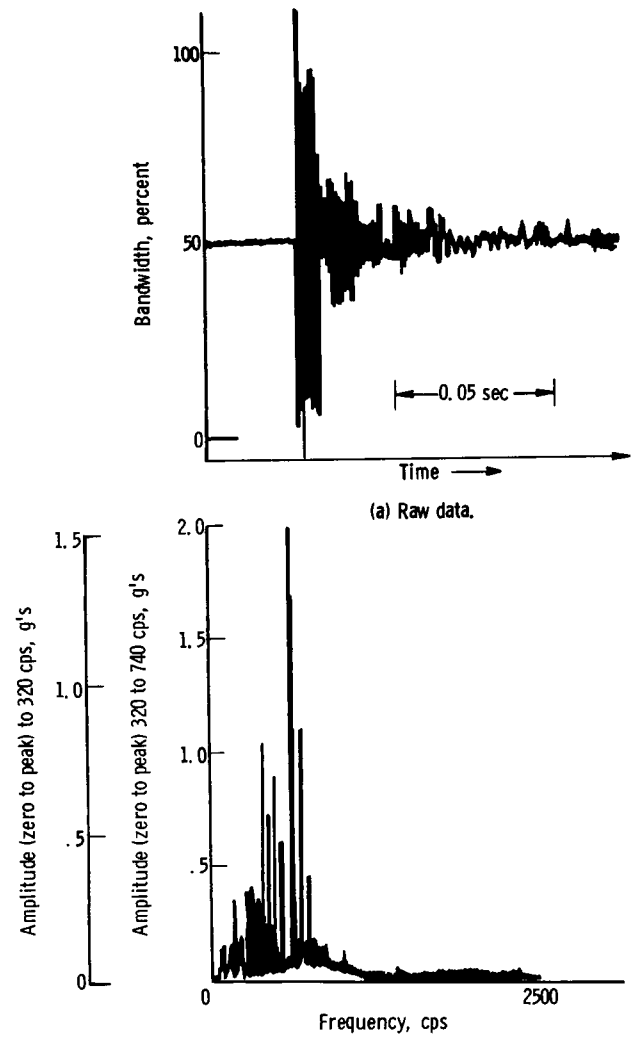

(a) Raw data.

(b) Amplitude spectrum.

Figure X-7. - Maximum vibration retroattachment 1. CY52φ.

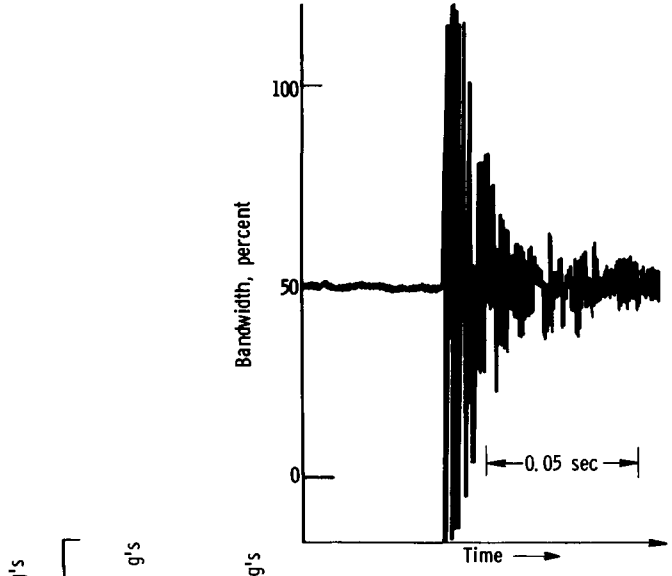

(a) Raw data.

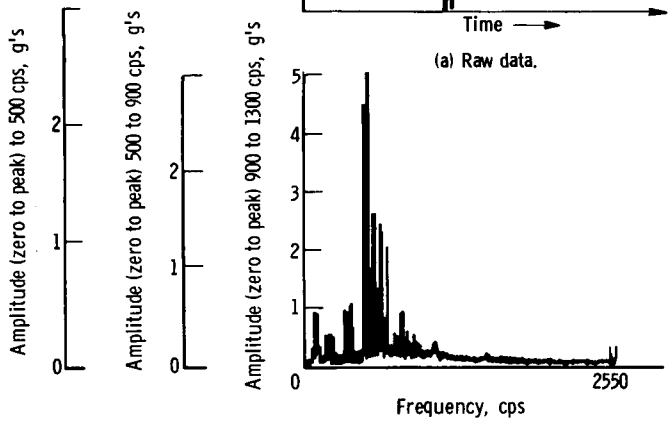

(b) Amplitude spectrum.

Figure X-8. - Maximum vibration retroattachment 2. CY53φ.

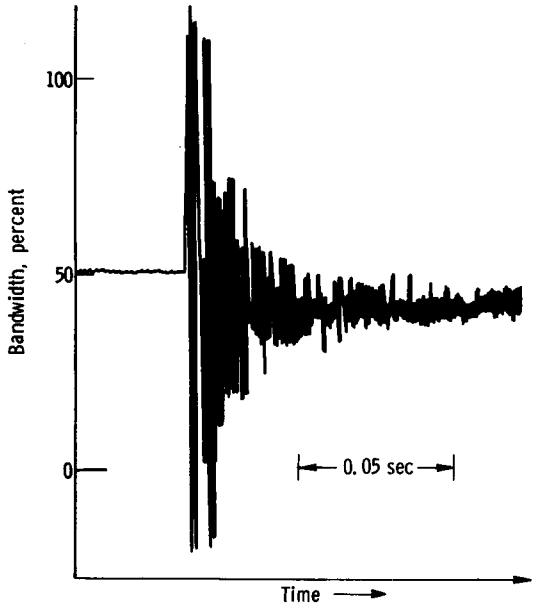

(a) Raw data.

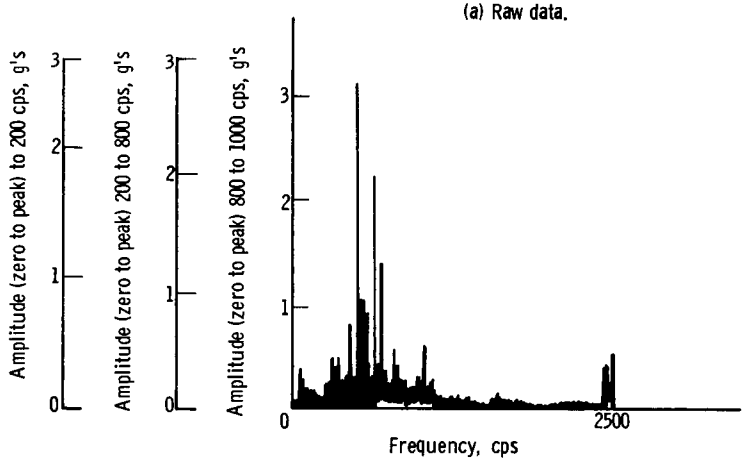

(b) Amplitude spectrum.

Figure X-9. - Maximum vibration retroattachment 3. CY54φ.

XI. FLIGHT CONTROL

SUMMARY

Analysis of the Atlas-Centaur flight-control telemetry data indicated satisfactory system performance throughout flight.

ATLAS

Flight-control measurements during Atlas-powered flight were taken from the Centaur rate gyros. Since the Centaur autopilot is not activated for control purpose until sustainer engine cutoff (SECO), the flight control measurements are monitored for correlation with the Atlas flight-control data and to supply supporting data during the booster phases of flight.

At lift-off the Centaur rate gyros indicated the usual clockwise roll transient at a frequency of 3.5 cps and a maximum rate of 1.2 degrees per second just prior to Atlas autopilot activation at 42-inch motion. Following lift-off, the axial accelerometer indicated longitudinal oscillations at a frequency of 6 cps reaching a maximum of 1.2 g's peak to peak at T + 0.5 second. The oscillations decayed to negligible levels by T + 15 seconds. All past Atlas-Centaur vehicles have shown similar oscillations (refs. 7 and 12).

Integration of the roll-rate gyro verified satisfactory accomplishment of the Atlas roll program, indicating a clockwise roll maneuver of 20.1 degrees, at an average rate of 1.55 degrees per second. The desired launch azimuth was 94.539 degrees, and the pad heading of 115 degrees resulted in a desired roll program of 20.46 degrees.

Low-order rigid-body and propellant slosh oscillations were observed throughout booster and sustainer flight. A comparison of analytical and flight telemetered data is shown in figure XI-1. Good correlation is evident indicating present methods of analysis in determining flight frequencies are acceptable.

The diverging oscillations in the pitch plane at the frequency of the Atlas LO_2 sloshing mode observed on AC-4 and to a lesser extent on AC-3 prior to booster engine cutoff (BECO) appear to have been stabilized on AC-6. Although the oscillations are evident prior to BECO, they approach a limit cycle with amplitudes reaching peak to peak rates of 0.12 degree per second as measured by the Centaur pitch-rate gyro.

Rates imparted to the vehicle during insulation-panel jettison were 1.96 degrees per second peak to peak in roll and less than 0.2 degree per second peak to peak in pitch and yaw. Telemetry received at the insulation-panel-jettison event indicated a roll transient of a higher magnitude than the roll

transients seen on AC-3 or AC-4. Figure XI-2 pitch- and yaw-rate gyro data showed little activity during the event other than high-frequency vibration at approximately 25 cps, which corresponds to the frequency of the third bending mode.

The area of interest, however, is the response that occurred in roll. By differentiating the roll-rate-gyro output, calculating resultant roll torques, and subtracting the torques due to vernier engine deflections, the net external torque on the vehicle can be calculated. The results are shown in figure XI-3.

The net torques on the vehicle were substantial in magnitude and changing in direction. A torque as shown in figure XI-3 is difficult to conceive since insulation-panel-hinge reactions are the only source of external forces on the vehicle. The hinges are mounted in such a manner as to cancel torques due to reactions normal to a line passing through the hinge points. No satisfactory explanation is known as to the source of the observed torques.

Rates due to nose-fairing-jettison were 0.64 degree per second peak to peak in pitch and less than 0.2 degree per second peak to peak in yaw and roll. During both insulation-panel and nose-fairing-jettison events, rates were reduced to less than 0.2 degree per second peak to peak within 1.5 seconds.

Sustainer engine cutoff was commanded at T + 234.3 seconds. Residual vehicle rates due to sustainer and vernier engine cutoff (SECO/VECO) were 0.2 degree per second in pitch and essentially zero in yaw and roll, at a point just prior to vehicle separation. These rates compared similarly with those observed during the AC-4 flight. Atlas-Centaur separation was commanded at T + 236.3 seconds following firing of the shaped charge, cutting the interstage adapter at T + 236.2 seconds. By T + 237.8 seconds, the previously mentioned residual vehicle rates had increased to 0.54 degree per second in pitch, 0.17 degree per second in yaw, and -0.16 degree per second in roll, indicating small external torques acting on the Centaur vehicle. These were probably the result of Atlas retrorocket gas impingement on the Centaur vehicle and also small torques due to the Centaur boost-pump exhaust gases (started at T + 203.8 sec).

CENTAUR

Main engine prestart was commanded at T + 237.8 seconds. The hydraulic circulating pumps were energized at T + 234.8 seconds (SECO + 0.5 sec). Main engines were then gimbaled toward a null position at an average rate of 0.6 degree per second. The engines, however, are enabled to respond to vehicle rates and approach gimbal positions in an attempt to reduce the vehicle rates, although engine thrusts are not yet available. Engine positions just prior to MES were C-1 pitch, 0.64 degree; C-2 pitch, 0.51 degree; C-1 yaw, -1.02 degrees; and C-2 yaw, -0.04 degree.

The AC-6 vehicle start transients were mild compared with AC-2 and comparable in magnitude to AC-4. Rates imparted to the vehicle due to the main engine ignition transients were -1.35 degrees per second in pitch, 0.11

degree per second in yaw, and 3.26 degrees per second in roll. These rates were primarily the result of engine differential thrust buildup, relative engine positions, and the residual vehicle rates. Corresponding maximum engine deflections due to these rates were C-1 pitch, 0.38 degree; C-2 pitch, 0.38 degree; C-1 yaw, 0.83 degree (peak to peak); and C-2 yaw, 0.45 degree (peak to peak).

At a point just prior to enabling the guidance steering signals (MES + 4 sec) vehicle rates had been reduced to 0.54 degree per second in pitch, -0.04 degree per second in yaw, and 0.7 degree per second in roll. Engine positions at this time were essentially at null.

The guidance steering commands were enabled at T + 246.8 seconds (MES + 4 sec). The guidance resolver chain outputs indicated errors of 5 degrees (nose up) in pitch and 3 degrees (nose right) in yaw. These errors had been accumulated during the separation and MES flight phases. Vehicle rates due to steering enable were -1.81 degrees per second in pitch and -1.40 degrees per second in yaw. Corresponding engine deflections were C-1 pitch, 0.64 degree; C-2 pitch, -0.64 degree; C-1 yaw, -0.64 degree; and C-2 yaw, -0.51 degree. This error was nulled in approximately 3 seconds.

Following the settling out of the MES and steering enable transients, the engines indicated trim positions of C-1 pitch, 0.014 degree; C-2 pitch, 0.17 degree; C-1 yaw, 0.01 degree; and C-2 yaw, -0.09 degree. At MES + 220 seconds, trim positions were C-1 pitch, 0.13 degree; C-2 pitch, 0.11 degree; C-1 yaw, -0.25 degree; and C-2 yaw, -0.12 degree. Low-level engine-limit cycling in the pitch and yaw planes was also observed during this period at a frequency of approximately 0.25 cps (rigid body) and peak-to-peak amplitudes of 0.12 degree.

Low-order slosh and rigid-body oscillations were observed throughout the powered phase at peak-to-peak amplitudes (average) of 0.2 degree per second. Frequency components agreed with the predicted engine-limit cycle frequencies as shown in figure XI-1.

CENTAUR COAST PHASE

At T + 747.8 seconds, spacecraft separation was commanded. A complete discussion of separation dynamics is presented in section X, VEHICLE DYNAMICS. Approximately 9 seconds prior to the separation sequence, vehicle rates were below the rated control engine switching thresholds, and no engines were commanded on during this time. The following table shows the residual rates of the Centaur vehicle just prior to separation, the rates imparted the Centaur vehicle after separation, and the differential change:

Plane of motion	T + 747.8 sec, deg/sec	T + 748.1 sec, deg/sec	Differential postseparation - preseparation, deg/sec
Pitch	-0.12	-0.11	0.01
Yaw	.19	.14	-.05
Roll	.04	.03	-.01

CENTAUR RETROMANEUVER

Centaur turnaround was commanded at T + 752.8 seconds as indicated by both attitude engine commands and rate-gyro data. At the initiation of turnaround, the guidance resolver-chain outputs indicated that the vehicle was approximately 18 degrees nose down and 12 degrees nose right with respect to the guidance steering vector generated at MECO. In response to the turnaround command, the vehicle reached maximum rates of 1.48 degrees per second in pitch and 1.45 degrees per second in yaw. Vehicle roll rates were maintained within the control thresholds. At T + 845 seconds, vehicle steering completed the turnaround maneuver approximately 15 seconds before the start of blowdown.

The blowdown maneuver was commanded at T + 872.8 seconds and enabled oxygen to be vented through the main engine and hydrogen through the chilldown valves, to produce thrust of sufficient magnitude in order to alter the orbital path of the expended Centaur stage. Coincident with the blowdown command, the hydraulic recirculating pumps were started to aline the thrust vector as commanded by attitude and rate errors. This was done in order to minimize blowdown torques and maximize the effect of the small axial thrust. Comparison of the Surveyor and Centaur orbital data indicates the separation distance was 1300 to 1600 kilometers 5 hours after separation.

Torquing moments were generally about the yaw and roll axes and were well within the capability of the attitude control system. During the first 100 seconds of blowdown, torquing moments were at their greatest, resulting in maximum duty cycles of approximately 65 percent. This duty cycle, however, was not maintained for long periods, and the average duty cycle was of the order of 10 percent. Duty cycles decreased with time thereafter as a result of tank pressure decay and subsequently lower torques.

Attitude control engine firings are plotted in figure VI-22, which show the attitude engine activity from MECO through the blowdown maneuver.

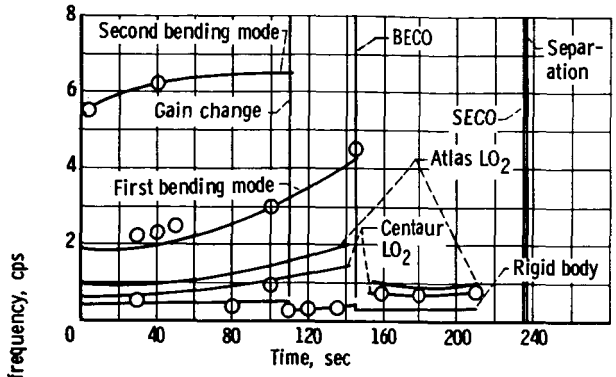

(a) Atlas powered flight.

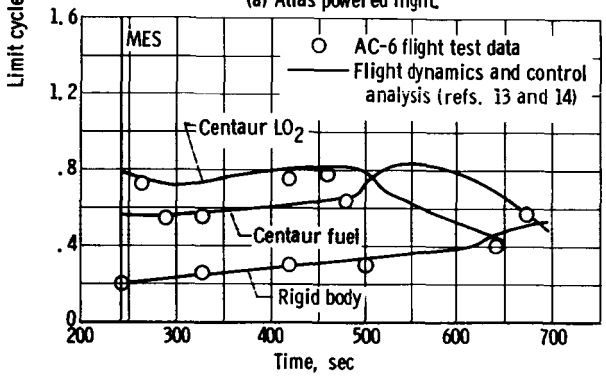

(b) Centaur powered flight.

Limit cycle frequency, cps

Figure XI-1. - Comparison of experimental and analytical frequencies.

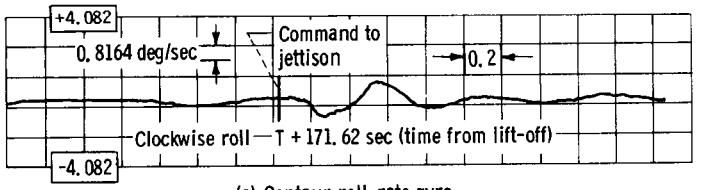

(a) Centaur roll-rate gyro.

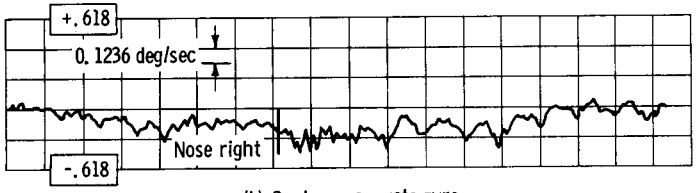

(b) Centaur yaw-rate gyro.

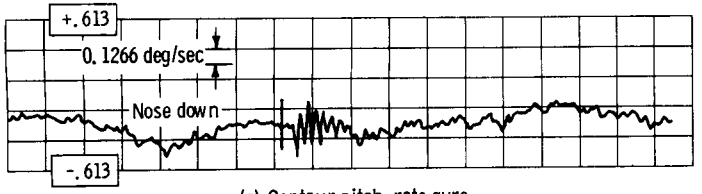

(c) Centaur pitch-rate gyro.

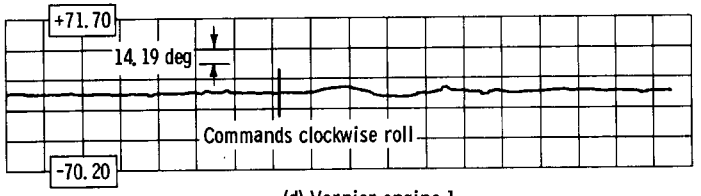

(d) Vernier engine 1.

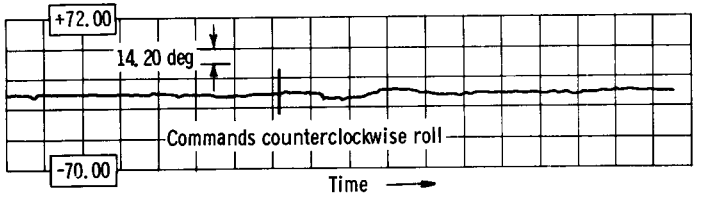

(e) Vernier engine 2.

Figure XI-2. - AC-6 flight response at insulation-panel jettison.

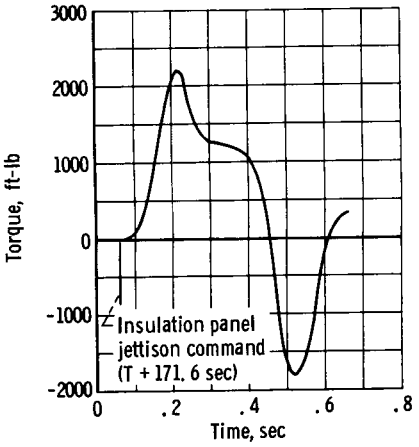

Figure XI-3. - Roll torque as function of time. (Positive torque causes clockwise roll.)

XII. GUIDANCE

The Centaur guidance system flown on the AC-6 vehicle exhibited nominal performance throughout the flight. Velocity errors at T_c + 689 seconds were as follows: δV_u = -0.4 foot per second, δV_v = -0.4 foot per second, and δV_w = 0.2 foot per second. One of the prime objectives of this flight was to demonstrate the capability of the inertial guidance system to inject the SD-2 Surveyor spacecraft on a lunar intercept trajectory. The maximum allowable spacecraft midcourse correction for miss only is 50 meters per second. Tracking data indicated a midcourse correction of 4.25 meters per second for the AC-6 flight.

The system was calibrated on F - 0 day, and the Day 2 Plan I "J" values (launch-on-time constants, ref. 15) were loaded into the airborne computer. After completion of calibration, the system was optically alined to an azimuth of 115 degrees from north. The system was advanced to the inertial mode 8.97 seconds prior to lift-off.

The computed steering vector successfully guided the vehicle during the sustainer and Centaur powered phases and provided a retrovector to which the vehicle was steered during retromaneuver and blowdown. The airborne computer generated booster cutoff, sustainer cutoff backup, and main engine cutoff discretes, as planned, with the significant times shown in the following table:

Function	Time, sec	Data source (ref. 5)
BECO	141.800	TLM CI21X
SECO backup	236.573	TLM CI22X
MECO	679.08	TLM CI19X

Table XII-I is a summary of the 21 digital words that were telemetered during each computer cycle by the digital data link.

A discussion of system performance is presented in the following sections. The times preceded by the symbol T are referenced to 2-inch motion, and those preceded by T_c are referenced to computer zero time. Figure XII-1 is a functional schematic drawing of the guidance system.

GIMBAL SERVOSIGNALS

Telemetry measurements of the gimbal torque motor input voltages and the 7.2-kilocycle demodulator outputs indicate that the platform remained stable throughout the flight. The maximum gimbal servoloop errors are shown in table XII-II. Gimbal 1, 2, and 3 demodulator error voltages indicate equivalent gyro

error angles well within the 60 arc-seconds of required dynamic accuracy. Gimbal 4 demodulator error does not represent an inertial misalinement but rather the gimbal 2 resolver error.

At T + 2.3 seconds, gimbal 2 reflected the start of the roll program and at T + 15.3 seconds, gimbal 3 responded to the initiation of the Atlas pitch program. At T + 43.6 seconds, gimbal 4 uncaged at a pitch angle of 16° (fig. XII-2(a)), as computed from the nominal Atlas pitch profile. During the Atlas powered phase of flight, gimbals 1 and 2 oscillated at approximately 1 cps, which is indicative of propellant sloshing. From T + 50 seconds until BECO, low-frequency oscillations from 0.25 to 0.33 cps observed on gimbal 1 were attributed to rigid body dynamics. During the Centaur phase of flight, oscillations of approximately 0.2 cps, which are characteristics of rigid body dynamics, were observed on gimbal 1. Propellant sloshing caused oscillations of 0.5 to 0.75 cps to appear on gimbal 2 during Centaur phase. At T + 496 seconds, the pitch gimbal voltage reflected a computer steering command for perigee correction. At T + 753 seconds, gimbals 1 and 3 responded to the beginning of retromaneuver and indicated satisfactory performance throughout the vehicle retromaneuver. Telemetered analog signals of gimbal 3 torque motor input and demodulator output show the occurrence of both the perigee correction and the beginning of retromaneuver (figs. XII-2(b) and (c)).

TORQUING LOOPS

The digital and analog torquing signals indicated that the guidance system went into the flight mode 7.8 seconds prior to lift-off. Analog signals revealed two unexplained shifts in the W-torquing loop. The first shift occurred at T - 0 and was equivalent to a 0.45 degree per hour change in the W-torquing rate. The second occurrence was at T + 204 seconds (same time as nose-fairing jettison) and was equivalent to a torquing change of 0.30 degree per hour. An equivalent change in torquing at the time of nose-fairing jettison occurred during the flight of the AC-4 vehicle. The digital torquing output did not give any indication of the two changes in W-torquing. The digital and analog data were reduced to the same units, "differenced," and the results are plotted in figure XII-3. The bias in the differences is a result of signal conditioner null offset, and figure XII-3(c) clearly indicates the two shifts previously discussed.

ACCELEROMETER LOOPS

Oscillograph recordings of the 14.4-kilocycle demodulator output voltages are shown in figure XII-4. These measurements indicate satisfactory performance of the accelerometer loops throughout the flight. Prior to T - 0 and U- and V-demodulator outputs showed a saw-toothed oscillation with a frequency from 0.17 to 0.25 cps. Similar cycling occurred in all three loops during the coast phase of flight. This is normal operation of the accelerometer loops when the inertial components are sensing zero gravity. The following table lists the largest pendulum offsets observed during flight:

Event	Accelerometer direction					
	A_u	$-A_u$	A_v	$-A_v$	A_w	$-A_w$
	Maximum pendulum excursion, arc-sec					
Lift-off	30	38	20	7	24	36
Mach 1	27	22	8	12	18	16
BECO	18	12	8	8	15	8
Booster jettison	14	20	--	16	15	12
Insulation-panel jettison	28	36	12	8	20	24
Nose-fairing jettison	30	37	16	16	36	50
SECO	20	22	6	14	12	8
Atlas-Centaur separation	20	40	8	8	8	8
MES	12	--	6	6	12	8

The demodulator outputs indicated small error voltages throughout powered flight with maximums occurring at the time of maximum shocks. At T + 742 seconds, the U and W demodulator outputs were no longer monitored. The two available channels allowed more spacecraft measurements to be telemetered. A histogram of the incremental velocity pulses (ΔV's) required to rebalance the pendulous accelerometers indicates that there were no large limit cycles or bursting of the loops.

STEERING LOOPS

The guidance steering loop performed exceptionally well throughout the flight. During the boost phase, the computer outputs were zero, and the X- and Y-resolver-chain outputs were maintained at null. Steering was enabled by the flight control system at T + 148 seconds, at which time the X- and Y-resolver-chain outputs moved off null indicating that the computer was compensating for trajectory errors built up during boost phase (fig. XII-5). Guidance steering was closed loop during sustainer and Centaur powered phases of flight. The steering vector was locked out by the flight control system at SECO until MES + 4 seconds when the autopilot reinitiated acceptance of guidance steering commands. At T + 497 seconds, the Y-resolver-chain output reflected a computer command perigee correction in the pitch plane. After MECO had been generated, guidance steering was disabled until T + 706 seconds, at which time the steering vector was switched to the negative of the velocity vector to provide the retro-vector to which the vehicle was steered after separation of the spacecraft (fig. XII-5).

FUNCTIONAL PERFORMANCE

The computer digital steering value minus the telemetered analog value as a function of time is shown in figure XII-6. Analysis indicates that the difference is a result of signal conditioner null offset. The computer-generated missile actual velocity is shown in figure XII-7, and the difference of nominal velocity from total velocity is shown in figure XII-8. The guidance computer correctly calculated the missile velocity, which was close to the nominal expected velocity as a function of time. Figure XII-9 shows plots of computer calculated position, and figure XII-10 shows the difference of the calculated posi-

tion from the nominal as a function of time. Figure XII-11 indicates that the platform skin temperature stayed within the 50° to 120° F specifications throughout the flight. It is also apparent that the inertial component temperatures were within their control bands.

TABLE XII-I. - TELEMETRY SEQUENCE (REF. 5)

Word order	Symbol	Function	Units	Discrete words length (W.T.)[a]
1	$V_{\sigma w}$	Sigmator W-velocity	ft/sec	16
2	t_i	Time	sec	8
3	$r_{\sigma v}$	Sigmator V-position	ft	8
4	$r_{\sigma w}$	Sigmator W-position	ft	8
5	$r_{\sigma u}$	Sigmator U-position	ft	8
6	$V_{\sigma u}$	Sigmator U-velocity	ft/sec	8
7	$V_{\sigma v}$	Sigmator V-velocity	ft/sec	8
8	r_{mv}	Total V-position	ft	8
9	r_{mw}	Total W-position	ft	8
10	t_e	Guidance launch time into window (first cycle)	sec	8
	Codeword	----------	none	8
11	r_{mu}	Total U-position	ft	8
12	V_{mw}	Total W-velocity	ft/sec	8
13	V_{mv}	Total V-velocity	ft/sec	8
14	Omega d_v	V-gyro torquing rate	rad/sec	8
15	Omega d_u	U-gyro torquing rate	rad/sec	8
16	Omega d_w	W-gyro torquing rate	rad/sec	8
17	a_t^2	Thrust acceleration squared; boost phase	$(ft/sec^2)^2$	8
	ϵ	Energy to be gained; sustainer-Centaur phase	$(ft/sec)^2$	8
	Δt_{co}	Time to go until MECO; first cycle postinjection phase	sec	8
18	V_{mu}	Total U-velocity	ft/sec	8
19	f_u^*	U-steering vector	---------	12
20	f_w^*	W-steering vector	---------	12
21	f_v^*	V-steering vector	---------	12

[a]W.T., word time where one W.T. = 0.15625 msec.

TABLE XII-II. - GIMBAL SERVOLOOP MAXIMUM ERRORS

Gimbal	Gimbal demodulator maximum errors			Torquer motor maximum errors	
	Signal conditioner output, V(dc)	Demodulator output, V(dc)	Displacement error, arc-sec	Signal conditioner output, V(dc)	Torque motor input, V(dc)
1	0.40 -.25	5.00 -3.13	7.2 -4.5	-0.28 .40	-2.80 4.00
2	.30 -.18	1.03 -.62	10.6 -6.18	-.20 .15	-2.00 1.50
3	.45 -.20	.74 -.33	16.4 -7.31	-.30 .34	-3.00 3.40
4	.20 -.30	.57 -.85	330 -500	-.10 .20	-1.00 2.00

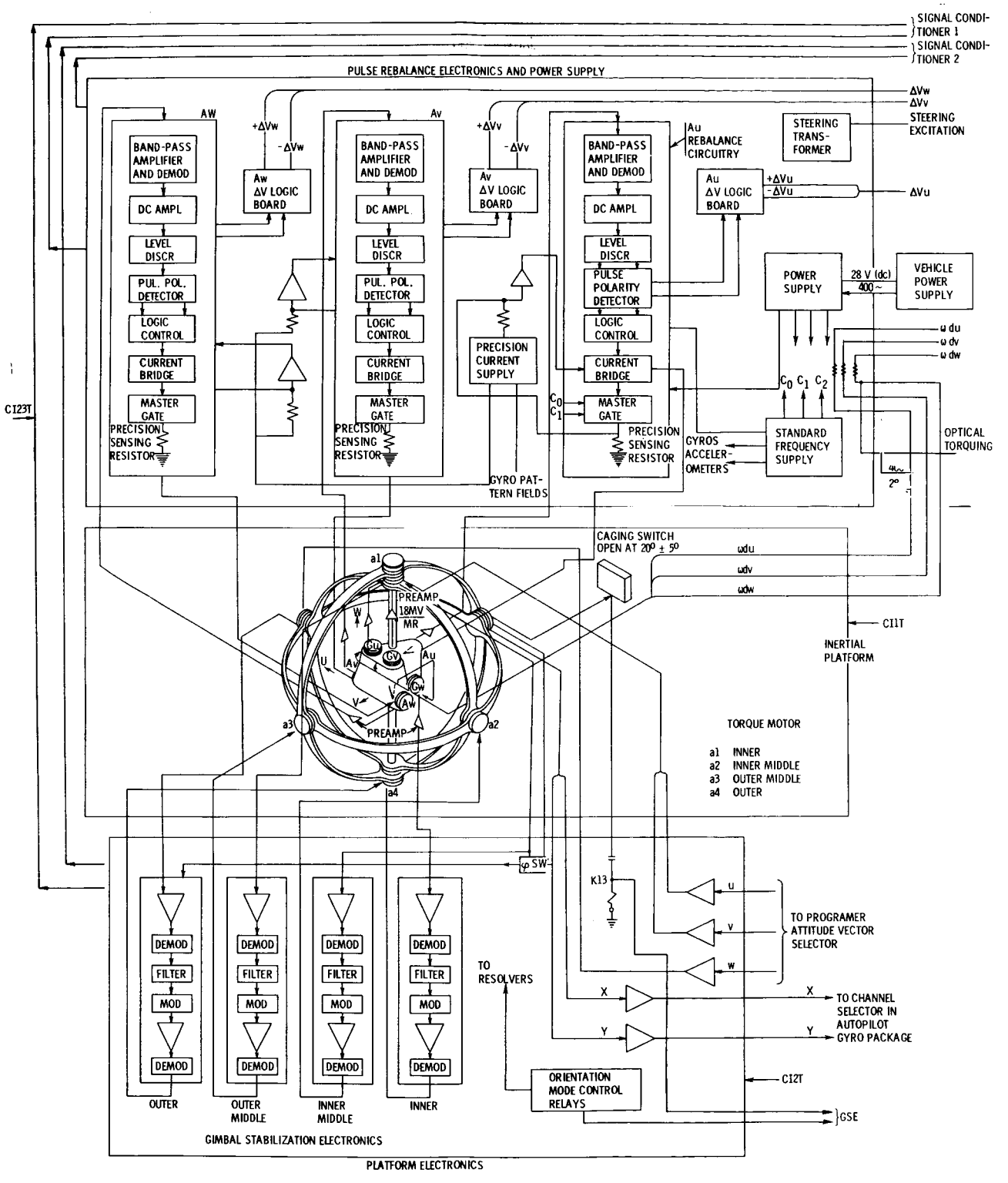

Figure XII-1. - Guidance system

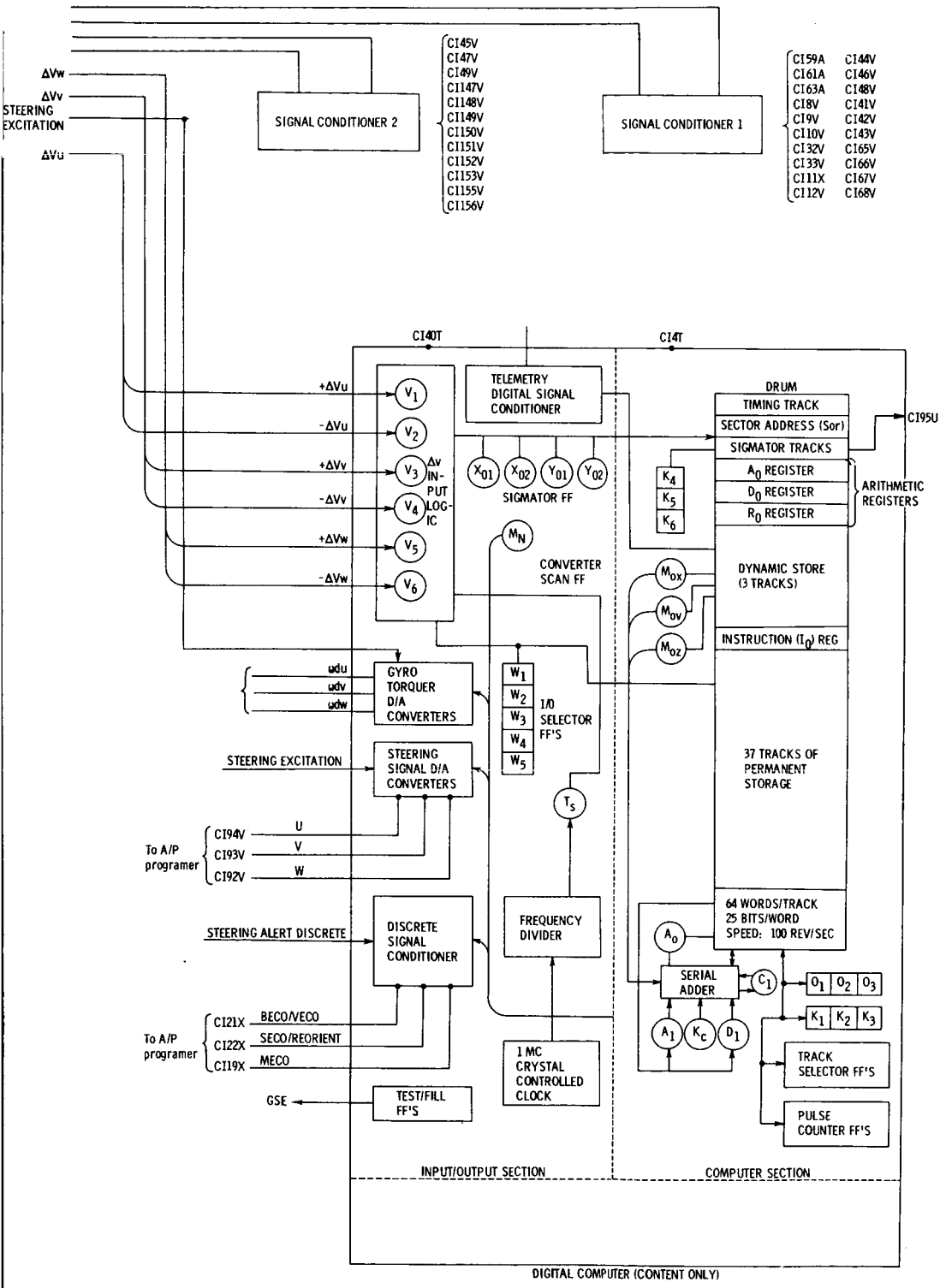

simplified schematic drawing.

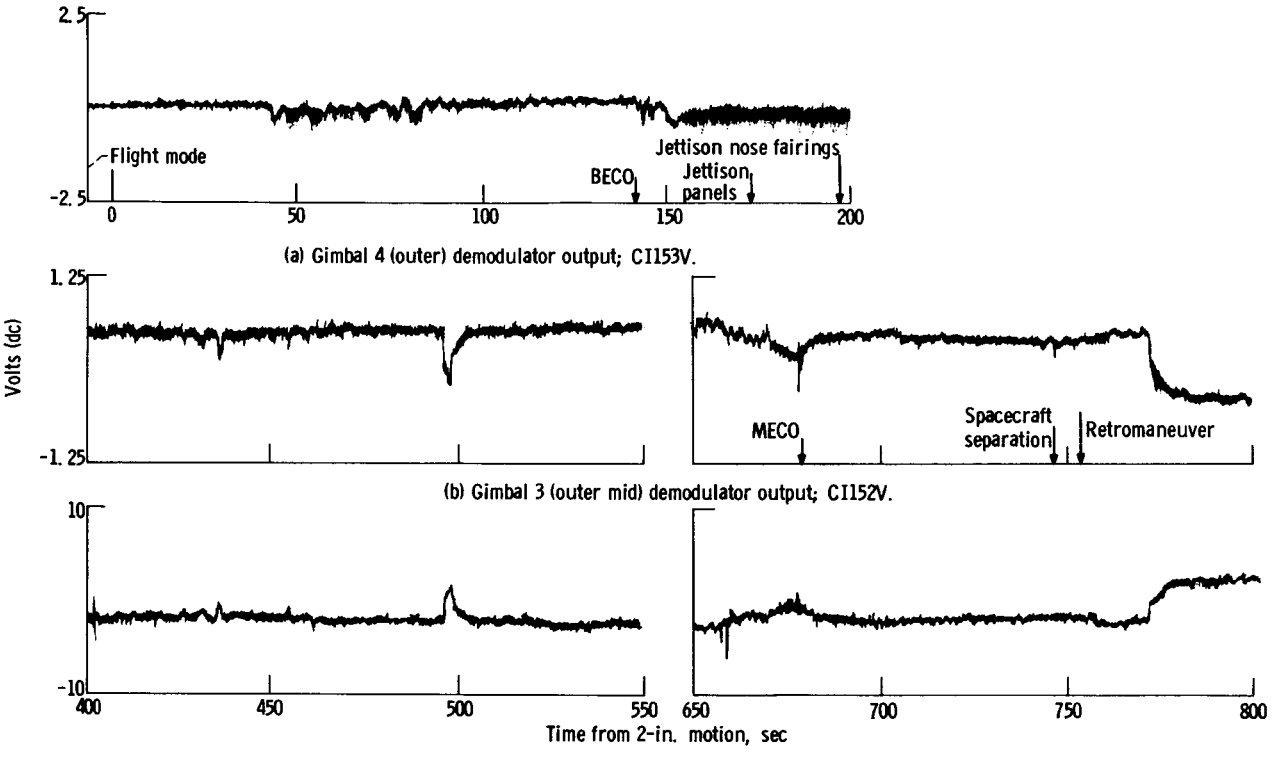

(a) Gimbal 4 (outer) demodulator output; CI153V.

(b) Gimbal 3 (outer mid) demodulator output; CI152V.

(c) Gimbal 3 torquer motor input; CI65V.

Figure XII-2. - Centaur guidance system telemetered data.

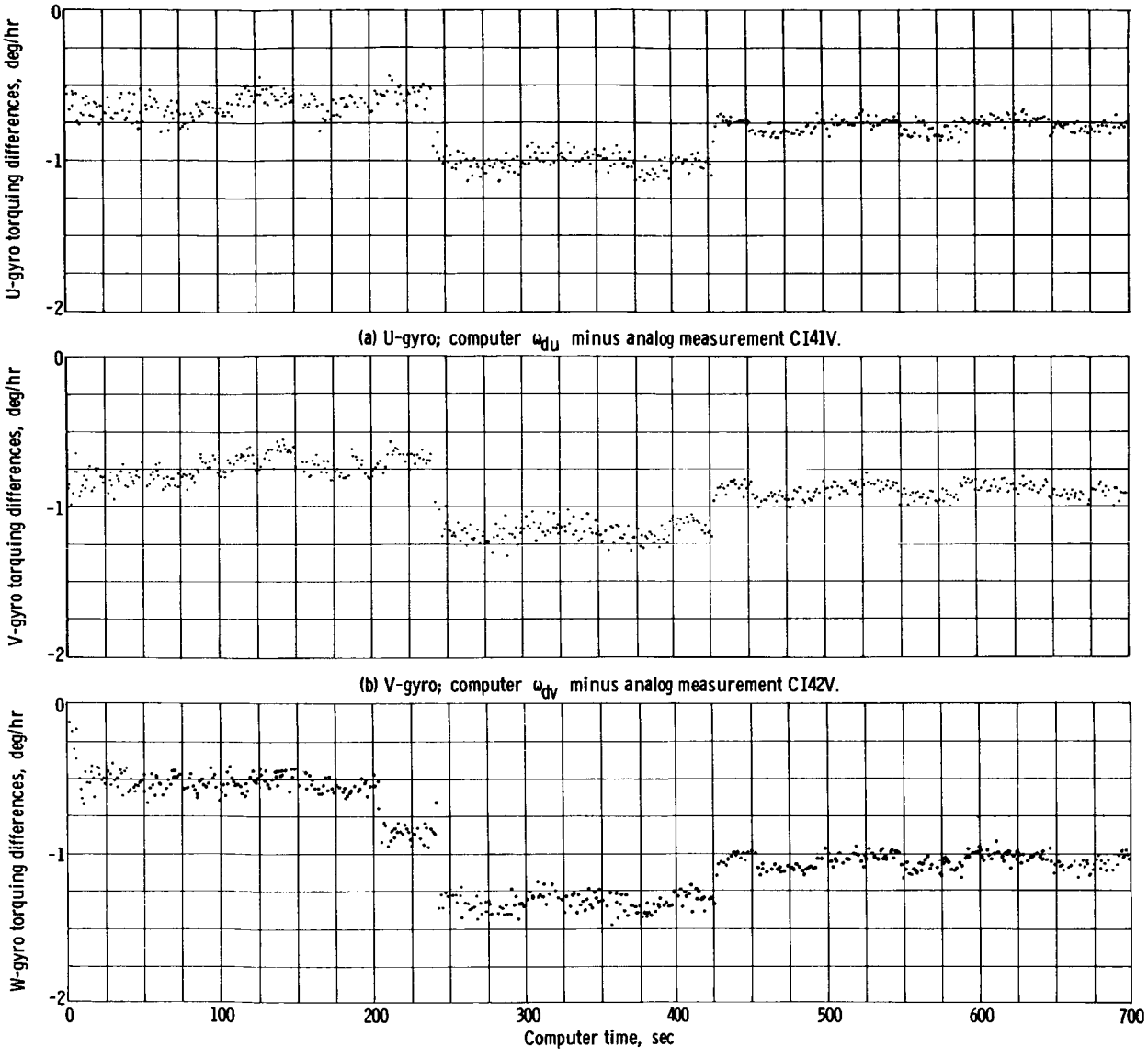

(a) U-gyro; computer ω_{du} minus analog measurement CI41V.

(b) V-gyro; computer ω_{dv} minus analog measurement CI42V.

(c) W-gyro; computer ω_{dw} minus analog measurement CI42V.

Figure XII-3. - Torquing differences.

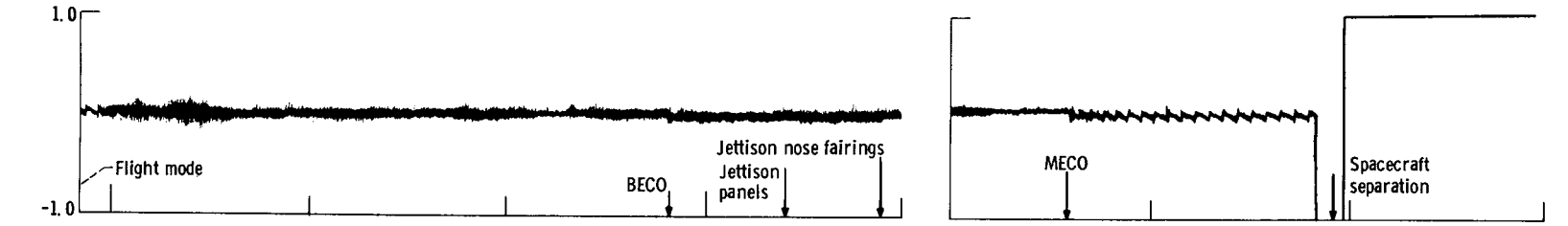

(a) U-accelerometer 14.4-kilocycle demodulator output; CI147V.

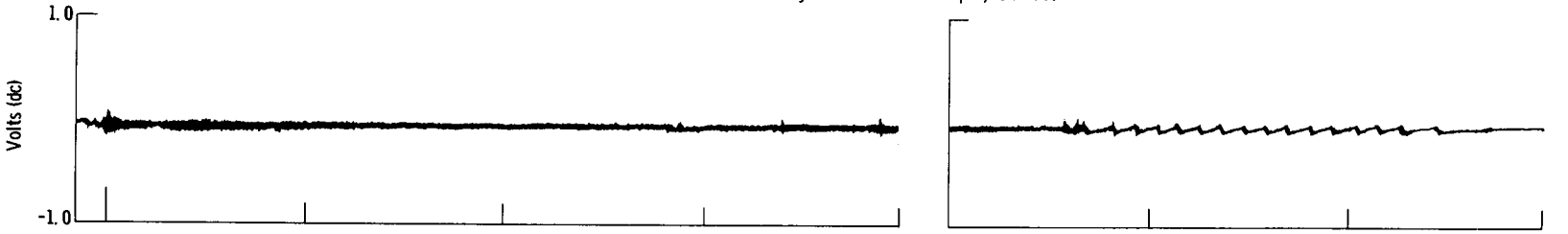

(b) V-accelerometer 14.4-kilocycle demodulator output; CI148V.

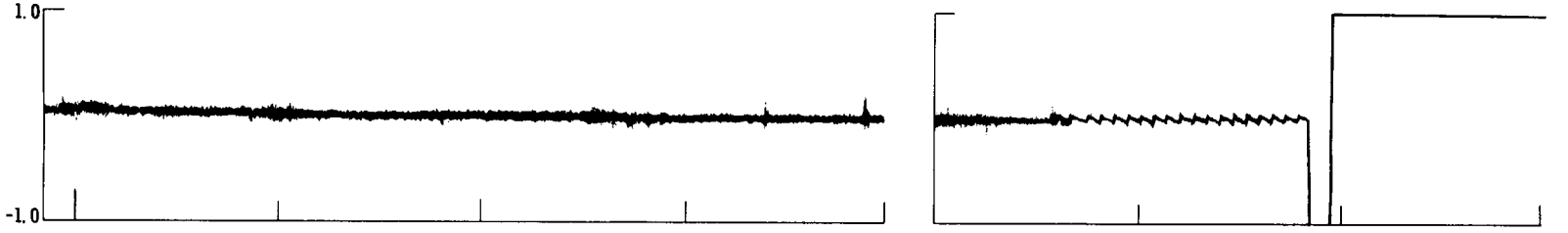

(c) W-accelerometer 14.4-kilocycle demodulator output; CI149V.

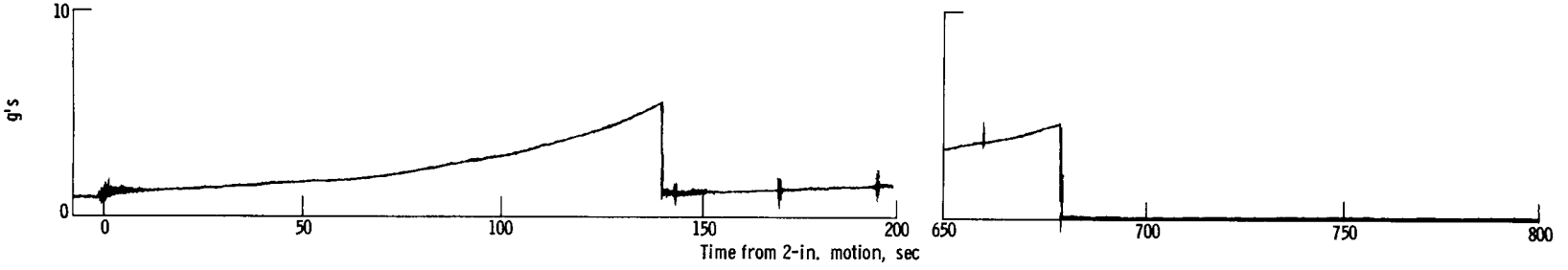

(d) Axial acceleration; CM101A.

Figure XII-4. - Centaur guidance system telemetered data.

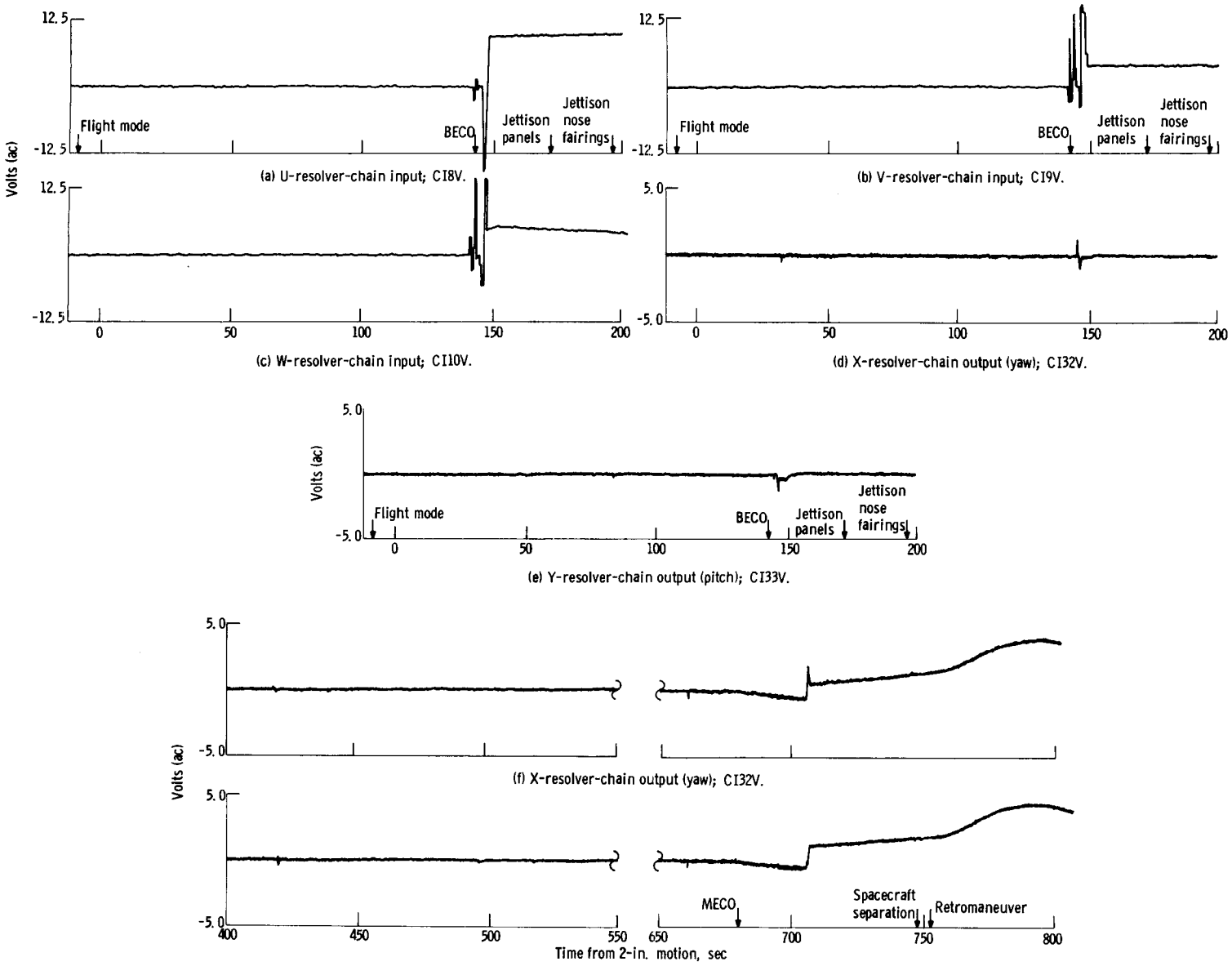

Figure XII-5. - Centaur guidance system telemetered data.

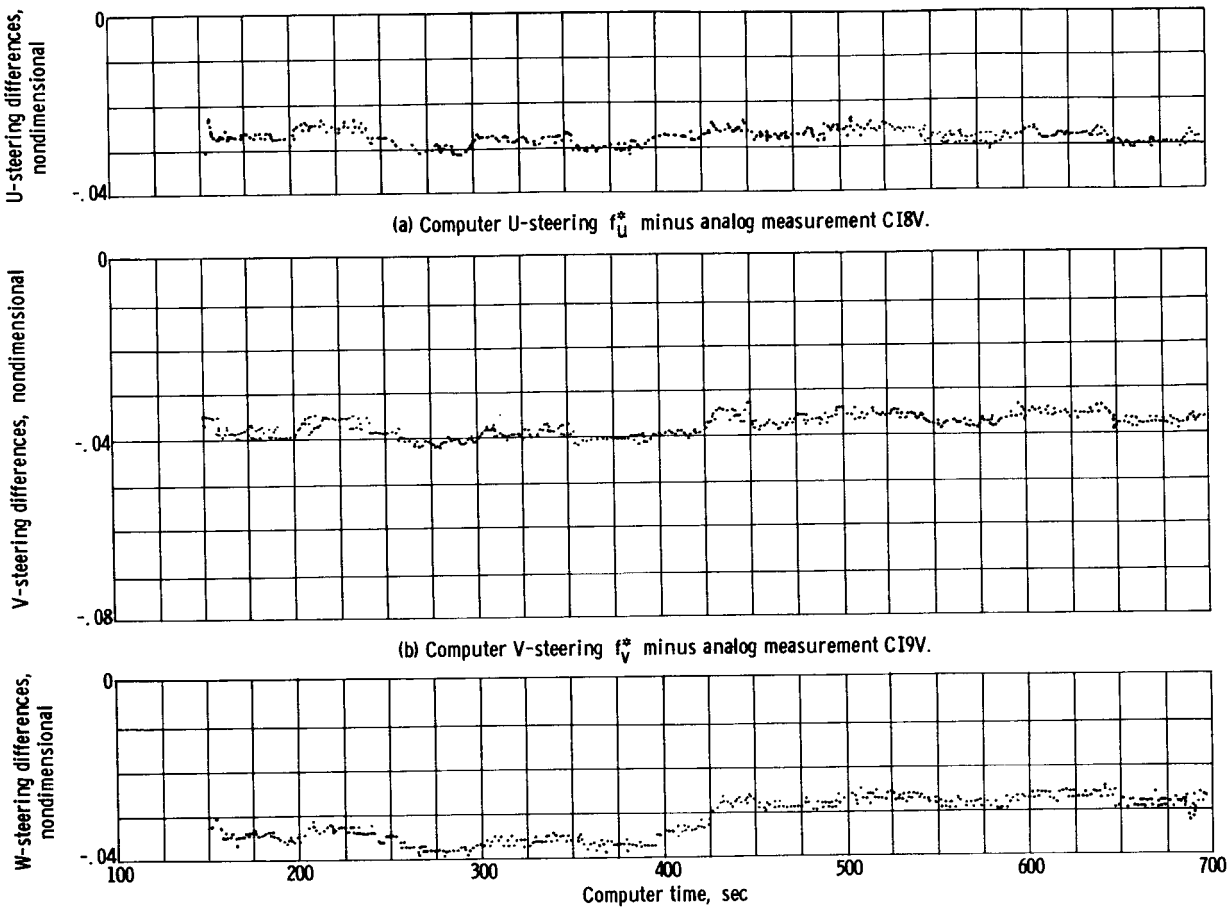

(a) Computer U-steering f_u^* minus analog measurement CI8V.

(b) Computer V-steering f_v^* minus analog measurement CI9V.

(c) Computer W-steering f_w^* minus analog measurement CI10V.

Figure XII-6. - Steering differences.

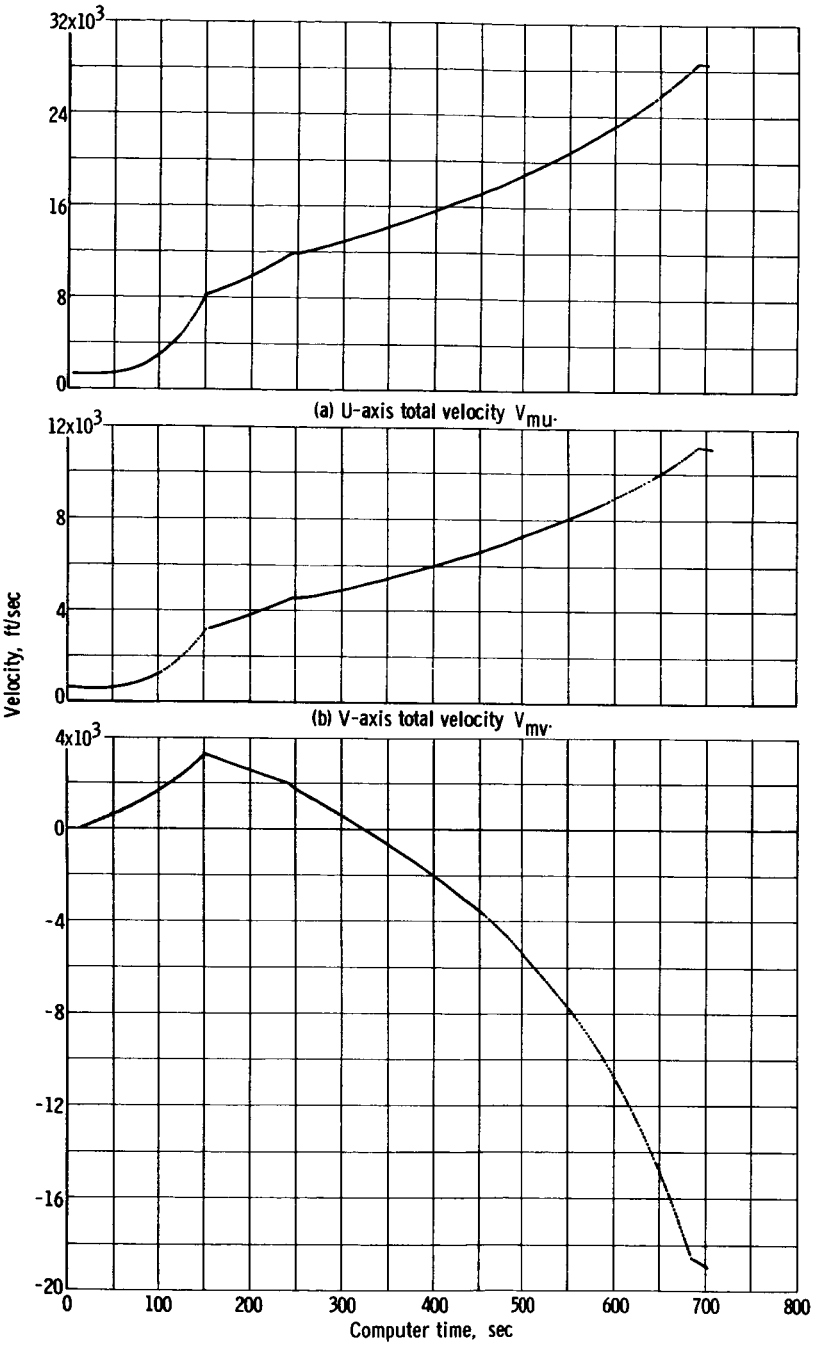

Figure XII-7. - Guidance computer total velocity.

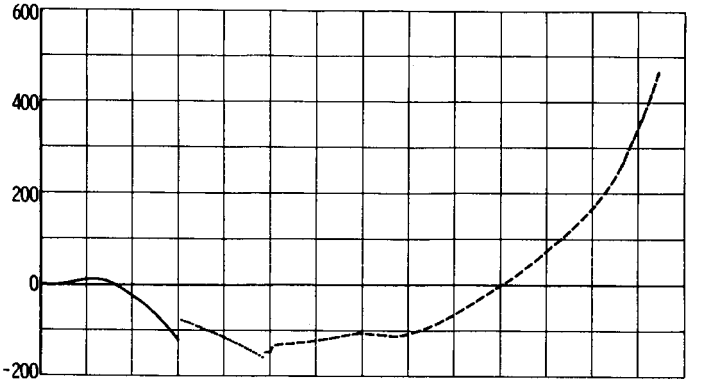

(a) Nominal U-velocity minus guidance computed velocity V_{mu}.

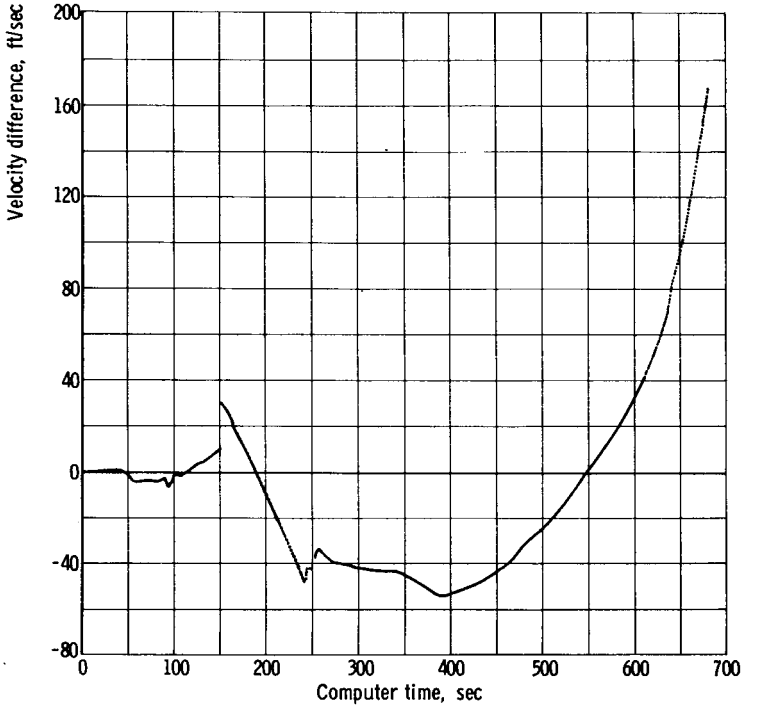

(b) Nominal V-velocity minus guidance computed velocity V_{mv}.

Figure XII-8. - Total velocity differences.

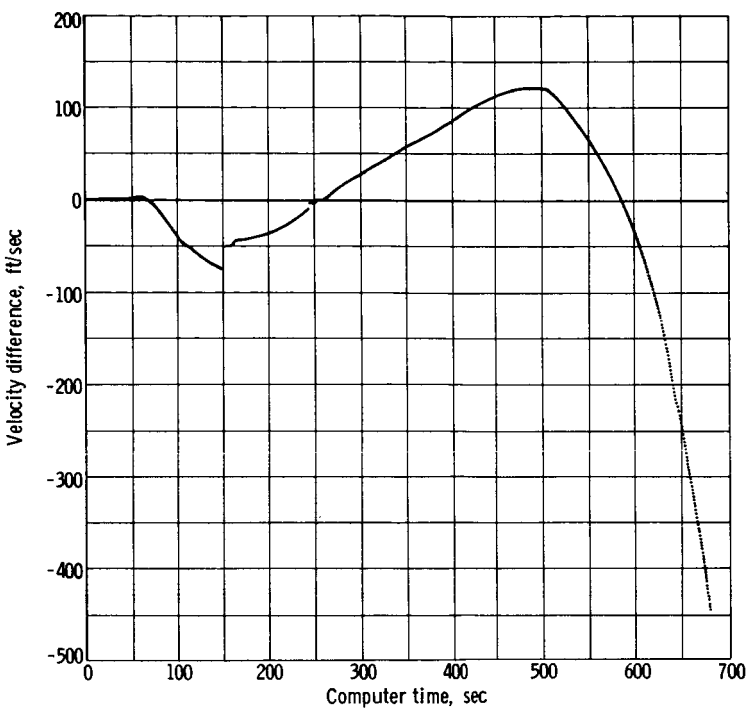

(c) Nominal W-velocity minus guidance computed velocity W_{mw}.

Figure XII-8. - Concluded.

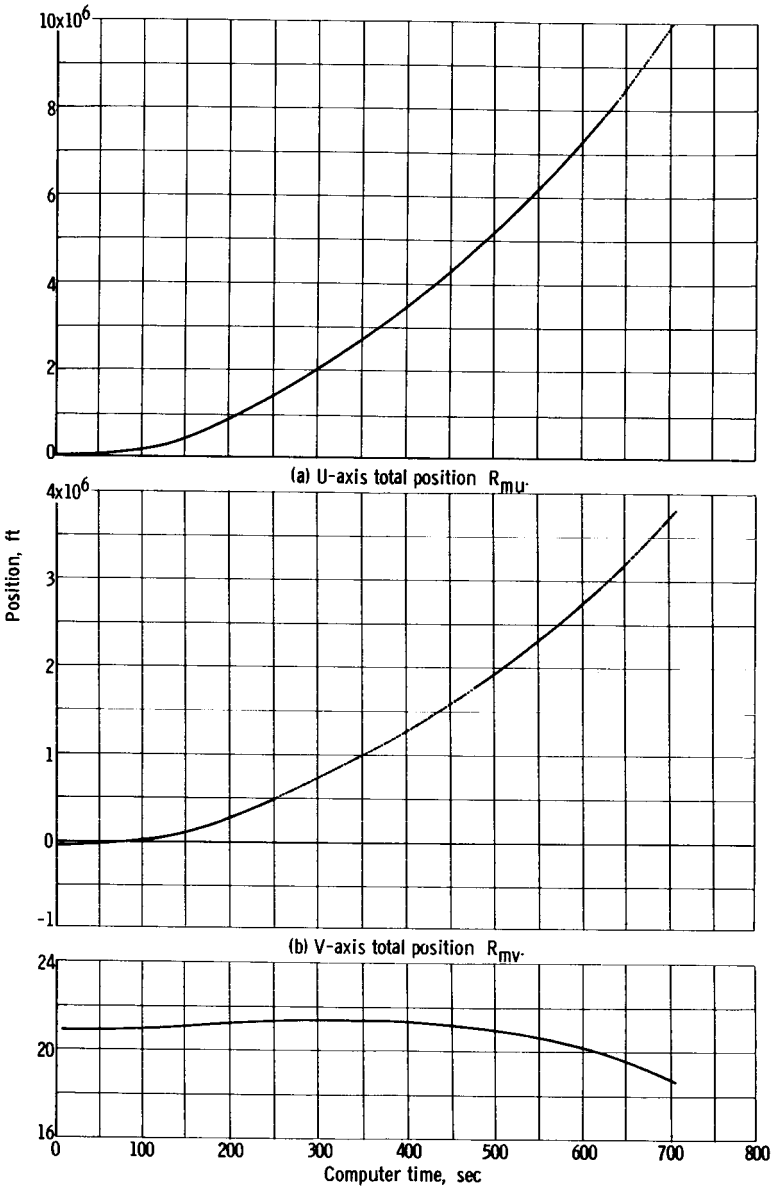

(a) U-axis total position R_{mu}.

(b) V-axis total position R_{mv}.

(c) W-axis total position R_{mw}.

Figure XII-9. - Guidance computer total position.

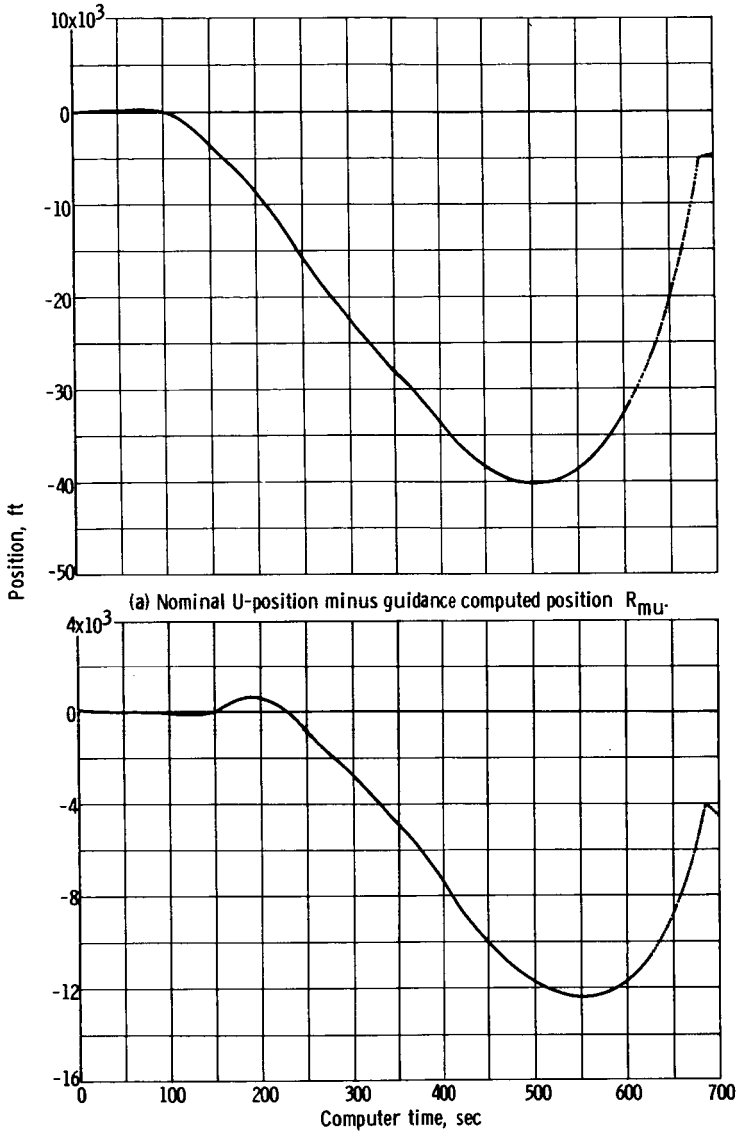

(a) Nominal U-position minus guidance computed position R_{mu}.

(b) Nominal V-position minus guidance computed position R_{mv}.

Figure XII-10. - Total position differences.

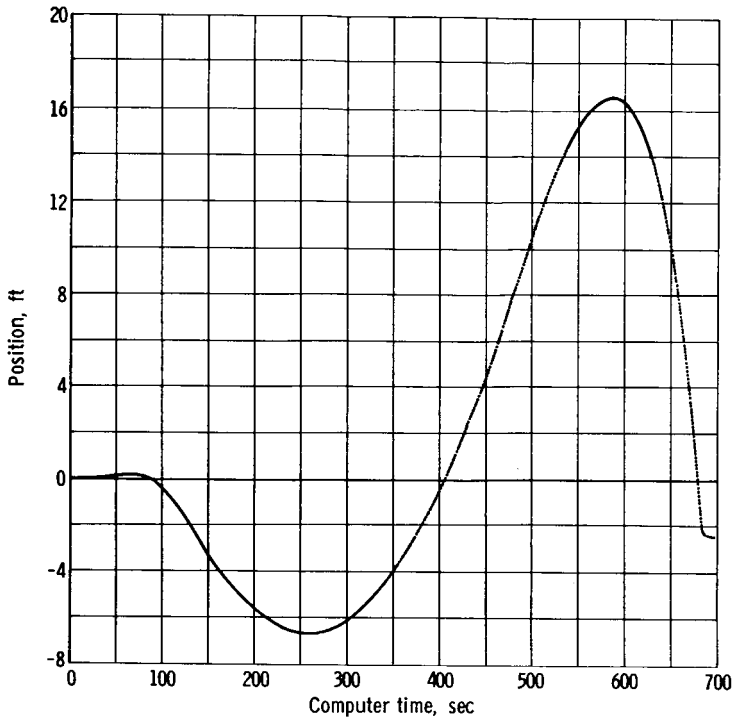

(c) Nominal W-position minus guidance computed position R_{mw}.

Figure XII-10. - Concluded.

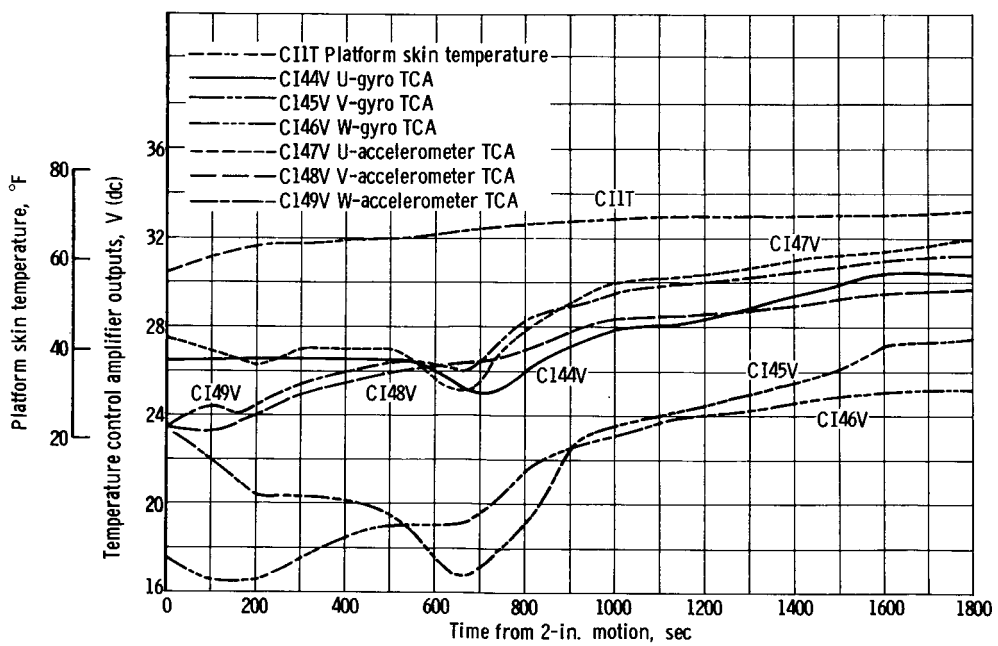

Figure XII-11. - Platform temperature history. Gyro and accelerometer temperature control amplifier outputs and platform skin temperature.

[redacted]

XIII. ATLAS-CENTAUR INSTRUMENTATION, RADIO FREQUENCY, AND ELECTRICAL SYSTEMS

SUMMARY

The Atlas-Centaur electrical system performed satisfactorily during ground operations, launch, and through all phases of programed flight. All electrical functions, voltage and current levels were within specifications. This was the first Centaur flight in which the new high-energy (1 amp - 1 W) squibs, that provided greater protection from stray currents and static discharges, were used exclusively. Squib simulators were used successfully during ground tests to provide assurance of adequate current flow to all pyrotechnics. Atlas-Centaur RF system performance was also satisfactory. Telemetry coverage was provided well beyond the end of retromaneuver. Main power cutoff was accomplished on schedule, and data quality was generally good. Approximately 98 percent of all instrumentation yielded valid data. Range Safety Command systems experienced no malfunctions during flight. The August 10, 1965 launch attempt, however, was scrubbed because of the failure to obtain a positive indication of an armed Centaur destruct system.

C-band tracking of the Centaur was adequate to provide acquisition of the spacecraft by the deep-space network, although it was intermittent. The JPL deep-space network acquired and tracked the SD-2 dynamic model S-band transponder as planned; signal strength from the spacecraft dropped off 2 hours sooner than the expected 20-hour minimum. Glotrac functioned normally and will permit a precision powered flight trajectory to be generated for the guidance component error analysis program.

Launch countdown logic and event times were modified from those at Complex 36A to improve probability of a successful launch. Upper umbilicals were ejected earlier in the countdown, while the time from engine start to vehicle release was reduced approximately 1/2 second to gain maximum thrust from the lower stage.

ELECTRICAL SYSTEM

Atlas

The major Atlas electrical system components were a manually activated main vehicle battery, two telemetry batteries, and a three-phase 400-cycle rotary inverter. The main battery bus voltage indicated near nominal voltage throughout powered flight. On transfer to internal power, the battery voltage dropped momentarily to 25.8 volts, recovering to 27.6 volts in approximately 200 milliseconds. A steady-state low of 27.3 volts was recorded at lift-off and reached a high of 27.8 volts at loss of signal.

[redacted]

The Atlas main power changeover switch satisfactorily transferred the launch vehicle load from external ground power to internal battery supply. Operation of the telemetry batteries was satisfactory, as verified by the performance of the telemetry system.

The Atlas vehicle utilizes a rotary inverter to deliver ac power at a nominal 115 volts, 400 cycles, three phase. The inverter operation was satisfactory with no recorded malfunction during flight. At launch, the voltage was 114.43 volts and the frequency was 402 cycles. Recorded data showed good recovery from load variations with the voltage varying from 114.33 to 114.72 volts during flight. The terminal value was 114.53 volts at T + 520 seconds when Atlas telemetry ended. The frequency varied from 402 to 402.7 cycles which maintained a differential frequency of two to three cycles with the Centaur 400-cycle inverter, required to avoid dangerous oscillations in the servoamplifier electromechanical loop.

Centaur

The Centaur vehicle power requirements were adequately supplied by one 100-ampere-hour battery, two range safety batteries, two pyrotechnic batteries, and a 400-cycle static inverter. Three notable configuration changes were made to the Centaur electrical power system:

(1) The main missile, telemetry, and tracking system power was supplied by a single 100-ampere-hour battery.

(2) A battery preload was used to precondition the main battery prior to power changeover to internal.

(3) The Range Safety Command system was supplied by two batteries of a new design.

The main battery voltage and current were near nominal throughout the flight. Vehicle system dc input (CE28V) indicated a level at lift-off of 27.8 volts. A low of 27.1 volts was recorded during main engine start sequence (maximum loading) and a high of 28.1 volts was reached during retromaneuver.

The 14-ampere preload of the main battery prior to changeover to internal power preconditioned the battery to accept Centaur load. Preconditioning of the battery minimized the voltage drop at changeover that could be detrimental to the user systems. The resulting battery voltage level dropped to approximately 26.5 volts on transfer (specification limit is 26 V minimum). The main missile battery current (CEIC) at lift-off was 56 amperes, reaching a high of 69 amperes at main engine start. Comparison of the profile for ground test battery load current with the flight recorded profile showed close correlation between sequential events (see fig. XIII-1). Several small spikes were noted on the current recording from T + 103 to T + 117 seconds, which were not identified with any specific event. The spikes appear to be valid data, although they could be attributed to spurious noise from a source as yet undetermined.

Transfer of the Centaur load was successfully accomplished by the main

power changeover switch in less than 250 milliseconds. No abnormal voltage or current transients occurred on transfer of load from external power source to internal battery supply.

On completion of the Centaur flight requirements at T + 1853.8 seconds the power changeover switch satisfactorily disconnected the main vehicle load from the battery while maintaining connection of the battery to the telemetry, C-band, and Azusa systems.

Satisfactory operation of the pyrotechnic batteries and relay system was verified by the successful jettison of the nose-fairing and insulation panels. The battery voltages were 35.0 volts at lift-off (minimum specification limit is 34.7 V).

Two new range safety system batteries, used for the first time, performed satisfactorily as verified by the range safety command receiver operation. The batteries were specially designed to provide the proper voltage level for receiver operation and vehicle destruct capability. The battery voltages at lift-off were 32.3 and 32.5 with receivers in operation (minimum specification limit is 30 V).

The staging disconnect functioned normally at T + 234.9 seconds after withstanding the shock produced by the jettison of the insulation panels. The actuator temperature was 72° F at lift-off (minimum value is 60° F).

The Centaur static inverter functioned normally and within specifications delivering three-phase 400-cycle power to the autopilot, guidance, and propellant-utilization systems. The inverter also supplied reference frequency to telemetry and gyros. The addition of the PU system on AC-6 caused a slightly leading power factor which accounts for the somewhat higher ac voltage. The voltages remained fairly constant throughout flight and were 116.3 to 116.5 volts for phase A, 115.5 to 115.7 volts for phase B, and 114.6 to 114.8 volts for phase C.

Since the inverter frequency was crystal controlled and was independent of load conditions, the frequency remained at 400.00 cycles throughout the flight. The ambient air temperature of the inverter at launch was 68° F and the inverter skin temperature was 87.5° F rising to a maximum of 183° F at termination of the programed flight. In figure XIII-2, it can be seen that the inverter immediately started to cool down and fell to 137° F at T + 3600 seconds when telemetry was lost.

INSTRUMENTATION SYSTEM

There were 442 measurements telemetered on AC-6, of which 267 were Centaur measurements, 150 were booster measurements, and 25 were payload measurements. The number of measurements by vehicle system is shown in table XIII-I. Three measurements were deleted prior to launch as a result of malfunction:

(1) C-1 engine pump LH_2 inlet temperatures (CP60T)

(2) LH_2 tank stem temperature (CP127T)

(3) Helium-purge-bottle discharge pressure (CP1146P)

The two temperature transducers were damaged during installation and were not easily accessible for repair or replacement during the countdown. The third measurement was deleted as a result of a transducer failure.

The following measurement anomalies were noted during the AC-6 flight:

(1) The high rate LH_2 vent dynamic pressure (CF190P) was consistently low during GH_2 venting and actually went negative during the early portion of flight. The cause of failure has not been determined; however, a more reliable transducer will be installed in an environmentally improved location on future vehicles.

(2) The low rate LH_2 vent dynamic pressure (CF191P) data was questionable. This transducer will also be relocated.

(3) The nose-cap surface-temperature (CA80T and CA958T) readings were erratic; at approximately T + 130 seconds, these readings increased abruptly and reached about twice the expected value. This failure has been attributed to improper installation.

(4) The LH_2 duct vibration (CA6010) operation was intermittent throughout the flight. A similar failure in this mode was caused by a defective coaxial cable. A new design has been initiated for a more reliable cable; however, the availability and implication have not been established.

(5) The spacecraft compartment A accelerometer (CY580) oscillated from band edge to band edge 0.7 second after nose-fairing jettison for no apparent reason.

(6) The interstage adapter panel radial vibration (AA1640) exhibited no useful data during flight. No resolution of this problem has been made.

TELEMETRY

The AC-6 telemetry system consisted of six RF links. Two of these links were on the Atlas booster. Atlas RF 1 transmitted booster operational measurements at 229.9 megacycles. Atlas RF 2 was used primarily for interstage adapter R&D measurements and operated at 232.4 megacycles. The Atlas transmitters radiated through a ring-coupler from two antennas, one on each Atlas pod.

The four telemetry links on the Centaur vehicle were coupled to a single antenna mounted on a ground plane located on the umbilical island. Signals were radiated through the nose fairing until nose-fairing jettison at T + 196.6 seconds. Centaur operational measurements were telemetered on SS 1, and Centaur R&D measurements were telemetered on SS 2. These two subsystems were located in the forward equipment area on the Centaur vehicle. Subsystems 3 and 4 were located in the retromotor simulator portion of the Surveyor dynamic model and

transmitted payload environmental information until spacecraft electrical disconnect, which occurred at T + 740 seconds. Subsystems 1 and 2 functioned until loss of signal at T + 6950 seconds. Telemetry transmitter frequency and nominal power were as follows:

Telemetry link	Frequency, Mc	Nominal power, W
Atlas RF:		
1	229.9	10
2	232.4	4
Centaur SS:		
1	225.7	4
2	235.0	4
3	243.8	4
4	251.5	4

Six measurements of telemetry parameters were made on AC-6. These were skin temperature measurements of SS 1 to 4 and thermocouple reference junction temperatures on the Atlas and Centaur. All measurements were as expected with the exception of telemetry SS 1 skin temperature (CT94T). This measurement went off scale (low) indicating a temperature less than 0° F shortly after the start of tanking. This low temperature was probably caused by the leakage of helium through the forward insulation-panel seal. The temperature remained off scale (low) until approximately T + 8 minutes. At that time, the measurement came on scale, and the temperature increased slowly to 24° F at T + 17 minutes. No data loss or anomalies resulted from this low temperature. Summary of the AC-6 telemetry coverage from time of lift-off to loss of signal at Pretoria is given in figures XIII-3 and 4.

Analysis of the signal strength records indicated that the performance of all the telemetry links was satisfactory throughout the flight. The only dropout of telemetry data was experienced by the TEL II ground station at booster engine jettison (T + 145 sec) for a period of 0.2 second. This dropout had occurred on previous vehicles also and may have been caused by flame attenuation (fig. XIII-5). At this time, flame attenuation is more prevalent because of the backscattering effect of the sustainer engine's flame impinging on the booster section as it is jettisoned. However, because of a different look angle, the telemetry data that is recorded from Grand Bahama Island at this same time does not have any dropout (fig. XIII-6).

RANGE SAFETY SYSTEM

A lightweight Range Safety Command system for the second stage (Centaur) and spacecraft (Surveyor) was flown on AC-6 for the first time. A block diagram of the system is shown in figure XIII-7. The functions of the system are to

(1) Cut off the Centaur main engines to an RF command, resulting in zero thrust

(2) Destroy the LH_2 and LO_2 tank structure, in response to an RF command to disperse the propellants

(3) Destroy the Surveyor engine, in response to an RF command, by causing a conical-shaped explosive charge to detonate and bore a hole through the engine housing, penetrate the propellant, and emerge through the opposite side (the shaped charge was inert for AC-6)

(4) Cause the actions in (2) and (3) on detection of premature separation of the Surveyor from Centaur (disarmed for AC-6)

The first-stage (Atlas) Range Safety Command system was the same for AC-6 as on previous Atlas-Centaur flights. Both systems performed properly except for the failure to obtain an armed destructor command during the August 10 attempted launch countdown. The launch was scrubbed at approximately T - 2 minutes as a result of a failure of the Centaur destructor to respond properly to the "ARM" command. The failure was subsequently determined to be due to inadequate design of the frost plug. It is inserted after removal of the safe-lock plug which mechanically prevents arming of the destructor. The design of this plug is such that it can be inserted improperly with resultant distortion of the plug that interferes with the arming of the destructor.

On August 11, 1965, after suitable replacement of the frost plug, the "ARM" function worked properly, and launch was successfully accomplished. Both Atlas and Centaur RSC systems performed satisfactorily throughout the flight. Signal strength was adequate to transmit commands to both the Atlas and Centaur RSC systems. The minimum gain margin for the Atlas system was 55 decibels, while the gains for the upper stage were 20 and 18 decibels, respectively, for receivers 1 and 2. The only command to the system was sent from the Antigua (station 91) transmitter shortly after main engine cutoff to disable the range safety system. Figure XIII-8 shows the operation of the various ground transmitters in supporting AC-6 range safety.

TRACKING SYSTEMS

C-Band

The Centaur stage C-band radar transponder and the pair of antennas under the insulation panels used in conjunction with ETR and Bermuda ground radar stations provided adequate tracking of the Centaur vehicle through the powered-flight phase. Real time computation of the Antigua and Twin Falls (ship) C-band tracking data after MECO enabled an early orbit to be determined. Look angles were transmitted to the DSIF station at Johannesberg permitting early acquisition of the S-band transponder in the dynamic model. C-band operation was satisfactory for the first 500 seconds of flight. Stations tracking later portions of the flight experienced tracking difficulty. The C-band radar coverage is shown in figure XIII-9. Extracts from the station logs follow:

Station 1. Cape Kennedy. - Beacon performance was satisfactory. All commitments were met. At loss of signal, the frequency deviation was 3 megacycles (see fig. XIII-9).

Station 19. Merritt Island. - The average signal strength was 45 decibels above the receiver threshold. Slight deterioration of the beacon return was noted from T + 90 to T + 100 seconds. At T + 500 seconds, the beacon return deteriorated both in amplitude and pulse width until the end of tracking.

Station 3. Grand Bahama Island. - FPS-16 lost tracking from T + 266 to T + 283 seconds, and the FPS-18 lost tracking from T + 412 to T + 447 seconds. Other stations operating showed no anomalies so these losses may be attributed to station problems or poor look angles. Final loss of signal occurred at T + 543 seconds, and at this time, the frequency deviation was down 7 to 9 megacycles.

Station 7. Grand Turk Island. - The beacon shifted in frequency and dropped 15 to 20 decibels in signal strength at approximately T + 435 seconds. The pulse was extremely narrow and the loss of signal frequency deviation was -6 megacycles.

Station 9. Antigua Island. - Shortly after 500 seconds, the signal dropped to approximately 15 decibels. A weak signal was confirmed by Grand Turk, and tracking was maintained to the horizon. The final beacon frequency reading was off -3 megacycles.

Station 86. Twin Falls Ship. - Tracking was complicated by locally generated noise interference.

Station 12. Ascension Island. - Lock-on was late as a result of computer program input and the beacon frequency shift.

Station 13. Pretoria. - This station reported negative tracking. The beacon transmitter frequency shift could have exceeded the radar receiver local oscillator tuning range of ±13 megacycles.

Indications are that the C-band transponder experienced the following symptoms:

(1) Width and amplitude deterioration of the return pulse

(2) Frequency deviation that may have gone out of specification

A magnetron failure within the transponder will produce frequency and pulse behavior identical to that recorded for AC-6. Conditions necessary include pulling, pushing, temperature change, or movement of the tuning mechanism which will produce a frequency shift. Temperature is discounted based on the telemetry data of the transponder skin temperature indicating normally (~36° F at T - 0, rising to ~65° F at T + 75 min). Pulling may be caused by either a change of VSWR and/or cable losses, while pushing may be caused by a power supply change. Analysis of this anomaly has been made with design engineering testing. The probable cause of failure was loss of internal cannister pressure through one of the seals. Future preflight checkout shall include more extensive testing of the electrical and mechanical aspects of the unit.

Glotrac

A Centaur stage Azusa type-C transponder and antenna system in conjunction with Glotrac segment 1 enabled powered flight position and velocity data to be determined with precision through the measurement of Doppler shift at three or more widely separated ground stations. Glotrac station coverage is shown in figure XIII-10. Handover at 400 seconds from the MARK II transmitter at the Cape to the Bermuda transmitter was satisfactorily accomplished within 4 seconds.

The Azusa interstage adapter antenna is used to provide coverage through the early flight phase when insulation panels cover the Centaur mounted antenna. At nose-fairing jettison (T + 197 sec) the dc power to the coaxial switch circuit is interrupted causing the switch to connect the Centaur mounted antenna to the transponder.

S-Band

The SD-2 dynamic model contained an S-band transponder assembly and an omnidirectional antenna mounted on top of the forward mast. The transponder operated on low-power (100 mW) mode until approximately 11 seconds prior to spacecraft separation, at which time the Centaur programer initiated a switchover command to the high-power (10 W) mode. The spacecraft was acquired by the Johannesberg DSIF approximately 20 minutes after injection, and two-way lock was obtained. Deep-space tracking of the spacecraft by Johannesberg, Goldstone, and Canberra continued for approximately 18 hours, at which time there was a marked dropoff in transponder power due to battery depletion. The precision deep-space tracking of the spacecraft after separation enabled an overall guidance system evaluation to be made. Tracking data indicated that the injection accuracy was excellent and that the spacecraft was well within the midcourse correction capability allowables. See section VI for discussion of trajectory (also ref. 17).

ELECTRICAL GSE

A modification to the ETR 36B GSE facilities provided the capability to monitor and record 23 channels of voltage and current data for the Atlas and Centaur electrical systems continuously through the preflight, countdown, and postflight operations.

A dual industrial power source was provided to the complex by completing an alternate route with capability for remote manual switchover in the event of an outage. The critical power shortage was relieved by requesting priority beforehand via an "express" bus which essentially provides preferential service similar to the service afforded manned launch complexes at ETR. This was provided to minimize outage possibilities such as occurred on previous Centaur countdowns.

No major electrical GSE anomalies occurred during either the aborted launch attempt of August 10 or the successful launch of August 11. Several minor GSE

problems were experienced during major preflight testing. A brief outline of these significant incidents appears in section III, PRELAUNCH HISTORY, and is discussed in greater detail, with corrective actions taken, in the analysis and evaluation of the corresponding system.

There were two significant problems observed in the electrical GSE both involving the dc power supplies:

(1) The 7-volt dc battery simulator supply to the Atlas vehicle exhibited an unstable voltage characteristic during the composite readiness test and necessitated replacement by a flight-type battery in order to complete the test. This same problem had occurred in an earlier test. The power supply was subsequently returned to the vendor.

(2) It was noted that a potential difference exists between the ground returns of the 28-volt dc power supplies in the transfer room and the blockhouse as well as with the battery simulator supply in the gantry. This potential difference is manifested by changes in landline calibrations and becomes evident at power transfer to the battery simulator supply, or when either the blockhouse or transfer room supplies are cut off. This is a condition that is prevalent at all Atlas launch complexes but which can be improved considerably by extensive modification to a single-point grounding system.

Corrective action is now in process to rectify two other anomalies in the GSE:

(1) Cooling air to the propellant level control unit chassis was inadequate resulting in improper operation of the tanking system. A supplementary source of cooling air effected a temporary fix to permit completion of tanking tests and launch preparations for the AC-6 flight.

(2) Unreliable operation of the vehicle optical alignment door and lack of position monitoring made it necessary to monitor the door position visually during launch preparations.

A listing of significant events and the time at which they occurred is shown in table XIII-II.

TABLE XIII-I. - AC-6 MEASUREMENT SUMMARY

Vehicle system	Measurement type															
	Acceleration	Rotation rate	Current	Deflection	Power	Vibration	Pressure	Frequency	Rate	Strain	Temperature	Voltage	Discrete position	Acoustic	Digital	Total
Atlas																
Airframe	--	--	--	--	--	4	9	--	--	10	40	--	4	--	--	67
Range safety command	--	--	--	--	--	--	--	--	--	--	---	2	1	--	--	3
Electrical	--	--	--	--	--	--	--	1	--	--	---	2	--	--	--	3
Pneumatic	--	--	--	--	--	--	7	--	--	--	2	--	--	--	--	9
Hydraulic	--	--	--	--	--	--	6	--	--	--	---	--	--	--	--	6
Guidance	--	--	--	--	--	--	--	--	--	--	---	--	--	--	--	---
Propulsion	--	3	--	2	--	--	20	--	--	--	2	--	8	--	--	35
Flight control	--	--	--	11	--	--	--	--	3	--	---	--	7	--	--	21
Telemetry	--	--	--	--	--	--	--	--	--	--	1	--	--	--	--	1
Propellant level control	--	--	--	--	--	--	2	--	--	--	---	1	--	--	--	3
Azusa	--	--	--	--	--	--	--	--	--	--	---	--	--	--	--	---
Payload	--	--	--	--	--	--	--	--	--	--	---	--	--	--	--	---
Miscellaneous	1	--	--	--	--	--	--	--	--	--	---	--	1	--	--	2
Total	1	3	--	13	--	4	44	1	3	10	45	5	21	--	--	150
Centaur																
Airframe	--	--	--	--	--	1	6	--	--	20	63	--	1	--	--	91
Range safety command	--	--	--	--	--	--	--	--	--	--	---	2	5	--	--	7
Electrical	--	--	1	--	--	--	--	1	--	--	1	4	--	--	--	7
Pneumatic	--	--	--	--	--	--	7	--	--	--	9	--	2	--	--	18
Hydraulic	--	--	--	--	--	--	2	--	--	--	2	--	--	--	--	4
Guidance	3	--	--	--	--	--	--	--	--	--	6	28	--	--	1	38
Propulsion	--	4	--	--	--	--	12	--	--	--	12	--	14	--	--	42
Flight control	--	6	--	--	--	--	--	--	--	--	2	8	28	--	--	44
Telemetry	--	--	--	--	--	--	--	--	--	--	6	--	--	--	--	6
Propellant level control	--	--	--	2	--	--	--	--	--	--	1	2	2	--	--	7
Azusa	--	--	--	--	1	--	--	--	--	--	---	--	--	--	--	1
Payload	--	--	--	5	--	10	1	--	--	1	6	--	--	2	--	25
Miscellaneous	1	--	--	1	--	--	--	--	--	--	---	--	--	--	--	2
Total	4	10	1	8	1	11	28	1	--	21	108	44	52	2	1	292

TABLE XIII-II. - SIGNIFICANT FLIGHT EVENTS

Event	Landline measurement number (a)	Time of occurrences, sec	
		Nominal	Actual
Engine start command	AP1161X (347)	T - 7.83	T - 8.27
Upper umbilicals ejected	CN1615X (354)	T - 3.21	T - 3.20
Ignition complete (main stage limiter)	AP1617X (28)	T - 2.17	T - 2.15
Vehicle release	AP1577X (363)	T - 0.80	T - 0.78
2-in. motion[b]	AM1030X (364)	T - 0	T - 0
Lower boom solenoid valve	CN1465X (88)	T - 0	T - 0
Auxiliary 2-in. motion	CN1474X (365)	T + 0.03	T + 0.04
Upper boom solenoid valve[c]	CN1464X (84)	T + 0.25	T + 0.26
8-in. rise	AN1827X (366)	T + 0.26	T + 0.27
42-in. rise (final umbilical ejected)	AN1066X (469)	T + 0.98	T + 0.85

[a]Numbers in parentheses refer to pen recording numbers.

[b]There was no evidence of erratic 2-in. rise switch operation, observed on previous flights between lift-off and 42-in. rise, which had been attributed to flame impingement. The switch cabling was wrapped with Blastape to prevent this from happening.

[c]The upper boom solenoid valve received its signal at T + 0.260 sec, indicating that the primary actuating device (240-msec time-delay relay) initiated upper boom motion rather than the backup signal from the 8-in.-rise switch that occurred at T + 0.270 sec.

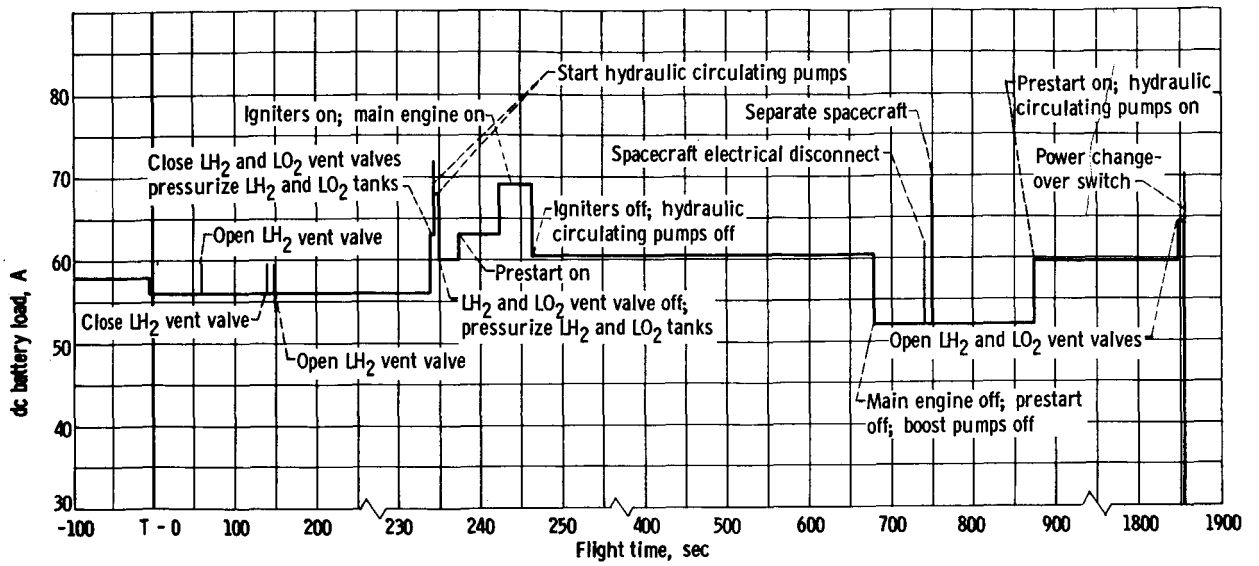

Figure XIII-1. - AC-6 main vehicle battery composite load profile.

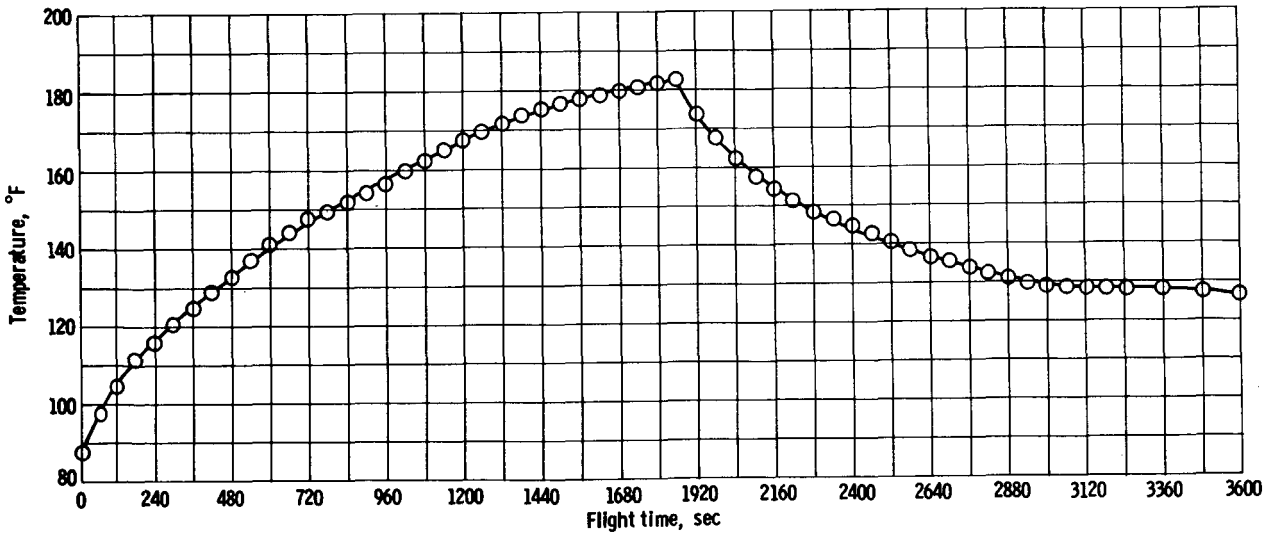

Figure XIII-2. - Variation of inverter skin temperature as function of flight time (CE29T).

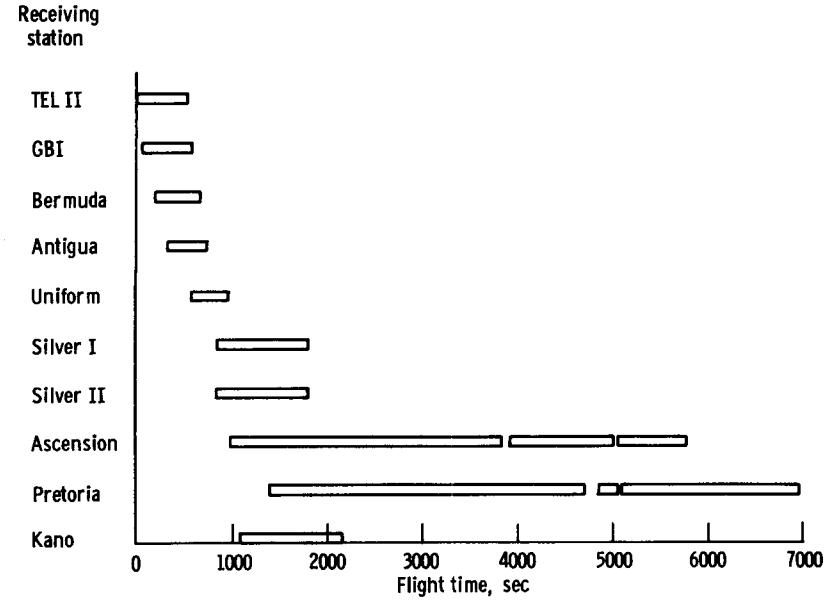

Figure XIII-3. - AC-6 Telemetry coverage.

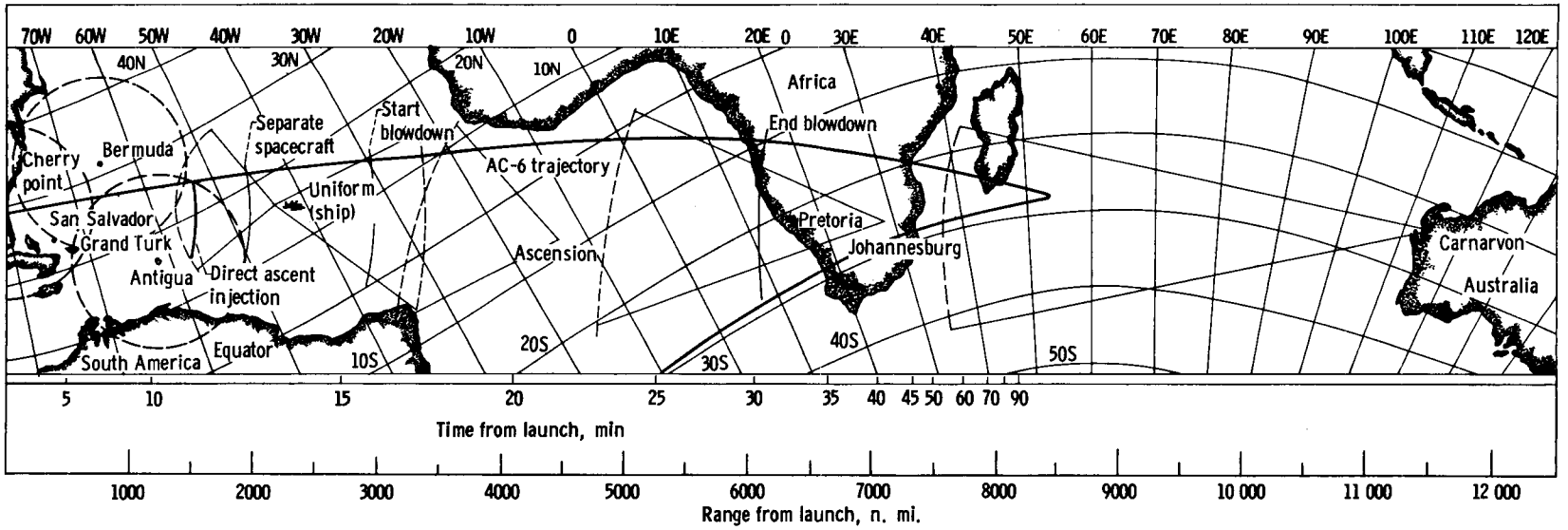

Figure XIII-4. - Centaur AC-6 direct ascent flight plan and data coverage. Axial rotation rate of Earth exceeds spacecraft angular rate about Earth center, thus, apparent westerly motion of spacecraft.

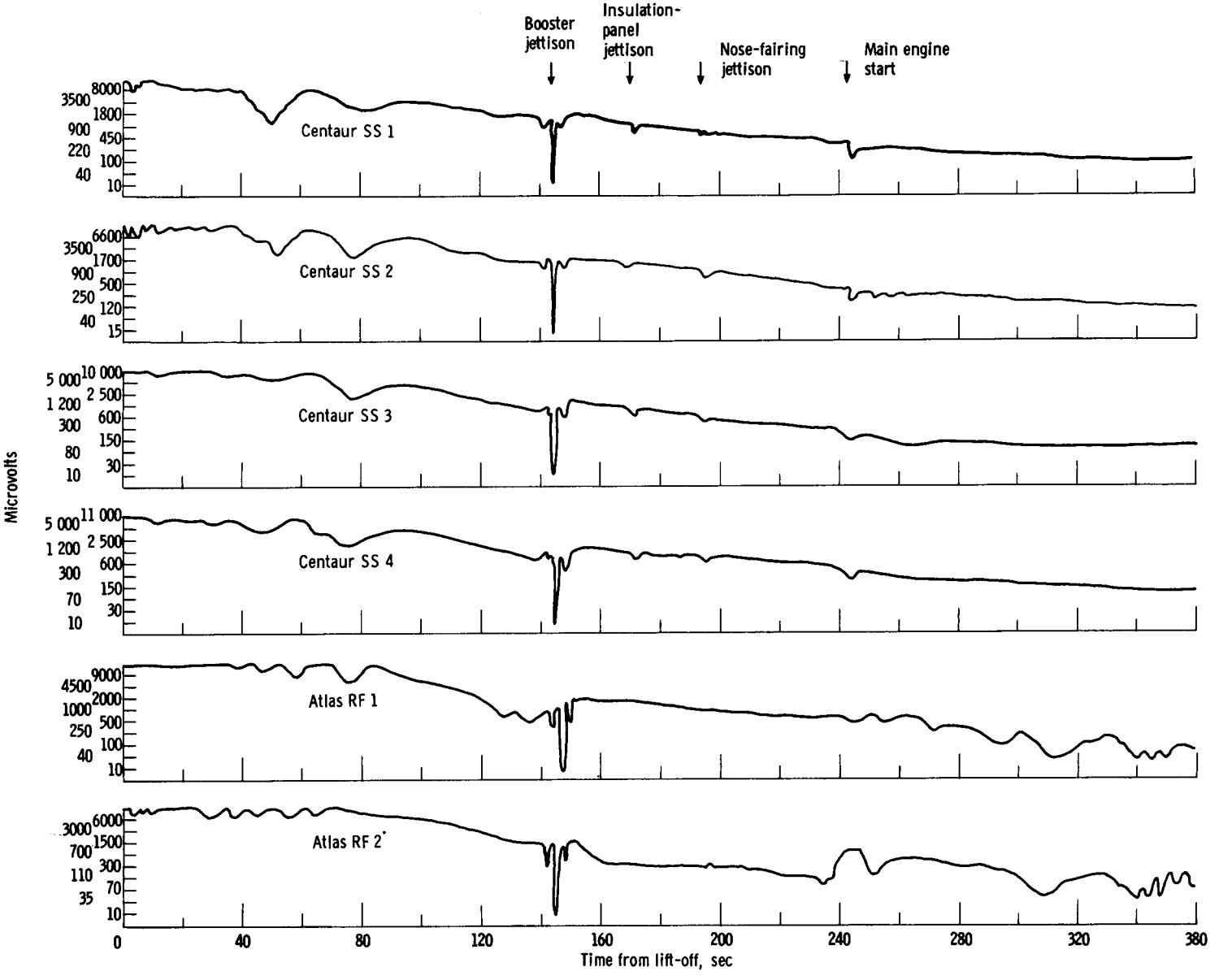

Figure XIII-5. - Signal strength from TEL II station at Cape Kennedy.

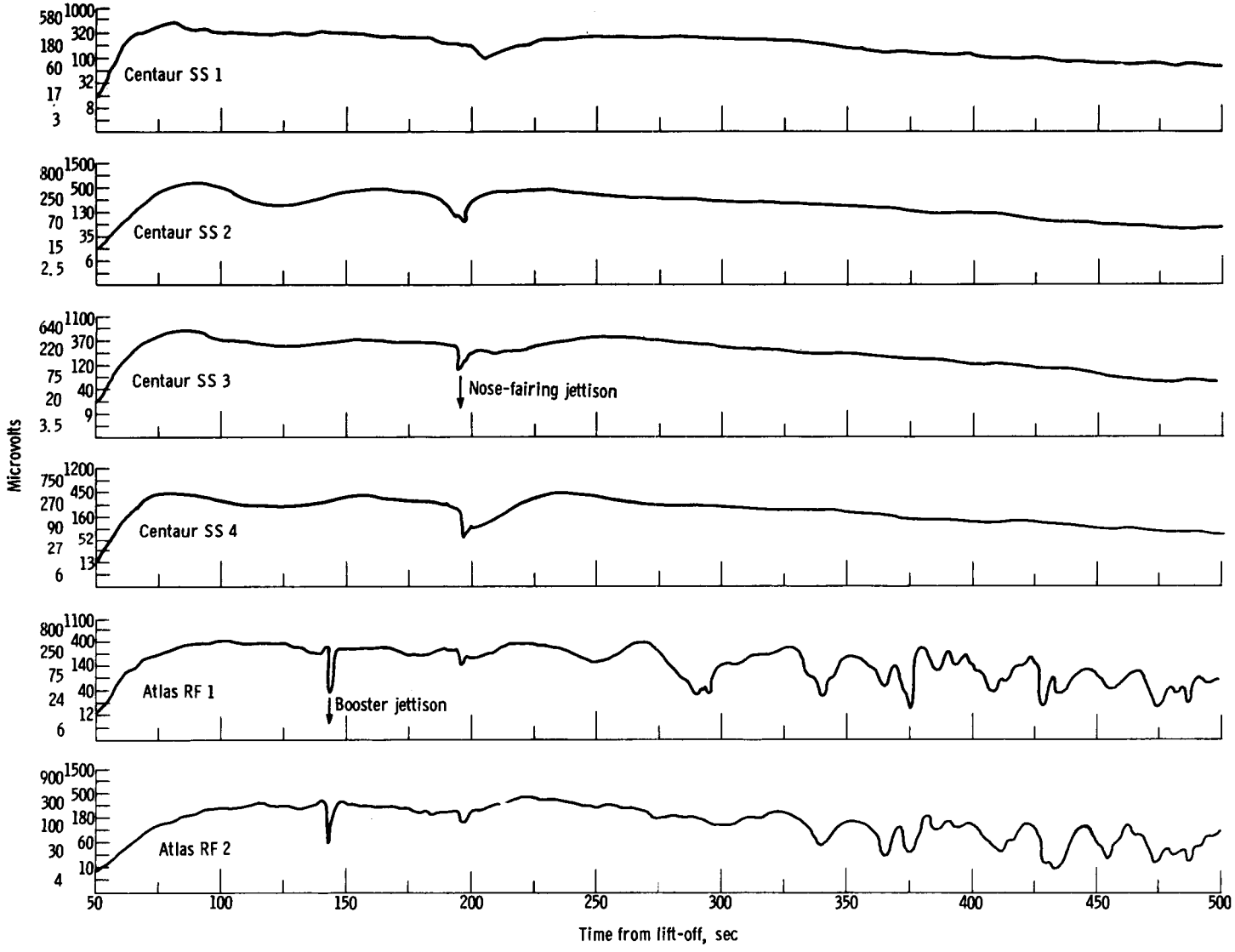

Figure XIII-6. - Signal strength from Grand Bahama Island.

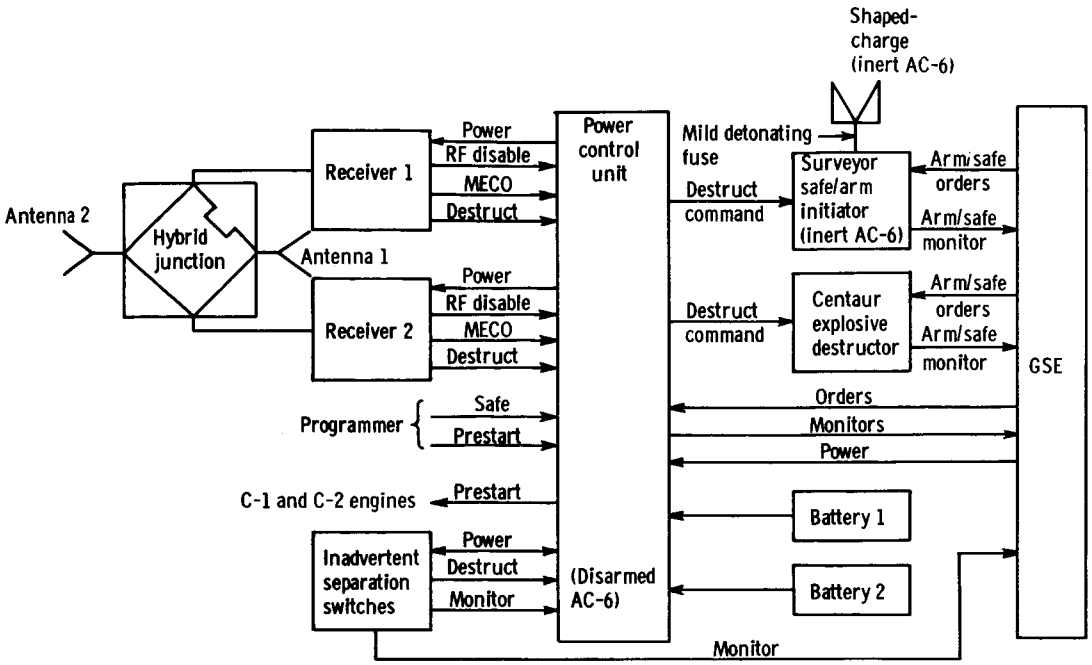

Figure XIII-7. - Block diagram of second stage range safety command subsystems.

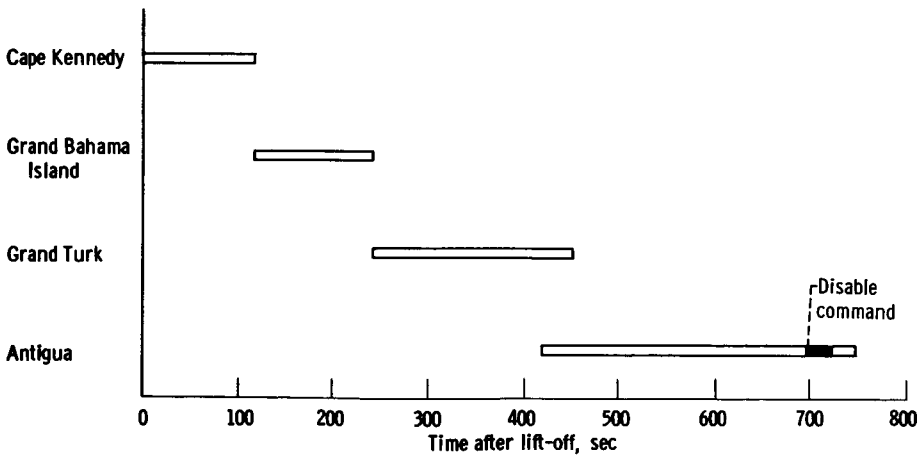

Figure XIII-8. - AC-6 Range Safety Command System transmitter utilization.

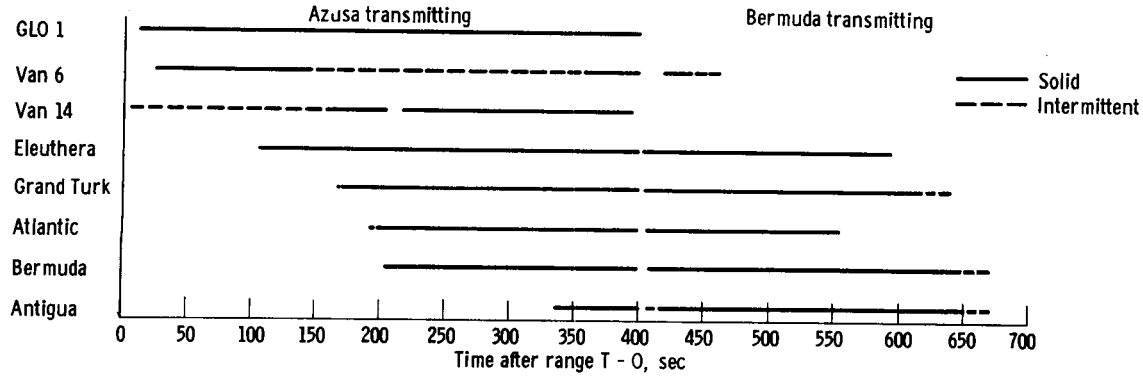

Figure XIII-10. - AC-6 Glotrac coverage.

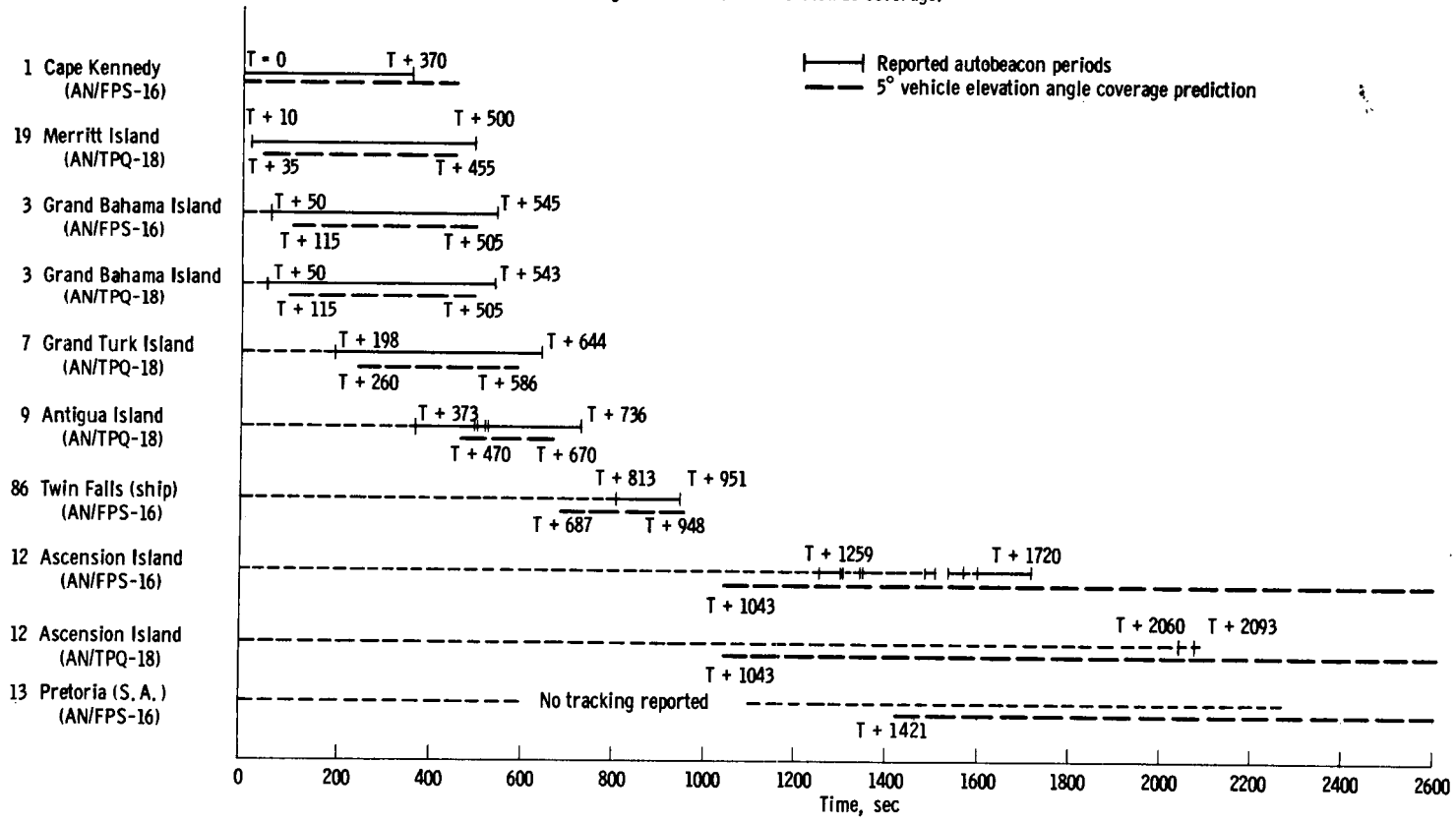

Figure XIII-9. - C-band transponder coverage and performance.

[redacted]

APPENDIX A

SYMBOLS

A	reference area
A-C	Atlas-Centaur
AFETR	Air Force Eastern Test Range
A/P	autopilot
ac	alternating current
BECO	booster engine cutoff
BET	best estimate of trajectory
BPS	boost-pump start
burp	step pressurization of propellant tank
C_x	standard aerodynamic drag coefficient
C-band	frequency band used in radar (range, 3.9 to 6.2 gigacycles)
CRT	composite readiness test
cps	cycles per second
D	drag
D/A	digital-analog
DSIF	deep-space instrumentation facility
dc	direct current
EST	Eastern Standard Time
ETR	Eastern Test Range
F -	days prior to launch
FPR	flight performance reserve
GD/C	General Dynamics/Convair
GET	best estimate of trajectory based on guidance data
GH_2	gaseous hydrogen

[redacted]

[redacted]

Glotrac	Global tracking
GMT	Greenwich Mean Time
gpm	gallons per minute
GN_2	gaseous nitrogen
GO_2	gaseous oxygen
GSE	ground support equipment
H_2	hydrogen
H_2O_2	hydrogen peroxide
JPL	Jet Propulsion Laboratory
LH_2	liquid hydrogen
LHe	liquid helium
LN_2	liquid nitrogen
LO_2	liquid oxygen
M	Mach number
MECO	main engine cutoff
MES	main engine start
max Q	maximum aerodynamic load
N	load factor, g's
N_x	load factor in x-direction
N_y	load factor in y-direction
N_z	load factor in z-direction
NPSH	net positive suction head
NPSP	net positive suction pressure
O_2	oxygen
P-P	peak to peak
PLIS	propellant level indicating system

[redacted]

psi	pounds per square inch
psia	pounds per square inch absolute
psid	pounds per square inch differential
psig	pounds per square inch gage
PU	propellant utilization
Q, QUAD	quadrant
q	dynamic pressure
RF	radio frequency
rms	root mean square
rpm	revolution per minute
RP-1	rocket propulsion fuel
RSC	Range Safety Command
S-band	frequency band used in radar (range, 1.55 to 5.20 gigacycles)
SD-2	Surveyor dynamic model 2
SECO	sustainer engine cutoff
T	time from lift-off (2-in. motion)
T_c	time referenced to computer zero time
t	MECO backup
TCA	temperature control amplifier
TEL	telemetry receiving station
Telepak	telemetry package
TLM	telemetry
ΔV	incremental velocity impulse
VECO	vernier engine cutoff
VSWR	voltage standing wave ratio

APPENDIX B

CALCULATIONS OF PROPELLANT RESIDUALS

The LO_2 and LH_2 residuals at MECO were calculated by using the time that the propellant level passed the bottom of the PU probe as a reference point. The calculations are summarized as follows:

Liquid oxygen:

Station level at bottom of probe	443.4
Level lag[a] in probe, in.	0.4
Actual propellant level station in tank	443.8
Total volume[b] below station 443.8, cu ft	14.9
Mass remaining at probe uncovery (69.5 lb/cu ft × 14.9 cu ft)[c], lb	1035
LO_2 burned from probe[d] uncovery to MECO, lb	
C-1 engine:	
29.2 lb/sec for 4.6 sec	134.3
31.3 lb/sec for 8.0 sec	250.4
Total LO_2 burned by C-1 engine, lb	384.7
C-2 engine:	
29.2 lb/sec for 7.2 sec	210.2
31.3 lb/sec for 5.4 sec	169.0
Total LO_2 burned by C-2 engine, lb	379.2
Total LO_2 consumed from probe uncovery to MECO, lb	
384.7 + 379.2	763.9
Total LO_2 residual[e], lb	
1035 lb - 763.9 lb	271.1
Usable LO_2 residual[f], lb	
271.1 lb - 68 lb	203.1

Liquid hydrogen:

Station level at bottom of probe	372.5
Level lag[a] in probe, in.	0.2
Actual propellant level station in tank	372.7
Total volume[b] below station 372.7, cu ft	62.3
Mass remaining at probe uncovery (4.29 lb/cu ft × 62.3 cu ft)[c], lb	267.3
LH_2 burned from probe[d] uncovery to MECO, lb	
C-1 engine:	
5.58 lb/sec for 2.4 sec	13.4
5.43 lb/sec for 8.0 sec	43.5
Total LH_2 burned by C-1 engine, lb	56.9
C-2 engine:	
5.57 lb/sec for 5 sec	27.9
5.43 lb/sec for 5.4 sec	29.3
Total LH_2 burned by C-2 engine, lb	57.2

Total LH_2 consumed from probe uncovery to MECO, lb	
56.9 lb + 57.2 lb	104.1
Total LH_2 residual[e], lb	
267.3 lb - 104.1 lb	163.2
Usable residual[f], lb	
163.2 lb - 71.8 lb	91.4

[a]The level lag is the difference in level inside the PU probe (level sensed) and the level outside the probe (actual level in tank).

[b]Volumes include 2.01 cu ft LO_2 and 3.47 cu ft LH_2 for lines, pumps, etc.

[c]Densities obtained from curves for vapor pressure against density from ref. 10.

[d]Flow rates based on PU valve positions.

[e]Accuracy of residuals is ±10 percent as a result of uncertainties in density, probe location, and volume.

[f]A total of 68 lb of LO_2 represents the LO_2 remaining in the boost-pump sump when zero NPSH point is reached; 71.8 lb of LH_2 represents the LH_2 remaining in tank and sump when the boost pump will cause vapor pull-through in the liquid (ref. 18).

[redacted]

APPENDIX C

SYMBOLS AND DETAILED LISTING OF TRAJECTORY RECONSTRUCTION FOR AC-6 FLIGHT

DESCRIPTIONS

Standard Output (OP 1)

TIME	elapsed time from lift-off
WEIGHT	total weight of vehicle
TOTAL FLOW	total weight flow
GRND RANGE	ground-range great-circle distance (spherical earth, R_o = 3441.3 n. mi.) from launch pad to vehicle subpoint
THETA I	inertial range angle, measured between launch radius vector and present radius vector
Q*ALPHA TOT	product of dynamic pressure and total angle of attack
ALTITUDE	altitude above oblate spheroidal earth, ft
RADIUS	magnitude of radius vector from Earth center to vehicle
VEL E	magnitude of velocity with respect to Earth
VEL R	magnitude of velocity with respect to air
VEL I	magnitude of velocity in inertial system
ALT	altitude above oblate spheroidal earth, n. mi.
ALPHA	angle of attack in pitch (XI, ZETA) plane, positive for ship above relative velocity vector, V_R
BETA	angle of attack in yaw (XI, ETA) plane, positive for ship left of relative velocity vector, V_R
PSI	inertial attitude angle, measure of angle between ship longitudinal axis and inertial u,v plane, positive above plane
PSIDOT	time rate of change of PSI
CROSS RANGE	minimum ground distance from vehicle subpoint to plane formed by launch vertical vector and launch down-range vector
DOWN RANGE	distance from vehicle subpoint to launch site along Great Circle at 94.539° azimuth through launch site

GEOCENT LAT	geocentric latitude, degrees north of equator
LONGITUDE	degrees from Greenwich, positive east
AZI E	azimuth of VEL E, angle between projection of VEL E into azimuth plane (plane perpendicular to radius vector) and north direction, positive clockwise from north
AZI R	azimuth of VEL R
AZI I	azimuth of VEL I
PHI	inertial attitude angle - angle between projection of minus ZETA axis in u,v plane and the u-axis
THRUST FIXED	fixed thrust magnitude - nongimbaled engines thrust
THRUST CONTL	controlled thrust magnitude - gimbaled engines
GAMMA E	flight path angle of VEL E, measured angle between velocity vector and local horizontal, positive above horizontal
GAMMA R	flight path angle of VEL R
GAMMA I	flight path angle of VEL I
EAST WIND	magnitude of wind velocity component from east
AXL FORCE	net aerodynamic force and holddown force along longitudinal axis, XI
SIDE FORCE	aerodynamic force along side axis, ETA
NORM FORCE	aerodynamic force normal to vehicle along ZETA
AXL LD FCTR	instantaneous value of (thrust - drag)/weight
WIND VEL	magnitude of wind velocity
NORTH WIND	magnitude of wind velocity component from north
ATM PRESS	atmospheric (ambient) pressure
DYNM PRESS	dynamic pressure, $\frac{1}{2} \rho_a V_r^2$
HEAT PARAM	heating parameter; time integral from lift-off of product of time, DYNM PRESS, and VEL R
MACH NUMBER	Mach number, ratio of VEL R and local speed of sound
RHO-VR CUBED	product of air density and VEL R cubed

[redacted]

TOTAL ISP	instantaneous quotient of total axial thrust by total flow

Detailed Propulsion (DEPRO)

THRUST ( )	total thrust of booster (B), sustainer (S), or vernier (V) engines, respectively, (vernier gimbaled)
THRUST TOT	total thrust of all engines
THRUST CORR (B)	change in booster thrust from C star table
THRUST CORR (S)	change in sustainer thrust from C star and PU tables
PC (B)	effective chamber pressure of booster engines
FUEL FLOW ( )	total fuel flow rate of booster (B), sustainer (S), or vernier (V) engines, respectively; vernier flow included in sustainer
FUEL FLOW TOT	total fuel flow rate for all engines
F FLOW CORR (B)	change in booster fuel flow rate from C star table
F FLOW CORR (S)	change in sustainer fuel flow rate from C star and PU table
PC (S)	effective chamber pressure of sustainer engine
OXID FLOW ( )	total LO_2 flow rate of booster (B), sustainer (S), or vernier (V) engines, respectively; vernier flow included in sustainer
OXID FLOW TOT	total LO_2 flow rate for all engines
O FLOW CORR (B)	change in booster LO_2 flow rate from C star table
O FLOW CORR (S)	change in sustainer LO_2 flow rate from C star and PU tables
PC (V)	effective chamber pressure of vernier engines
FP INLTP ( )	fuel pump inlet pressure, booster (B) or sustainer (S)
FUEL DENSITY	fuel density
OXID DENSITY	LO_2 density based on telemetry measurements
MIX RATIO (B)	ratio of LO_2 to fuel (booster)
MIX RATIO (S)	ratio of LO_2 to fuel (sustainer)
BASE FORCE	force of interaction of jet exhaust and base configuration
OP INLTP ( )	LO_2 pump inlet pressure, booster (B) or sustainer (S)

[redacted]

FUEL WEIGHT	weight of fuel above sustainer pump inlet
OXID WEIGHT	weight of LO_2 above sustainer pump inlet
AXL LD FCTR	axial load factor, required by propulsion model to calculate effect of headrise on pump inlet conditions
CAP RATIO (PU)	capacitance output from fuel manometer divided by capacitance output from oxidizer manometer; this ratio is calculated from telemetry values of PU valve angle position
HOLD - DOWN	restraining force on vehicle during first 10 sec
OIL WEIGHT ( )	weight of lubrication oil remaining, booster (B) or sustainer (S)
FUEL LEVEL	height of fuel above sustainer pump inlet
OXID LEVEL	height of LO_2 above sustainer pump inlet
NPSH	net positive suction head of sustainer LO_2 pump
VALVE ANGLE (PU)	propellant utilization fuel valve angle, value used is from telemetry
ATM PRESS	atmosphere (ambient) pressure
VAPOR PRESS	vapor pressure of LO_2
FUEL TNK PR (G)	gage pressure of fuel tank (telemetry)
OXID TNK PR (G)	gage pressure of LO_2 tank (telemetry)
ACS ITER	internal counter

Vehicle Dynamic Parameters (OP 5)

THRUST XI ETA ZETA	thrust components in vehicle axes system
DEL XI-ETA	thrust deflection angle in XI-ETA plane to compensate for center-of-gravity offset and aerodynamic moments
DEL XI-ZETA	thrust deflection angle in XI-ZETA plane to compensate for center-of-gravity offset and aerodynamic moments
CG XI	center of gravity measured from zero station along longitudinal (XI) axis
CG ETA	center of gravity measured from longitudinal axis along pitch (ETA) axis

CG ZETA	center of gravity measured from longitudinal axis along yaw (ZETA) axis
CP NORM	center of pressure measured from zero station for forces perpendicular to pitch (XI-ETA) plane
CP SIDE	center of pressure measured from zero station for forces perpendicular to yaw (XI-ZETA) plane
AERO MOM XI ETA ZETA	aerodynamic moments about center of gravity in vehicle axes system
INERTIA XI ETA ZETA	moments of inertia in vehicle axes system
INERTIA XI-ETA ETA-ZETA XI-ZETA	products of inertia in vehicle axes system

Centaur

THRUST	total Centaur thrust
LH2 FLOW	total LH_2 flow
LO2 FLOW	total LO_2 flow
RATIO	ratio of LO_2 to LH_2, total
C-1 THRUST	thrust of C-1 engine
C-1 LH2 FLOW	LH_2 flow for C-1 engine
C-1 LO2 FLOW	LO_2 flow for C-1 engine
C-1 RATIO	ratio of LO_2 to LH_2 for C-1 engine
PERCENT T1	percent change in thrust due to inlet pressures, temperatures, and PU valve setting for C-1 engine
C-2 THRUST	thrust of C-2 engine
C-2 LH2 FLOW	LH_2 flow for C-2 engine
C-2 LO2 FLOW	LO_2 flow for C-2 engine
C-2 RATIO	ratio of LO_2 to LH_2 for C-2 engine

PERCENT T2	percent change in thrust due to inlet pressures, temperatures, and PU valve setting for C-2 engine
LH2 WEIGHT	weight of LH_2
LO2 WEIGHT	weight of LO_2
C-1 LH2 PRESS	pump inlet pressure for C-1 engine LH_2 (telemetry)
C-2 LH2 PRESS	pump inlet pressure for C-2 engine LH_2 (telemetry)
PERCENT ISP1	percent change in engine specific impulse due to inlet conditions and valve setting for C-1 engine
C-1 ISP	specific impulse of C-1 engine equals ratio of C-1 thrust to C-1 flow
C-1 FLOW	total propellant flow for C-1 engine
C-1 LO2 PRESS	pump inlet pressure for C-1 engine LO_2 (telemetry)
C-2 LO2 PRESS	pump inlet pressure for C-2 engine LO_2 (telemetry)
PERCENT ISP2	percent change in engine specific impulse due to inlet conditions and valve setting for C-2 engine
C-2 ISP	specific impulse of C-2 engine equals ratio of C-2 thrust to C-2 flow
C-2 FLOW	total propellant flow for C-2 engine
C-1 LH2 TEMP	pump inlet temperature for C-1 engine LH_2 (telemetry)
C-2 LH2 TEMP	pump inlet temperature for C-2 engine LH_2 (telemetry)
PERCENT MR1	percent change in propellant mixture ratio due to engine inlet conditions and PU valve setting for C-1 engine
C-1 PU VALVE	propellant utilization valve setting for C-1 engine (telemetry)
C-2 PU VALVE	propellant utilization valve setting for C-2 engine (telemetry)
C-1 LO2 TEMP	pump inlet temperature for C-1 engine LO_2 (telemetry)
C-2 LO2 TEMP	pump inlet temperature for C-2 engine LO_2 (telemetry)
PERCENT MR2	percent change in propellant mixture ratio due to engine inlet conditions and PU valve setting for C-2 engine

Orbit Elements (OP 4)

PERIGEE RAD	radius at perigee of instantaneous conic
APOGEE RAD	radius at apogee of instantaneous conic
PERIGEE ALT	perigee altitude (above spherical Earth with radius = 3443.9 n. mi.)
APOGEE ALT	apogee altitude (above spherical Earth with radius = 3443.9 n. mi.)
PERIGEE VEL	velocity at perigee
APOGEE VEL	velocity at apogee
SEMI LAT REC	semilatus rectum of trajectory
PERIOD	period of eliptical trajectory
SEMI MAJ AXIS	semimajor axis
ENERGY	energy, $v^2/2 - \mu/r$
ECCENTRICITY	orbit eccentricity
INCLINATION	orbit inclination
TRUE ANOMALY	true anomaly
ASCEND NODE	ascending node

DETAILED TRAJECTORY LISTING

0 1	TIME	ALTITUDE	ALPHA	GEOCENT LAT	THRUST FIXED	AXL FORCE	ATM PRESS
P 2	WEIGHT	RADIUS	BETA	LONGITUDE	THRUST CONTL	SIDE FORCE	DYNM PRESS
1 3	TOTAL FLOW	VEL E	PSI	AZI E	GAMMA E	NORM FORCE	HEAT PARAM
4	GRND RANGE	VEL R	PSIDOT	AZI R	GAMMA R	AXL LD FCTR	MACH NUMBER
5	THETA I	VEL I	CROSS RANGE	AZI I	GAMMA I	WIND VEL	RHO-VR CUBED
6	Q*ALPHA TOT	ALT	DOWN RANGE	PHI	EAST WIND	NORTH WIND	TOTAL ISP
0 1	SEC	FT	DEG	DEG	LBS	LBS	PSI
P 2	LBS	FT	DEG	DEG	LBS	LBS	LBS/FT SQD
1 3	LBS/SEC	FT/SEC	DEG	DEG	DEG	LBS	FT*LBS/FT SQD
4	N. MI.	FT/SEC	DEG/SEC	DEG	DEG		
5	DEG	FT/SEC	N.MI.	DEG	DEG	FT/SEC	LBS/SEC CUBED
6	DEG-PSF	N.MI	N.MI.	DEG	FT/SEC	FT/SEC	SEC
0 1	THRUST (B)	FUEL FLOW (B)	OXID FLOW (B)	FP INLTP (B)	OP INLTP (B)	OIL WEIGHT (B)	ATM PRESS
E 2	THRUST (S)	FUEL FLOW (S)	OXID FLOW (S)	FP INLTP (S)	OP INLTP (S)	OIL WEIGHT (S)	VAPOR PRESS
P 3	THRUST (V)	FUEL FLOW (V)	OXID FLOW (V)	FUEL DENSITY	FUEL WEIGHT	FUEL LEVEL	FUEL TNK PR (G)
R 4	THRUST TOT	FUEL FLOW TOT	OXID FLOW TOT	OXID DENSITY	OXID WEIGHT	OXID LEVEL	OXID TNK PR (G)
0 5	THRUST CORR (B)	F FLOW CORR (B)	O FLOW CORR (B)	MIX RATIO (B)	AXL LD FCTR	NPSH	ACS ITER
6	THRUST CORR (S)	F FLOW CORR (S)	O FLOW CORR (S)	MIX RATIO (S)	CAP RATIO (PU)	VALVE ANGLE (PU)	
7	PC(B)	PC(S)	PC(V)	BASE FORCE	HOLD-DOWN		
0 1	LBS	LBS/SEC	LBS/SEC	PSI	PSI	LBS	PSI
E 2	LBS	LBS/SEC	LBS/SEC	PSI	PSI	LBS	PSI
P 3	LBS	LBS/SEC	LBS/SEC	LBS/CUBIC FT	LBS	INCHES	PSI
R 4	LBS	LBS/SEC	LBS/SEC	LBS/CUBIC FT	LBS	INCHES	PSI
0 5	LBS	LBS/SEC	LBS/SEC			FEET	
6	LBS	LBS/SEC	LBS/SEC			DEG	
7	PSIA	PSIA	PSIA	LBS	LBS		
0 1	THRUST XI	DEL XI-ETA	CG XI	CP NORM	AERO MOM XI	INERTIA XI	INERTIA XI-ETA
P 2	THRUST ETA	DEL XI-ZETA	CG ETA	CP SIDE	AERO MOM ETA	INERTIA ETA	INERTIA ETA-ZETA
5 3	THRUST ZETA		CG ZETA		AERO MOM ZETA	INERTIA ZETA	INERTIA XI*ZETA
0 1	LBS	DEG	INCHES	INCHES	FT-LBS	SLUG-FT SQD	SLUG-FT SQD
P 2	LBS	DEG	INCHES	INCHES	FT-LBS	SLUG-FT SQD	SLUG-FT SQD
5 3	LBS		INCHES		FT-LBS	SLUG-FT SQD	SLUG-FT SQD
0*1	0	-94.500000	90.202411	28.307490	58521.604	-4059.5250	14.661513
P 2	303536.00	0.2090976E 08	91.089153	-80.541179	325075.55	43.532346	0.8414420E-01
1 3	1575.2291	0.2543216E-04	90.079948	102.03122	-4.7390165	32.380253	0
4	0.5520337E-04	8.6176617	0	125.57289	-0.9536743E-06	1.2503855	0.7545577E-02
5	0.7227983E-06	1342.4258	0.5519358E-04	90.000001	0.9536743E-06	8.6176623	46.660424
6	7.5562331	-0.1555270E-01	-0.1039724E-05	-0.2834380E-01	7.0094011	-5.0132224	243.51833
0 1	325075.55	408.25398	889.85269	69.597418	52.531308	166.00000	14.661513
E 2	56995.596	94.796268	180.76768	71.673851	57.152909	53.000000	28.611137
P 3	1526.0075	0	0	50.380000	76103.000	937.69234	58.338486
R 4	383597.15	503.05025	1070.6204	68.889999	172286.00	551.35773	24.838486
0 5	-181.84886	0.1100356	0.2591751	2.1796546	1.2503862	59.660548	4.0000000
6	-976.49999	9.9399999	-9.9399999	1.9069072	0.4516520	14.100000	
7	574.20450	688.40168	315.27214	13.090707	4070.0978		
0 1	383596.55	0.7191021E-01	797.99998	298.47157	0	0	0
P 2	481.44076	0.5979738E-01	0.5000000	624.74978	-16140.178	0	0
5 3	400.34498		0.3900000		7518.2086	0	0

O*1	2.0000000	-77.500000	26.487728	28.307490	59835.999	-2383.0916	14.653006
P 2	300384.92	0.2090978E 08	3.2316061	-80.541179	325231.59	7.8699333	0.4083280
1 3	1575.8149	17.003596	90.079948	40.868798	88.981075	46.328034	5.3360091
4	0.3803400E-04	18.986295	0	121.29905	63.563803	1.2739783	0.1662689E-01
5	0.7356352E-02	1342.3367	0.1431421E-04	89.990241	0.7256804	8.7409658	498.86660
6	10.875362	-0.1275486E-01	-0.3523774E-04	-0.2834380E-01	7.4203514	-4.6198340	244.36092
D 1	325231.59	408.16779	890.52763	69.567023	53.040716	164.10000	14.653006
E 2	58309.886	79.282924	196.27811	71.671313	57.683414	52.700000	28.640030
P 3	1526.1134	0	0	50.380000	75113.631	941.49165	58.286993
R 4	385067.58	487.45071	1086.8057	68.885999	170127.41	556.97995	25.046994
O 5	-175.11980	0.1059643	0.2496105	2.1817685	1.2739782	60.712587	42.000000
6	324.19999	-5.5737776	5.5737776	2.4756669	0.4347981	-4.1022221	
7	574.40135	699.46621	315.29380	15.984401	2386.8503		
O 1	385066.96	0.7003726E-01	799.19998	299.21912	0	0	0
P 2	470.69867	0.6278981E-01	0.5013333	624.74998	-22994.848	0	0
5 3	421.99080		0.3926667		1257.5164	0	0

O*1	2.0000000	-77.500000	26.487728	28.307490	59835.999	-2383.0916	14.653006
P 2	300384.92	0.2090978E 08	3.2316061	-80.541179	325231.59	7.8699333	0.4083280
1 3	1575.8149	17.003596	90.079948	40.868798	88.981075	46.328034	5.3360091
4	0.3803400E-04	18.986295	0	121.29905	63.563803	1.2739783	0.1662689E-01
5	0.7356352E-02	1342.3367	0.1431421E-04	89.990241	0.7256804	8.7409658	498.86660
6	10.875362	-0.1275486E-01	-0.3523774E-04	-0.2834382E-01	7.4203514	-4.6198340	244.36092
D 1	325231.59	408.16779	890.52763	69.567023	53.040716	164.10000	14.653006
E 2	58309.886	79.282924	196.27811	71.671313	57.683414	52.700000	28.640030
P 3	1526.1134	0	0	50.380000	75113.631	941.49165	58.286993
R 4	385067.58	487.45071	1086.8057	68.885999	170127.41	556.97995	25.046994
O 5	-175.11980	0.1059643	0.2496105	2.1817685	1.2739782	60.712587	43.000000
6	324.19999	-5.5737776	5.5737776	2.4756669	0.4347981	-4.1022221	
7	574.40135	699.46621	315.29380	15.984401	2386.8503		
O 1	385066.96	0.7003726E-01	799.19998	299.21912	0	0	0
P 2	470.69867	0.6278981E-01	0.5013333	624.74998	-22994.848	0	0
5 3	421.99080		0.3926667		1257.5164	0	0

O*1	9.9999998	366.50000	6.3960503	28.307505	60053.484	-229.81629	14.431659
P 2	287772.32	0.2091023E 08	-1.8904111	-80.541198	326274.95	-112.90607	10.675694
1 3	1577.2112	96.926457	90.079948	53.842976	88.881361	295.86516	2446.3177
4	0.1398597E-02	97.541192	0	84.661310	83.467972	1.3416770	0.8566623E-01
5	0.3676688E-01	1344.4248	-0.8233720E-03	89.952325	4.1335449	12.576276	67006.851
6	71.155015	0.6031814E-01	-0.1130550E-02	12.330644	12.576000	-0.8333253E-01	244.94400
D 1	326274.95	407.84449	892.33156	69.307250	54.473969	156.50000	14.431659
E 2	58524.003	81.783713	193.69303	71.491478	59.177110	51.500000	28.755585
P 3	1529.4817	0	0	50.380000	71216.876	954.32954	58.268339
R 4	386328.43	489.62820	1086.0246	68.869999	161424.03	576.73292	26.068340
O 5	-155.53472	0.9411472E-01	0.2217726	2.1879211	1.3416769	63.608242	120.00000
6	186.20000	-3.0655001	3.0655001	2.3683569	0.4363835	-2.3900001	
7	574.88435	698.21640	315.98254	91.272480	0.2390502E-14		
O 1	386327.32	0.6254431E-01	803.99999	299.95150	0	0	0
P 2	421.71669	0.1092502	0.5066667	620.99998	-144730.67	0	0
5 3	736.64056		0.4033333		-23678.763	0	0

0*1	15.000000	994.50000	2.7548628	28.307525	60617.316	-609.05181	14.122938
P 2	279886.42	0.2091085E 08	0.8847233	-80.541231	327292.43	152.98536	26.686758
1 3	1577.1461	155.47007	90.079948	58.725236	88.803411	323.95700	14134.999
4	0.3483488E-02	155.60573	0	110.86109	87.325059	1.3837737	0.1369163
5	0.5512978E-01	1348.7076	-0.1815362E-02	89.927983	6.6179438	10.471728	267212.30
6	77.205461	0.1636736	-0.2973084E-02	20.055011	9.5615999	-4.2699992	245.95676
D 1	327292.43	407.63671	892.60740	68.891796	54.780973	151.75000	14.122938
E 2	59083.080	80.449087	194.89441	71.125731	59.521639	50.750000	28.845860
P 3	1534.2367	0	0	50.380000	68770.167	961.75739	58.177062
R 4	387909.74	488.08580	1087.5018	68.857499	155992.63	588.68318	26.327062
O 5	-149.83090	0.9066373E-01	0.2136653	2.1897129	1.3837736	64.151505	184.00000
6	258.99999	-4.3849998	4.3849998	2.4225807	0.4355409	-3.2999999	
7	574.88481	698.68919	316.95485	196.27973	0		
O 1	387908.54	0.7956819E-01	806.99999	385.32631	0	0	0
P 2	538.69938	0.1038117	0.5100000	624.74998	-125605.86	0	0
5 3	702.83543		0.4100000		20339.905	0	0

0*1	15.000000	994.50000	2.7548628	28.307525	60617.316	-609.05181	14.122938
P 2	279886.42	0.2091085E 08	0.8847233	-80.541231	327292.43	152.98536	26.686758
1 3	1577.1461	155.47007	90.079948	58.725236	88.803411	323.95700	14134.999
4	0.3483488E-02	155.60573	0.4824402	110.86109	87.325059	1.3837737	0.1369163
5	0.5512978E-01	1348.7076	-0.1815362E-02	89.927983	6.6179438	10.471728	267212.30
6	77.205461	0.1636736	-0.2973084E-02	20.055011	9.5615999	-4.2699992	245.95676
D 1	327292.43	407.63671	892.60740	68.891796	54.780973	151.75000	14.122938
E 2	59083.080	80.449087	194.89441	71.125731	59.521639	50.750000	28.845860
P 3	1534.2367	0	0	50.380000	68770.167	961.75739	58.177062
R 4	387909.74	488.08580	1087.5018	68.857499	155992.63	588.68318	26.327062
O 5	-149.83090	0.9066373E-01	0.2136653	2.1897129	1.3837736	64.151505	185.00000
6	258.99999	-4.3849998	4.3849998	2.4225807	0.4355409	-3.2999999	
7	574.88481	698.68919	316.95485	196.27973	0		
O 1	387908.54	0.7956819E-01	806.99999	385.32631	0	0	0
P 2	538.69938	0.1038117	0.5100000	624.74998	-125605.86	0	0
5 3	702.83543		0.4100000		20339.905	0	0

0*1	20.000000	1932.5000	0.3394084	28.307551	61364.505	-1242.5184	13.671721
P 2	272001.01	0.2091179E 08	1.7606265	-80.541260	328767.26	566.98078	52.564540
1 3	1577.0027	221.04637	87.667747	19.979073	89.418265	94.896011	51217.801
4	0.5648172E-02	221.34168	0.4824402	127.26459	86.983444	1.4297302	0.1953010
5	0.7349703E-01	1361.3854	-0.3282023E-02	89.910045	9.3439264	12.500988	748671.20
6	94.248358	0.3180486	-0.4596777E-02	20.055011	8.5049576	-9.1618992	247.38813
D 1	328767.26	407.39435	892.87419	68.487040	55.136643	147.00000	13.671721
E 2	59823.258	80.053598	195.12217	70.775239	59.918281	50.000000	28.936138
P 3	1541.2472	0	0	50.380000	66332.392	969.07626	58.228279
R 4	390131.76	487.44795	1087.9964	68.844999	150552.79	600.65314	26.728279
O 5	-143.59997	0.8689382E-01	0.2048088	2.1916705	1.4297303	64.803958	231.00000
6	279.80000	-4.7620000	4.7620000	2.4373941	0.4353002	-3.5600000	
7	574.86661	698.72547	318.38836	349.75491	0		
O 1	390130.59	0.1072969	809.49998	277.20958	0	0	0
P 2	730.59205	0.7078773E-01	0.5233333	624.74997	-28849.076	0	0
5 3	481.99838		0.4233333		89894.970	0	0

O*1	20.000000	1932.5000	0.3394084	28.307551	61364.505	-1242.5184	13.671721
P 2	272001.01	0.2091179E 08	1.7606265	-80.541260	328767.26	566.98078	52.564540
1 3	1577.0027	221.04637	87.667747	19.979073	89.418265	94.896011	51217.801
4	0.5648172E-02	221.34168	0.4824402	127.26459	86.983444	1.4297302	0.1953010
5	0.7349703E-01	1361.3854	-0.3282023E-02	89.910045	9.3439264	12.500988	748671.20
6	94.248358	0.3180486	-0.4596777E-02	20.055011	8.5049576	-9.1618992	247.38813
D 1	328767.26	407.39435	892.87419	68.487040	55.136643	147.00000	13.671721
E 2	59823.258	80.053598	195.12217	70.775239	59.918281	50.000000	28.936138
P 3	1541.2472	0	0	50.380000	66332.392	969.07626	58.228279
R 4	390131.76	487.44795	1087.9964	68.844999	150552.79	600.65314	26.728279
O 5	-143.59997	0.8689382E-01	0.2048088	2.1916705	1.4297303	64.803958	232.00000
6	279.80000	-4.7620000	4.7620000	2.4373941	0.4353002	-3.5600000	
7	574.86661	698.72547	318.38836	349.75491	0		
O 1	390130.59	0.1072969	809.49998	277.20958	0	0	0
P 2	730.59205	0.7078773E-01	0.5233333	624.74997	-28849.076	0	0
5 3	481.99838		0.4233333		89894.970	0	0
O*1	29.999999	4889.7500	0.7137683E-01	28.307602	63678.811	-3477.6857	12.323769
P 2	256203.96	0.2091475E 08	1.2596738	-80.540757	333745.11	1116.8508	141.44509
1 3	1579.2258	377.51923	82.843346	88.295714	84.132222	93.158265	337622.74
4	0.2324998E-01	378.49046	0.4824402	103.99221	82.842731	1.5376206	0.3374364
5	0.1107239	1431.4609	-0.8444539E-02	89.950727	15.209443	14.494280	3444909.8
6	178.46029	0.8047493	0.2166229E-01	20.055011	7.1815171	-12.590074	251.65744
D 1	333745.11	406.32534	896.66630	67.316554	58.267037	137.50000	12.323769
E 2	62116.589	77.168285	197.50739	69.732149	63.144728	48.500000	29.174477
P 3	1562.2215	0	0	50.380000	61484.417	983.63178	58.376230
R 4	397423.91	483.49362	1094.1737	68.811998	139619.30	624.62925	30.176230
O 5	-107.13534	0.6483061E-01	0.1529197	2.2067693	1.5376209	71.088127	305.00000
6	423.71999	-7.5913997	7.5913997	2.5594373	0.4337502	-5.2339998	
7	575.69186	699.53279	322.67717	808.24188	0		
O 1	397422.19	0.1416411	814.49997	267.96249	0	0	0
P 2	982.47101	0.6196086E-01	0.5500000	624.74998	8002.0820	0	0
5 3	429.78085		0.4500000		171950.05	0	0
O*1	32.000000	5675.2500	-0.4671421E-01	28.307607	64236.952	-4089.9925	11.984071
P 2	253046.12	0.2091553E 08	0.9060293	-80.540479	334747.04	968.89505	165.46576
1 3	1578.6167	413.37678	81.878466	89.361306	82.862528	25.988382	459216.98
4	0.3765832E-01	414.15001	0.4824402	100.53530	82.053832	1.5605558	0.3701022
5	0.1183263	1453.2396	-0.9902581E-02	89.974133	16.394400	12.143299	4409616.9
6	150.11588	0.9340260	0.3633315E-01	20.055011	4.9297504	-11.097624	252.74279
D 1	334747.04	406.19794	896.31729	66.979795	58.118064	135.60000	11.984071
E 2	62669.444	76.804242	197.73874	69.422471	63.016154	48.200000	29.227917
P 3	1567.5087	0	0	50.380000	60517.920	986.53320	58.375928
R 4	398983.98	483.00218	1094.0560	68.804599	137431.07	629.42239	30.155929
O 5	-107.37981	0.6497855E-01	0.1532686	2.2066022	1.5605557	70.714839	343.00000
6	437.00000	-7.9399999	7.9399999	2.5745810	0.4335965	-5.4000000	
7	575.51145	699.52277	323.75830	923.78552	0		
O 1	398982.59	0.1305776	815.69998	265.49998	0	0	0
P 2	909.28635	0.4580654E-01	0.5566667	624.74998	55259.610	0	0
5 3	318.97668		0.4553333		138249.88	0	0

O*1	32.000000	5675.2500	-0.4671421E-01	28.307607	64236.952	-4089.9925	11.984071
P 2	253046.12	0.2091553E 08	0.9060293	-80.540479	334747.04	968.89505	165.46576
1 3	1578.6167	413.37678	81.878466	89.361306	82.862528	25.988382	459216.98
4	0.3765832E-01	414.15001	0.6633552	100.53530	82.053832	1.5605558	0.3701022
5	0.1183263	1453.2396	-0.9902581E-02	89.974133	16.394400	12.143299	4409616.9
6	150.11588	0.9340260	0.3633315E-01	20.055011	4.9297504	-11.097624	252.74279
D 1	334747.04	406.19794	896.31729	66.979795	58.118064	135.60000	11.984071
E 2	62669.444	76.804242	197.73874	69.422471	63.016154	48.200000	29.227917
P 3	1567.5087	0	0	50.380000	60517.920	986.53320	58.375928
R 4	398983.98	483.00218	1094.0560	68.804599	137431.07	629.42239	30.155929
O 5	-107.37981	0.6497855E-01	0.1532686	2.2066022	1.5605557	70.714839	344.00000
6	437.00000	-7.9399999	7.9399999	2.5745810	0.4335965	-5.4000000	
7	575.51145	699.52277	323.75830	923.78552	0		
O 1	398982.59	0.1305776	815.69998	265.49998	0	0	0
P 2	909.28635	0.4580654E-01	0.5566667	624.74998	55259.610	0	0
S 3	318.97668		0.4553333		138249.88	0	0
O*1	40.000000	9544.7500	-0.4978502	28.307579	66760.001	-7182.2672	10.416903
P 2	240427.31	0.2091940E 08	1.1895844	-80.538343	339422.28	2122.7864	283.35539
1 3	1576.0619	574.59356	76.571624	91.638327	77.189988	-492.35731	1346492.7
4	0.1499887	574.51738	0.6633552	99.791181	77.223469	1.6595304	0.5194768
5	0.1496333	1573.5309	-0.1716748E-01	90.135064	20.859241	18.267021	0.1047538E 08
6	365.38821	1.5708638	0.1490035	20.055011	-2.1476239	-18.140336	257.71975
D 1	339422.28	405.63434	894.90906	65.634136	57.589394	128.00000	10.416903
E 2	65168.047	76.737247	197.22279	68.193679	62.575516	47.000000	29.441689
P 3	1591.9544	0	0	50.380000	56656.365	998.12705	58.583097
R 4	406182.28	482.37159	1092.1318	68.775000	128686.29	648.58788	30.283097
O 5	-107.97362	0.6533788E-01	0.1541162	2.2061965	1.6595300	69.375080	417.00000
6	436.99999	-7.9399998	7.9399998	2.5701051	0.4335965	-5.3999999	
7	574.76060	699.03460	328.75695	1456.8356	0		
O 1	406178.70	0.2074403	820.49999	265.49999	0	0	0
P 2	1470.5832	-0.7341166E-01	0.5833333	624.74998	397359.00	0	0
S 3	-520.42699		0.4766667		338795.74	0	0
O*1	40.000000	9544.7500	-0.4978502	28.307579	66760.001	-7182.2672	10.416903
P 2	240427.31	0.2091940E 08	1.1895844	-80.538343	339422.28	2122.7864	283.35539
1 3	1576.0619	574.59356	76.571624	91.638327	77.189988	-492.35731	1346492.7
4	0.1499887	574.51738	0.7538127	99.791181	77.223469	1.6595304	0.5194768
5	0.1496333	1573.5309	-0.1716748E-01	90.135064	20.859241	18.267021	0.1047538E 08
6	365.38821	1.5708638	0.1490035	20.055011	-2.1476239	-18.140336	257.71975
D 1	339422.28	405.63434	894.90906	65.634136	57.589394	128.00000	10.416903
E 2	65168.047	76.737247	197.22279	68.193679	62.575516	47.000000	29.441689
P 3	1591.9544	0	0	50.380000	56656.365	998.12705	58.583097
R 4	406182.28	482.37159	1092.1318	68.775000	128686.29	648.58788	30.283097
O 5	-107.97362	0.6533788E-01	0.1541162	2.2061965	1.6595300	69.375080	418.00000
6	436.99999	-7.9399998	7.9399998	2.5701051	0.4335965	-5.3999999	
7	574.76060	699.03460	328.75695	1456.8356	0		
O 1	406178.70	0.2074403	820.49999	265.49999	0	0	0
P 2	1470.5832	-0.7341166E-01	0.5833333	624.74998	397359.00	0	0
S 3	-520.42699		0.4766667		338795.74	0	0

O*1	49.999998	16179.250	-0.1536195	28.307378	70323.914	-12962.776	8.1278249
P 2	224688.13	0.2092604E 08	0.4604396	-80.532060	346122.16	1629.9621	473.75257
1 3	1571.7179	823.13828	69.033498	92.565230	69.339205	-140.35732	3991657.0
4	0.4822555	822.68612	0.7538127	96.001675	69.422889	1.7957399	0.7604285
5	0.1919506	1806.1353	-0.3146654E-01	90.438298	25.241510	17.924995	0.2507961E 08
6	229.95380	2.6627621	0.4812297	20.055011	-2.5999983	-17.735429	264.96236
D 1	346122.16	404.85096	892.22288	63.521492	56.370275	118.50000	8.1278249
E 2	68696.297	79.024981	194.06062	66.241867	61.477274	45.500000	29.781147
P 3	1627.6173	0	0	50.380000	51832.165	1012.6114	58.772173
R 4	416446.08	483.87594	1086.2835	68.727998	117786.89	672.47033	30.172175
O 5	-111.43574	0.6743291E-01	0.1590578	2.2038304	1.7957392	66.410231	515.00000
6	323.00005	-5.5511119	5.5511119	2.4556870	0.4348105	-4.0888894	
7	573.46545	697.28925	336.04930	2235.4337	0		
O 1	416444.23	0.1509342	825.49999	308.60540	0	0	0
P 2	1097.0411	-0.3693258E-01	0.6233333	645.90878	314749.67	0	0
5 3	-268.43795		0.5066667		164422.83	0	0

O*1	54.000000	19437.500	0.1814791	28.307204	71756.412	-17006.413	7.1655341
P 2	218405.53	0.2092930E 08	-0.1744148E-01	-80.527917	348862.14	300.56964	556.47168
1 3	1569.5257	938.98008	66.018245	93.092863	66.225939	752.77845	5807963.2
4	0.7014757	939.94690	0.7538127	94.719205	66.092517	1.8479884	0.8777422
5	0.2103119	1924.3290	-0.3841509E-01	90.656147	26.522263	11.733509	0.3365747E 08
6	101.45327	3.1990011	0.7004257	20.055011	1.6143385	-11.621925	267.99087
D 1	348862.14	404.52502	890.74864	62.471813	55.606063	114.70000	7.1655341
E 2	70113.849	80.902243	191.79130	65.253882	60.759252	44.900000	29.951584
P 3	1642.5641	0	0	50.380000	49893.521	1018.4329	58.734464
R 4	420618.55	485.42726	1082.5399	68.704399	113449.16	681.97313	30.014466
O 5	-114.17005	0.6908752E-01	0.1629607	2.2019618	1.8479884	64.570889	567.00000
6	217.22222	-3.6277777	3.6277777	2.3706549	0.4360245	-2.7777778	
7	572.80334	695.99680	339.10563	2562.7435	0		
O 1	420617.30	0.8299099E-01	827.09999	352.96625	0	0	0
P 2	609.25031	0.9576332E-01	0.6420000	654.47407	-51869.189	0	0
5 3	703.01424		0.5200000		-35535.863	0	0

O*1	54.000000	19437.500	0.1814791	28.307204	71756.412	-17006.413	7.1655341
P 2	218405.53	0.2092930E 08	-0.1744148E-01	-80.527917	348862.14	300.56964	556.47168
1 3	1569.5257	938.98008	66.018245	93.092863	66.225939	752.77845	5807963.2
4	0.7014757	939.94690	0.7538127	94.719205	66.092517	1.8479884	0.8777422
5	0.2103119	1924.3290	-0.3841509E-01	90.656147	26.522263	11.733509	0.3365747E 08
6	101.45327	3.1990011	0.7004257	20.055011	1.6143385	-11.621925	267.99087
D 1	348862.14	404.52502	890.74864	62.471813	55.606063	114.70000	7.1655341
E 2	70113.849	80.902243	191.79130	65.253882	60.759252	44.900000	29.951584
P 3	1642.5641	0	0	50.380000	49893.521	1018.4329	58.734464
R 4	420618.55	485.42726	1082.5399	68.704399	113449.16	681.97313	30.014466
O 5	-114.17005	0.6908752E-01	0.1629607	2.2019618	1.8479884	64.570889	568.00000
6	217.22222	-3.6277777	3.6277777	2.3706549	0.4360245	-2.7777778	
7	572.80334	695.99680	339.10563	2562.7435	0		
O 1	420617.30	0.8299099E-01	827.09999	352.96625	0	0	0
P 2	609.25031	0.9576332E-01	0.6420000	654.47407	-51869.189	0	0
5 3	703.01424		0.5200000		-35535.863	0	0

O*1	59.999998	24986.250	0.2167363	28.306786	73938.029	-40268.783	5.7465147
P 2	209004.94	0.2093485E 08	-0.1977431	-80.519473	352457.52	-70.192196	661.77822
1 3	1564.2345	1122.0648	61.495369	93.552414	61.695132	1073.3900	9601208.2
4	1.1485244	1123.4698	0.7538127	94.424048	61.562378	1.8474448	1.0688671
5	0.2398174	2119.6921	-0.4874749E-01	90.973541	27.778962	9.6854819	0.4784195E 08
6	194.15743	4.1122078	1.1474938	20.055011	2.3177105	-9.4040829	272.59055
D 1	352457.52	404.19267	886.44266	60.497546	52.853840	109.00000	5.7465147
E 2	72273.484	81.962076	190.07869	63.278974	58.005692	44.000000	30.207253
P 3	1664.5450	0	0	50.380000	46977.882	1027.1888	58.653484
R 4	426395.55	486.15474	1076.5213	68.668999	106973.57	696.16972	29.753485
O 5	-138.98991	0.8410458E-01	0.1982561	2.1931191	1.8474444	58.293776	649.00000
6	154.20001	-2.4870002	2.4870002	2.3191053	0.4367539	-1.9900001	
7	571.14247	694.68038	343.60028	3045.4032	0		
O 1	426393.89	-0.3244040E-01	829.49998	327.30995	0	0	0
P 2	-241.42076	0.1415932	0.6700000	594.59126	-172801.15	0	0
5 3	1053.7355		0.5400000		-378027.34	0	0
O*1	64.000000	29102.500	0.4731671E-01	28.306380	75442.699	-41003.095	4.8474337
P 2	202750.59	0.2093896E 08	-0.9627425E-01	-80.512154	355204.43	674.99542	718.42864
1 3	1563.0900	1252.9798	58.480117	93.867531	58.725282	649.83930	0.1288145E 08
4	1.5362615	1252.8011	0.7538127	94.695011	58.738745	1.9217867	1.2125666
5	0.2609775	2263.2494	-0.5517574E-01	91.219602	28.240415	10.836292	0.5791630E 08
6	77.068320	4.7896555	1.5352763	20.055011	-1.1399394	-10.776166	275.51013
D 1	355204.43	403.78225	886.07830	59.475126	53.040431	105.20000	4.8474337
E 2	73764.335	80.673805	190.99717	62.344336	58.257692	43.400000	30.513477
P 3	1678.3645	0	0	50.380000	45038.653	1033.0146	58.512565
R 4	430647.13	484.45605	1077.0755	68.626598	102664.68	705.56561	30.132566
O 5	-134.76689	0.8154953E-01	0.1922536	2.1944459	1.9217867	58.216013	702.00000
6	223.17142	-3.7356071	3.7356071	2.3675240	0.4359556	-2.8521428	
7	570.81125	694.88876	346.42609	3351.2130	0		
O 1	430646.47	-0.3078844E-01	829.89999	199.31581	0	0	0
P 2	-231.41209	0.8537090E-01	0.6940000	560.76283	-6889.2000	0	0
5 3	641.66511		0.5533333		-387291.21	0	0
C*1	64.000000	29102.500	0.4731671E-01	28.306380	75442.699	-41003.095	4.8474337
P 2	202750.59	0.2093896E 08	-0.9627425E-01	-80.512154	355204.43	674.99542	718.42864
1 3	1563.0900	1252.9798	58.480117	93.867531	58.725282	649.83930	0.1288145E 08
4	1.5362615	1252.8011	0.7538127	94.695011	58.738745	1.9217867	1.2125666
5	0.2609775	2263.2494	-0.5517574E-01	91.219602	28.240415	10.836292	0.5791630E 08
6	77.068320	4.7896555	1.5352763	20.055011	-1.1399394	-10.776166	275.51013
D 1	355204.43	403.78225	886.07830	59.475126	53.040431	105.20000	4.8474337
E 2	73764.335	80.673805	190.99717	62.344336	58.257692	43.400000	30.513477
P 3	1678.3645	0	0	50.380000	45038.653	1033.0146	58.512565
R 4	430647.13	484.45605	1077.0755	68.626598	102664.68	705.56561	30.132566
O 5	-134.76689	0.8154953E-01	0.1922536	2.1944459	1.9217867	58.216013	703.00000
6	223.17142	-3.7356071	3.7356071	2.3675240	0.4359556	-2.8521428	
7	570.81125	694.88876	346.42609	3351.2130	0		
O 1	430646.47	-0.3078844E-01	829.89999	199.31581	0	0	0
P 2	-231.41209	0.8537090E-01	0.6940000	560.76283	-6889.2000	0	0
5 3	641.66511		0.5533333		-387291.21	0	0

O*1	69.999997	35914.250	0.1960529	28.305532	77421.375	-38010.769	3.6022101
P 2	193375.74	0.2094578E 08	-0.1105525	-80.498178	359112.83	621.40588	798.06741
1 3	1561.9846	1476.5203	53.957243	94.262465	54.429804	1233.5948	0.1913052E 08
4	2.2769209	1482.6205	0.7538127	94.749709	54.101485	2.0608637	1.4825352
5	0.2953583	2508.4913	-0.6308133E-01	91.607092	28.605528	14.078476	0.7613855E 08
6	179.62441	5.9107254	2.2760558	20.055011	9.6831489	-10.219595	279.47408
D 1	359112.83	403.14074	886.12786	58.010647	53.723474	99.500004	3.6022101
E 2	75723.906	80.787389	190.37016	61.044076	59.063304	42.500000	30.972809
P 3	1697.4693	0	0	50.380000	42133.489	1041.7423	58.197790
R 4	436534.20	483.92812	1076.4980	68.562999	96204.347	719.67327	30.597789
O 5	-123.26088	0.7458803E-01	0.1758991	2.1980608	2.0608637	58.997292	780.00000
6	213.91428	-3.5678214	3.5678214	2.3564341	0.4360628	-2.7364286	
7	570.51235	694.28184	350.33264	3774.7585	0		
O 1	436531.82	-0.6739856E-01	830.49998	254.39101	0	0	0
P 2	-513.50431	0.1579092	0.7300000	522.62182	-208704.59	0	0
5 3	1203.1004		0.5733333		-514570.11	0	0
O*1	72.000000	38360.000	-0.4436596E-01	28.305175	78037.719	-36406.338	3.2208212
P 2	190251.91	0.2094822E 08	-0.3533762E-01	-80.492613	360345.33	983.75119	814.12049
1 3	1561.8468	1559.1994	52.449615	94.337140	53.009749	171.39251	0.2158183E 08
4	2.5719378	1562.5499	0.7538127	94.895601	52.846965	2.1128588	1.5835463
5	0.3076177	2599.3485	-0.6512023E-01	91.723411	28.627741	12.784745	0.8185734E 08
6	46.176389	6.3132440	2.5711233	20.055011	4.6281191	-11.917643	280.68248
D 1	360345.33	402.99794	886.25642	57.790051	54.157149	97.600001	3.2208212
E 2	76334.428	80.834163	190.19986	60.884874	59.542648	42.200000	31.169250
P 3	1703.2918	0	0	50.380000	41165.729	1044.6501	58.319179
R 4	438383.04	483.83210	1076.4563	68.535799	94051.390	724.35887	30.859178
O 5	-119.76657	0.7247386E-01	0.1709323	2.1991587	2.1128581	59.615111	822.00000
6	210.82857	-3.5118927	3.5118927	2.3529638	0.4360985	-2.6978571	
7	570.47530	694.18394	351.52322	3904.4825	0		
O 1	438381.77	0.4987941E-01	830.69999	260.68024	0	0	0
P 2	381.63768	-0.1149960	0.7420000	510.53974	589751.66	0	0
5 3	-879.85899		0.5800000		-179760.81	0	0
O*1	72.000000	38360.000	-0.4436596E-01	28.305175	78038.062	-36406.338	3.2208212
P 2	190127.91	0.2094822E 08	-0.3533762E-01	-80.492613	360352.40	983.75119	814.12049
1 3	1561.8796	1559.1994	52.449615	94.337140	53.009749	171.39251	0.2158183E 08
4	2.5719378	1562.5499	0.6633552	94.895601	52.846965	2.1142758	1.5835463
5	0.3076177	2599.3485	-0.6512023E-01	91.723411	28.627741	12.784745	0.8185734E 08
6	46.176389	6.3132440	2.5711233	20.055011	4.6281191	-11.917643	280.68133
D 1	360352.40	402.99532	886.29077	57.795889	54.183101	97.600001	3.2208212
E 2	76334.771	80.834353	190.20075	60.892386	59.569865	42.200000	31.169250
P 3	1703.2926	0	0	50.380000	41165.729	1044.6501	58.319179
R 4	438390.46	483.82967	1076.4915	68.535799	94051.390	724.35887	30.859178
O 5	-119.44965	0.7228211E-01	0.1704819	2.1992582	2.1142758	59.672296	826.00000
6	210.82857	-3.5118927	3.5118927	2.3529693	0.4360985	-2.6978571	
7	570.48617	694.18685	351.52338	3904.4825	0		
O 1	438385.18	0.4988045E-01	830.69999	260.68024	0	0	0
P 2	381.65210	-0.1149926	0.7420000	510.53974	589751.66	0	0
5 3	-879.84770		0.5800000		-179760.81	0	0

O*1	79.999997	49057.000	0.1619624	28.303324	80214.780	-26827.323	1.9054108
P 2	177633.37	0.2095892E 08	-0.4513068E-01	-80.465013	364714.47	728.99931	800.99030
1 3	1561.9939	1935.9767	47.142775	94.665470	47.704864	1074.9363	0.3314835E 08
4	4.0354576	1945.8123	0.6633552	94.950631	47.387495	2.3537276	2.0421567
5	0.3613634	3009.0066	-0.7053696E-01	92.217043	28.418681	17.754376	0.1002913E 09
6	134.67257	8.0737438	4.0348567	20.055011	13.685203	-11.310751	284.84699
D 1	364714.47	402.42358	887.40678	56.945216	56.266192	90.000004	1.9054108
E 2	78491.515	80.045456	190.55957	60.324452	61.863307	41.000000	31.955032
P 3	1723.2661	0	0	50.380000	37301.017	1056.2610	58.594589
R 4	444929.25	482.46904	1077.9664	68.426998	85434.026	743.15416	31.694589
O 5	-109.49634	0.6625932E-01	0.1562896	2.2051560	2.3537274	62.939945	920.00000
6	252.73483	-4.2714438	4.2714438	2.3806420	0.4356134	-3.2216854	
7	570.52933	694.28360	355.60756	4351.9011	0		
O 1	444927.89	0.1028109	830.49997	303.57721	0	0	0
P 2	798.37482	0.7605617E-01	0.8000000	481.51730	49053.990	0	0
5 3	550.61123		0.6166666		-51362.280	0	0
O*1	84.000000	54980.750	-0.2288800	28.302113	81006.406	-20689.299	1.4136417
P 2	171384.79	0.2096485E 08	-0.2452971E-01	-80.447586	366388.44	694.52480	733.84932
1 3	1562.3107	2154.8955	44.489352	94.689645	45.258921	-604.56066	0.3946615E 08
4	4.9598052	2158.7771	0.6633552	95.010857	45.155064	2.4897463	2.2693606
5	0.3914360	3244.3918	-0.7157366E-01	92.396632	28.149349	14.056833	0.1019412E 09
6	168.92526	9.0486677	4.9593081	20.055011	4.4153482	-13.345383	286.36740
D 1	366388.44	402.22923	888.06609	56.678370	57.520584	86.200002	1.4136417
E 2	79275.870	80.221678	190.23522	60.218215	63.236619	40.400000	32.460587
P 3	1730.5368	0	0	50.380000	35371.182	1062.0600	58.726357
R 4	447394.84	482.45090	1078.3013	68.356998	81121.520	752.55274	32.026358
O 5	-105.53883	0.6386452E-01	0.1506409	2.2078606	2.4897462	64.832405	1008.0000
6	242.84719	-4.0922302	4.0922302	2.3713692	0.4357279	-3.0980898	
7	570.61189	694.13302	357.09428	4519.1694	0		
O 1	447393.96	0.1134047E-01	830.09999	314.92267	0	0	0
P 2	88.552048	-0.1021239	0.8320000	475.26121	589977.91	0	0
5 3	-797.43538		0.6380000		-338413.74	0	0
O*1	84.000000	54980.750	-0.2288800	28.302113	81006.406	-20689.299	1.4136417
P 2	171384.79	0.2096485E 08	-0.2452971E-01	-80.447586	366388.44	694.52480	733.84932
1 3	1562.3107	2154.8955	44.489352	94.689645	45.258921	-604.56066	0.3946615E 08
4	4.9598052	2158.7771	0.5427452	95.010857	45.155064	2.4897463	2.2693606
5	0.3914360	3244.3918	-0.7157366E-01	92.396632	28.149349	14.056833	0.1019412E 09
6	168.92526	9.0486677	4.9593081	20.055011	4.4153482	-13.345383	286.36740
D 1	366388.44	402.22923	888.06609	56.678370	57.520584	86.200002	1.4136417
E 2	79275.870	80.221678	190.23522	60.218215	63.236619	40.400000	32.460587
P 3	1730.5368	0	0	50.380000	35371.182	1062.0600	58.726357
R 4	447394.84	482.45090	1078.3013	68.356998	81121.520	752.55274	32.026358
O 5	-105.53883	0.6386452E-01	0.1506409	2.2078606	2.4897462	64.832405	1009.0000
6	242.84719	-4.0922302	4.0922302	2.3713692	0.4357279	-3.0980898	
7	570.61189	694.13302	357.09428	4519.1694	0		
O 1	447393.96	0.1134047E-01	830.09999	314.92267	0	0	0
P 2	88.552048	-0.1021239	0.8320000	475.26121	589977.91	0	0
5 3	-797.43538		0.6380000		-338413.74	0	0

O*1	89.999997	64623.000	0.5471212	28.299865	81856.938	-13724.656	0.8781079
P 2	162009.71	0.2097449E 08	-0.3897452	-80.416162	368214.56	-1046.9921	621.06242
I 3	1562.7195	2523.0804	41.232882	94.932760	41.943488	2262.2521	0.4902291E 08
4	6.6269175	2561.7915	0.5427452	94.573563	41.170140	2.6932505	2.6488869
5	0.4412073	3635.4705	-0.7006521E-01	92.768343	27.637731	52.078544	0.1023797E 09
6	417.18775	10.635578	6.6265729	20.055011	52.048060	1.7816021	288.00530
D 1	368214.56	401.98740	888.89971	56.189951	59.193958	80.500004	0.8781079
E 2	80118.702	80.489079	189.78486	59.970090	65.087443	39.500000	33.218918
P 3	1738.2364	0	0	50.380000	32476.428	1070.7606	58.721891
R 4	450071.50	482.47648	1078.6846	68.251999	74650.546	766.69379	32.321891
O 5	-100.56106	0.6085233E-01	0.1435359	2.2112626	2.6932502	67.237117	1100.0000
6	228.01573	-3.8234101	3.8234101	2.3578958	0.4358995	-2.9126967	
7	570.70670	693.87267	358.66869	4701.3238	0		
O 1	450057.40	-0.9282521E-01	829.49999	311.37268	0	0	0
P 2	-729.14117	0.3994890	0.8800000	469.01955	-898758.25	0	0
S 3	3138.0305		0.6700000		-674946.99	0	0

O*1	100.00000	82836.750	-0.1873564	28.294727	82732.088	-5864.0319	0.3732913
P 2	146378.68	0.2099271E 08	-0.2396710	-80.347588	370022.88	-359.07388	417.78825
I 3	1563.7081	3244.0965	35.805429	95.144146	37.106089	-278.35962	0.6380302E 08
4	10.266299	3284.4287	0.5427452	94.864855	36.575709	3.0529718	3.3321451
5	0.5384671	4392.0134	-0.5418506E-01	93.252341	26.462590	50.531514	0.8829805E 08
6	127.09540	13.633176	10.266196	20.055011	50.527729	-0.6184507	289.53931
D 1	370022.88	401.76698	890.27828	55.608608	62.064084	71.000002	0.3732913
E 2	80987.238	79.411119	190.69325	59.813499	68.269659	38.000000	34.598362
P 3	1744.8504	0	0	50.380000	27658.672	1085.2409	58.726708
R 4	452754.97	481.17810	1080.9715	68.060999	63852.851	790.34962	32.726708
O 5	-93.765494	0.5674014E-01	0.1338362	2.2159070	3.0529715	71.240017	1247.0000
6	288.43999	-4.9185999	4.9185999	2.4013420	0.4352002	-3.6680000	
7	570.92978	694.25728	360.02112	4873.0301	0		
O 1	452754.01	0.1061975	825.49999	331.04511	0	0	0
P 2	839.17869	-0.6110547E-02	0.9800000	466.48006	349172.89	0	0
S 3	-48.285838		0.7300000		-119356.35	0	0

O*1	100.00000	82836.750	-0.1873564	28.294727	82732.088	-5864.0319	0.3732913
P 2	146378.68	0.2099271E 08	-0.2396710	-80.347588	370022.88	-359.07388	417.78825
I 3	1563.7081	3244.0965	35.805429	95.144146	37.106089	-278.35962	0.6380302E 08
4	10.266299	3284.4287	0.3316776	94.864855	36.575709	3.0529718	3.3321451
5	0.5384671	4392.0134	-0.5418506E-01	93.252341	26.462590	50.531514	0.8829805E 08
6	127.09540	13.633176	10.266196	20.055011	50.527729	-0.6184507	289.53931
D 1	370022.88	401.76698	890.27828	55.608608	62.064084	71.000002	0.3732913
E 2	80987.238	79.411119	190.69325	59.813499	68.269659	38.000000	34.598362
P 3	1744.8504	0	0	50.380000	27658.672	1085.2409	58.726708
R 4	452754.97	481.17810	1080.9715	68.060999	63852.851	790.34962	32.726708
O 5	-93.765494	0.5674014E-01	0.1338362	2.2159070	3.0529715	71.240017	1248.0000
6	288.43999	-4.9185999	4.9185999	2.4013420	0.4352002	-3.6680000	
7	570.92978	694.25728	360.02112	4873.0301	0		
O 1	452754.01	0.1061975	825.49999	331.04511	0	0	0
P 2	839.17869	-0.6110547E-02	0.9800000	466.48006	349172.89	0	0
S 3	-48.285838		0.7300000		-119356.35	0	0

O*1	110.00000	103822.50	0.6297035	28.287572	83163.939	-817.89899	0.1382768
P 2	130724.61	0.2101370E 08	-0.1067720	-80.254949	371546.97	-20.406121	240.41963
1 3	1567.2285	4108.7977	32.488655	95.288598	33.168719	1050.3627	0.7591387E 08
4	15.184375	4176.8026	0.3316776	95.115643	32.561096	3.4720770	4.1531726
5	0.6569918	5286.6202	-0.2329492E-01	93.642538	25.164263	81.007221	0.6461732E 08
6	153.55361	17.086986	15.184417	20.055011	80.400000	-9.8999945	290.13695
D 1	371546.97	401.07361	894.55809	55.075521	64.983003	61.500006	0.1382768
E 2	81415.376	78.544322	191.49406	59.775286	71.559996	36.500000	34.598362
P 3	1748.5635	0	0	50.380000	22851.902	1099.6938	58.661722
R 4	454710.91	479.61793	1086.0521	68.060999	53021.137	814.55772	32.661723
O 5	-72.547753	0.4390069E-01	0.1035511	2.2304088	3.4720776	78.201544	1339.0000
6	335.02486	-5.7782474	5.7782474	2.4380382	0.4346868	-4.2224985	
7	572.08279	694.63880	360.78038	4952.9670	0		
O 1	454703.82	0.1770984	820.49998	391.89264	0	0	0
P 2	1405.4716	0.2283887	1.0933333	488.04763	-341291.73	0	0
5 3	1812.5205		0.8100000		53099.321	0	0
O*1	112.00000	108378.50	0.6293370	28.285867	83275.170	-106.20795	0.1132131
P 2	127589.42	0.2101826E 08	-0.1072034	-80.233159	371784.33	-23.899064	211.99531
1 3	1567.9587	4300.7429	31.825298	95.312285	32.495080	924.48615	0.7784418E 08
4	16.341340	4369.2462	0.3316776	95.132676	31.924701	3.5657082	4.3100717
5	0.6835804	5483.6980	-0.1520386E-01	93.710711	24.918927	81.007221	0.5960296E 08
6	135.33801	17.836807	16.341397	20.055011	80.400000	-9.8999945	290.22416
D 1	371784.33	400.93377	895.43654	54.951464	65.569366	59.600001	0.1132131
E 2	81526.212	77.205817	192.82417	59.761785	72.229335	36.200000	34.598362
P 3	1748.9585	0	0	50.380000	21894.140	1102.5736	58.626786
R 4	455059.50	478.13958	1088.2607	68.060999	50846.828	819.42146	32.586786
O 5	-68.203983	0.4127215E-01	0.9735098E-01	2.2333777	3.5657074	79.617698	1381.0000
6	405.59999	-7.1157498	7.1157498	2.4975342	0.4339599	-5.0074999	
7	572.32082	695.23403	360.86115	4961.4921	0		
O 1	455052.86	0.1777559	819.29999	399.81576	0	0	0
P 2	1411.7725	0.2159064	1.1186667	491.06331	-295697.71	0	0
5 3	1714.7735		0.8300000		45350.604	0	0
O*1	112.00000	108378.50	0.6293370	28.285867	83275.170	-106.20795	0.1132131
P 2	127589.42	0.2101826E 08	-0.1072034	-80.233159	371784.33	-23.899064	211.99531
1 3	1567.9587	4300.7429	31.825298	95.312285	32.495080	924.48615	0.7784418E 08
4	16.341340	4369.2462	0.2713726	95.132676	31.924701	3.5657082	4.3100717
5	0.6835804	5483.6980	-0.1520386E-01	93.710711	24.918927	81.007221	0.5960296E 08
6	135.33801	17.836807	16.341397	20.055011	80.400000	-9.8999945	290.22416
D 1	371784.33	400.93377	895.43654	54.951464	65.569366	59.600001	0.1132131
E 2	81526.212	77.205817	192.82417	59.761785	72.229335	36.200000	34.598362
P 3	1748.9585	0	0	50.380000	21894.140	1102.5736	58.626786
R 4	455059.50	478.13958	1088.2607	68.060999	50846.828	819.42146	32.586786
O 5	-68.203983	0.4127215E-01	0.9735098E-01	2.2333777	3.5657074	79.617698	1382.0000
6	405.59999	-7.1157498	7.1157498	2.4975342	0.4339599	-5.0074999	
7	572.32082	695.23403	360.86115	4961.4921	0		
O 1	455052.86	0.1777559	819.29999	399.81576	0	0	0
P 2	1411.7725	0.2159064	1.1186667	491.06331	-295697.71	0	0
5 3	1714.7735		0.8300000		45350.604	0	0

O*1	120.00000	127904.75	0.8345654	28.278013	83407.472	2076.0753	0.5008224E-01
P 2	115033.21	0.2103779E 08	-0.1080218	-80.133874	372676.64	-26.517287	123.29157
1 3	1571.1934	5138.7155	29.654319	95.410323	30.112420	687.17193	0.8407769E 08
4	21.613785	5208.9130	0.2713726	95.205853	29.665610	3.9827958	4.9419070
5	0.8006616	6339.8630	0.2381848E-01	93.967766	23.994365	81.007221	0.4132525E 08
6	103.75298	21.050415	21.613858	20.055011	80.400000	-9.8999945	290.27877
D 1	372676.64	400.32746	899.30342	54.392137	68.129482	52.000007	0.5008224E-01
E 2	81657.522	76.378215	193.62590	59.694948	75.159080	35.000000	34.598362
P 3	1749.9499	0	0	50.380000	18077.570	1114.0498	58.449916
R 4	456084.11	476.70567	1092.9293	68.060999	42119.657	838.93031	32.249917
O 5	-49.123694	0.2972613E-01	0.7011673E-01	2.2464195	3.9827964	85.816302	1435.0000
6	436.99998	-7.9399997	7.9399997	2.5350932	0.4335965	-5.3999999	
7	573.37318	695.47523	361.06385	4982.9652	0		
O 1	456077.73	0.1832561	814.49998	416.80429	0	0	0
P 2	1458.7346	0.2035057	1.2199999	496.89214	-228889.20	0	0
5 3	1619.9242		0.9099999		23432.246	0	0
O*1	129.99999	155529.50	0.6078844	28.265548	83466.654	3591.8757	0.1743915E-01
P 2	99297.449	0.2106543E 08	-0.1089386	-79.979252	373841.88	-17.480006	59.541084
1 3	1576.2204	6368.1218	26.940593	95.541580	27.686688	243.82350	0.8912985E 08
4	29.826971	6439.9314	0.2713726	95.308942	27.351969	4.6415567	5.8198995
5	0.9740177	7587.9616	0.8993392E-01	94.262551	22.950859	81.007221	0.2467363E 08
6	36.770623	25.596864	29.826955	20.055011	80.400000	-9.8999945	290.12980
D 1	373841.88	399.47159	905.17761	53.732837	72.052947	42.500008	0.1743915E-01
E 2	81716.176	76.380358	193.63243	59.813499	79.666346	33.500001	34.598362
P 3	1750.4790	0	0	50.380000	13314.575	1128.3802	58.382560
R 4	457308.53	475.85194	1098.8100	68.060999	31162.472	863.43147	31.682561
O 5	-20.570796	0.1244797E-01	0.2936173E-01	2.2659374	4.6415563	95.352547	1477.0000
6	436.99999	-7.9399998	7.9399998	2.5351076	0.4335965	-5.3999999	
7	574.99973	695.52129	361.17204	4994.0682	0		
O 1	457302.87	0.1950672	796.49999	436.72728	0	0	0
P 2	1556.9234	0.1683508	1.3933332	503.42917	-68987.466	0	0
5 3	1343.6858		1.0699999		9726.4092	0	0
O*1	132.00000	161527.25	0.5142667	28.262651	83472.563	3768.5769	0.1403299E-01
P 2	96143.960	0.2107143E 08	-0.1092412	-79.943766	374075.25	-16.259134	52.087046
1 3	1577.2767	6642.5963	26.397846	95.569283	27.258000	181.74630	0.8986292E 08
4	31.712270	6714.6787	0.2713726	95.331303	26.941560	4.7981248	6.0681943
5	1.0127279	7865.7748	0.1058057	94.319118	22.754069	81.007221	0.2250557E 08
6	27.384243	26.583966	31.712221	20.055011	80.400000	-9.8999945	290.08723
D 1	374075.25	399.28114	906.42423	53.554498	72.872801	40.600002	0.1403299E-01
E 2	81722.030	76.380434	193.63241	59.820034	80.624950	33.200000	34.598370
P 3	1750.5335	0	0	50.380000	12363.057	1131.2461	58.345966
R 4	457547.81	475.66157	1100.0566	68.060998	28963.618	868.34584	31.445967
O 5	-14.422571	0.8727504E-02	0.2058606E-01	2.2701404	4.7981248	97.380700	1522.0000
6	436.99998	-7.9399997	7.9399997	2.5351049	0.4335965	-5.3999999	
7	575.34138	695.52384	361.18320	4995.2268	0		
O 1	457542.15	0.1976454	792.89999	432.51684	0	0	0
P 2	1578.3266	0.1655114	1.4280000	501.89474	-49719.153	0	0
5 3	1321.7146		1.1020000		8106.5056	0	0

0*1	132.00000	161527.25	0.5142667	28.262651	83472.563	3768.5769	0.1403299E-01
P 2	96143.960	0.2107143E 08	-0.1092412	-79.943766	374075.25	-16.259134	52.087046
1 3	1577.2767	6642.5963	26.397846	95.569283	27.258000	181.74630	0.8986292E 08
4	31.712270	6714.6787	0.2110676	95.331303	26.941560	4.7981248	6.0681943
5	1.0127279	7865.7748	0.1058057	94.319118	22.754069	81.007221	0.2250557E 08
6	27.384243	26.583966	31.712221	20.055011	80.400000	-9.8999945	290.08723
D 1	374075.25	399.28114	906.42423	53.554498	72.872801	40.600002	0.1403299E-01
E 2	81722.030	76.380434	193.63241	59.820034	80.624950	33.200000	34.598370
P 3	1750.5335	0	0	50.380000	12363.057	1131.2461	58.345966
R 4	457547.81	475.66157	1100.0566	68.060998	28963.618	868.34584	31.445967
0 5	-14.422571	0.8727504E-02	0.2058606E-01	2.2701404	4.7981248	97.380700	1523.0000
6	436.99998	-7.9399997	7.9399997	2.5351049	0.4335965	-5.3999999	
7	575.34138	695.52384	361.18320	4995.2268	0		
0 1	457542.15	0.1976454	792.89999	432.51684	0	0	0
P 2	1578.3266	0.1655114	1.4280000	501.89474	-49719.153	0	0
5 3	1321.7146		1.1020000		8106.5056	0	0
0*1	139.99999	187286.75	0.4559739	28.249502	83490.743	4293.5477	0.5455301E-02
P 2	83505.479	0.2109721E 08	-0.1111630	-79.784641	375225.34	-11.725822	29.919180
1 3	1582.7468	7856.4606	24.709307	95.685866	25.735468	90.113364	0.9217494E 08
4	40.167679	7929.4821	0.2110676	95.427241	25.481408	5.5445865	7.3762429
5	1.1827866	9091.5914	0.1795291	94.540448	22.038323	81.007221	0.1526615E 08
6	14.041896	30.823435	40.167442	20.055011	80.400000	-9.8999945	289.82277
D 1	375225.34	398.33584	912.83003	52.747653	76.962441	33.000008	0.5455301E-02
E 2	81739.975	76.379750	193.64279	59.894597	85.377053	32.000001	34.504475
P 3	1750.7694	0	0	50.380000	8561.2512	1142.9212	58.194544
R 4	458716.07	474.71559	1106.4728	68.073998	20139.411	888.03210	30.494545
0 5	-6.9650672	0.4120998E-02	0.9693052E-02	2.2916091	5.5445864	107.61306	1579.0000
6	436.99999	-7.9399998	7.9399998	2.5352634	0.4335965	-5.3999999	
7	577.06657	695.55748	361.23143	4998.1444	0		
0 1	458709.80	0.2109586	771.50000	441.94792	0	0	0
P 2	1688.9411	0.1701356	1.6133332	505.49361	-22034.850	0	0
5 3	1362.1093		1.2599999		3926.8229	0	0

BEGIN BOOSTER DECAY

0*1	141.87926	193784.50	0.4068391	28.246017	83489.146	4386.8190	0.4236529E-02
P 2	80528.882	0.2110371E 08	-0.1118575	-79.742957	375704.14	-10.308137	25.976219
1 3	1585.1061	8172.4529	24.312655	95.714700	25.419181	69.797919	0.9259921E 08
4	42.383048	8245.6636	0.2110676	95.451375	25.177662	5.7566136	7.7992455
5	1.2265490	9410.0952	0.1994283	94.591716	21.887357	81.007221	0.1378277E 08
6	10.960281	31.892827	42.382753	20.055011	80.400000	-9.8999945	289.69246
D 1	375704.14	397.93916	915.59789	52.413280	78.731556	31.214708	0.4236529E-02
E 2	81738.332	76.376708	193.63386	59.810581	87.334471	31.718112	34.469185
P 3	1750.8143	0	0	50.380000	7669.5076	1145.8246	58.083007
R 4	459193.29	474.31587	1109.2318	68.078885	18057.486	892.63190	30.815237
0 5	0	0	0	2.3008489	5.7566133	111.82030	1627.0000
6	436.99999	-7.9399998	7.9399998	2.5352475	0.4335965	-5.3999999	
7	577.79671	695.52660	361.24060	4998.5590	0		
0 1	459186.84	0.2144120	765.48636	444.13515	0	0	0
P 2	1718.3749	0.1714184	1.6634468	506.22935	-15863.483	0	0
5 3	1373.8065		1.3013436		3444.9427	0	0

O*1	141.87926	193784.50	0.4068391	28.246017	377454.95	4386.8190	0.4236529E-02
P 2	80528.882	0.2110371E 08	-0.1118575	-79.742957	81738.301	-10.308137	25.976219
1 3	1585.1060	8172.4529	24.312655	95.714700	25.419181	69.797919	0.9259921E 08
4	42.383048	8245.6636	0	95.451375	25.177662	5.7563255	7.7992455
5	1.2265490	9410.0952	0.1994283	94.591716	21.887357	81.007221	0.1378277E 08
6	10.960281	31.892827	42.382753	20.055011	80.400000	-9.8999945	289.69246
D 1	375704.14	397.93916	915.59789	52.412944	78.728235	31.214708	0.4236529E-02
E 2	81738.301	76.376691	193.63378	59.809906	99.300896	31.718112	34.469185
P 3	1750.8142	0	0	50.380000	7669.5076	1145.8246	58.083007
R 4	459193.25	474.31585	1109.2317	68.078885	18057.486	892.63190	30.815237
O 5	0	0	0	2.3008489	5.7563259	137.13160	1629.0000
6	436.99999	-7.9399998	7.9399998	2.5352470	0.4335965	-5.3999999	
7	577.79671	695.52633	361.24059	4998.5590	0		
D 1	459163.64	0.2144120	765.48636	444.13515	0	0	0
P 2	1718.2885	0.1714186	1.6634468	506.22935	-15863.483	0	0
5 3	1373.7389		1.3013436		3444.9427	0	0

END BOOSTER DECAY

O*1	143.66000	200022.00	0.7447207	28.242609	1749.6677	4499.4861	0.3296921E-02
P 2	79721.291	0.2110995E 08	-0.1095624	-79.702397	81234.123	-8.0839808	21.205621
1 3	269.97408	8233.4742	24.312655	95.745293	25.119306	99.041218	0.9294685E 08
4	44.538830	8306.8647	0	95.478019	24.882207	1.0973489	7.9880532
5	1.2689589	9473.9805	0.2190349	94.621459	21.649071	81.007221	0.1133504E 08
6	15.962216	32.919387	44.538476	20.055011	80.400000	-9.8999945	307.37687
D 1	0	0	0	46.837747	25.146922	30.560654	0.3296921E-02
E 2	81234.123	76.095363	192.32026	48.733476	41.589726	31.451000	34.435753
P 3	1749.6677	0	0	50.380000	7435.0162	1146.5996	57.977102
R 4	82983.790	76.095363	192.32026	68.083514	17487.162	893.90269	31.118902
O 5	0	0	0	0	1.0973490	15.131007	1854.0000
6	436.99999	-7.9399998	7.9399998	2.5273584	0.4335965	-5.3999999	
7	0.1670513E-01	691.22352	361.00615	4998.8785	0		
O 1	82982.587	0.2212744	759.78798	440.32893	0	0	0
P 2	320.47763	0.2100168	1.7109333	506.47728	-26310.773	0	0
5 3	304.17278		1.3405200		2946.1647	0	0

O*1	143.66000	200022.00	0.7447207	28.242609	1749.6677	4499.4861	0.3296921E-02
P 2	79721.291	0.2110995E 08	-0.1095624	-79.702397	81234.123	-8.0839808	21.205621
1 3	269.97408	8233.4742	24.312655	95.745293	25.119306	99.041218	0.9294685E 08
4	44.538830	8306.8647	0	95.478019	24.882207	1.0973489	7.9880532
5	1.2689589	9473.9805	0.2190349	94.621459	21.649071	81.007221	0.1133504E 08
6	15.962216	32.919387	44.538476	20.055011	80.400000	-9.8999945	307.37687
D 1	0	0	0	46.837747	25.146922	30.560654	0.3296921E-02
E 2	81234.123	76.095363	192.32026	48.733476	41.589726	31.451000	34.435753
P 3	1749.6677	0	0	50.380000	7435.0162	1146.5996	57.977102
R 4	82983.790	76.095363	192.32026	68.083514	17487.162	893.90269	31.118902
O 5	0	0	0	0	1.0973490	15.131007	1855.0000
6	436.99999	-7.9399998	7.9399998	2.5273584	0.4335965	-5.3999999	
7	0.1670513E-01	691.22352	361.00615	4998.8785	0		
O 1	82982.587	0.2212744	759.78798	440.32893	0	0	0
P 2	320.47763	0.2100168	1.7109333	506.47728	-26310.773	0	0
5 3	304.17278		1.3405200		2946.1647	0	0

O*1	145.06000	204900.75	1.0088991	28.239901	1749.6942	4576.8705	0.2693984E-02
P 2	79343.336	0.2111483E 08	-0.1075611	-79.670302	81231.550	-6.5914937	17.928368
I 3	269.96255	8264.4025	24.312655	95.769596	24.885732	111.33262	0.9317436E 08
4	46.244815	8337.9316	0	95.499256	24.651568	1.1035186	8.1253605
5	1.3024867	9507.1560	0.2347615	94.643554	21.456987	81.007221	9619093.2
6	18.190376	33.722326	46.244410	20.055011	80.400000	-9.8999945	307.38057
D 1	0	0	0	46.749217	25.430462	30.560654	0.2693984E-02
E 2	81231.550	76.092633	192.31146	48.652231	41.878788	31.241000	34.409454
P 3	1749.6942	0	0	50.380000	7328.4847	1146.9602	57.893705
R 4	82981.243	76.092633	192.31146	68.087155	17217.920	894.50337	31.357505
O 5	0	0	0	0	1.1035186	15.797164	1889.0000
6	436.99999	-7.9399998	7.9399998	2.5273335	0.4335965	-5.3999999	
7	0.1670513E-01	691.19325	361.01159	4999.0836	0		
O 1	82979.979	0.2232386	755.30799	437.15736	0	0	0
P 2	323.31220	0.2188126	1.7482666	506.63033	-30934.578	0	0
5 3	316.90215		1.3713200		2582.9734	0	0

O*1	145.06000	204900.75	1.0088991	28.239901	1749.7051	-398.28766	0.2693984E-02
P 2	71987.775	0.2111483E 08	-0.1075611	-79.670302	81236.175	-4.5431647	17.928368
I 3	268.63277	8264.4025	24.312655	95.769596	24.885732	100.92751	0.9317436E 08
4	46.244815	8337.9316	0	95.499256	24.651568	1.1472364	8.1253605
5	1.3024867	9507.1560	0.2347615	94.643554	21.456987	81.007221	9619093.2
6	18.190376	33.722326	46.244410	20.055011	80.400000	-9.8999945	308.91942
D 1	0	0	0	0	0	0	0.2693984E-02
E 2	81236.175	76.095197	192.32348	48.753485	42.419498	31.241000	34.409454
P 3	1749.7051	0	0	50.380000	7328.4847	1146.9602	57.893705
R 4	82985.880	76.095197	192.32348	68.087155	17217.920	894.50337	31.357505
O 5	0	0	0	0	1.1472363	16.940733	1892.0000
6	436.99999	-7.9399998	7.9399998	2.5274062	0.4335965	-5.3999999	
7	0.1670513E-01	691.23260	361.01381	0	0		
O 1	82985.286	0.1051755	689.46999	379.35316	0	0	0
P 2	152.33286	0.1865798	0.9251800	381.32268	-27077.188	0	0
5 3	270.23683		1.3753000		2822.1667	0	0

O*1	149.96000	221792.50	1.9141677	28.230213	1749.7874	-214.94059	0.1281268E-02
P 2	70671.572	0.2113173E 08	-0.9843878E-01	-79.556559	81226.141	-1.9861772	9.6752533
I 3	268.59295	8383.2032	24.312655	95.857449	24.088884	102.34720	0.9372681E 08
4	52.291647	8457.1969	0	95.576365	23.864960	1.1710559	8.6552763
5	1.4210998	9633.4974	0.2921421	94.723979	20.804523	81.007221	5265308.6
6	18.544494	36.502351	52.291050	20.055011	80.400000	-9.8999945	308.92816
D 1	0	0	0	0	0	0	0.1281268E-02
E 2	81226.141	76.085722	192.29313	48.471570	43.449690	30.506000	34.317448
P 3	1749.7874	0	0	50.380000	6955.6415	1148.2220	57.601118
R 4	82975.928	76.085722	192.29313	68.099895	16275.609	896.61456	32.191917
O 5	0	0	0	0	1.1710559	19.310499	1926.0000
6	436.99999	-7.9399998	7.9399998	2.5273221	0.4335965	-5.3999999	
7	0.1670513E-01	691.12762	361.03064	0	0		
O 1	82975.302	0.1047757	687.01999	364.41623	0	0	0
P 2	151.73554	0.1932037	0.9398800	381.29531	-30739.068	0	0
5 3	279.79712		1.3998000		1671.2987	0	0

0*1	149.96000	221792.50	0.9377259	28.230213	1749.7874	-214.94059	0.1281268E-02
P 2	70671.572	0.2113173E 08	0.1049550	-79.556559	81226.141	7.9803038	9.6752533
1 3	268.59295	8383.2032	23.336219	95.857449	24.088884	50.780005	0.9372681E 08
4	52.291647	8457.1969	1.2470491	95.576365	23.864960	1.1710572	8.6552763
5	1.4210998	9633.4974	0.2921421	94.723979	20.804523	81.007221	5265308.6
6	9.1293664	36.502351	52.291050	20.274927	80.400000	-9.8999945	308.92816
D 1	0	0	0	0	0	0	0.1281268E-02
E 2	81226.141	76.085722	192.29313	48.471573	43.449707	30.506000	34.317448
P 3	1749.7874	0	0	50.380000	6955.6415	1148.2220	57.601118
R 4	82975.928	76.085722	192.29313	68.099895	16275.609	896.61456	32.191917
O 5	0	0	0	0	1.1710572	19.310533	1928.0000
6	436.99999	-7.9399998	7.9399998	2.5273221	0.4335965	-5.3999999	
7	0.1670513E-01	691.12762	361.03064	0	0		
0 1	82975.397	0.1087833	687.01999	379.35987	0	0	0
P 2	157.53944	0.1703244	0.9398800	381.31486	-13344.460	0	0
5 3	246.66353		1.3998000		4718.1420	0	0
0*1	149.99999	221929.25	0.9946426	28.230132	1749.7880	-213.81515	0.1273198E-02
P 2	70660.830	0.2113187E 08	0.1318016	-79.555621	81226.053	9.1960893	9.6245931
1 3	268.59262	8384.1971	23.385709	95.858124	24.082330	53.442575	0.9373008E 08
4	52.341494	8458.1945	1.2361742	95.576953	23.858488	1.1712499	8.6599023
5	1.4220762	9634.5525	0.2926301	94.724602	20.799148	81.007221	5238356.9
6	9.6566788	36.524857	52.340895	20.303908	80.400000	-9.8999945	308.92821
D 1	0	0	0	0	0	0	0.1273198E-02
E 2	81226.053	76.085645	192.29288	48.469260	43.458073	30.500001	34.316692
P 3	1749.7880	0	0	50.380000	6952.5984	1148.2323	57.598725
R 4	82975.840	76.085645	192.29288	68.099999	16267.919	896.63186	32.198725
O 5	0	0	0	0	1.1712498	19.329792	1940.0000
6	436.99999	-7.9399998	7.9399998	2.5273215	0.4335965	-5.3999999	
7	0.1670513E-01	691.12676	361.03077	0	0		
0 1	82975.305	0.1092642	686.99999	379.48794	0	0	0
P 2	158.23569	0.1714225	0.9400000	381.39540	-14167.644	0	0
5 3	248.25346		1.4000000		5076.9587	0	0
0*1	159.96000	255488.25	5.0779343	28.209517	1749.9039	-50.470067	0.2252039E-03
P 2	67986.195	0.2116545E 08	1.2990901	-79.317452	81193.173	15.146750	2.2718403
1 3	268.48217	8641.9751	25.798372	95.969178	22.634534	69.795513	0.9417438E 08
4	65.006801	8716.7781	-0.3937769	95.667006	22.429673	1.2192477	10.003931
5	1.6694172	9905.8162	0.4138775	94.830535	19.618159	81.007221	1274291.6
6	11.903976	42.047958	65.005762	21.591674	80.400000	-9.8999945	308.93327
D 1	0	0	0	0	0	0	0.2252039E-03
E 2	81193.173	76.061161	192.20691	47.688020	43.940578	29.006000	34.129669
P 3	1749.9039	0	0	50.380000	6194.9068	1150.8718	56.802973
R 4	82943.076	76.061161	192.20691	68.125895	14353.108	900.93486	32.299374
O 5	0	0	0	0	1.2192477	20.737648	1987.0000
6	436.99999	-7.9399998	7.9399998	2.5270047	0.4335965	-5.3999999	
7	0.1670513E-01	690.83247	361.05446	0	0		
0 1	82942.483	0.1111673	676.24318	388.97746	0	0	0
P 2	160.92810	0.1829775	0.9798400	384.89727	-19514.840	0	0
5 3	264.88273		1.4756960		4947.9620	0	0

O*1	159.96000	255488.25	5.0319546	28.209517	1749.9039	-50.470066	0.2252039E-03
P 2	67986.195	0.2116545E 08	1.3194320	-79.317452	81193.173	15.377543	2.2718402
I 3	268.48217	8641.9751	25.752568	95.969178	22.634534	69.019829	0.9417438E 08
4	65.006801	8716.7780	-0.2170110	95.667006	22.429673	1.2192477	10.003931
5	1.6694172	9905.8162	0.4138775	94.830535	19.618159	81.007221	1274291.6
6	11.814363	42.047958	65.005762	21.613437	80.400000	-9.8999945	308.93327
D 1	0	0	0	0	0	0	0.2252039E-03
E 2	81193.173	76.061161	192.20691	47.688020	43.940578	29.006000	34.129669
P 3	1749.9039	0	0	50.380000	6194.9068	1150.8718	56.802973
R 4	82943.076	76.061161	192.20691	68.125895	14353.108	900.93486	32.299374
O 5	0	0	0	0	1.2192477	20.737648	1988.0000
6	436.99999	-7.9399998	7.9399998	2.5270047	0.4335965	-5.3999999	
7	0.1670513E-01	690.83247	361.05446	0	0		
O 1	82942.484	0.1112527	676.24318	388.25328	0	0	0
P 2	161.05185	0.1827547	0.9798400	384.95829	-19341.995	0	0
S 3	264.56012		1.4756960		5014.2643	0	0
O*1	159.99999	255621.25	5.0298378	28.209431	1749.9043	-50.146088	0.2234756E-03
P 2	67975.457	0.2116558E 08	1.3170945	-79.316477	81193.036	15.252473	2.2572568
I 3	268.48173	8643.0554	25.743894	95.969642	22.628936	68.541359	0.9417517E 08
4	65.058672	8717.8613	-0.2166517	95.667385	22.424149	1.2194431	10.010255
5	1.6704274	9906.9476	0.4143712	94.830976	19.613595	81.007221	1266269.0
6	11.732579	42.069847	65.057631	21.611071	80.400000	-9.8999945	308.93328
D 1	0	0	0	0	0	0	0.2234756E-03
E 2	81193.036	76.061063	192.20657	47.684862	43.942515	29.000001	34.128922
P 3	1749.9043	0	0	50.380000	6191.8647	1150.8827	56.799776
R 4	82942.940	76.061063	192.20657	68.125998	14345.421	900.95213	32.299776
O 5	0	0	0	0	1.2194431	20.743291	2000.0000
6	436.99999	-7.9399998	7.9399998	2.5270034	0.4335965	-5.3999999	
7	0.1670513E-01	690.83128	361.05455	0	0		
O 1	82942.350	0.1112088	676.20000	388.21994	0	0	0
P 2	160.98796	0.1825984	0.9800000	384.95128	-19206.961	0	0
S 3	264.33345		1.4759999		4973.8473	0	0
O*1	169.99999	288400.00	4.9312296	28.187522	1749.9847	-7.6761953	0.3036552E-04
P 2	65291.343	0.2119838E 08	1.0405019	-79.067693	81149.132	1.8594637	0.3455333
I 3	268.34113	8924.9739	24.026501	96.096657	21.251595	10.240501	0.9426720E 08
4	78.293311	9000.5022	-0.1268268	95.773297	21.064726	1.2695547	10.624887
5	1.9274075	10201.154	0.5365364	94.951149	18.488795	81.007221	200120.56
6	1.7410565	47.464535	78.291817	21.341142	80.400000	-9.8999945	308.93183
D 1	0	0	0	0	0	0	0.3036552E-04
E 2	81149.132	76.031240	192.09579	46.692647	44.333764	27.500001	33.941143
P 3	1749.9847	0	0	50.380000	5431.4031	1153.6532	55.799970
R 4	82899.116	76.031240	192.09579	68.151999	12423.909	905.26632	32.299969
O 5	0	0	0	0	1.2695547	21.958819	2046.0000
6	436.99999	-7.9399998	7.9399998	2.5265375	0.4335965	-5.3999999	
7	0.1670513E-01	690.45503	361.07098	0	0		
O 1	82898.610	0.1076827	665.39999	386.66686	0	0	0
P 2	155.80128	0.1661898	1.0200000	384.12150	-2772.9939	0	0
S 3	240.45304		1.5519999		604.40023	0	0

0*1	171.72000	293947.25	4.9989934	28.183620	1749.9925	-5.5332985	0.2164278E-04
P 2	64829.822	0.2120393E 08	1.0544031	-79.023890	81139.158	1.3575226	0.2490738
1 3	268.30944	8975.8356	23.821645	96.119612	21.021062	7.5062259	0.9427177E 08
4	80.624016	9051.4811	-0.1113769	95.792627	20.837168	1.2784719	10.685067
5	1.9725140	10254.020	0.5578567	94.972841	18.300278	81.007221	145071.70
6	1.2722395	48.377495	80.622444	21.359342	80.400000	-9.8999945	308.93118
D 1	0	0	0	0	0	0	0.2164278E-04
E 2	81139.158	76.024791	192.07055	46.469842	44.402901	27.242000	33.908848
P 3	1749.9925	0	0	50.380000	5300.6346	1154.1393	55.576378
R 4	82889.150	76.024791	192.07055	68.156470	12093.525	906.00820	32.299978
O 5	0	0	0	0	1.2784719	22.171682	2074.0000
6	436.99999	-7.9399998	7.9399998	2.5264199	0.4335965	-5.3999999	
7	0.1670513E-01	690.37006	361.07258	0	0		
D 1	82888.643	0.1078270	663.54239	387.73414	0	0	0
P 2	155.99129	0.1660334	1.0268800	384.16321	-2011.6221	0	0
S 3	240.19780		1.5650720		437.92041	0	0

0*1	171.72000	293947.25	5.4571823	28.183620	1749.9981	-5.5332986	0.2164278E-04
P 2	63604.822	0.2120393E 08	1.6722167	-79.023890	81141.530	2.1273192	0.2490738
1 3	268.31692	8975.8356	24.284797	96.119612	21.021062	8.3648424	0.9427177E 08
4	80.624016	9051.4812	-0.1875684	95.792627	20.837167	1.3031321	10.685067
5	1.9725140	10254.020	0.5578567	94.972841	18.300278	81.007221	145071.71
6	1.4208887	48.377495	80.622444	22.008304	80.400000	-9.8999945	308.93143
D 1	0	0	0	0	0	0	0.2164278E-04
E 2	81141.530	76.026107	192.07671	46.521795	44.696724	27.242000	33.908848
P 3	1749.9981	0	0	50.380000	5300.6346	1154.1393	55.576378
R 4	82891.528	76.026107	192.07671	68.156470	12093.525	906.00820	32.299978
O 5	0	0	0	0	1.3031320	22.792469	2077.0000
6	436.99999	-7.9399998	7.9399998	2.5264573	0.4335965	-5.3999999	
7	0.1670513E-01	690.39024	361.07372	0	0		
D 1	82891.019	0.1080930	663.54239	394.95061	0	0	0
P 2	156.38067	0.1662557	1.0268800	386.01665	-2188.0710	0	0
S 3	240.52630		1.5650720		649.04272	0	0

0*1	179.99999	320309.75	5.5775167	28.164272	1750.0353	-1.1135236	0.4717097E-05
P 2	61383.791	0.2123032E 08	0.9365026	-78.808665	81093.434	0.2442007	0.5012373E-01
1 3	268.16425	9237.0756	23.132205	96.225278	19.961176	1.7297105	0.9428112E 08
4	92.078423	9313.2421	-0.1045595	95.880940	19.791080	1.3495718	10.267247
5	2.1935618	10524.329	0.6609394	95.073740	17.435264	81.007221	30038.573
6	0.2834305	52.716205	92.076468	21.260047	80.400000	-9.8999945	308.92809
D 1	0	0	0	0	0	0	0.4717097E-05
E 2	81093.434	75.995037	191.95511	45.448225	45.060406	26.000001	33.753365
P 3	1750.0353	0	0	50.380000	4671.2674	1156.5539	54.499995
R 4	82843.469	75.995037	191.95511	68.177999	10503.634	909.57455	32.299995
O 5	0	0	0	0	1.3495718	23.881809	2102.0000
6	436.99999	-7.9399998	7.9399998	2.5258901	0.4335965	-5.3999999	
7	0.1670513E-01	689.98077	361.08131	0	0		
D 1	82842.949	0.1091721	653.09999	396.84588	0	0	0
P 2	157.85017	0.1680433	1.0640000	383.80950	-431.44128	0	0
S 3	242.97157		1.6339999		77.565064	0	0

O*1	183.96000	332727.25	5.7792558	28.154663	1750.0441	-0.5635106	0.2500467E-05
P 2	60322.027	0.2124274E 08	0.9358240	-78.703108	81066.678	0.1234966	0.2536565E-01
1 3	268.07943	9368.0530	22.745321	96.281992	19.474404	0.9151411	0.9428246E 08
4	97.697765	9444.4507	-0.9396356E-01	95.929336	19.310596	1.3728920	10.031876
5	2.3016318	10659.369	0.7111145	95.127479	17.037537	81.007221	15415.504
6	0.1484784	54.759862	97.695623	21.266625	80.400000	-9.8999945	308.92606
O 1	0	0	0	0	0	0	0.2500467E-05
E 2	81066.678	75.978102	191.88723	44.852823	45.242815	25.406000	33.678997
P 3	1750.0441	0	0	50.380000	4370.3602	1157.7754	53.905997
R 4	82816.722	75.978102	191.88723	68.188295	9743.6249	911.27843	32.299997
O 5	0	0	0	0	1.3728920	24.420465	2138.0000
6	436.99999	-7.9399998	7.9399998	2.5255596	0.4335965	-5.3999999	
7	0.1670513E-01	689.75310	361.08312	0	0		
O 1	82816.193	0.1099969	647.63519	400.02328	0	0	0
P 2	158.99140	0.1696957	1.0830080	383.80747	-220.62623	0	0
5 3	245.28153		1.6688480		38.555439	0	0
O*1	183.96000	332727.25	5.7792558	28.154663	1750.0444	-0.5635106	0.2500467E-05
P 2	60248.027	0.2124274E 08	0.9358240	-78.703108	81066.832	0.1234966	0.2536565E-01
1 3	268.07991	9368.0530	22.745321	96.281992	19.474404	0.9151411	0.9428246E 08
4	97.697765	9444.4507	-0.9396356E-01	95.929336	19.310596	1.3745808	10.031876
5	2.3016318	10659.369	0.7111145	95.127479	17.037537	81.007221	15415.504
6	0.1484784	54.759862	97.695623	21.266625	80.400000	-9.8999945	308.92607
O 1	0	0	0	0	0	0	0.2500467E-05
E 2	81066.832	75.978188	191.88763	44.856202	45.262587	25.406000	33.678997
P 3	1750.0444	0	0	50.380000	4370.3602	1157.7754	53.905997
R 4	82816.876	75.978188	191.88763	68.188295	9743.6249	911.27843	32.299997
O 5	0	0	0	0	1.3745808	24.462218	2141.0000
6	436.99999	-7.9399998	7.9399998	2.5255620	0.4335965	-5.3999999	
7	0.1670513E-01	689.75441	361.08319	0	0		
O 1	82816.348	0.1099969	647.63519	400.02328	0	0	0
P 2	158.99170	0.1696957	1.0830080	383.80747	-220.62623	0	0
5 3	245.28198		1.6688480		38.555439	0	0
O*1	189.99999	351443.00	6.0454653	28.139540	1750.0576	-0.2177465	0.1043130E-05
P 2	58629.217	0.2126147E 08	1.0455839	-78.538732	81025.890	0.5299308E-01	0.9801558E-02
1 3	267.95013	9575.8160	22.139122	96.367897	18.760216	0.3749056	0.9428340E 08
4	106.45025	9652.5427	-0.1140688	96.002604	18.605598	1.4118419	9.6549072
5	2.4694904	10872.997	0.7889973	95.209130	16.453644	81.007221	6087.9615
6	0.6012180E-01	57.840079	106.44782	21.393719	80.400000	-9.8999945	308.92295
O 1	0	0	0	0	0	0	0.1043130E-05
E 2	81025.890	75.952286	191.78375	43.945216	45.554422	24.500001	33.565586
P 3	1750.0576	0	0	50.380000	3911.5305	1159.7076	53.000000
R 4	82775.946	75.952286	191.78375	68.203999	8584.9379	913.87397	32.299998
O 5	0	0	0	0	1.4118418	25.312187	2166.0000
6	436.99998	-7.9399997	7.9399997	2.5250557	0.4335965	-5.3999999	
7	0.1670513E-01	689.40603	361.08588	0	0		
O 1	82775.403	0.1112690	639.30000	404.55706	0	0	0
P 2	160.75096	0.1723806	1.1119999	384.13675	-85.698168	0	0
5 3	249.03952		1.7219999		15.830154	0	0

O*1	196.49000	371268.75	6.0138624	28.122641	1750.0779	-0.7545220E-01	0.5187425E-06
P 2	56890.644	0.2128132E 08	0.9179036	-78.357434	80984.568	0.1623956E-01	0.3396376E-02
1 3	267.81911	9809.7651	21.197631	96.461128	18.026230	0.1288981	0.9428377E 08
4	116.10658	9886.8177	-0.1845008	96.082316	17.880978	1.4542639	8.0593816
5	2.6540487	11112.853	0.8741577	95.297943	15.852757	81.007221	2160.7643
6	0.2065845E-01	61.102978	116.10384	21.278160	80.400000	-9.8999945	308.91986
D 1	0	0	0	0	0	0	0.5187425E-06
E 2	80984.568	75.925937	191.67908	43.024888	45.886248	23.526500	33.443718
P 3	1750.0779	0	0	50.380000	3418.6851	1161.9297	52.091399
R 4	82734.646	75.925937	191.67908	68.220873	7340.5993	916.67464	32.299999
O 5	0	0	0	0	1.4542639	26.263580	2203.0000
6	436.99998	-7.9399997	7.9399997	2.5245534	0.4335965	-5.3999999	
7	0.1670513E-01	689.05444	361.09004	0	0		
O 1	82734.086	0.1126112	630.34379	403.82230	0	0	0
P 2	162.60883	0.1752839	1.1431520	383.75370	-28.398346	0	0
5 3	253.10758		1.7791120		4.8043609	0	0
O*1	196.49000	371268.75	6.1073989	28.122641	1750.0887	-0.7545220E-01	0.5187425E-06
P 2	54885.644	0.2128132E 08	0.9395306	-78.357434	80989.137	0.1659706E-01	0.3396376E-02
1 3	267.83352	9809.7651	21.291260	96.461128	18.026230	0.1319033	0.9428377E 08
4	116.10658	9886.8177	-0.1143397	96.082316	17.880978	1.5074723	8.0593816
5	2.6540487	11112.853	0.8741577	95.297943	15.852757	81.007221	2160.7643
6	0.2098338E-01	61.102978	116.10384	21.300278	80.400000	-9.8999945	308.92035
D 1	0	0	0	0	0	0	0.5187425E-06
E 2	80989.137	75.928469	191.69095	43.124900	46.497859	23.526500	33.443718
P 3	1750.0887	0	0	50.380000	3418.6851	1161.9297	52.091399
R 4	82739.225	75.928469	191.69095	68.220873	7340.5993	916.67464	32.299999
O 5	0	0	0	0	1.5074722	27.554563	2206.0000
6	436.99998	-7.9399997	7.9399997	2.5246255	0.4335965	-5.3999999	
7	0.1670513E-01	689.09331	361.09225	0	0		
O 1	82738.664	0.1126113	630.34379	405.99702	0	0	0
P 2	162.61798	0.1752843	1.1431520	383.81859	-28.792240	0	0
5 3	253.12226		1.7791120		4.8914393	0	0
O*1	199.99999	381878.50	6.1664414	28.113205	1750.0995	-0.4961549E-01	0.3913642E-06
P 2	53945.674	0.2129194E 08	0.9061711	-78.257277	80966.666	0.1055120E-01	0.2233373E-02
1 3	267.76228	9947.1448	20.874284	96.513433	17.647196	0.8799426E-01	0.9428386E 08
4	121.44250	10024.361	-0.1232002	96.127316	17.506851	1.5333230	7.5241905
5	2.7557535	11253.236	0.9209298	95.348135	15.543490	81.007221	1440.6316
6	0.1391761E-01	62.849118	121.43958	21.273994	80.400000	-9.8999945	308.91866
D 1	0	0	0	0	0	0	0.3913642E-06
E 2	80966.666	75.914152	191.63403	42.624504	46.700238	23.000001	33.377808
P 3	1750.0995	0	0	50.380000	3152.2017	1163.2179	51.600000
R 4	82716.765	75.914152	191.63403	68.229999	6667.8649	918.24320	32.299999
O 5	0	0	0	0	1.5333230	28.117105	2222.0000
6	436.99998	-7.9399997	7.9399997	2.5243518	0.4335965	-5.3999999	
7	0.1670513E-01	688.90211	361.09444	0	0		
O 1	82716.196	0.1133251	625.50000	407.36976	0	0	0
P 2	163.60419	0.1768422	1.1599999	383.71851	-18.668248	0	0
5 3	255.30260		1.8099999		3.0770440	0	0

0*1	209.99999	411737.25	6.1251504	28.085092	1750.1275	-0.2052358E-01	0.2131879E-06
P 2	51269.078	0.2132182E 08	0.8743115	-77.963299	80901.594	0.4221280E-02	0.9238404E-03
1 3	267.55598	10358.878	19.522741	96.667636	16.621532	0.3603481E-01	0.9428401E 08
4	137.10957	10436.519	-0.1466710	96.260781	16.494331	1.6121042	6.5567246
5	3.0532554	11672.944	1.0575911	95.496182	14.705274	81.007221	620.42271
6	0.5715154E-02	67.763236	137.10616	21.263946	80.400000	-9.8999945	308.91375
D 1	0	0	0	0	0	0	0.2131879E-06
E 2	80901.594	75.872774	191.46910	41.175731	47.263741	21.500001	33.190029
P 3	1750.1275	0	0	50.380000	2393.2661	1167.3432	50.200000
R 4	82651.721	75.872774	191.46910	68.255999	4752.3450	923.55154	32.299999
0 5	0	0	0	0	1.6121042	29.691376	2270.0000
6	436.99998	-7.9399997	7.9399997	2.5235548	0.4335965	-5.3999999	
7	0.1670513E-01	688.34845	361.10019	0	0		
0 1	82651.119	0.1164260	605.70000	406.40974	0	0	0
P 2	167.94875	0.1820157	1.2319999	383.62293	-6.9638214	0	0
5 3	262.56475		1.9259999		1.1550139	0	0
0*1	219.99999	441102.75	5.8052907	28.055032	1750.2121	-0.1110942E-01	0.1373659E-06
P 2	48594.156	0.2135122E 08	0.8640732	-77.655950	80432.083	0.2260061E-02	0.5000750E-03
1 3	267.42506	10801.908	17.949611	96.827682	15.665887	0.1814379E-01	0.9428408E 08
4	153.49802	10879.923	-0.1675175	96.400215	15.550702	1.6911839	6.0096308
5	3.3627704	12123.217	1.1995772	95.650148	13.921779	81.007221	350.10317
6	0.2934629E-02	72.596176	153.49410	21.277319	80.400000	-9.8999945	307.30963
D 1	0	0	0	0	0	0	0.1373659E-06
E 2	80432.083	83.646213	183.56474	40.250416	47.559832	20.000001	33.002254
P 3	1750.2121	0	0	50.380000	1609.9981	1172.6462	49.400000
R 4	82182.295	83.646213	183.56474	68.281999	2862.8318	930.92700	32.199999
0 5	0	0	0	0	1.6911839	30.700494	2289.0000
6	8.6523916	-0.1384383	0.1384383	2.1945374	0.4384897	-0.1153652	
7	0.1670513E-01	684.35364	361.11747	0	0		
0 1	82181.665	0.1193324	585.90001	400.43332	0	0	0
P 2	171.16349	0.1868708	1.3039999	383.59221	-3.2473018	0	0
5 3	268.03737		2.0419999		0.5749956	0	0
0*1	229.99999	470029.00	5.2447738	28.022850	1750.3298	-0.7022040E-02	0.9741856E-07
P 2	45920.311	0.2138018E 08	0.7856002	-77.334395	80833.339	0.1307817E-02	0.3160874E-03
1 3	267.33851	11280.697	16.181139	96.994871	14.769499	0.1010562E-01	0.9428413E 08
4	170.65374	11359.044	-0.1857396	96.546919	14.665338	1.7983982	5.6735187
5	3.6850622	12608.633	1.3471408	95.811407	13.184169	81.007221	231.03834
6	0.1676097E-02	77.356824	170.64930	21.221523	80.400000	-9.8999945	308.91048
D 1	0	0	0	0	0	0	0.9741856E-07
E 2	80833.339	75.824331	191.30008	39.633230	47.272853	18.500001	32.814476
P 3	1750.3298	0	0	50.380000	843.02725	1179.9930	49.000000
R 4	82583.668	75.824331	191.30008	68.307999	958.09844	950.10765	32.099999
0 5	0	0	0	0	1.7983982	30.479685	2321.0000
6	436.99999	-7.9399998	7.9399998	2.5229379	0.4335965	-5.3999999	
7	0.1670513E-01	687.76771	361.14156	0	0		
0 1	82583.010	0.1219210	561.60001	391.60518	0	0	0
P 2	175.73061	0.1902822	1.3839999	383.35680	-1.6434643	0	0
5 3	274.26343		2.1599999		0.3075481	0	0

BEGIN SUSTAINER AND VERNIER SOFT SHUT-DOWN

O*1	231.97000	475680.00	5.1092315	28.016242	1750.3538	-0.6499937E-02	0.9177719E-07
P 2	45393.667	0.2138584E 08	0.7545784	-77.269289	80828.319	0.1166402E-02	0.2925857E-03
1 3	267.32246	11379.525	15.811982	97.029104	14.598986	0.9057020E-02	0.9428413E 08
4	174.12856	11457.933	-0.1890199	96.577128	14.496888	1.8191525	5.6237873
5	3.7501380	12708.702	1.3769484	95.844449	13.043493	81.007221	215.72197
6	0.1510933E-02	78.286860	174.12402	21.194378	80.400000	-9.8999945	308.91035
D 1	0	0	0	0	0	0	0.9177719E-07
E 2	80828.319	75.820504	191.28786	39.518604	41.679256	18.204500	32.777481
P 3	1750.3538	0	0	50.380000	693.65654	1181.9408	48.960599
R 4	82578.673	75.820504	191.28786	68.313121	581.24782	1031.0915	32.099999
O 5	0	0	0	0	1.8191525	18.764413	2351.0000
6	0	0	0	2.5229040	0.4335965	-5.3999999	
7	0.1670513E-01	687.72500	361.14645	0	0		
O 1	82578.012	0.1223806	555.92639	389.47039	0	0	0
P 2	176.38235	0.1907010	1.4013360	383.26373	-1.4386914	0	0
5 3	274.85038		2.1836399		0.2702981	0	0
O*1	231.97000	475680.00	5.1092315	28.016242	82578.673	-0.6499937E-02	0.9177719E-07
P 2	45393.667	0.2138584E 08	0.7545784	-77.269289	0	0.1166402E-02	0.2925857E-03
1 3	267.32246	11379.525	15.811982	97.029104	14.598986	0.9057020E-02	0.9428413E 08
4	174.12856	11457.933	0	96.577128	14.496888	1.8191671	5.6237873
5	3.7501380	12708.702	1.3769484	95.844449	13.043493	81.007221	215.72197
6	0.1510933E-02	78.286860	174.12402	21.194378	80.400000	-9.8999945	308.91035
D 1	0	0	0	0	0	0	0.9177719E-07
E 2	80828.319	75.820504	191.28786	39.518623	41.679358	18.204500	32.777481
P 3	1750.3538	0	0	50.380000	693.65654	1181.9408	48.960599
R 4	82578.673	75.820504	191.28786	68.313121	581.24782	1031.0915	32.099999
O 5	0	0	0	0	1.8191671	18.764629	2353.0000
6	0	0	0	2.5229040	0.4335965	-5.3999999	
7	0.1670513E-01	687.72500	361.14645	0	0		
O 1	82578.673	0	555.92639	389.47039	0	0	0
P 2	0	0	1.4013360	383.26373	-1.4386914	0	0
5 3	0		2.1836399		0.2702981	0	0

FUEL MANIFOLD PRESSURE SWITCH ACTIVATED...END SOFT SHUT-DOWN

BEGIN SUSTAINER DECAY

BEGIN VERNIER DECAY

O*1	234.39000	482600.50	5.3972446	28.007998	65879.554	-0.5933258E-02	0.8554827E-07
P 2	44783.616	0.2139277E 08	0.7520142	-77.188501	0	0.1061380E-02	0.2670774E-03
1 3	211.75460	11495.968	15.811982	97.073732	14.389217	0.8847232E-02	0.9428414E 08
4	178.44093	11574.449	0	96.616808	14.289569	1.4710636	5.5652245
5	3.8308082	12826.655	1.4140325	95.887000	12.869223	81.007221	198.91729
6	0.1455244E-02	79.425827	178.43625	21.194378	80.400000	-9.8999945	311.11274
D 1	0	0	0	0	0	0	0.8554827E-07
E 2	64421.894	76.525639	135.01486	38.895282	33.184644	17.841500	32.732037
P 3	1457.6602	0	0	50.380000	506.00121	1184.8256	48.912199
R 4	65879.554	76.525639	135.01486	68.319413	159.36938	1135.6877	32.099999
O 5	0	0	0	0	1.4710636	0.9539811	2369.0000
6	0	0	0	1.7643088	0.4335965	-5.3999999	
7	0.1670513E-01	548.13148	301.29648	0	0		

O 1	65879.554	0	548.95679	394.00660	0	0	0
P 2	0	0	1.4226320	383.25604	-1.3079836	0	0
S 3	0		2.2126800		0.2387682	0	0
O*1	234.39000	482600.50	5.3972446	28.007998	65879.554	-0.5933258E-02	0.8554827E-07
P 2	44783.616	0.2139277E 08	0.7520142	-77.188501	0	0.1061380E-02	0.2670774E-03
I 3	211.75460	11495.968	15.811982	97.073732	14.389217	0.8847232E-02	0.9428414E 08
4	178.44093	11574.449	0	96.616808	14.289569	1.4710636	5.5652245
5	3.8308082	12826.655	1.4140325	95.887000	12.869223	81.007221	198.91729
6	0.1455244E-02	79.425827	178.43625	21.194378	80.400000	-9.8999945	311.11274
D 1	0	0	0	0	0	0	0.8554827E-07
E 2	64421.894	76.525639	135.01486	38.895282	33.184644	17.841500	32.732037
P 3	1457.6602	0	0	50.380000	506.00121	1184.8256	48.912199
R 4	65879.554	76.525639	135.01486	68.319413	159.36938	1135.6877	32.099999
D 5	0	0	0	0	1.4710636	0.9539811	2370.0000
6	0	0	0	1.7643088	0.4335965	-5.3999999	
7	0.1670513E-01	548.13148	301.29648	0	0		
O 1	65879.554	0	548.95679	394.00660	0	0	0
P 2	0	0	1.4226320	383.25604	-1.3079836	0	0
S 3	0		2.2126800		0.2387682	0	0

END SUSTAINER DECAY

O*1	235.89000	486857.75	5.6090377	28.002832	272.05860	-0.5549718E-02	0.8204448E-07
P 2	44731.058	0.2139703E 08	0.7553962	-77.138151	0	0.9968817E-03	0.2498129E-03
I 3	0.2141025	11492.962	15.811982	97.106560	14.226611	0.8681616E-02	0.9428414E 08
4	181.12893	11571.500	0	96.646553	14.128041	0.6081972E-02	5.4960726
5	3.8810611	12824.769	1.4373103	95.913820	12.722930	81.007221	186.01141
6	0.1413700E-02	80.126480	181.12417	21.194378	80.400000	-9.8999945	1270.6932
D 1	0	0	0	0	0	0	0.8204448E-07
E 2	0	0	0	37.089516	28.985316	17.662236	32.703873
P 3	272.05860	0	0	50.380000	490.49810	1185.1326	48.882199
R 4	272.05860	0	0	68.323313	122.63571	1144.4845	32.099999
D 5	0	0	0	0	0.6081960E-02	-7.8373277	2449.0000
6	0	0	0	0	0.4335965	-5.3999999	
7	0.1670513E-01	0.1138524E-05	58.864788	0	0		
O 1	272.05860	0	544.63680	397.34234	0	0	0
P 2	0	0	1.4358320	383.26618	-1.2199229	0	0
S 3	0		2.2306800		0.2196983	0	0
O*1	235.89000	486857.75	5.6090377	28.002832	272.05860	-0.5549718E-02	0.8204448E-07
P 2	44731.058	0.2139703E 08	0.7553962	-77.138151	0	0.9968817E-03	0.2498129E-03
I 3	0.2141025	11492.962	15.811982	97.106560	14.226611	0.8681616E-02	0.9428414E 08
4	181.12893	11571.500	0	96.646553	14.128041	0.6081972E-02	5.4960726
5	3.8810611	12824.769	1.4373103	95.913820	12.722930	81.007221	186.01141
6	0.1413700E-02	80.126480	181.12417	21.194378	80.400000	-9.8999945	1270.6932
D 1	0	0	0	0	0	0	0.8204448E-07
E 2	0	0	0	37.089516	28.985316	17.662236	32.703873
P 3	272.05860	0	0	50.380000	490.49810	1185.1326	48.882199
R 4	272.05860	0	0	68.323313	122.63571	1144.4845	32.099999
D 5	0	0	0	0	0.6081960E-02	-7.8373277	2450.0000
6	0	0	0	0	0.4335965	-5.3999999	

7	0.1670513E-01	0.1138524E-05	58.864788	0	0		
O 1	272.05860	0	544.63680	397.34234	0	0	0
P 2	0	0	1.4358320	383.26618	-1.2199229	0	0
5 3	0		2.2306800		0.2196983	0	0
O*1	236.22000	487787.50	5.6565087	28.001692	92.499965	-0.5468816E-02	0.8130972E-07
P 2	44730.987	0.2139796E 08	0.7562588	-77.127077	0	0.9833829E-03	0.2461712E-03
1 3	0.2141025	11490.524	15.811982	97.113898	14.189969	0.8645652E-02	0.9428415E 08
4	181.72018	11569.075	0	96.653214	14.091626	0.2067795E-02	5.4804612
5	3.8921148	12822.580	1.4424902	95.919726	12.689763	81.007221	183.26136
6	0.1404700E-02	80.279497	181.71541	21.194378	80.400000	-9.8999945	432.03589
D 1	0	0	0	0	0	0	0.8130972E-07
E 2	0	0	0	37.078086	28.975206	17.662236	32.697674
P 3	92.499965	0	0	50.380000	490.49810	1185.1326	48.875599
R 4	92.499965	0	0	68.324171	122.63571	1144.4848	32.099999
D 5	0	0	0	0	0.2067818E-02	-7.8454711	2462.0000
6	0	0	0	0	0.4335965	-5.3999999	
7	0.1670513E-01	0.1138524E-05	58.864788	0	0		
O 1	92.499965	0	543.68639	398.09001	0	0	0
P 2	0	0	1.4387360	383.26877	-1.2008023	0	0
5 3	0		2.2346400		0.2157253	0	0
O*1	236.22000	487787.50	5.6565087	28.001692	92.499965	-0.5468816E-02	0.8130972E-07
P 2	36408.000	0.2139796E 08	0.7562588	-77.127077	0	0.9833829E-03	0.2461712E-03
1 3	0.2141025	11490.524	15.811982	97.113898	14.189969	0.8645652E-02	0.9428415E 08
4	181.72018	11569.075	0	96.653214	14.091626	0.2540499E-02	5.4804612
5	3.8921148	12822.580	1.4424902	95.919726	12.689763	81.007221	183.26136
6	0.1404700E-02	80.279497	181.71541	21.194378	80.400000	-9.8999945	432.03589
D 1	0	0	0	0	0	0	0.8130972E-07
E 2	0	0	0	37.078655	28.976397	17.662236	32.697674
P 3	92.499965	0	0	50.380000	490.49810	1185.1326	48.875599
R 4	92.499965	0	0	68.324171	122.63571	1144.4848	32.099999
D 5	0	0	0	0	0.2540499E-02	-7.8429626	2464.0000
6	0	0	0	0	0.4335965	-5.3999999	
7	0.1670513E-01	0.1128328E-05	22.148656	0	0		
O 1	92.499965	0	543.68639	398.09001	0	0	0
P 2	0	0	1.4387360	383.26877	-1.2008023	0	0
5 3	0		2.2346400		0.2157253	0	0

0 1	TIME	ALTITUDE	ALPHA	GEOCENT LAT	THRUST FIXED	AXL FORCE	ATM PRESS
P 2	WEIGHT	RADIUS	BETA	LONGITUDE	THRUST CONTL	SIDE FORCE	DYNM PRESS
1 3	TOTAL FLOW	VEL E	PSI	AZI E	GAMMA E	NORM FORCE	HEAT PARAM
4	GRND RANGE	VEL R	PSIDOT	AZI R	GAMMA R	AXL LD FCTR	MACH NUMBER
5	THETA I	VEL I	CROSS RANGE	AZI I	GAMMA I	WIND VEL	RHO-VR CUBED
6	Q*ALPHA TOT	ALT	DOWN RANGE	PHI	EAST WIND	NORTH WIND	TOTAL ISP
0 1	SEC	FT	DEG	DEG	LBS	LBS	PSI
P 2	LBS	FT	DEG	DEG	LBS	LBS	LBS/FT SQD
1 3	LBS/SEC	FT/SEC	DEG	DEG	DEG	LBS	FT*LBS/FT SQD
4	N. MI.	FT/SEC	DEG/SEC	DEG	DEG		
5	DEG	FT/SEC	N.MI.	DEG	DEG	FT/SEC	LBS/SEC CUBED
6	DEG-PSF	N.MI	N.MI.	DEG	FT/SEC	FT/SEC	SEC
0 1	PERIGEE RAD	PERIGEE ALT	PERIGEE VEL	SEMI LAT REC	SEMI MAJ AXIS	ECCENTRICITY	TRUE ANOMALY
4 2	APOGEE RAD	APOGEE ALT	APOGEE VEL	PERIOD	ENERGY	INCLINATION	ASCEND NODE
0 1	NM	NM	FT/SEC	NM	NM		DEG
4 2	NM	NM	FT/SEC	MIN	FT**2/SEC**2	DEG	DEG
0*1	236.22000	487787.50	5.5581583	28.001692	8.7199999	-0	0.8130972E-07
P 2	36408.000	0.2139796E 08	0.7534464	-77.127077	0	0	0.2428397E-03
1 3	4.4400000	11490.524	15.811982	97.113899	14.189969	0	0.9428415E 08
4	181.72018	11490.524	0	96.650549	14.189970	0.2395078E-03	5.4432505
5	3.8921148	12822.581	1.4424891	95.919726	12.689763	0	179.55378
6	0.1361933E-02	80.279497	181.71541	21.194378	0	-0	1.9639639
0 1	474.89109	-2969.0424	92765.799	837.71051	2012.2975	0.7640055	175.97983
4 2	3549.7039	105.77036	12410.514	37.736184	-0.5756356E 09	28.570975	-178.59392
0*1	24C.00000	498254.00	0	27.988566	8.7199999	-0	0
P 2	36391.216	0.2140844E 08	0	-77.000321	0	0	0
1 3	4.4400000	11462.597	15.811982	97.197918	13.768950	0	0.9428415E 08
4	188.48861	11462.597	0	96.727356	13.768951	0.2396183E-03	0
5	4.0186629	12797.473	1.5027681	95.987320	12.308842	0	0
6	0	82.002062	188.48362	21.194378	0	-0	1.9639639
0 1	474.89479	-2969.0387	92765.393	837.71625	2012.2989	0.7640039	175.10643
4 2	3549.7030	105.76944	12410.560	37.736223	-0.5756352E 09	28.571106	-178.59532

O 1	TIME	ALTITUDE	ALPHA	GEOCENT LAT	THRUST FIXED	AXL FORCE	ATM PRESS
P 2	WEIGHT	RADIUS	BETA	LONGITUDE	THRUST CONTL	SIDE FORCE	DYNM PRESS
I 3	TOTAL FLOW	VEL E	PSI	AZI E	GAMMA E	NORM FORCE	HEAT PARAM
4	GRND RANGE	VEL R	PSIDOT	AZI R	GAMMA R	AXL LD FCTR	MACH NUMBER
5	THETA I	VEL I	CROSS RANGE	AZI I	GAMMA I	WIND VEL	RHO-VR CUBED
6	Q*ALPHA TOT	ALT	DOWN RANGE	PHI	EAST WIND	NORTH WIND	TOTAL ISP
O 1	SEC	FT	DEG	DEG	LBS	LBS	PSI
P 2	LBS	FT	DEG	DEG	LBS	LBS	LBS/FT SQD
I 3	LBS/SEC	FT/SEC	DEG	DEG	DEG	LBS	FT*LBS/FT SQD
4	N. MI.	FT/SEC	DEG/SEC	DEG	DEG		
5	DEG	FT/SEC	N.MI.	DEG	DEG	FT/SEC	LBS/SEC CUBED
6	DEG-PSF	N.MI	N.MI.	DEG	FT/SEC	FT/SEC	SEC
O 1	PERIGEE RAD	PERIGEE ALT	PERIGEE VEL	SEMI LAT REC	SEMI MAJ AXIS	ECCENTRICITY	TRUE ANOMALY
4 2	APOGEE RAD	APOGEE ALT	APOGEE VEL	PERIOD	ENERGY	INCLINATION	ASCEND NODE
O 1	NM	NM	FT/SEC	NM	NM		DEG
4 2	NM	NM	FT/SEC	MIN	FT**2/SEC**2	DEG	DEG
C 1	THRUST	C-1 THRUST	C-2 THRUST	LH2 WEIGHT	C-1 ISP	C-2 ISP	C-1 PU VALVE
E 2	LH2 FLOW	C-1 LH2 FLOW	C-2 LH2 FLOW	LO2 WEIGHT	C-1 FLOW	C-2 FLOW	C-2 PU VALVE
N 3	LO2 FLOW	C-1 LO2 FLOW	C-2 LO2 FLOW	C-1 LH2 PRESS	C-1 LO2 PRESS	C-1 LH2 TEMP	C-1 LO2 TEMP
T 4	RATIO	C-1 RATIO	C-2 RATIO	C-2 LH2 PRESS	C-2 LO2 PRESS	C-2 LH2 TEMP	C-2 LO2 TEMP
5		PER CENT T1	PER CENT T2	PER CENT ISP1	PER CENT ISP2	PER CENT MR1	PER CENT MR2
C 1	LBS	LBS	LBS	LBS	SEC	SEC	DEG
E 2	LBS/SEC	LBS/SEC	LBS/SEC	LBS	LBS/SEC	LBS/SEC	DEG
N 3	LBS/SEC	LBS/SEC	LBS/SEC	PSI	PSI	DEG R	DEG R
T 4				PSI	PSI	DEG R	DEG R
O*1	242.63374	505349.00	0	27.979340	8.7199999	-0	0
P 2	36379.523	0.2141554E 08	0	-76.912107	0	0	0
I 3	0.1030000	11443.644	15.811982	97.256376	13.474454	0	0.9428415E 08
4	193.20024	11443.644	0	96.780796	13.474455	0.2396953E-03	0
5	4.1067641	12780.439	1.5459533	96.034350	12.042634	0	0
6	0	83.169748	193.19508	21.194378	0	-0	84.660193
O 1	474.89740	-2969.0361	92765.107	837.72028	2012.2998	0.7640027	176.19457
4 2	3549.7022	105.76871	12410.592	37.736249	-0.5756350E 09	28.571198	-178.59629
C 1	8.7199999	0	0	4974.0000	432.07177	433.04969	0
E 2	0	0	0	25180.000	0	0	0
N 3	0	0	0	47.383130	103.05217	39.444650	180.94650
T 4	1.0000000	5.4869566	5.5855885	46.889234	102.10522	39.444650	180.67325
5		102.00125	101.97909	99.227134	99.223093	109.73913	109.73651
O*1	244.73374	510893.00	0	27.971935	29834.589	-0	0
P 2	36280.825	0.2142109E 08	0	-76.841798	0	0	0
I 3	68.686529	11449.048	15.811982	97.301565	13.251060	0	0.9428415E 08
4	196.95609	11449.049	0	96.821985	13.251060	0.8223239	0
5	4.1769956	12787.285	1.5810801	96.071736	11.842956	0	0
6	0	84.082173	196.95081	21.194378	0	-0	434.35867
O 1	476.54739	-2967.3861	92585.635	840.29067	2013.2017	0.7632888	176.24557
4 2	3549.8560	105.92245	12429.079	37.761621	-0.5753771E 09	28.571254	-178.59589

C 1	29834.589	14886.770	14939.099	4958.1744	434.25336	435.51556	0
E 2	11.098199	5.5736467	5.5245527	25097.344	34.281364	34.302166	0
N 3	57.485331	28.707718	28.777613	36.916965	69.121115	38.917097	177.31291
T 4	5.1796988	5.1506166	5.2090394	36.393592	68.650145	38.917097	178.62532
5		100.53730	100.41331	99.728148	99.788089	103.01233	102.33869
O*1	246.77000	516199.25	0	27.964690	29806.243	-0	0
P 2	36141.059	0.2142641E 08	0	-76.773428	0	0	0
1 3	68.590554	11488.447	15.811982	97.343127	13.056136	0	0.9428415E 08
4	200.60894	11488.447	0	96.859673	13.056138	0.8247197	0
5	4.2452785	12827.947	1.6156466	96.107919	11.672452	0	0
6	0	84.955470	200.60352	21.194378	0	-0	434.55317
O 1	480.93233	-2963.0012	92113.074	847.11161	2015.5970	0.7613946	176.26281
4 2	3550.2617	106.32819	12477.997	37.829035	-0.5746933E 09	28.571279	-178.59715
C 1	29806.243	14872.479	14925.044	4935.5434	434.45079	435.70755	0
E 2	11.129921	5.5896221	5.5402990	24980.419	34.232827	34.254728	0
N 3	57.357634	28.643205	28.714429	36.449823	66.845295	38.912306	177.16917
T 4	5.1534628	5.1243545	5.1828302	35.722824	66.422236	38.912306	178.58460
5		100.44059	100.31865	99.773488	99.832079	102.48709	101.82378
O*1	248.77000	521354.25	0	27.957508	29779.044	-0	0
P 2	36003.971	0.2143157E 08	0	-76.706020	0	0	0
1 3	68.497487	11527.474	17.661339	97.384048	12.867025	0	0.9428415E 08
4	204.21093	11527.474	-1.5982462	96.896791	12.867026	0.8271044	0
5	4.3125813	12868.188	1.6500899	96.143565	11.506991	0	0
6	0	85.803874	204.20537	19.229014	0	-0	434.74652
O 1	485.27745	-2958.6561	91650.996	853.85622	2017.9681	0.7595217	175.27970
4 2	3550.6587	106.72519	12526.172	37.895806	-0.5740181E 09	28.571303	-178.59740
C 1	29779.044	14858.628	14911.696	4913.2518	434.64842	435.89861	0
E 2	11.161784	5.6056353	5.5561482	24865.829	34.185396	34.209093	0
N 3	57.232705	28.579760	28.652944	35.991000	64.610001	38.907599	177.02800
T 4	5.1275591	5.0983980	5.1569798	35.064000	64.234000	38.907599	178.54460
5		100.34705	100.22893	99.818874	99.875857	101.96796	101.31591
O*1	254.07000	534741.25	0	27.938136	29737.400	-0	0
P 2	35641.471	0.2144498E 08	0	-76.526156	0	0	0
1 3	68.352577	11632.835	12.989772	97.501077	12.362873	0	0.9428415E 08
4	213.82471	11632.835	0.2413857	97.003757	12.362875	0.8343483	0
5	4.4920747	12976.684	1.7446191	96.245858	11.065454	0	0
6	0	88.007091	213.81877	22.122121	0	-0	435.05894
O 1	497.06527	-2946.8683	90427.334	872.08022	2024.3606	0.7544581	176.32772
4 2	3551.6560	107.72244	12655.586	38.076018	-0.5722054E 09	28.572819	-178.61301
C 1	29737.400	14836.211	14892.469	4853.9020	434.98328	436.19161	0
E 2	11.213784	5.6328387	5.5809450	24563.224	34.107544	34.142034	0
N 3	57.035794	28.474705	28.561089	35.250000	60.704285	38.905914	176.68171
T 4	5.0862220	5.0551252	5.1176079	34.000000	60.699999	38.905914	178.39720
5		100.19566	100.09969	99.895775	99.942990	101.10251	100.54240
O*1	260.00000	549230.00	0	27.915898	29738.643	-0	0
P 2	35236.124	0.2145949E 08	0	-76.322742	0	0	0

1 3	66.357274	11754.155	13.949902	97.612599	11.803724	0	0.9428415E 08
4	224.70182	11754.155	0.9273585E-01	97.104046	11.803725	0.8439817	0
5	4.6949115	13101.407	1.8539603	96.343241	10.575107	0	0
6	0	90.391632	224.69543	21.833292	0	-0	435.04724
0 1	510.71104	-2933.2225	89062.786	893.04468	2031.7110	0.7486301	176.38460
4 2	3552.7110	108.77747	12802.997	38.283586	-0.5701353E 09	28.570899	-178.59358
C 1	29738.643	14834.844	14895.079	4787.4126	435.00389	436.14727	0
E 2	11.211468	5.6342619	5.5772066	24224.977	34.102785	34.151490	0
N 3	57.042807	28.468523	28.574284	35.246589	60.013642	38.916316	176.38635
T 4	5.0878978	5.0527511	5.1234042	34.000000	60.699999	38.916316	178.19454
5		100.18643	100.11724	99.900508	99.932831	101.05502	100.65627
0*1	264.22000	559235.50	0	27.899714	29738.744	-0	0
P 2	34947.656	0.2146951E 08	0	-76.176572	0	0	0
1 3	66.357337	11842.413	14.172476	97.695782	11.423797	0	0.9428415E 08
4	232.52073	11842.414	0.1875443E-01	97.179249	11.423798	0.8509510	0
5	4.8405625	13191.917	1.9334036	96.416053	10.241812	0	0
6	0	92.038326	232.51402	21.519128	0	-0	435.04831
0 1	520.63905	-2923.2945	88103.180	908.21111	2037.0565	0.7444160	176.42320
4 2	3553.4739	109.54041	12908.482	38.434772	-0.5686392E 09	28.570106	-178.58569
C 1	29738.744	14835.316	14894.707	4740.0996	434.99793	436.15540	0
E 2	11.211759	5.6338230	5.5779365	23984.257	34.104338	34.150001	0
N 3	57.042578	28.470515	28.572064	35.232195	60.071214	38.900772	176.32878
T 4	5.0877454	5.0534983	5.1223359	34.000000	60.699999	38.900772	178.17151
5		100.18962	100.11474	99.899140	99.934694	101.06997	100.63528
0*1	274.02000	581531.75	0	27.860914	29738.979	-0	0
P 2	34277.754	0.2149185E 08	0	-75.832545	0	0	0
1 3	66.357502	12053.762	13.807991	97.898937	10.582086	0	0.9428415E 08
4	250.93340	12053.762	-0.7929710E-01	97.363935	10.582087	0.8675883	0
5	5.1830500	13408.062	2.1254779	96.594481	9.5027418	0	0
6	0	95.707817	250.92588	21.652579	0	-0	435.05070
0 1	544.52272	-2899.4108	85900.745	944.40012	2049.8759	0.7343631	176.51082
4 2	3555.2290	111.29550	13156.651	38.798153	-0.5650831E 09	28.569774	-178.58243
C 1	29738.979	14836.417	14893.842	4630.2211	434.98400	436.17422	0
E 2	11.212426	5.6327982	5.5796276	23425.243	34.107959	34.146544	0
N 3	57.042077	28.475161	28.566916	35.198771	60.204911	38.864674	176.19509
T 4	5.0873984	5.0552425	5.1198606	34.000000	60.699999	38.864674	178.11803
5		100.19705	100.10893	99.895943	99.939007	101.10485	100.58666
0*1	280.00000	594508.00	0	27.836373	29739.124	-0	0
P 2	33868.976	0.2150485E 08	0	-75.619422	0	0	0
1 3	66.357613	12187.263	13.321577	98.022842	10.089115	0	0.9428415E 08
4	262.34709	12187.263	-0.8178531E-01	97.476609	10.089116	0.8780639	0
5	5.3950042	13544.255	2.2483083	96.703617	9.0692749	0	0
6	0	97.843432	262.33904	21.336598	0	-0	435.05212
0 1	559.73916	-2884.1944	84569.982	967.23946	2058.0023	0.7280182	176.56471
4 2	3556.2655	112.33200	13310.910	39.029096	-0.5628517E 09	28.569327	-178.57815
C 1	29739.124	14837.091	14893.313	4563.1696	434.97545	436.18569	0

[redacted]

[redacted]

E 2	11.212827	5.6321699	5.5806569	23084.132	34.110180	34.144433	0
N 3	57.041786	28.478010	28.563776	35.178376	60.286493	38.842646	176.11350
T 4	5.0871904	5.0563124	5.1183537	34.000000	60.699999	38.842646	178.08540
5		100.20160	100.10537	99.893978	99.941632	101.12625	100.55705
O*1	286.00000	607058.75	0	27.811071	29739.272	-0	0
P 2	33458.830	0.2151742E 08	0	-75.403105	0	0	0
1 3	68.357737	12324.710	12.742861	98.148410	9.6088505	0	0.9428415E 08
4	273.93756	12324.710	-0.7433578E-01	97.590938	9.6088514	0.8888318	0
5	5.6099750	13684.235	2.3758754	96.814479	8.6464853	0	0
6	0	99.909020	273.92896	21.357634	0	-0	435.05349
O 1	575.53151	-2868.4020	83243.735	990.76687	2066.4034	0.7214815	175.61944
4 2	3557.2752	113.34171	13468.003	39.268322	-0.5605634E 09	28.568933	-178.57446
C 1	29739.272	14837.771	14892.782	4495.8914	434.96682	436.19716	0
E 2	11.213225	5.6315374	5.5816875	22741.882	34.112420	34.142317	0
N 3	57.041512	28.480883	28.560629	35.157912	60.368349	38.820545	176.03165
T 4	5.0869854	5.0573902	5.1168450	34.000000	60.699999	38.820545	178.05266
5		100.20619	100.10180	99.891995	99.944262	101.14781	100.52741
O*1	300.00000	634551.75	0	27.749292	29739.622	-0	0
P 2	32501.819	0.2154498E 08	0	-74.888461	0	0	0
1 3	68.358053	12659.126	11.638535	98.445976	8.5425262	0	0.9428415E 08
4	301.53604	12659.127	-0.8182717E-01	97.862415	8.5425272	0.9150141	0
5	6.1207976	14023.958	2.6907936	97.078238	7.7058287	0	0
6	0	104.43379	301.52600	21.346988	0	-0	435.05659
O 1	614.57218	-2829.3613	80182.224	1048.1710	2087.0416	0.7055295	175.75003
4 2	3559.5110	115.57745	13843.970	39.858078	-0.5550202E 09	28.568180	-178.56759
C 1	29739.622	14839.364	14891.538	4338.8998	434.94650	436.22384	0
E 2	11.214135	5.6300514	5.5840839	21943.305	34.117676	34.137378	0
N 3	57.040918	28.487625	28.553294	35.110163	60.559345	38.768976	175.84065
T 4	5.0865195	5.0599227	5.1133354	34.000000	60.699999	38.768976	177.97626
5		100.21695	100.09344	99.887328	99.950375	101.19845	100.45846
O*1	320.00000	669635.50	0	27.653966	29740.136	-0	0
P 2	31134.653	0.2158016E 08	0	-74.128322	0	0	0
1 3	68.358593	13170.263	9.8789929	98.880898	7.1526613	0	0.9428415E 08
4	342.36197	13170.264	-0.9252915E-01	98.260407	7.1526613	0.9552101	0
5	6.8738444	14541.349	3.1848411	97.466240	6.4752083	0	0
6	0	110.20783	342.34957	21.333874	0	-0	435.06068
O 1	676.22243	-2767.7111	75886.479	1136.6797	2119.3260	0.6809257	175.94209
4 2	3562.4295	118.49600	14404.815	40.786491	-0.5465653E 09	28.567194	-178.55903
C 1	29740.136	14841.662	14889.754	4114.6045	434.91703	436.26176	0
E 2	11.215394	5.6279069	5.5874870	20802.494	34.125272	34.130322	0
N 3	57.040200	28.497365	28.542835	35.041950	60.832196	38.695306	175.56780
T 4	5.0858847	5.0635815	5.1083491	34.000000	60.699999	38.695306	177.86712
5		100.23247	100.08145	99.880562	99.959063	101.27163	100.36050
O*1	340.00000	700036.00	0	27.549632	30284.195	-0	0
P 2	29755.643	0.2161067E 08	0	-73.337325	0	0	0
1 3	70.317154	13725.170	7.9054109	99.327509	5.9112587	0	0.9428415E 08

4	384.92752	13725.170	-0.1032311	98.670536	5.9112587	1.0177631	0
5	7.6558534	15101.185	3.7342681	97.867832	5.3709641	0	0
6	0	115.21111	384.91237	21.323225	0	-0	430.68005
O 1	746.33996	-2697.5936	71648.233	1234.2823	2155.6833	0.6537803	177.13946
4 2	3565.0266	121.09308	14999.590	41.840526	-0.5373471E 09	28.566300	-178.55170
C 1	30284.195	15064.385	15211.090	3893.8517	431.37985	430.99743	-29.500000
E 2	10.636795	5.3901013	5.2466937	19646.297	34.921392	35.292764	-50.300000
N 3	59.577360	29.531291	30.046070	35.801281	58.500000	38.616666	175.30897
T 4	5.6010631	5.4788007	5.7266675	35.000000	59.000000	38.616666	177.74949
5		101.73662	102.24131	99.068233	98.752866	109.57602	112.50820
O*1	360.00000	726054.75	0	27.435382	30281.871	-0	0
P 2	28349.428	0.2163680E 08	0	-72.513191	0	0	0
1 3	70.304338	14330.847	5.7177894	99.786161	4.8104792	0	0.9428415E 08
4	429.36962	14330.847	-0.1139331	99.093211	4.8104801	1.0681652	0
5	8.4691036	15710.694	4.3430653	98.283712	4.3871155	0	0
6	0	119.49324	429.35128	21.315041	0	-0	430.72551
O 1	827.28255	-2616.6510	67427.048	1343.0933	2197.2979	0.6235000	177.33996
4 2	3567.3133	123.37973	15636.760	43.057926	-0.5271703E 09	28.565480	-178.54534
C 1	30281.871	15063.498	15209.654	3681.0613	431.42534	431.04317	-29.500000
E 2	10.642236	5.3929477	5.2492889	18454.932	34.915653	35.285685	-50.299999
N 3	59.559102	29.522706	30.036396	36.057692	58.499999	38.549999	175.10384
T 4	5.5964835	5.4743171	5.7219934	35.000000	59.000000	38.549999	177.64692
5		101.73063	102.23165	99.078679	98.763348	109.48634	112.41638
O*1	380.00000	747941.75	0	27.310239	30013.437	-0	0
P 2	26945.752	0.2165881E 08	0	-71.653749	0	0	0
1 3	69.321608	14981.204	3.3161281	100.25801	3.8314514	0	0.9428415E 08
4	475.82170	14981.204	-0.1246351	99.529645	3.8314524	1.1138467	0
5	9.3158166	16363.996	5.0156596	98.714612	3.5072632	0	0
6	0	123.09538	475.79971	21.309322	0	-0	432.95934
O 1	920.20463	-2523.7289	63270.225	1463.1799	2244.7260	0.5900593	177.55636
4 2	3569.2474	125.31390	16311.997	44.459515	-0.5160319E 09	28.564745	-178.53995
C 1	30013.437	14930.955	15073.762	3467.5619	433.57798	433.37825	-11.195566
E 2	10.909307	5.5275967	5.3817102	17266.816	34.436609	34.782000	-22.995673
N 3	58.309301	28.909012	29.400289	35.315217	59.804346	38.486956	174.91521
T 4	5.3449135	5.2299424	5.4630013	34.130435	60.304347	38.486956	177.54391
5		100.83551	101.31826	99.573042	99.298374	104.59885	107.32812
O*1	400.00000	765873.50	0	27.173193	29647.786	-0	0
P 2	25582.225	0.2167688E 08	0	-70.757221	0	0	0
1 3	68.037110	15665.732	0.7004272	100.74413	2.9525204	0	0.9428415E 08
4	524.39856	15665.733	-0.1353371	99.981000	2.9525204	1.1589213	0
5	10.197904	17050.744	5.7570011	99.161038	2.7125034	0	0
6	0	126.04657	524.37240	21.306068	0	-0	435.75904
O 1	1025.6886	-2418.2449	59239.541	1593.6194	2298.2392	0.5537068	177.80954
4 2	3570.7898	126.85623	17016.214	46.058792	-0.5040164E 09	28.564106	-178.53552
C 1	29647.786	14788.249	14850.817	3241.5930	435.72884	436.85296	6.0000152
E 2	11.341057	5.6995702	5.6414865	16131.318	33.939109	33.995002	4.7615561

N 3	56.593054	28.239539	28.353515	34.676922	60.915385	38.420768	174.80000
T 4	4.9901041	4.9546787	5.0258943	33.442307	61.607693	38.420768	177.43230
5		99.871748	99.819732	100.06699	100.09452	99.093575	98.740558
0*1	420.00000	779988.50	0	27.023126	29667.267	-0	0
P 2	24213.884	0.2169115E 08	0	-69.821692	0	0	0
1 3	68.103382	16402.101	-2.1293135	101.24396	2.1685009	0	0.9428415E 08
4	575.22541	16402.102	-0.1460391	100.44677	2.1685019	1.2252172	0
5	11.117449	17788.719	6.5724127	99.623322	1.9993973	0	0
6	0	128.36960	575.19450	21.305280	0	-0	435.62105
0 1	1148.9192	-2295.0144	55239.174	1738.6151	2360.4441	0.5132614	178.10171
4 2	3571.9690	128.03543	17767.608	47.941351	-0.4907340E 09	28.563518	-178.53166
C 1	29667.267	14796.961	14861.586	3017.5204	435.59909	436.70519	5.2461421
E 2	11.316140	5.6882853	5.6278546	14989.109	33.969220	34.031163	3.1307555
N 3	56.684243	28.280935	28.403309	34.415384	61.269229	38.353076	174.64538
T 4	5.0091501	4.9717855	5.0469158	33.480769	61.446152	38.353076	177.32846
5		99.930588	99.892114	100.03720	100.06067	99.435711	99.153554
0*1	440.00000	790417.00	0	26.858745	29743.319	-0	0
P 2	22855.745	0.2170174E 08	0	-68.844687	0	0	0
1 3	66.363759	17188.506	-5.1730935	101.75833	1.4642372	0	0.9428415E 08
4	628.46098	17188.507	-0.1567410	100.92789	1.4642382	1.3013498	0
5	12.077095	18576.215	7.4677532	100.10213	1.3548336	0	0
6	0	130.08591	628.42474	21.306957	0	-0	435.07437
0 1	1293.2283	-2150.7052	51289.570	1899.0598	2433.0044	0.4684645	178.46180
4 2	3572.7805	128.84702	18565.126	50.168839	-0.4760987E 09	28.562970	-178.52826
C 1	29743.319	14835.295	14899.305	2789.4813	435.05761	436.14763	0.3428456
E 2	11.220307	5.6407649	5.5795420	13861.069	34.099609	34.161150	-1.5285848
N 3	57.040452	28.458844	28.581608	34.864286	60.978570	38.273571	174.46285
T 4	5.0836802	5.0452102	5.1225724	33.178571	61.278571	38.273571	177.26286
5		100.18947	100.14564	99.912846	99.932914	100.90421	100.63993
0*1	460.00000	797236.00	0	26.678615	29476.197	-0	0
P 2	21500.581	0.2170873E 08	0	-67.823609	0	0	0
1 3	67.459013	18032.025	-8.4309134	102.28760	0.8284149	0	0.9428415E 08
4	684.27466	18032.026	-0.1674430	101.42482	0.8284159	1.3709489	0
5	13.079662	19420.381	8.4494574	100.59809	0.7691898	0	0
6	0	131.20817	684.23241	21.311099	0	-0	436.94972
0 1	1464.6820	-1979.2515	47367.854	2077.7069	2518.9637	0.4185379	178.93113
4 2	3573.2453	129.31180	19416.199	52.850921	-0.4598519E 09	28.562443	-178.52516
C 1	29476.197	14713.557	14753.920	2560.0673	436.76303	438.21425	17.000011
E 2	11.597304	5.8089085	5.7883953	12737.379	33.687734	33.668281	18.000012
N 3	55.758710	27.878825	27.879885	33.750000	62.199999	38.199999	174.30000
T 4	4.8079029	4.7993225	4.8165137	33.499999	62.500000	38.199999	177.10000
5		99.367320	99.168440	100.30450	100.40643	95.986451	94.626990
0*1	479.99999	800472.50	0	26.481131	29736.003	-0	0
P 2	20145.444	0.2171216E 08	0	-66.755621	0	0	0
1 3	66.338411	18939.344	-11.902772	102.83223	0.2486486	0	0.9428415E 08
4	742.85340	18939.344	-0.1781450	101.93813	0.2486496	1.4760659	0

5	14.128264	20327.956	9.5247402	101.11184	0.2316637	0	0
6	0	131.74083	742.60448	21.317706	0	-0	435.12869
O 1	1671.4058	-1772.5277	43459.562	2277.5329	2622.4097	0.3626450	179.59283
4 2	3573.4136	129.48004	20327.500	56.139754	-0.4417121E 09	28.561906	-178.52218
C 1	29736.063	14826.936	14900.348	2330.6279	435.18012	436.13399	0.8000295
E 2	11.230554	5.6514174	5.5791370	11613.742	34.070802	34.164610	-1.7333015
N 3	57.004858	28.419384	28.585473	34.316665	60.400002	38.126666	174.03333
T 4	5.0758721	5.0287180	5.1236371	32.699998	61.333334	38.126666	176.96666
5		100.13302	100.15265	99.940981	99.929788	100.57436	100.66085
O*1	495.83000	800477.75	0	26.311284	29704.449	-0	0
P 2	19061.915	0.2171234E 08	0	-65.874716	0	0	0
1 3	68.230238	19712.608	-15.545808	103.27441	-0.1776857	0	0.9428415E 08
4	791.33109	19712.609	0.6121850	102.35634	-0.1776848	1.5583141	0
5	14.993404	21101.171	10.447493	101.53165	-0.1659918	0	0
6	0	131.74169	791.27638	20.978558	0	-0	435.35609
O 1	1868.7981	-1575.1354	40348.078	2454.1474	2721.1107	0.3132223	-179.63604
4 2	3573.4233	129.48975	21100.890	59.338836	-0.4256902E 09	28.561454	-178.51979
C 1	29704.449	14808.994	14886.735	2153.4172	435.42584	436.34529	3.4613948
E 2	11.270854	5.6737357	5.5971186	10709.053	34.010371	34.116868	-0.5454051
N 3	56.856385	28.336635	28.519750	33.713600	60.917699	38.065510	173.80653
T 4	5.0445497	4.9943522	5.0954343	32.603400	61.024499	38.065510	175.87585
5		100.01185	100.06116	99.997412	99.978203	99.887046	100.10677
O*1	499.83000	800115.00	0	26.266340	29546.274	-0	0
P 2	18790.105	0.2171202E 08	0	-65.646901	0	0	0
1 3	67.693067	19914.558	-14.225898	103.38697	-0.2797709	0	0.9428415E 08
4	803.89230	19914.558	-0.2159379	102.46296	-0.2797699	1.5724379	0
5	15.217200	21303.078	10.691167	101.63884	-0.2615356	0	0
6	0	131.68199	803.83605	21.299951	0	-0	436.47416
O 1	1923.9570	-1519.9765	39565.496	2501.2327	2748.6909	0.3000461	-179.38985
4 2	3573.4248	129.49124	21302.341	60.243272	-0.4214189E 09	28.561035	-178.51763
C 1	29546.274	14732.936	14804.618	2107.8950	436.49466	437.52461	13.781395
E 2	11.488863	5.7791055	5.7097577	10483.178	33.752844	33.837224	9.9345946
N 3	56.101204	27.973738	28.127466	33.393600	61.677699	38.053509	173.77053
T 4	4.8830944	4.8404962	4.9262100	32.523399	61.624499	38.053509	175.85585
5		99.498198	99.509206	100.24287	100.24841	96.809924	96.782123
O*1	499.99999	800096.50	0	26.264411	29540.197	-0	0
P 2	18778.600	0.2171200E 08	0	-65.637172	0	0	0
1 3	67.672714	19923.184	-14.262739	103.39182	-0.2835941	0	0.9428415E 08
4	804.42896	19923.185	-0.2159228	102.46755	-0.2835932	1.5730777	0
5	15.226758	21311.703	10.701602	101.64345	-0.2651157	0	0
6	0	131.67895	804.37265	21.300109	0	-0	436.51563
O 1	1926.3487	-1517.5848	39532.328	2503.2530	2749.8867	0.2994807	-179.37983
4 2	3573.4247	129.49112	21310.943	60.282589	-0.4212356E 09	28.561034	-178.51762
C 1	29540.197	14730.021	14801.456	2105.9412	436.53428	437.56839	14.219980
E 2	11.497918	5.7834718	5.7144467	10473.644	33.743104	33.826612	10.379980
N 3	56.071796	27.959632	28.112165	33.380000	61.709998	38.052999	173.76900

T 4	4.8766911	4.8344027	4.9194903	32.520000	61.649998	38.052999	175.85500
5		99.478511	99.487952	100.25197	100.25845	96.688054	96.650195
0*1	519.99999	796225.25	0	26.026398	29442.569	-0	0
P 2	17426.564	0.2170836E 08	0	-64.464750	0	0	0
1 3	67.349561	20978.384	-18.569456	103.97021	-0.7322340	0	0.9428415E 08
4	869.23708	20978.384	-0.2126601	103.01710	-0.7322330	1.6895223	0
5	16.379069	22366.490	11.989084	102.19625	-0.6867867	0	0
6	0	131.04182	869.17265	21.318111	0	-0	437.16051
0 1	2242.7420	-1201.1915	35627.743	2755.9124	2908.1720	0.2288138	-177.68398
4 2	3573.6020	129.66849	22359.467	65.561646	-0.3983087E 09	28.560772	-178.51633
C 1	29442.569	14695.343	14738.505	1875.2943	436.99421	438.40684	19.454560
E 2	11.652687	5.8374206	5.8152665	9354.3153	33.628233	33.618329	20.000015
N 3	55.593874	27.790812	27.803062	33.045454	61.893637	37.967272	173.50000
T 4	4.7709060	4.7608034	4.7810470	31.736363	61.945454	37.967272	176.71454
5		99.244314	99.064830	100.35759	100.45056	95.216069	93.930198
0*1	539.99999	788775.00	0	25.764745	29592.607	-0	0
P 2	16070.663	0.2170116E 08	0	-63.234517	0	0	0
1 3	67.850555	22124.101	-22.781478	104.56546	-1.1773891	0	0.9428415E 08
4	937.53963	22124.102	-0.2064536	103.58497	-1.1773882	1.8414055	0
5	17.589557	23511.493	13.398918	102.76903	-1.1079035	0	0
6	0	129.81567	937.46629	21.334806	0	-0	436.14391
0 1	2647.9786	-795.95490	31706.003	3042.5806	3111.6817	0.1490201	-173.65277
4 2	3575.3847	131.45117	23481.898	72.562534	-0.3722586E 09	28.560358	-178.51438
C 1	29592.607	14750.594	14833.293	1646.3030	436.24683	437.10818	11.000010
E 2	11.422338	5.7534610	5.6688766	8229.4657	33.812495	33.935061	6.2500063
N 3	56.325219	28.059034	28.266185	33.049999	61.425001	37.905000	173.40250
T 4	4.9311463	4.8768966	4.9862056	31.650000	61.675000	37.905000	176.60000
5		99.617448	99.701945	100.18595	100.15300	97.537932	97.960819
0*1	559.99999	777392.50	0	25.476712	29722.757	-0	0
P 2	14709.145	0.2169006E 08	0	-61.941723	0	0	0
1 3	68.293040	23374.590	-26.839933	105.17838	-1.6151342	0	0.9428415E 08
4	1009.6573	23374.591	-0.1973031	104.17219	-1.6151333	2.0206992	0
5	18.863563	24760.946	14.943159	103.36293	-1.5246811	0	0
6	0	127.94235	1009.5742	21.350193	0	-0	435.22380
0 1	3175.2065	-268.72702	27827.622	3369.9721	3382.6996	0.6133951E-01	-155.81758
4 2	3590.1927	146.25919	24611.060	82.246013	-0.3424336E 09	28.559813	-178.51197
C 1	29722.757	14827.676	14886.361	1419.3837	435.15565	436.35026	1.0714624
E 2	11.249856	5.6510869	5.5987695	7096.9266	34.074419	34.115623	-0.5713337
N 3	56.940185	28.423331	28.516853	33.335713	60.842858	37.830714	173.20500
T 4	5.0614144	5.0297105	5.0934144	31.935713	61.371430	37.830714	176.47786
5		100.13802	100.05864	99.935361	99.979341	100.59421	100.06708
0*1	579.99999	761724.25	0	25.159122	29668.722	-0	0
P 2	13344.585	0.2167469E 08	0	-60.580956	0	0	0
1 3	68.109258	24746.209	-30.685935	105.80982	-2.0388184	0	0.9428415E 08
4	1085.9588	24746.209	-0.1852087	104.77985	-2.0388184	2.2232773	0
5	20.207223	26131.194	16.636235	103.97917	-1.9307165	0	0

6	0	125.36369	1085.8653	21.364273	0	-0	435.60483
O 1	3529.4787	85.545197	26395.440	3746.3564	3760.5555	0.6144752E-01	-35.179876
4 2	3991.6324	547.69882	23339.360	96.404590	-0.3080263E 09	28.559167	-178.50926
C 1	29668.722	14796.427	14863.575	1193.8270	435.59606	436.67553	4.8750105
E 2	11.319180	5.6907785	5.6284015	5959.9872	33.968229	34.038030	2.1250124
N 3	56.687078	28.277450	28.409628	32.812500	61.075000	37.758749	173.01000
T 4	5.0080552	4.9689950	5.0475482	31.412499	61.475000	37.758749	176.36125
5		99.926978	99.905483	100.03650	100.05387	99.379901	99.165977
O*1	599.99999	741445.25	0	24.808285	29440.428	-0	0
P 2	11987.598	0.2165474E 08	0	-59.146031	0	0	0
1 3	67.345472	26254.774	-34.260614	106.46079	-2.4367752	0	0.9428415E 08
4	1166.8694	26254.774	-0.1701704	105.40924	-2.4367752	2.4559071	0
5	21.627621	27638.052	18.495308	104.61902	-2.3147478	0	0
6	0	122.02619	1166.7646	21.377044	0	-0	437.15527
O 1	3544.6495	100.71600	27765.568	4181.0934	4320.3754	0.1795506	-15.314361
4 2	5096.1012	1652.1677	19312.647	118.71399	-0.2681133E 09	28.558450	-178.50643
C 1	29440.428	14694.478	14737.230	965.15644	436.98526	438.40538	19.285742
E 2	11.656584	5.8384901	5.8180936	4833.7274	33.626943	33.615531	20.142894
N 3	55.585890	27.788452	27.797438	32.228570	61.900001	37.704285	172.85286
T 4	4.7686262	4.7555272	4.7777570	30.828570	62.357144	37.704285	176.26000
5		99.238474	99.056257	100.35554	100.45022	95.190545	93.865561
O*1	602.00000	739153.75	0	24.771214	29551.305	-0	0
P 2	11852.551	0.2165248E 08	0	-58.998200	0	0	0
1 3	67.712603	26414.055	-34.508231	106.52700	-2.4746456	0	0.9428415E 08
4	1175.2321	26414.055	-0.1583216	105.47342	-2.4746456	2.4932443	0
5	21.774182	27797.144	18.691105	104.68435	-2.3514442	0	0
6	0	121.64906	1175.1261	21.378250	0	-0	436.42253
O 1	3544.8443	100.91077	27920.220	4228.2647	4391.4923	0.1927928	-14.638713
4 2	5238.1403	1794.2068	18894.651	121.65722	-0.2637714E 09	28.558374	-178.50615
C 1	29551.305	14743.400	14799.186	942.01572	436.33317	437.58309	11.857143
E 2	11.482798	5.7638142	5.7189838	4722.0269	33.789317	33.820287	10.428571
N 3	56.126805	28.025502	28.101303	32.485714	61.499999	37.692857	172.81857
T 4	4.8879032	4.8623189	4.9136881	31.085714	61.871428	37.692857	176.24000
5		99.568861	99.472692	100.20578	100.26182	97.246378	96.536115
O*1	619.99998	716329.50	0	24.419793	29535.101	-0	0
P 2	10627.524	0.2162999E 08	0	-57.629494	0	0	0
1 3	67.660435	27941.756	-37.062461	107.13173	-2.7868996	0	0.9428415E 08
4	1252.9021	27941.757	-0.1216920	106.06111	-2.7868996	2.7791141	0
5	23.133294	29323.017	20.541307	105.28387	-2.6555262	0	0
6	0	117.89267	1252.7853	21.388509	0	-0	436.51953
O 1	3544.1963	100.26276	29420.800	4693.2602	5244.5231	0.3242100	-10.871477
4 2	6944.8500	3500.9164	15014.448	158.77375	-0.2208685E 09	28.557648	-178.50346
C 1	29535.101	14710.942	14815.439	737.80684	436.76036	437.34991	16.636340
E 2	11.507418	5.8121836	5.6952342	3703.0624	33.681953	33.875483	8.1817918
N 3	56.050018	27.869770	28.180248	32.036364	61.772726	37.619091	172.61000
T 4	4.8707728	4.7950602	4.9480403	30.636364	61.772726	37.619091	176.11363

5		99.349662	99.581940	100.30389	100.20839	95.901203	97.211009
O*1	639.99998	686463.50	0	23.988184	29714.908	-0	0
P 2	9274.6086	0.2160052E 08	0	-56.021728	0	0	0
1 3	68.269669	29848.450	-38.977847	107.82370	-3.0419083	0	0.9428415E 08
4	1344.7128	29848.450	-0.6553493E-01	106.73693	-3.0419073	3.2038988	0
5	24.735166	31227.470	22.800321	105.97555	-2.9074574	0	0
6	0	112.97736	1344.5833	21.398667	0	-0	435.25783
O 1	3541.2288	97.295258	31308.446	5305.9255	7058.8658	0.4983289	-8.7494856
4 2	10576.503	7132.5692	10482.706	247.92601	-0.1640986E 09	28.556728	-178.50024
C 1	29714.908	14807.784	14898.404	507.28770	435.41556	436.15796	3.4615197
E 2	11.260078	5.6758510	5.5842267	2582.7264	34.008394	34.158276	-2.3846353
N 3	56.906591	28.332543	28.574049	32.107692	61.038459	37.542307	172.41000
T 4	5.0538365	4.9917700	5.1169214	30.707693	61.238460	37.542307	175.98923
5		100.00368	100.13959	99.995051	99.935279	99.835401	100.52891
O*1	659.99998	652510.25	0	23.506378	29735.535	-0	0
P 2	7914.9586	0.2156700E 08	0	-54.309585	0	0	0
1 3	68.340871	32065.882	-39.607381	108.53751	-3.1341743	0	0.9428415E 08
4	1443.1865	32065.883	0.6893145E-02	107.43803	-3.1341743	3.7568781	0
5	26.447972	33442.604	25.305869	106.69654	-3.0050306	0	0
6	0	107.38938	1443.0439	21.407517	0	-0	435.10618
O 1	3537.7666	93.833099	33507.113	6065.4431	12390.766	0.7144836	-7.2127596
4 2	21243.766	17799.833	5580.0061	576.58980	-0.9348494E 08	28.555544	-178.49537
C 1	29735.535	14822.658	14904.157	279.80687	435.19619	436.07259	1.6666768
E 2	11.234260	5.6569269	5.5773327	1452.6172	34.059714	34.178157	-3.2222154
N 3	57.003612	28.402787	28.600824	31.955555	60.933333	37.473332	172.21555
T 4	5.0740871	5.0208864	5.1280469	30.555555	61.188889	37.473332	175.87222
5		100.10413	100.17826	99.944671	99.915718	100.41773	100.74749
O*1	679.31673	617530.50	0	22.984429	30290.964	-0	0
P 2	6580.3719	0.2153248E 08	0	-52.539395	0	0	0
1 3	70.359889	34641.183	-38.689235	109.24898	-2.9663315	0	0.9428415E 08
4	1545.7817	34641.182	0	108.14109	-2.9663315	4.6032297	0
5	28.226853	36015.892	28.001511	107.42419	-2.8530121	0	0
6	0	101.63245	1545.6260	21.414823	0	-0	430.51466
O 1	3534.9416	91.008087	36061.303	7014.1889	224364.23	0.9842446	-5.7517335
4 2	445193.52	441749.58	286.33525	44427.321	-5162808.0	28.553900	-178.49135
C 1	30290.964	15071.201	15211.043	67.067810	431.23122	430.81429	-29.000000
E 2	10.627820	5.3859240	5.2418955	332.75916	34.949234	35.307656	-50.000000
N 3	59.629070	29.563309	30.065761	30.811387	59.000000	37.402277	172.02683
T 4	5.6106588	5.4889948	5.7356657	26.753021	59.000000	37.402277	175.75455
5		101.78265	102.24099	99.034100	98.710903	109.77990	112.68499

REFERENCES

1. Hofeller, G. W.: Centaur Unified Test Plan. AC-6/SD-2 Flight Test Plan - Sec. 8.6., Rev. B. Rep. No. AY 62-0047, General Dynamics/Convair, Aug. 11, 1965.

2. Anon: Centaur Test Report (AC-6), Propellant Tanking (CTP-INT-1003A), Conducted July 13, 1965. Test Summary, NASA, Goddard Launch Operations, July 1965.

3. Anon: Centaur Test Report (AC-6), Flight Acceptance Composite Test (CTP-INT-1000), Conducted July 28, 1965. Test Summary, NASA, Goddard Launch Operations, July 1965.

4. Anon: Centaur Test Report (AC-6), Composite Readiness Test, Conducted July 31, 1965. Test Summary, NASA, Goddard Launch Operations, Aug. 1965.

5. Anon: Atlas-Centaur Flight Evaluation Report. Vehicle AC-6. Rep. No. GD/C BNZ65-037, General Dynamics/Convair, Oct. 22, 1965.

6. Staff of Lewis Research Center: Postflight Evaluation of Atlas-Centaur AC-4 (Launched Dec. 11, 1964). NASA TM X-1108, 1965.

7. Anon: Centaur Monthly Configuration, Performance, and Weight Status Report. Rep. No. GDC63-0495-26, General Dynamics/Convair, July 21, 1965.

8. O'Connor, H. T.: A Comparison of Six- and Twelve-Variable Engine Models for the MA-5 Booster Engine. Rep. No. GD/C-CHA65-016, General Dynamics/Convair, Apr. 15, 1965.

9. Tulino, J. N.; and Staley, C. F.: Investigation of Effect of Hydrogen Snow Accumulation of the Centaur Retromaneuver and the Surveyor Payload. Rep. No. PWA FR-1595, Pratt and Whitney Aircraft Corp., Sept. 30, 1965.

10. Foushee, B. R.: Liquid Hydrogen and Liquid Oxygen Density Data for use in Centaur Propellant Loading Analysis. Rep. No. AE62-0471, General Dynamics/Astronautics, May 1, 1962.

11. Galleher, V. R.; Giberson, W. E.; Margraf, H. J.; and Gautschi, T. F.: Surveyor Spacecraft/Launch Vehicle. Interface Requirements. Surveyor Project Control Document. Project Document No. 1 (Rev. 1), Calif. Inst. of Tech., Jet Propulsion Lab., Dec. 19, 1963.

12. Staff of Lewis Research Center: Postflight Evaluation of Atlas-Centaur AC-3 (Launched June 30, 1964) NASA TM X-1094, 1965.

13. McGowan, P. R.: Flight Dynamics and Control Analyses of the LV-3C Launch Vehicle (Atlas/Centaur AC-6 and AC-7). Rep. No. GD/C-DDE65-021, General Dynamics/Convair, Apr. 1965.

14. Stubblefield, W. O.: Flight Dynamics and Control Analysis of the Centaur Vehicle (Atlas/Centaur AC-6). Rep. No. GD/C-DDE65-033, General Dynamics/Convair, May 1965.

15. Zobal, S. A.: AC-6 Firing Tables. Rep. No. GD/C-BTD65-042, Rev. I, General Dynamics/Convair, July 6, 1965.

16. Roberts, R. E.: Final Guidance Equations and Performance Analysis for Centaur AC-6. Rep. No. GD/C-BTD65-059, General Dynamics/Convair, Apr. 15, 1965.

17. Rung, R. B.; and Renzetti, N. A.: Summary of Deep Space Network Operations Support of Atlas/Centaur AC-6 Mission. Rep. No. EPD 314, Calif. Inst. of Tech., Jet Propulsion Lab., Aug. 26, 1965.

18. Anon: Centaur Monthly Configuration, Performance, and Weight Status Report. Rep. No. GDC63-0495-29, General Dynamics/Convair, Oct. 21, 1965.

NASA-Langley, 1966 E-3268

[redacted]

"The aeronautical and space activities of the United States shall be conducted so as to contribute . . . to the expansion of human knowledge of phenomena in the atmosphere and space. The Administration shall provide for the widest practicable and appropriate dissemination of information concerning its activities and the results thereof."

—NATIONAL AERONAUTICS AND SPACE ACT OF 1958

NASA SCIENTIFIC AND TECHNICAL PUBLICATIONS

TECHNICAL REPORTS: Scientific and technical information considered important, complete, and a lasting contribution to existing knowledge.

TECHNICAL NOTES: Information less broad in scope but nevertheless of importance as a contribution to existing knowledge.

TECHNICAL MEMORANDUMS: Information receiving limited distribution because of preliminary data, security classification, or other reasons.

CONTRACTOR REPORTS: Technical information generated in connection with a NASA contract or grant and released under NASA auspices.

TECHNICAL TRANSLATIONS: Information published in a foreign language considered to merit NASA distribution in English.

SPECIAL PUBLICATIONS: Information derived from or of value to NASA activities. Publications include conference proceedings, monographs, data compilations, handbooks, sourcebooks, and special bibliographies.

TECHNOLOGY UTILIZATION PUBLICATIONS: Information on technology used by NASA that may be of particular interest in commercial and other nonaerospace applications. Publications include Tech Briefs; Technology Utilization Reports and Notes; and Technology Surveys.

Details on the availability of these publications may be obtained from:

SCIENTIFIC AND TECHNICAL INFORMATION DIVISION

NATIONAL AERONAUTICS AND SPACE ADMINISTRATION

Washington, D.C. 20546

[redacted]